

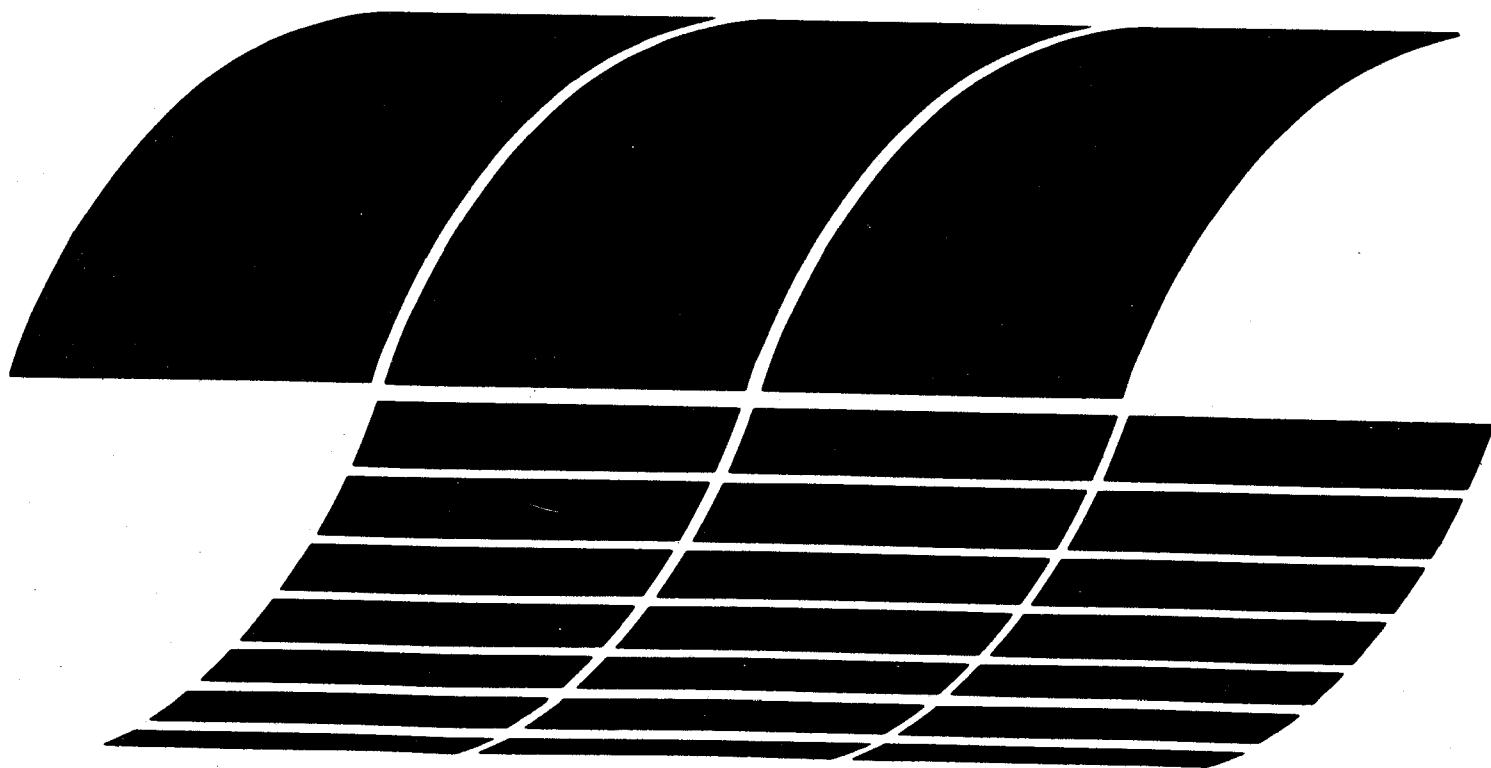


# Third Symposium on Fabric Filters for Particulate Collection

Interagency  
Energy/Environment  
R&D Program Report

\*\*\*\*\*  
\*\*\*\*\*

\*\*\*\*\*  
\*\*\*\*\*



## **RESEARCH REPORTING SERIES**

Research reports of the Office of Research and Development, U.S. Environmental Protection Agency, have been grouped into nine series. These nine broad categories were established to facilitate further development and application of environmental technology. Elimination of traditional grouping was consciously planned to foster technology transfer and a maximum interface in related fields. The nine series are:

1. Environmental Health Effects Research
2. Environmental Protection Technology
3. Ecological Research
4. Environmental Monitoring
5. Socioeconomic Environmental Studies
6. Scientific and Technical Assessment Reports (STAR)
7. Interagency Energy-Environment Research and Development
8. "Special" Reports
9. Miscellaneous Reports

This report has been assigned to the ENVIRONMENTAL PROTECTION TECHNOLOGY series. This series describes research performed to develop and demonstrate instrumentation, equipment, and methodology to repair or prevent environmental degradation from point and non-point sources of pollution. This work provides the new or improved technology required for the control and treatment of pollution sources to meet environmental quality standards.

## **REVIEW NOTICE**

This report has been reviewed by the U.S. Environmental Protection Agency, and approved for publication. Approval does not signify that the contents necessarily reflect the views and policy of the Agency, nor does mention of trade names or commercial products constitute endorsement or recommendation for use.

This document is available to the public through the National Technical Information Service, Springfield, Virginia 22161.

**EPA-600/7-78-087**

**June 1978**

# **Third Symposium on Fabric Filters for Particulate Collection**

Richard Dennis, Compiler

GCA Technology Division  
Burlington Road  
Bedford, Massachusetts 01730

Contract No. 68-02-2177  
Program Element No. EHE624

EPA Project Officer: Dennis C. Drehmel

Industrial Environmental Research Laboratory  
Office of Energy, Minerals, and Industry  
Research Triangle Park, NC 27711

Prepared for

U.S. ENVIRONMENTAL PROTECTION AGENCY  
Office of Research and Development  
Washington, DC 20460

Environmental Protection Agency  
Region V, Library  
230 South Dearborn Street  
Chicago, Illinois 60604

## ABSTRACT

The Third Symposium on Fabric Filters for Particle Collection was held on December 5-6, 1977 in Tucson, Arizona. The Symposium was sponsored by the U.S. EPA's Industrial Environmental Research Laboratory and was organized by GCA/Technology Division.

The conference was intended to emphasize current field experience and engineering-oriented research so that potential users may better select and/or design their control systems. The technical content of the meeting focused on fabrics for high temperature filtration, their field behavior with fly ash and other effluents, design criteria and shakedown experience, and new filtration concepts that appear amenable to combustion and other process effluents.

This report presents the 17 technical papers presented at the symposium.



#### ACKNOWLEDGMENT

GCA wishes to express its appreciation for assistance in organizing and conducting this symposium to Dr. Dennis Drehmel, EPA Project Officer. Members of the GCA/Technology Division staff who provided assistance were: Mr. Stephen V. Capone, Dr. Paul F. Fennelly, and Mr. Norman F. Surprenant.

## TABLE OF CONTENTS

	<u>Page</u>
Abstract . . . . .	iii
Acknowledgments . . . . .	iv
List of Figures . . . . .	vi
List of Tables . . . . .	xii
 Paper 1 - Selection Criteria for Emission Control System and Status Report of Fabric Filter Performance Testing . . . . .	 1
Paper 2 - Modeling Coal Fly Ash Filtration With Glass Fabrics . . . . .	13
Paper 3 - A Pilot Plant Study of Various Filter Media Applied to a Refuse Boiler . . . . .	 41
Paper 4 - Field Tests With a Mobile Fabric Filter . . . . .	75
Paper 5 - Australian Experience, Filtration of Flyash From Very Low Sulfur Coals . . . . .	 105
Paper 6 - Demonstration of a High Velocity Fabric Filtration System Used to Control Flyash Emissions . . . . .	 119
Paper 7 - Baghouse Performance on a Small Electric Arc Furnace . . . . .	155
Paper 8 - Fume Control at Small Smelters . . . . .	167
Paper 9 - Fabric Filters in the Cement Industry . . . . .	177
Paper 10 - New Applications for Fabric Filters . . . . .	189
Paper 11 - Effect of Modified Cleaning Pulses on Pulse Jet Filter Performance . . . . .	 205
Paper 12 - Current and Future EPA Filtration Research . . . . .	229
Paper 13 - Contributing Role of Single Fiber Properties to Nonwoven Fabric Performance . . . . .	 235
Paper 14 - Specific Resistance ( $K_2$ ) of Filter Dust Cakes: Comparison of Theory and Experiments . . . . .	 251
Paper 15 - The Influence of Electrostatically-Induced Cage Voltage Upon Bag Collection Efficiency During the Pulse-Jet Fabric Filtration of Room Temperature Flyash . . . . .	  289
Paper 16 - Textile Filter Media Durability . . . . .	329
Paper 17 - High-Temperature Filtration . . . . .	331
List of Attendees . . . . .	359

## LIST OF FIGURES

<u>Figure</u>		<u>Page</u>
<u>PAPER 1</u>		
1	Comparison of Costs (%) . . . . .	6
2	Harrington No. 2 Flue Gas Flow Diagram and Monitoring Points . . . . .	11
<u>PAPER 2</u>		
1	Schematic, Dust Accumulation on Woven Glass Fabrics . . . . .	16
2	Massive Pinhole Leaks With all Multifilament Yarns and Large, ~200 $\mu$ m, pores . . . . .	17
3	Typical Drag Versus Loading Curves for Filters With Different Degrees of Cleaning and a Maximum Allowable Level for Terminal Drag, $S_T$ , and Terminal Fabric Loading, $W_T$ . . . . .	20
4	Fly Ash Dislodgement From 10 ft x 4 in. Woven Glass Bag (Inside Illumination) . . . . .	21
5	Fly Ash Filtration With Completely and Partially Cleaned Woven Glass Fabric (Menardi Southern) . . . . .	24
6	Relationship Between Cleaned Area Fraction and Initial Fabric Loading. GCA Fly Ash and Woven Glass Fabric . . . . .	26
7	Effect of Inlet Concentration on Predicted Outlet Concen- trations at a Face Velocity of 0.61 m/min. GCA Fly Ash and Sunbury Fabric . . . . .	28
8	Predicted and Observed Outlet Concentrations for Bench Scale Tests. GCA Fly Ash and Sunbury Fabric . . . . .	29
9	System Breakdown for I Bags and J Areas Per Bag . . . . .	32
10	NUCLA Baghouse Simulation, Resistance Versus Time . . . . .	35
11	Test Run No. 0422 Nucla Baghouse Simulation - Linear Penetration Versus Time Graph . . . . .	36
<u>PAPER 3</u>		
1	Schematic Diagram of the Enviro-Clean RA-1 Dust Collector Model 144-RA1-5-104 . . . . .	46
2	Temperature Profile for the Enviro-Systems Baghouse . . . . .	47
3	Fabric Filter Pilot Plant Installed at Nashville Thermal Transfer Corp. . . . .	48
4	Inlet Particle Size Distribution for Two Brinks Impactor Runs . . . . .	52
5	Outlet Particle Size Distribution . . . . .	54
6	Outlet Particle Size Distribution, Globe Albany . . . . .	55

## LIST OF FIGURES

<u>Figure</u>	PAPER 3 (cont)	<u>Page</u>
7	Outlet Particle Size Distribution for Gore-Tex Fabric . . . .	57
8	Comparison of Three (3) Fabrics for Outlet Concentration versus Air-to-Cloth Ratio . . . . .	60
9	Comparison of Installed Costs for Four (4) Filter Media and Electrostatic Precipitators . . . . .	62
10	Installed Cost Comparisons for Different Air Pollution Control Techniques . . . . .	64
11	Comparison of Annual Operating Costs of Four (4) Filter Media and ESP Assuming Four Year Bag Life . . . . .	65
12	Comparison of Annual Operating Costs of Four (4) Filter Media and ESP Assuming Four Year Bag Life . . . . .	66
13	Annual Operating Cost Comparison for Three Air Pollution Control Techniques . . . . .	68
14	Comparison of Annual Operating Costs of Four (4) Filter Media and ESP Assuming Two Year Bag Life . . . . .	69
15	Comparison of Annual Operating Costs of Four (4) Filter Media and ESP Assuming Four Year Bag Life . . . . .	70
16	Annualized Cost for the Three Air Pollution Control Techniques . . . . .	71

### PAPER 4

1	Average Mass Penetration versus Geometric Mean Particle Diameter . . . . .	103
---	---	-----

### PAPER 5

1	Typical Coal Analysis . . . . .	113
2	ECNSW Fabric Filter Installations . . . . .	114
3A	ECNSW Tallawarra Station - Section A Pilot Unit . . . . .	115
3B	ECNSW Tallawarra Station - Section A and B Full Scale . . . .	116
4	ECNSW Wangi Station - Units 4, 5, 6 - Pulse Jet Filters . . .	117
5	ECNSW Wangi Station - Unit 5 PC Boiler - Reverse Air Baghouse Design Conditions . . . . .	118

# LIST OF FIGURES

<u>Figure</u>		<u>Page</u>
<u>PAPER 6</u>		
1	SD-10 General Arrangement With Pyramid Hoppers . . . . .	123
2	Fabric Filter Module Cell . . . . .	124
3	Baghouse Pictorial Showing Gas Flow . . . . .	126
4	Step 2 - The Fabric Filter . . . . .	127
5	Step 3 - Shock . . . . .	128
6	Step 4 - Drag . . . . .	129
7	Kerr Pilot Plant Photo . . . . .	131
8	Outlet Concentration versus Air-to-Cloth Ratio for Various Bag Materials . . . . .	132
9	Comparison of Operating Pressures for Various Bag Materials . . . . .	133
10	Installed Costs versus Air-to-Cloth Ratio . . . . .	134
11	Operating Costs versus Air-to-Cloth Ratio . . . . .	135
12	Teflon Felt - Annual Operating Costs versus Air-to-Cloth Ratio for Different Bag Life Assumptions . . . . .	136
13	Annualized Cost Comparison . . . . .	137
14	EPA Demonstration of the Enviro-Systems Fabric Filter Sys- tem at Kerr Finishing Div. FabricsAmerica, Concord, North Carolina . . . . .	139
15	One House on Truck . . . . .	140
16	House Being Lifted Onto Hopper - Far View . . . . .	141
17	House Being Lifted Onto Hopper - Near View . . . . .	142
18	Completed System . . . . .	143
19	Control Panel. . . . .	144
20	Fabric Filter Schematic . . . . .	145
21	Total Annualized Cost Versus Air-to-Cloth Ratio Teflon Felt . . . . .	150
22	Annualized Costs Versus Air-to-Cloth Ratio . . . . .	152
23	Annualized Costs Versus Air-to-Cloth Ratio . . . . .	153

## LIST OF FIGURES

<u>Figure</u>		<u>Page</u>
<u>PAPER 7</u>		
1	Photograph of Side of Fabric Filter . . . . .	157
2	Photograph of End of Fabric Filter . . . . .	158
3	Concentration Versus Process Cycle for 10 $\mu$ m Particles. . . . .	160
4	Time in Process Cycle at Which Inlet Samples Were Collected . . . . .	162
5	Composited Differential Size Distribution Curves of Baghouse Inlet Aerosol . . . . .	163
6	Average Outlet Differential Size Distribution Curves . . . . .	164
7	Fabric Filter Fractional Penetration Curves . . . . .	165
<u>PAPER 10</u>		
1	Flow Sheet . . . . .	191
2	Typical Filter Pressure Loss Curve . . . . .	193
3	Coke Oven Exhaust Tar Removal Efficiency . . . . .	192
4	Coke Oven Pilot Unit . . . . .	194
5	Coke Oven Pilot Unit . . . . .	195
6	Galvanizing Line Fabric Filter Operating Conditions . . . . .	197
7	Galvanizing Line Fabric Filter Design Features . . . . .	197
8	Sinter Machine Windbox Fabric Filter . . . . .	199
9	Fabric Filter - Nahcolite System . . . . .	201
10	SO <sub>2</sub> Removal as a Function of Stoichiometric Ratio Under Optimum Conditions . . . . .	202
11	Fabric Filter-Nahcolite System Costs . . . . .	203
<u>PAPER 11</u>		
1	Schematic Drawing of Fabric Filter Apparatus Used . . . . .	210
2	Cumulative Size Distribution by Count for Fly Ash . . . . .	211
3	Valve Arrangement for Pulse-Air Manifold. . . . .	212
4	Photograph Tracing of Oscilloscope Display: Pulse Pressure Versus Time for Normal Pulse . . . . .	214

## LIST OF FIGURES

<u>Figure</u>	PAPER 11 (cont)	<u>Page</u>
5	Photograph Tracing of Oscilloscope Display: Pulse Pressure Versus Time for Modified Pulse . . . . .	216
6	Photograph Tracing of Oscilloscope Display: Pulse Pressure Versus Time for Modified Pulse With Twice Normal Chamber Volume . . . . .	217
7	Penetration Versus Filtration Velocity, Pulse Type as Parameter . . . . .	220
8	Penetration Versus Filtration Velocity, Relative Humidity as Parameter . . . . .	221
9	Pressure Drop Versus Filtration Velocity, Relative Humidity as Parameter . . . . .	223

### PAPER 13

1	Capture Efficiencies of Three Nonwoven PET Fabrics Made of Various Fibers, as Shown, When Filtering a Flyash Aerosol. .	241
2	Ratios of Outlet Concentrations for Filters Made of Fibers With 2, 3 and 5 Lobes to Outlet Concentrations for Round Fiber Filter . . . . .	242
3	Capture Efficiencies for Nonwoven Rayon Filters Made of Fibers With Various Levels of Crimp as Shown, When Filtering a Flyash Aerosol . . . . .	243
4	Penetration (Equal to 1-Efficiency) for PET and Polypropylene Filters of Constant Weight and Density but Made of Fibers of Different Diameters . . . . .	244
5	Specific Cake Resistance for the Filters in Figure 4 . . . . .	245
6	Pressure Drops at Beginning and End of Filter Cycle ( $\Delta P_i$ and $\Delta P_f$ ) for Conditioned Bags Made of Round and Trilobal PET Fibers . . . . .	246
7	Outlet Concentration Ratios for Bags in Figure 6 . . . . .	247
8	Single Fiber Efficiencies for Each Layer in Layered Filters Made of Round and Trilobal Fibers . . . . .	248
9	Calculated Single Fiber Efficiencies for Fibers With Cross Sections $\rho = 1 + \epsilon \cos m(\phi + C)$ Where $m$ = Number of Lobes and $\epsilon$ Indicates the Lobe Depth . . . . .	249

## LIST OF FIGURES

<u>Figure</u>		<u>Page</u>
<u>PAPER 14</u>		
1	Experimental Apparatus . . . . .	273
2	Cross Section of Dust Cake on Woven Fabric . . . . .	275
3	Dust Cake Shadow Cast on Woven Fabric . . . . .	277
4	Particle Size Distribution . . . . .	278
5	Specific Resistance Versus Solidity . . . . .	282
<u>PAPER 15</u>		
1	Cage Contact . . . . .	297
2	Cage Voltage Forms . . . . .	299
3	Basic Electrical Equivalent Circuit . . . . .	302
4	Gas Flow Rate Through One Bag of a Four-Row Pulse-Jet Array . . . . .	304
5	Modified Equivalent Circuit Containing Distributed Components . . . . .	306
6	Cage Voltage During Fly Ash Filtration At High Relative Humidity . . . . .	314
7	Cage Voltage Under an External Bias of -2000 Volts . . . . .	316
<u>PAPER 17</u>		
1	3-M Company Thermacomb . . . . .	334
2	Calculated Performance 3.0 $\mu$ m Alumina Fiber Bed . . . . .	339
3	D.O.P. Efficiency fn Airflow Velocity . . . . .	341
4	D.O.O. Efficiency fn Basis Weight. . . . .	346
5	Dust Loading of Ceramic Felts . . . . .	348
6	Dust Loading of Ceramic Paper . . . . .	349
7	Dust Loading of Woven Ceramic Media . . . . .	350
8	Saffil Alumina - Post Test Dust Cake . . . . .	353
9	Woven Fiberfrax - Post Test Dust Cake . . . . .	355
10	Fiberfrax Blanket - Post Test Dust Cake . . . . .	356



## LIST OF TABLES

<u>Table</u>		<u>Page</u>
<u>PAPER 2</u>		
1	Required Data Inputs for Specific Model Application . . . . .	33
2	Predicted and Measured Resistance Characteristics for Nucla Filter System . . . . .	34
3	Measured and Predicted Values for Filter System Penetration and Resistance, Coal Fly Ash Filtration With Woven Glass Fabrics . . . . .	38
<u>PAPER 3</u>		
1	Nashville Thermal Transfer. . . . .	49
2	Inlet Emission Profile . . . . .	50
3	Outlet Concentration and Cumulative % . . . . .	53
4	Outlet Concentration and Cumulative % . . . . .	56
5	Outlet Concentration and Cumulative % . . . . .	58
6	Bag Cost as Percent of Installed Cost . . . . .	61
<u>PAPER 4</u>		
1	Brass and Bronze Foundry Pulse Cleaning Test Results. . . . .	89
2	Brass and Bronze Foundry Shake Cleaning Test Results. . . . .	89
3	Hot Mix Asphalt Plant Pulse Cleaning Test Results . . . . .	90
4	Coal-Fired Power Plant (Cyclone-Fired Boiler) Shake Cleaning Test Results . . . . .	90
5	Operating Conditions for Coal-Fired Power Plant (Anthracite Coal) Tests . . . . .	91
6	Coal-Fired Power Plant (Anthracite Coal) Mass Efficiency Test Results . . . . .	92
7	Operating Conditions for Pulp Mill Lime Recovery Kiln Tests . .	94
8	Pulp Mill Lime Recovery Kiln Mass Efficiency Test Results . . .	95
9	Pulp Mill Lime Recovery Kiln Fractional Efficiency Test Results . . . . .	96
10	Pressure Drop Results of Pulp Mill Lime Recovery Kiln Tests . .	97
11	Operating Conditions for Coal-Fired Power Plant (Subbituminous Coal) Tests . . . . .	98
12	Pressure Drop Results of Coal-Fired Power Plant (Subbituminous Coal) Shake Cleaning Tests. . . . .	99

## LIST OF TABLES

<u>Table</u>	PAPER 4 (cont)	<u>Page</u>
13	Pressure Drop Results of Coal-Fired Power Plant (Subbituminous Coal) Reverse Cleaning Tests (Teflon/Glass Bags) . . . . .	100
14	Pressure Drop Results of Coal-Fired Power Plant (Subbituminous Coal) Reverse Cleaning Tests (Graphite/Glass Bags) . . . . .	101
15	Coal-Fired Power Plant (Subbituminous Coal) Mass Efficiency Test Results . . . . .	102
<u>PAPER 6</u>		
1	Alarms and Shut-Down Functions . . . . .	147
<u>PAPER 7</u>		
1	Average Results of Total Mass Measurements . . . . .	159
<u>PAPER 8</u>		
1	Fume Control in Small Smelters . . . . .	175
<u>PAPER 11</u>		
1	Fractional Mass Penetration/Pressure Drop, MM Water Gauge/% Relative Humidity . . . . .	219
<u>PAPER 14</u>		
1	Minimum Specific Resistance . . . . .	258
2	Comparison of Resistance Factors Predicted by Kozeny-Carman Equation and "Free Surface" Model. . . . .	263
3	Comparison of $\bar{D}_{vs}$ and $\bar{D}_{v1}$ . . . . .	268
4	Porosities and Particle Diameters for which $C_s = 1.1$ . . . . .	271
<u>PAPER 15</u>		
1	Experimental Nomex Test Bags (Scrimless Felts) . . . . .	311
2	Bag Performance Series . . . . .	312
3	Control Bag Performance Under Cage Electrical Bias (All Runs at 50% Relative Humidity). . . . .	315
4	Control Bag Performance at Various Cage Electrical Terminations (All Runs at 50% Relative Humidity). . . . .	318
5	Properties of Needled Polyester Felt Fabric. . . . .	320
6	Filtration Performance of the Test Polyester Felts . . . . .	322

## LIST OF TABLES

<u>Table</u>		<u>Page</u>
	<u>PAPER 17</u>	
1	Summary of 3M ThermaComb Performance . . . . .	336
2	Effect of Changing Cleaning Conditions . . . . .	336
3	Summary Room Ambient Test Data . . . . .	342

SELECTION CRITERIA  
for  
EMISSION CONTROL SYSTEM  
and  
STATUS REPORT OF FABRIC FILTER  
PERFORMANCE TESTING

Presented by:

Jack D. Jones  
Principal Engineer, Mechanical  
and

Kenneth L. Ladd, Jr.  
Senior Environmentalist

Southwestern Public Service Co.  
Amarillo, Texas

Presented at:

Third EPA Symposium  
on Fabric Filters for  
Particle Collection

December 5, 1977

Tucson, Arizona

ABSTRACT

SELECTION CRITERIA FOR  
EMISSION CONTROL SYSTEM AND  
STATUS REPORT OF FABRIC FILTER PERFORMANCE TESTING

After studying the technological and economic aspects of emission control devices for its second coal-fired generating unit, Southwestern Public Service Company selected a fabric filter system for particulate control. Problems with electrostatic precipitators and the desire to install an emission control device which would not require particulate scrubbing prompted Southwestern to investigate the feasibility of a fabric filter installation. The study revealed that a fabric filter system would be economically justifiable as well as technically appropriate for the Company's coal-fired plant which utilizes low sulfur Western coal.

As a result of its choice, Southwestern, under a contract with the U. S. Environmental Protection Agency, will conduct a study to assess the performance of the fabric filter system as an emission control device. Continuous monitoring of the flue gas emission stream will be made at five different sampling points. Special inlet and outlet sample testing will define the particulate characteristics. The collected data will be processed into a determination of the economics and industrial acceptability of operating and maintaining the commercial emission control system. The resultant report should be a guide on the selection, design, operation and maintenance of a fabric filter system for Western coal-fired boilers.

## SELECTION CRITERIA FOR EMISSION CONTROL SYSTEM

### PART I

Southwestern Public Service Company is an electric utility headquartered in Amarillo, Texas, with 2,240 employees serving approximately 280,000 customers in Texas, Oklahoma, New Mexico and a small area of Kansas. The Company has a generating capacity of 2740 MW produced by five major and three smaller power stations; seven of these installations are fueled by natural gas. The number one unit of Southwestern's first coal-fired station went on line in July, 1976; it has a 356 MW capability. By July, 1984, the Company will have approximately 2150 MW of coal-fired steam generating capability on line.

Southwestern Public Service Company designs its own power plants through the Generation Plant Design Group, which is part of the System Engineering Department organized in 1945. When we began design of our first coal-fired unit, the Generating Plant Design Group had 30 employees, of whom 12 were engineers. We now have 87 employees in plant design, 36 of whom are engineers.

The basic problem in designing the Company's second coal-fired unit was the selection of a coal-fired furnace flue gas treating and control system which would satisfy EPA's New Source Standards. These standards require that a coal-fired facility not emit more than .1 pounds per million Btu particulate, and emissions cannot exceed 1.2 pounds per million input of sulfur dioxide.

Southwestern Public Service Company looked at the alternatives for controlling coal-fired boiler emissions and an effort was made to select a type of emission control device which would not require scrubbing for particulate removal.

The 350 MW Harrington Station unit (located near Amarillo, Texas) uses sub-bituminous low sulfur Western coal, and, therefore, the EPA standards for SO<sub>2</sub> could be met by selecting low sulfur coal as fuel.

The primary systems initially studied for particulate control were electrostatic precipitators. Since the construction of Harrington Station Unit #1, electrostatic precipitator guarantees, performance and technology had improved to the point that consideration was given to the purchase of a 99.5% removal-of-ash electrostatic precipitator. At the time that a decision was required by Generation Plant Design staff, numerous utilities were having problems with hot-side precipitators; therefore, this type of precipitator was not considered.

While obtaining bids and information from suppliers of electrostatic precipitators some mention was made of the use of fabric filters for particulate control. The use of this type of filter system in Southwestern's service area is very common (in the carbon black industry) and we were somewhat familiar with this application. After a study was made of fabric filters, and how they were applied at the Sunbury and NUCLA facilities, a decision was made to compare electrostatic precipitators with baghouse systems.

Baghouse vendors were contacted and the only specifications given these suppliers for preparing their quotations were flue gas flow, ash characteristics, and grain loading. Meetings were held with fabric filter suppliers to determine a common base for comparison with each other and with electrostatic precipitator proposals. These comparisons were based on physical design, physical operation, capital cost and operating cost.

Comparison Charts: This comparison chart (Figure 1) will show the comparative costs of three fabric filters and three

99.5% effective precipitators. The comparison is in percentages with the fabric filter purchased for Harrington Station, Unit #2, being the base. There are two areas in which the competitors were lower than the base. The #3 fabric filter was lower in capital cost due to the cost of bag replacement for fabric filters being classified as maintenance. Replacement for the fabric filters was based on a two year life of the bags; however, experience at Sunbury indicates that bag life is much longer than two years. From a discounted cash flow analysis it can be seen that the fabric filters have less effect on the cost to stockholders than any of the precipitators. It should be noted, however, that the parameters used in this analysis may not necessarily apply to other utilities, or to other areas.

Our first fabric filter was selected for Harrington Station, Unit #2. For the #3 unit at Harrington we wrote a set of specifications and then negotiated a contract for a fabric filter system to be supplied by Wheelabrator-Frye, Inc. Essentially it is the same as the system designed for Unit #2.

The Company's next coal-fired station will be Tolk Station Units #1 and #2. Unit #1 is scheduled to go on line in June, 1982. Southwestern Public Service will prepare a set of specifications for a fabric filter system based on knowledge gained from the purchase and use of two fabric filter systems at our Harrington Station, enhanced by the knowledge gained in studying the system for Unit #2.

In the second part of this paper, Kenneth Ladd will describe Southwestern Public Service Company's plans to obtain this knowledge.



# COMPARISON OF COSTS (%)

	FABRIC FILTER			99.5 % PRECIPITATOR			
	BASE	2	3	1	2	3	
CAPITAL COST	100	101	86	142	143	166	
OPERATING COST	100	132	110	228	175	153	
MAINTENANCE COST	100	101	144	20	20	20	
COST TO STOCKHOLDER	100	115	105	133	132	148	

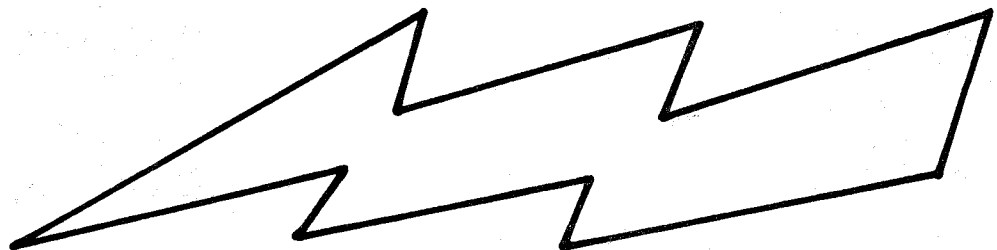


FIGURE 1

## SELECTION CRITERIA FOR EMISSION CONTROL SYSTEM

### PART II

The preceding comments describe Southwestern Public Service Company's reasons for selecting a fabric filter system for emission control. Because such a small amount of information is available on the performance testing of fabric filters at other utility installations, it was necessary for Southwestern Public Service to make its own evaluation of emission control devices for the specified Harrington Station application.

Southwestern has no previous experience in fabric filter system operations so when asked the question, "Why a baghouse?" we encourage each utility to make its own analysis. Factors to consider are specific requirements, boiler design, fuel, and other engineering and economic considerations. Southwestern is not qualified to present general criteria at this time.

To assist in the collection of information to formulate a more complete data base for fabric filter performance, Southwestern and EPA have agreed to make a comprehensive study of a commercial, operating unit. The study will require two years to complete the collection and assessment of one full operating year's worth of data. After this experience and testing, Southwestern Public Service can offer more expert opinion concerning fabric filters. In the last part of this paper, the status of the testing program will be discussed.

The objective of the study is to implement an overall program of testing and evaluation design to (1) fully characterize the fabric filter system applied to Harrington Station, Unit #2; (2) study the technical and economic feasibility of the system; (3) demonstrate long-term reliability of the system; and (4) determine the system's optimum operating conditions.

A description of the emission source and the fabric filter system to be tested is as follows:

The emission source is a pulverized coal-fired Combustion Engineering tangentially-fired boiler. It will use low sulfur Western coal, supplying steam to a 356 MW rated steam turbine generator. The fabric filter is a Wheelabrator-Frye, Inc. unit with 28 compartments, operating at 313° F, cleaning 2,650,000 acfm at full load; the normal net air-to-cloth ratio is 3.4:1. The fabric filter cleaning method is reverse air and shaking with the control flexibility of using either or both. The filter medium is fiberglass coated with silicone and graphite. The bags are 11.5 inches in diameter and 30.5 feet long.

The test plan will characterize the fabric filter system by manual sampling and continuous monitoring. The plan also calls for analyses of all solids and gases in and out of the system. Additionally, data will be collected and recorded which describes all significant fuel and operation information.

Major manual sampling and testing of the particulate entering and leaving the fabric filter system will be used to determine performance characteristics that cannot be measured with continuous monitoring equipment. Three detailed manual samplings will be equally spaced during the year of operating tests. Five sampling ports will be sampled at the same time to determine mass particulate flow and particle size distribution down to .01  $\mu$ m. The particulate ash will be analyzed for organic material, elemental constituents, sulfates, sulfites and nitrates.

Manual sampling and testing will also be used to determine flue gas characteristics. The parameters to be determined are hydrogen chloride, hydrogen fluoride, oxides of sulfur, oxide of nitrogen, organic vapors, and elemental constituents.

All major sampling and testing will be performed according

to EPA and other approved testing procedures. The manual sampling results will be correlated with operating data to define the performance of the fabric filter at full load on the system.

The same five sampling ports will be used to locate the continuous monitoring equipment (see Figure 2, Harrington #2 Flue Gas Flow Diagram and Monitoring Points).

The parameters listed below will be continuously monitored (flue gas stream - at all 5 points):

- |                               |                  |
|-------------------------------|------------------|
| 1. $\text{SO}_2$              | 5. $\text{O}_2$  |
| 2. $\text{NO}_x$              | 6. Temperature   |
| 3. Particulate (grain/cu.ft.) | 7. Duct pressure |
| 4. Flue gas flow (acfm)       |                  |

Additional operating parameters that will be measured or calculated on a continuous basis will be pressure drop across the system, power consumption, load on the unit, fuel flow, particulate removal, cleaning mode and frequency and flue gas flow. There are approximately 30 analog inputs and another 20 contact inputs that will direct operational data into the plant computer. This data will not be as specialized as the manual sampling information, but rather will represent every day operation of the fabric filter system. Daily records will be kept of the maintenance required by the fabric filter system.

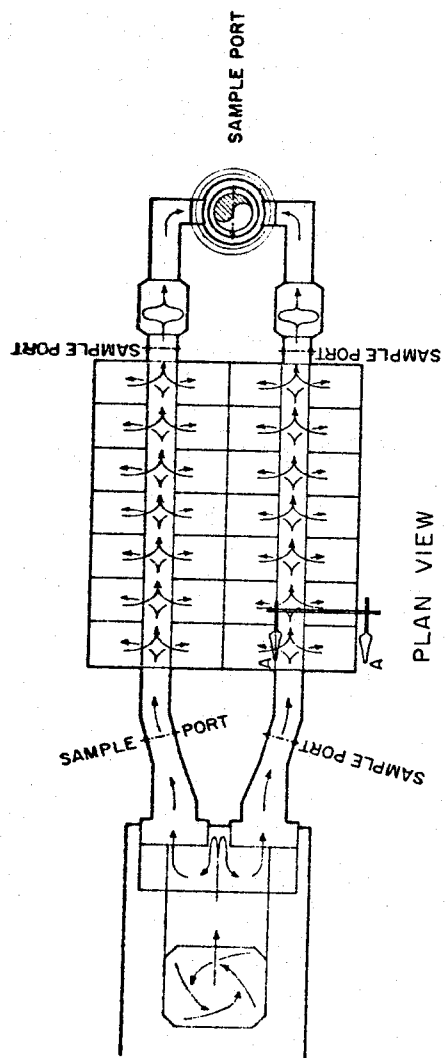
The test program should produce an assessment of the performance of a fabric filter system that determines particulate collection, pressure drop, temperature, energy consumption,  $\text{SO}_2/\text{SO}_3$  removal, optimum cleaning procedures, fabric care and maintenance, corrosion, system reliability and bottom line cost of operation and maintenance.

An option for a future study exists which would permit the determination of operation and maintenance parameters for five years of operation after performance has been defined.

During the present study, the fabric filter system will operate as designed and required for the generation of electric power from a commercially operating unit. This limits the special testing of parameters outside of the normal operation. Another future option would include special testing of fabrics, air-to-cloth ratios, or other related research. These objectives would be accomplished by installing a small slipstream fabric filter test module (about 10,000 acfm).

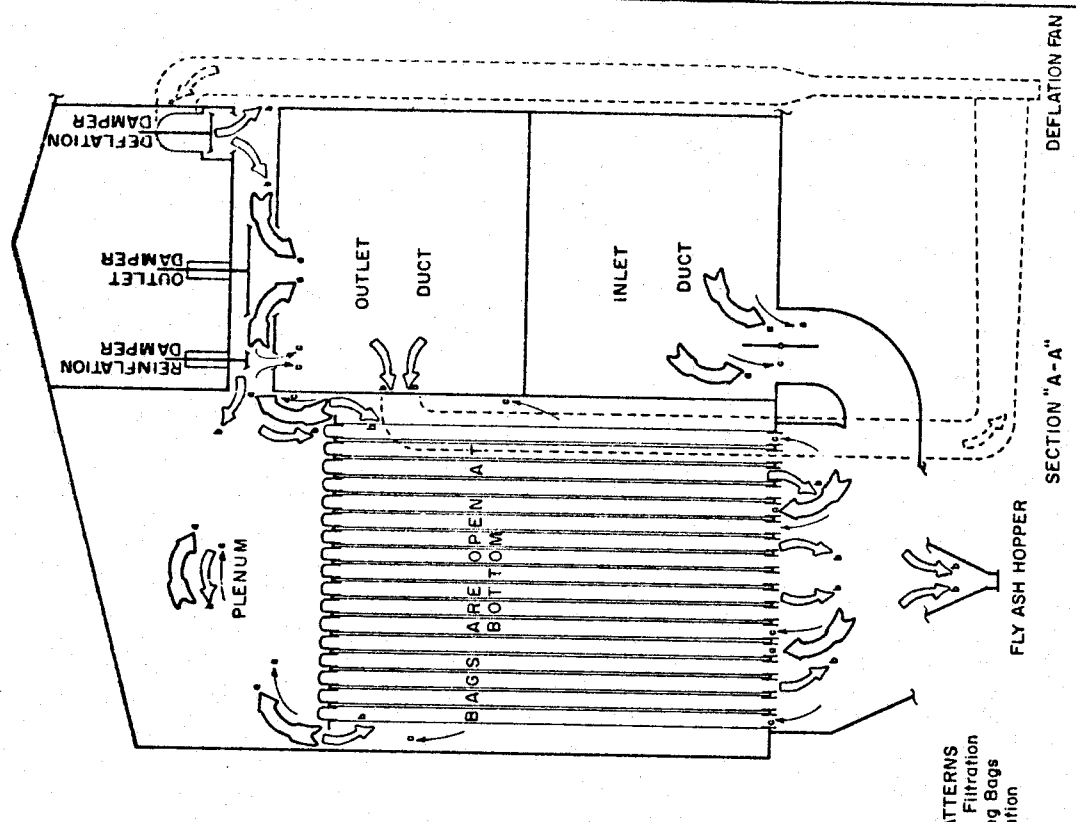
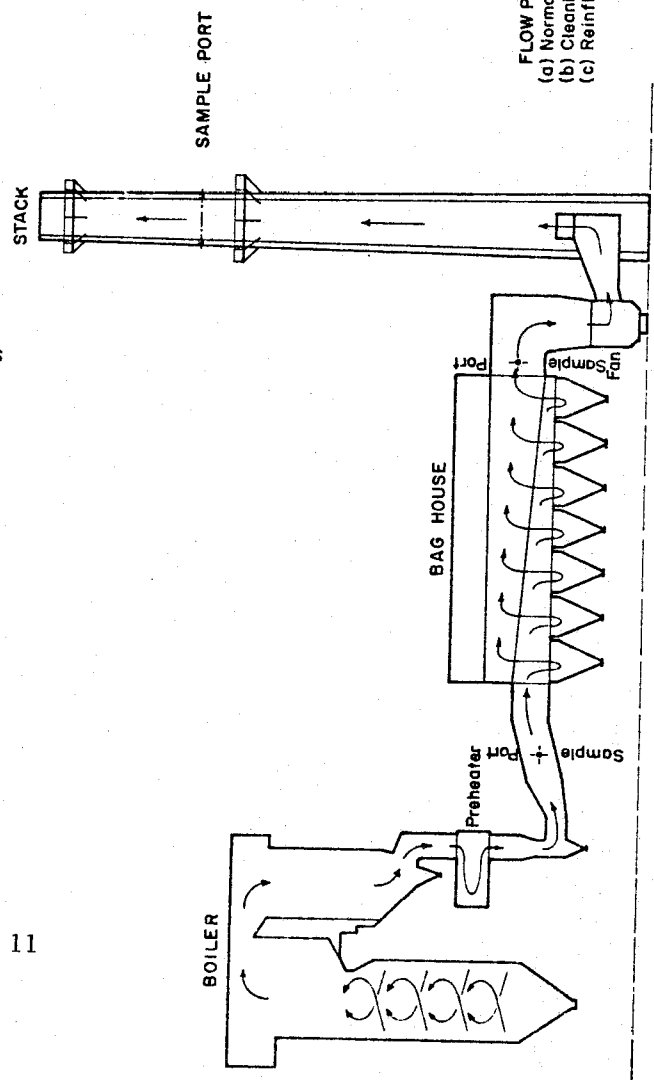
Southwestern Public Service Company wants to gain experience in the application of fabric filters as well as provide to other utilities information which might be useful in their evaluations of their own unique emission control problems. A performance report submitted by a utility would present utility knowledge and application to the air quality regulatory groups, and thus better represent the industry's problems and solutions.

As a result of the testing program, Southwestern Public Service Company will, two years from now, be able to make an assessment based on sound and well-documented operating experience



11

FIGURE 2



REVISIONS

HARRINGTON No 2 FLUE GAS FLOW DIAGRAM AND MONITORING POINTS					
Southwestern PUBLIC SERVICE Company					
DRAWN	DATE	CHECKED	APPROVED	SCALE	ENGINEERING DEPT.
SIX	10/18/76			NONE	NO
					76101808E



MODELING COAL FLY ASH FILTRATION  
WITH GLASS FABRICS

by

Richard Dennis

and

Hans Klemm

GCA CORPORATION  
GCA/TECHNOLOGY DIVISION  
Bedford, Massachusetts



## ABSTRACT

A new mathematical model for predicting the performance of woven glass filters with coal fly ash aerosols from utility boilers is described in this paper. The data base includes bench and pilot scale studies in which several dust/fabric combinations were investigated; field data from prior GCA studies of coal fly ash filtration with glass fabrics; past GCA studies of fabric filter cleaning mechanisms and a broad-based literature survey.

Two new concepts were instrumental in model design. The first relates to the manner in which dust dislodges from a fabric and its subsequent impact upon resistance and penetration in a multichambered system. The second concept is associated with the relatively large fractions of fly ash that pass with minimal collection through temporarily or permanently unblocked pores or pinholes. Additionally, the quantitation of the cleaning action with dust removal in terms of method, intensity and duration of cleaning was essential to the overall modeling process. The examination of specific resistance coefficient,  $K_2$ , for the dust layer in the light of polydispersed rather than monodispersed particle components provided improved estimates of  $K_2$ . Trial applications of the modeling technique to field filter systems operating at Sunbury, Pennsylvania and Nucla, Colorado indicate excellent agreement between theory and practice for both penetration and resistance characteristics.

## SECTION 1

### BACKGROUND

The prospect of stricter particulate emission regulations for coal-fired boilers suggests that fabric filtration may be the best control technique for many applications. Limited field experience with large utility boilers<sup>1,2</sup> has demonstrated that glass fabric filters perform well with respect to moderate pressure loss, very high collection efficiency and acceptable service life (at least 2 years). A possible drawback, however, in the eyes of utility groups has been the inability to predict accurately how a new filter system will perform without extensive pilot testing and field trials.<sup>3,4</sup> Only when the new plant design replicates an existing (and successful) installation with respect to power level, boiler design and fuel characteristics can the filter performance be predicted safely.

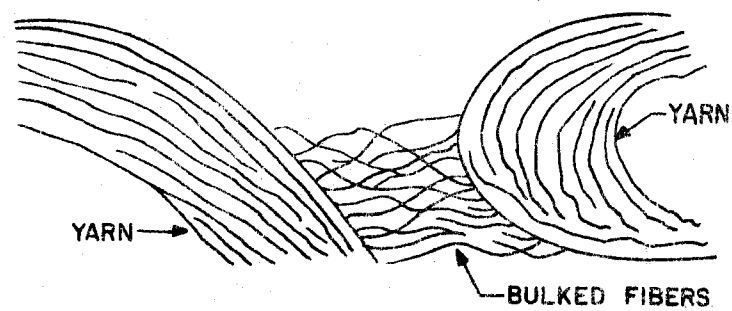
In this paper, a filtration model is described which, based upon limited field validation, provides rational estimates for the performance of woven glass bags with coal fly ash in real filter systems.<sup>4,5</sup> The apparent success of the model is attributed to the introduction of three new concepts or approaches to the modeling process.

The first relates to the fact that dust remaining on a fabric surface after cleaning is characterized by a distinctive, nonuniform distribution in which the unique resistance and collection properties of cleaned and uncleaned areas are definable and thus amenable to mathematical analysis.

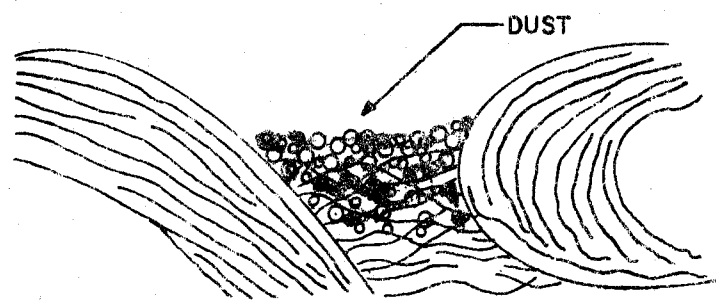
The second approach allows us to quantify the relationship between the amount of dust removed from a filter and the method of cleaning and the filter dust loading prior to cleaning.<sup>5,6</sup>

The third approach centers on the unique dust penetrating properties observed for fly ash/woven glass fabric systems in which the failure to obtain rapid and/or complete pore bridging allows significant direct leakage (bypassing) of the upstream aerosol to the clean air side of the system. Such penetration arises because of a characteristic nonuniformity in both pore dimensions and in the dispersion of the loose fiber substrate that screens the pore openings.<sup>4,5</sup>

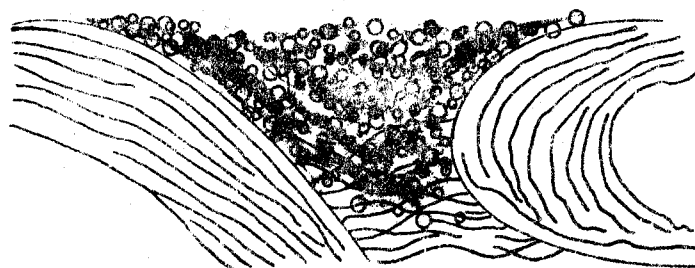
Were it not for the above imperfections, a continuous and highly impenetrable dust layer would form above the substrate as shown in Figure 1. On the other hand, an overly loose weave coupled with a sparsity and nonuniform distribution of substrate fibers can lead to the critical pinhole leak problem illustrated in Figure 2. The relatively low resistance to gas flow presented by the larger pores results in the passage of a disproportionately large



UNUSED  
FABRIC



EARLY DUST  
BRIDGING OF  
FIBER SUBSTRATE



SUB SURFACE  
DUST CAKE  
DEVELOPMENT

Figure 1. Schematic, dust accumulation on woven glass fabrics.

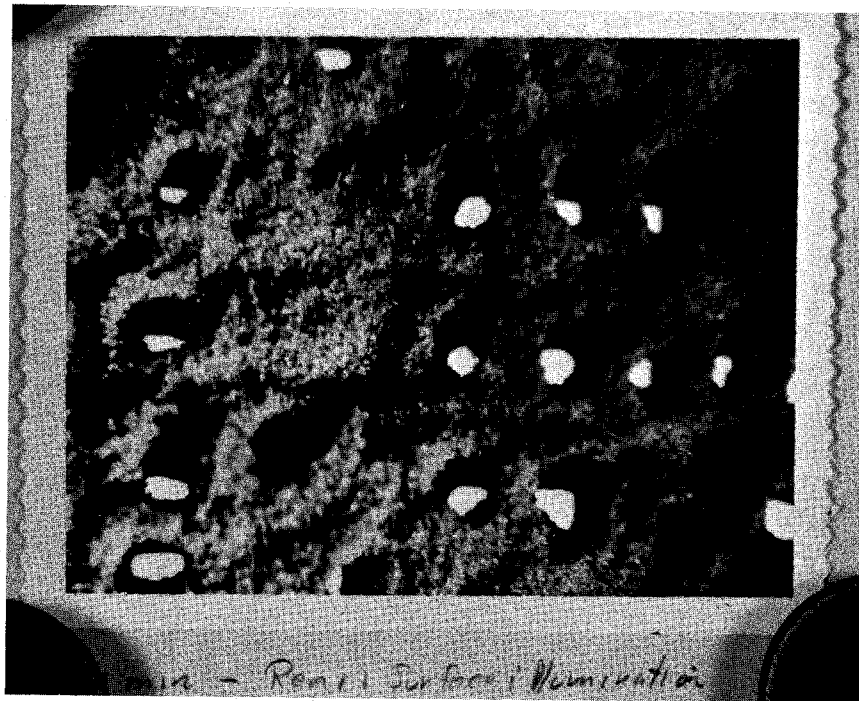


Figure 2. Massive pinhole leaks with all multifilament yarns and large, ~200  $\mu\text{m}$ , pores.

fraction of the uncleaned gas along with most dust particles  $< 15 \mu\text{m}$  diameter. Because the quantity of fly ash penetrating woven glass fabrics via the pore or pinhole leak route exceeds that which penetrates the unbroken dust cake by some 100 to 1000 times, the particle size properties of the effluent particles are essentially the same as those in the entering aerosol.

The above phenomenon explain why the reported fractional efficiencies for glass fabric systems often indicate the same degree of collection for all particle sizes. It is also pointed out that periodic rear face slough-off of agglomerated particles due to mechanical vibration or aerodynamic drag may contribute significantly to the effluent loading.<sup>4,7</sup>

Another consideration in the modeling process is the fact that the dust collection capability for any specified area of a fabric surface depends upon both the local dust cover and the local filtration velocity.<sup>3,4,6,8</sup> Additionally, the specific resistance coefficient,  $K_2$ , for a given dust depends not only upon the physical properties of the particles, gas and bed structure but also upon the gas velocity at the time of particle deposition.<sup>3,5</sup>

Introduction of variables and concepts discussed above into the classical filtration equations constitutes the basis for a comparatively simple model which can serve two major roles. The first application relates to the design of a filter system based upon specified dust and fabric properties, air to cloth ratios, proposed frequency and/or intensity of cleaning and pressure loss constraints. The second application is that of determining whether the operating regimen and basic design approach specified by a system designer will allow the user to meet particle emission requirements while conforming to system gas flow and resistance requirements. Thus, the second or diagnostic role of the filtration model should prove particularly valuable to environmental control groups who must assess the adequacy of proposed control measures.

In the following sections, we have outlined briefly the basic structure and development of the model and its preliminary trial runs. We have not attempted, however, to describe fine operating details nor the programming routines per se, both aspects having been dealt with extensively in a recent study.<sup>4</sup> Although the basic mathematical model has been established, it is emphasized that peripheral modifications in the model with respect to what constitutes direct or indirect data inputs are expected based upon specific user requirements and precise model applications.

## SECTION 2

### MODEL DEVELOPMENT

#### BASIC FILTRATION RELATIONSHIPS

The classical filter drag-fabric loading relationships, which have been discussed extensively in the literature, need not be elaborated upon in this paper. Deposition of a uniformly distributed dust layer at constant inlet concentration and face velocity upon an unused or completely cleaned fabric leads to the characteristic relationship shown by the solid Curve 1, Figure 3. The origin for the curvilinear form of Curve 1 depicts the true residual drag,  $S_R$ , when the permanent residual loading,  $W_R$ , for a cleaned glass fabric is approximately 50 grams/M<sup>2</sup>. In most cases, however, linear extrapolation to the zero loading state is sufficient to specify the curve path and what is referred to as the "effective residual drag,"  $S_E$ . For many applications, there is no need to employ the curvilinear mathematics in the modeling process.

The linear expression

$$S = S_E + K_2 W \quad (1)$$

in which  $S$  is the resultant filter drag,  $S_E$  the effective residual drag,  $K_2$  the specific resistance coefficient for the dust, and  $W$  the fabric surface area dust loading in mass/unit area completely describes the drag properties for any element of the filter surface for which the dust loading is uniformly distributed and the local filtration velocity is known.

When a fabric bag is cleaned by bag collapse and reverse flow or by mechanical shaking, the dust sloughs off as flakes or slabs with the separation occurring at the dust/fabric interface where the adhesive bonds are weakest.<sup>4</sup> Figure 4 shows the appearance of a full scale glass bag (10 ft x 4 in.) in which a fluorescent light tube within the bag reveals clearly the cleaned (bright) areas and the uncleaned (dark) regions. Typical drag/loading curves for fabrics with varying fractions of their dust loading removed are represented by Curves 2 through 4, Figure 3.

#### PARALLEL FLOW CONCEPT

The varying slopes of the curves, Figure 3, have sometimes been incorrectly interpreted as signifying a dependency of  $K_2$  (the specific resistance coefficient for the dust) on the underlying fabric substrate. Except for very heavily napped surfaces, however, the reported variability in  $K_2$  can usually be attributed to (a) the partial cleaning effect indicated in Figure 3 or to massive

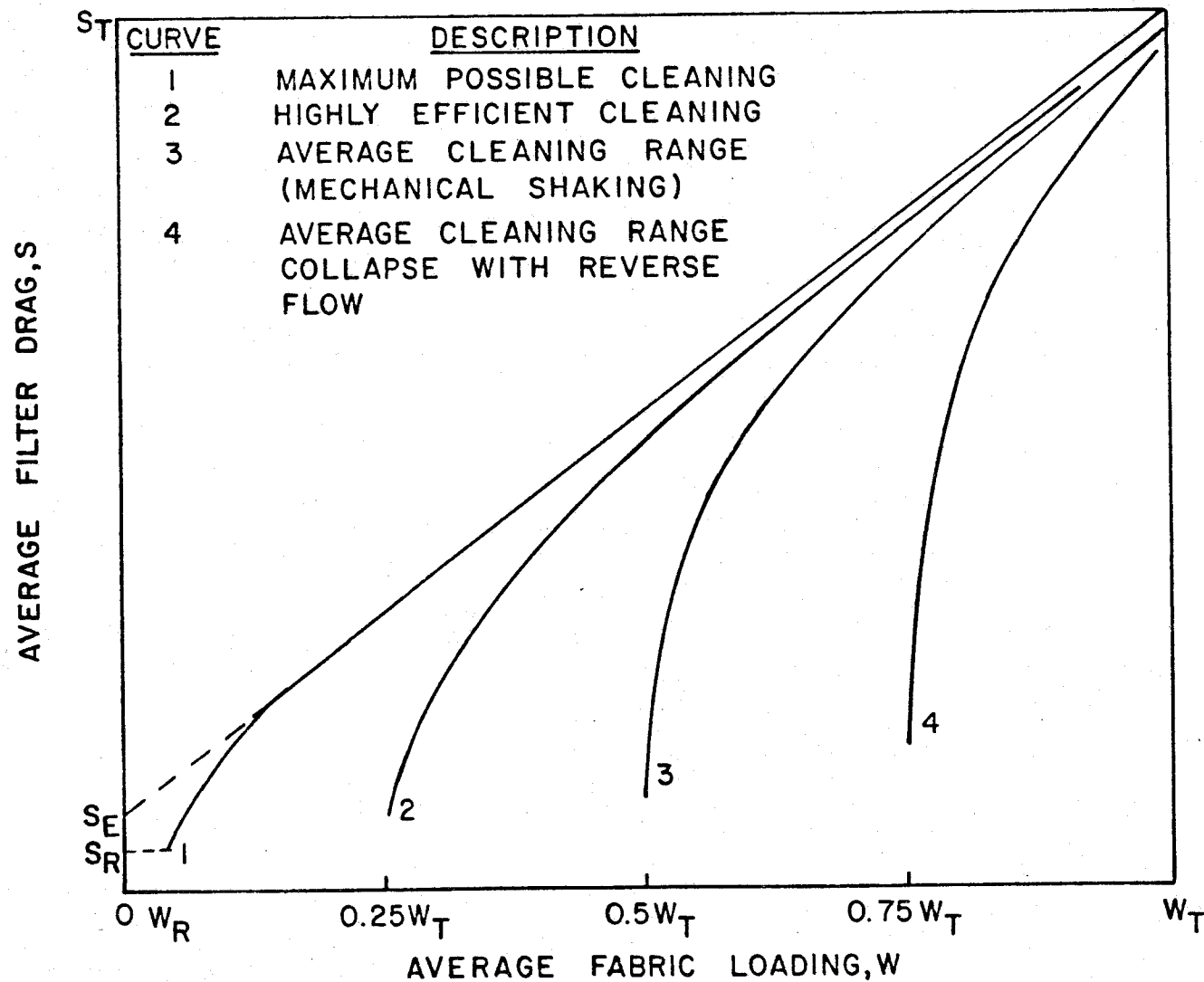


Figure 3. Typical drag versus loading curves for filters with different degrees of cleaning and a maximum allowable level for terminal drag,  $S_T$ , and terminal fabric loading,  $W_T$ .



Figure 4. Fly ash dislodgement from 10 ft x 4 in. woven glass bag (inside illumination).



pinhole leakage that may divert as much as 20 percent of the approaching gas flow through as little as < 0.1 percent of the filter face area.<sup>4</sup>

The path of these curves is governed by several parallel flow paths in which the approaching gas stream is apportioned according to the local drag values at any specified time for cleaned and uncleaned surfaces.<sup>3,4,9</sup>

$$S = \sum_{i=1}^n \left( \frac{A_c}{S_c} + \frac{A_{u1}}{S_{u1}} \cdot \cdot \cdot \frac{A_{un}}{S_{un}} \right)^{-1} A \quad (2)$$

In Equation (2), S and A refer to overall drag and filter area, respectively, i designates the i<sup>th</sup> fractional area and its associated properties, n is the total number of filter areas making up the whole surface, and the subscripts c and u refer to the cleaned and uncleaned filter areas.

The resulting pressure losses, P, after a time increase, Δt, for cleaned and uncleaned filter surfaces are equal and expressable by the following general relationship:

$$P_{t + \Delta t} = (S_E V)_{t + \Delta t} + (K_2 V W)_{t + \Delta t} \quad (3)$$

in which S<sub>E</sub> is the characteristic effective residual drag, V the instantaneous face velocity and W the total surface loading at the time t + Δt. Equations (2) and (3) form the building blocks for the iteration process from which the local and overall drag and resistance parameters may be estimated by computer for any time and/or average filter dust loading during a filtration cycle. Two critical parameters must be defined, however, before undertaking the modeling process.

#### SPECIFIC RESISTANCE COEFFICIENT (K<sub>2</sub>)

The first parameter is K<sub>2</sub>, which has been demonstrated in past and current studies to increase with the velocity of dust deposition, presumably due to increased dust layer compaction and hence lower cake porosity.<sup>3,4</sup> For many coal fly ash/woven glass fabric systems, K<sub>2</sub> values computed as shown below may be used in Equation (3):

$$K_2 = 1.8 V^{1/2} \quad (\text{Metric units})^* \quad (4)$$

For broader applications, however, Equation (4) is better expressed as

$$(K_2)_2 = (K_2)_1 (V_2/V_1)^{1/2} \quad (5)$$

when K<sub>2</sub> has been measured at a different velocity. Although several theoretical approaches have been proposed for the estimation of K<sub>2</sub> in terms of particle

---

\* V = face velocity, m/min. K<sub>2</sub> = specific resistance coefficient, N.min/g.m

and fluid parameters, the direct measurement of  $K_2$  is recommended. In the absence of direct measurements, a modified form of the Carman-Kozeny equation<sup>4</sup> provides a rough ( $\pm 25$  percent) estimate of  $K_2$ ; i.e.,

$$K_2 = 2.5\mu (S'_o)^2 (1-\epsilon)/\rho_p \epsilon^3 \quad (6)$$

where  $\mu$  is the gas viscosity,  $\epsilon$  the cake porosity,  $\rho_p$  the discrete particle density, and  $S'_o$  the specific surface parameter for the size distribution as a whole, i.e.

$$S'_o = \frac{\sum \text{particle surface area}}{\sum \text{particle volume}}$$

for any unit volume of dust cake. Although cake porosity is a measureable quantity, it should be noted that a 10 percent error in porosity estimation will lead to a 50 percent error in the porosity function  $(1-\epsilon)/\epsilon^3$ . Particle density measurements over the size spectrum of polydispersed dusts such as fly ash are also subject to error. Hence, there is a strong argument for direct measurement of  $K_2$  (and  $S_E$ ) whenever possible.

Use of the parallel flow concept involving Equations (2) and (3) for several partially cleaned fabrics indicated excellent agreement between observed and predicted drag values.<sup>4,5</sup> The modeling process used in Figure 5 is based on the fact that the cleaned area fraction,  $a_c$ , is always associated with a characteristic fabric drag,  $S_c$ .

#### FRACTION OF FILTER SURFACE CLEANED ( $a_c$ )

The fraction of the filtration surface cleaned by the cleaning process,  $a_c$ , must also be determined prior to the modeling effort. In the case of fabric cleaning by bag collapse and reverse flow, the amount of dust removed can be related to the fabric dust loading immediately before cleaning ( $W_T$ ), the characteristic residual dust loading for the cleaned region ( $W_R$ ) and the average filter dust loading after cleaning, ( $W_R'$ ).

$$a_c = 1 - \frac{W_R' - W_R}{W_T - W_R} \quad (7)$$

or

$$a_c = 1.51 \times 10^{-8} W_T^{2.52} = 1.51 \times 10^{-8} W_p^{2.52} \quad (8)$$

in which the fabric loading prior to cleaning,  $W_T$  or  $W_p$ , is expressed in grams/m<sup>2</sup>. Equation (7) can only be used to estimate  $a_c$  when the average filter dust holding after cleaning,  $W_R'$ , is known. Ordinarily, such data are obtainable only when special experimental testing procedures are employed. Hence, Equation (8) which depends upon the measureable or readily calculable  $W_p$  or  $W_T$  term, is chosen to compute the cleaned area fraction,  $a_c$ .<sup>4</sup>

The term  $W_p$  has the special significance of identifying the fabric loading associated with the fabric pressure loss just before initiating the cleaning

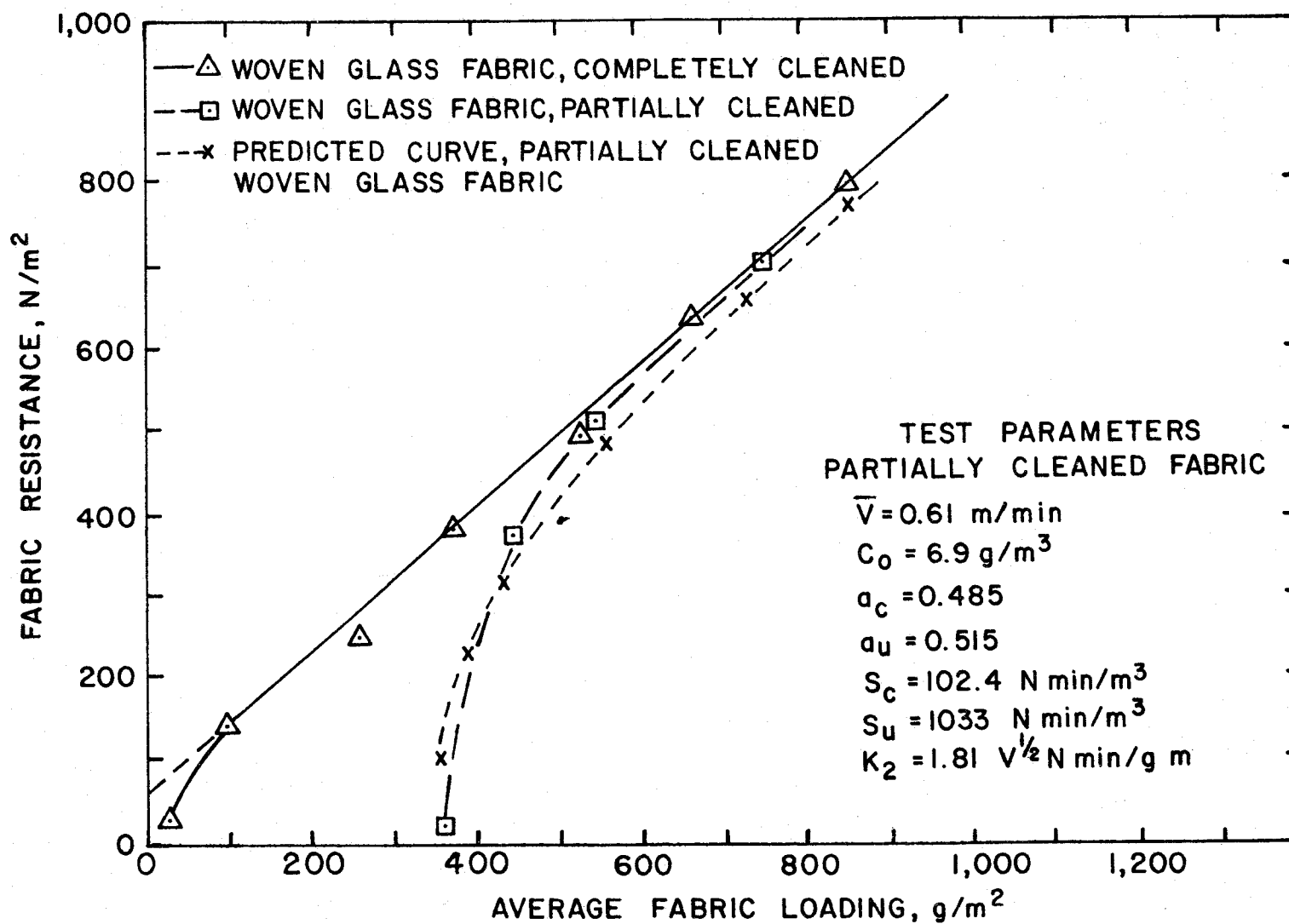


Figure 5. Fly ash filtration with completely and partially cleaned woven glass fabric (Menardi Southern)

action. In many systems,  $W_p$  represents the fabric dust loading corresponding to the preset pressure loss at which the filter cleaning cycle is to be activated.

#### DUST DISLODGE MENT AND ADHESIVE FORCES

Dust separation from any element of the filter surface is assumed to take place when the local separating force equals or exceeds the local adhesive force bonding the dust layer to the fabric surface. The dislodging force for bag collapse-reverse flow systems is that resulting from the tensile or shear stresses (assumed to be approximately the same) exerted by the local surface loading in mass per unit area,  $M_a$ , in a gravity field,  $g$ . If the system is cleaned by mechanical shaking, the acceleration,  $\bar{a}$ , imparted to the dust layer by the mechanical shaking action is substituted for the gravitational acceleration,<sup>4,6,10</sup>

$$\bar{a} = 0.75 \ 4 \ \pi^2 \ f^2 A \quad (9)$$

such that the dislodging force is now defined by the relation  $M_a \cdot \bar{a}$  rather than  $M_a \cdot g$ . In Equation (9),  $f$  refers to the shaking frequency and  $A$  to the amplitude (half-stroke) of the shaker arm motion (assumed to be essentially horizontal). After cleaning by the above mechanisms, the dust remaining on the filter is assumed to be held by an adhesive force in excess of the computed  $M_a \cdot \bar{a}$  or  $M_a \cdot g$  values.

The relationship between  $a_c$  and fabric loading shown in Figure 6 is also a measure of the distribution of adhesive forces over the fabric surface. The range of adhesive forces encountered exhibits a pattern similar to that displayed for particle to particle adhesive forces<sup>3,11,12</sup> while the average adhesive forces binding the cake to the fabric agree with those described by Zimon.<sup>13</sup> The cleaned area values reflect those to be expected after a fabric element has undergone successive flexings. Recent measurements have shown that a single cleaning by bag collapse and reverse flow removes about 67 percent of the dust separable by repeated cleanings at the same initial dust load level.<sup>4</sup>

#### DUST PENETRATION WITH WOVEN GLASS FABRICS

Extensive laboratory and field measurements coupled with a detailed analysis of the filtration process with conventional twill-weave glass fabrics have shown that coal fly ash emissions are due mainly to gas flow through the low resistance paths afforded by unblocked pores, pinholes or other lead regions in a filter.<sup>4,5</sup> Furthermore, because relatively few particles are removed from the gas fraction passing through the pores (nearly 100 percent penetration for diameters  $< 15 \mu m$ ), the particle size distributions are nearly the same for up- and downstream aerosols provided that size measurements are made in the immediate vicinity of the dirty and cleaned filter faces.<sup>1,4</sup>

The above factors suggest, therefore, that mass emissions from glass fabrics should depend in part upon (2) the inlet concentration and (b) the total remaining unblocked pore region at any time. The latter item, (b), is governed

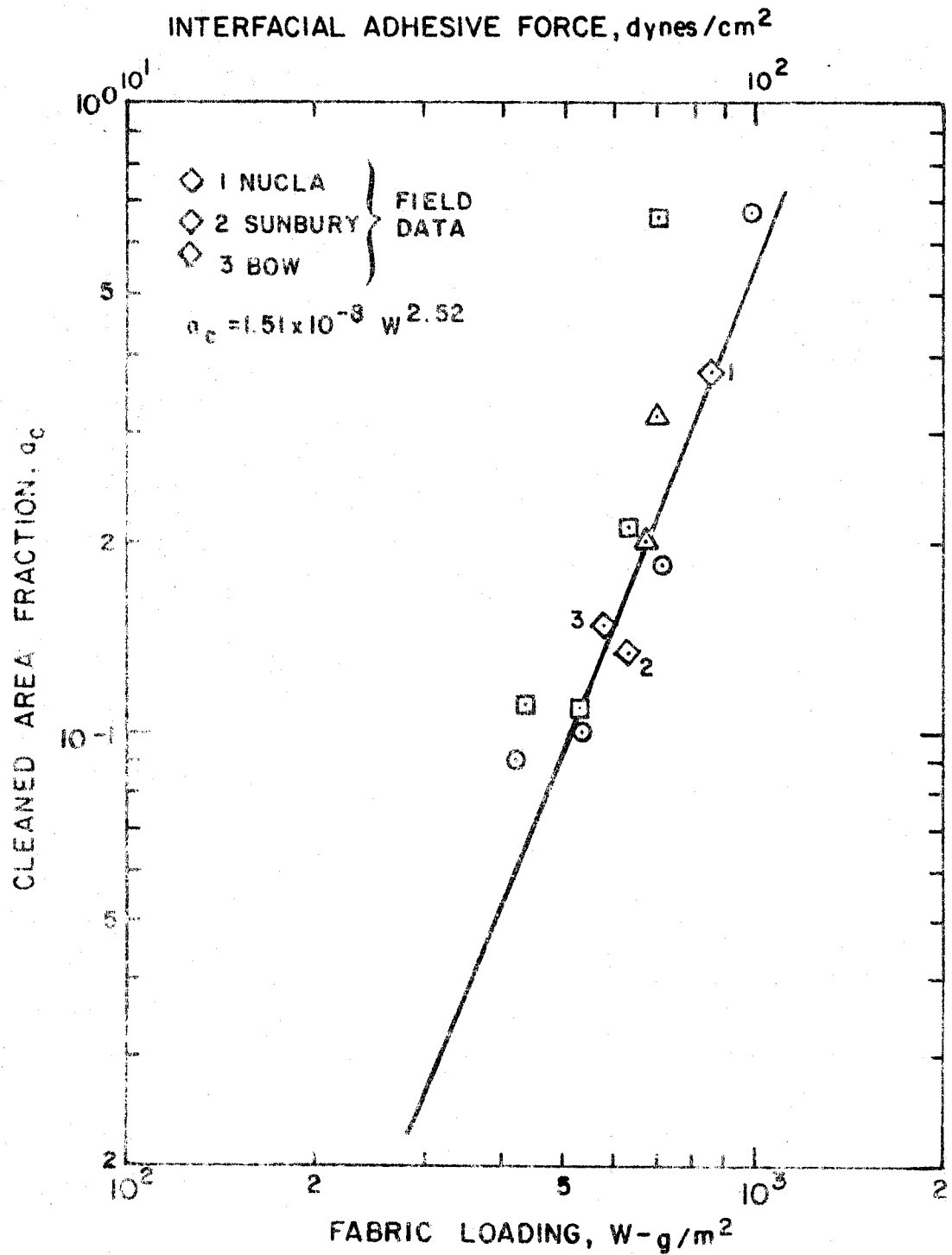


Figure 6. Relationship between cleaned area fraction and initial fabric loading. GCA fly ash and woven glass fabric

by the amount of dust deposited on the cleaned filter face following resumption of filtration. Given a glass fabric with no visible signs of weave imperfections and with a relatively uniform pore structure, the relationship between outlet concentration,  $C_o$ , and fabric dust loading,  $W$ , appears as shown in Figure 7 for an average filtration velocity of 0.61 m/min (2 ft/min). After fabric loadings increase to 60 to 80 grams/m<sup>2</sup>, however, the direct proportionality between inlet and outlet concentrations disappears because of a second contributor to outlet loading. The latter is the low level, essentially steady state, slough-off of agglomerated dust from the downstream region of the dust deposit as the result of aerodynamic reentrainment augmented by mechanically generated vibrations.<sup>4,7</sup> A conservative estimate of the magnitude of this source strength place it as less than a 0.5 mg/m<sup>3</sup> contributor,  $C_R$ , to the overall effluent loading.

Average face velocity has been shown to play a major role in determining filter effluent concentrations. Following deposition of about 60 to 80 gram/m<sup>2</sup>, Figure 8, steady state emissions are seen to increase from ~ 0.5 to 150 mg/m<sup>3</sup> over the face velocity range of 0.39 to 3.35 m/min (1.3 to 11 ft/min). This relationship indicates that seeking to reduce collector size by increasing the face velocity (air to cloth ratio) may lead to unacceptably high emission levels.

The solid line curves shown in Figure 8 represent the best mathematical fits to the indicated data points. The outlet concentration,  $C_o$ , is defined by the local penetration level ( $P_n$ ), the inlet dust concentration ( $C_i$ ), and the previously cited residual concentration,  $C_R = 0.5 \text{ mg/m}^3$ .

$$C_o = P_n C_i + C_R \quad (10)$$

The formal equation structures and the precise manner in which they are applied in the modeling process are presented in Reference 4. For present purposes, it suffices to point out that the following expression

$$P_n \text{ or } C_o \sim (\phi, C_i, W, V, C_R)$$

describes penetration or effluent concentration as a function of  $\phi$ , a parameter characterizing the dust/fabric combination under test; constant inlet and residual concentrations,  $C_i$  and  $C_R$ , respectively; and the time and position dependent variables; i.e., local face velocity,  $V$ , and local fabric dust loading,  $W$ .

The total (and average) filter system penetration,  $P_n$ , at some time,  $t$ , for a system consisting of  $I$  compartments and  $J$  areal subdivisions per bag is determined by successive iterations in accordance with the general summation

$$P_{n_t} = \frac{1}{V_t I J} \sum_{i=1}^I \sum_{j=1}^J P_{n_{ij_t}} V_{ij_t} \quad (11)$$

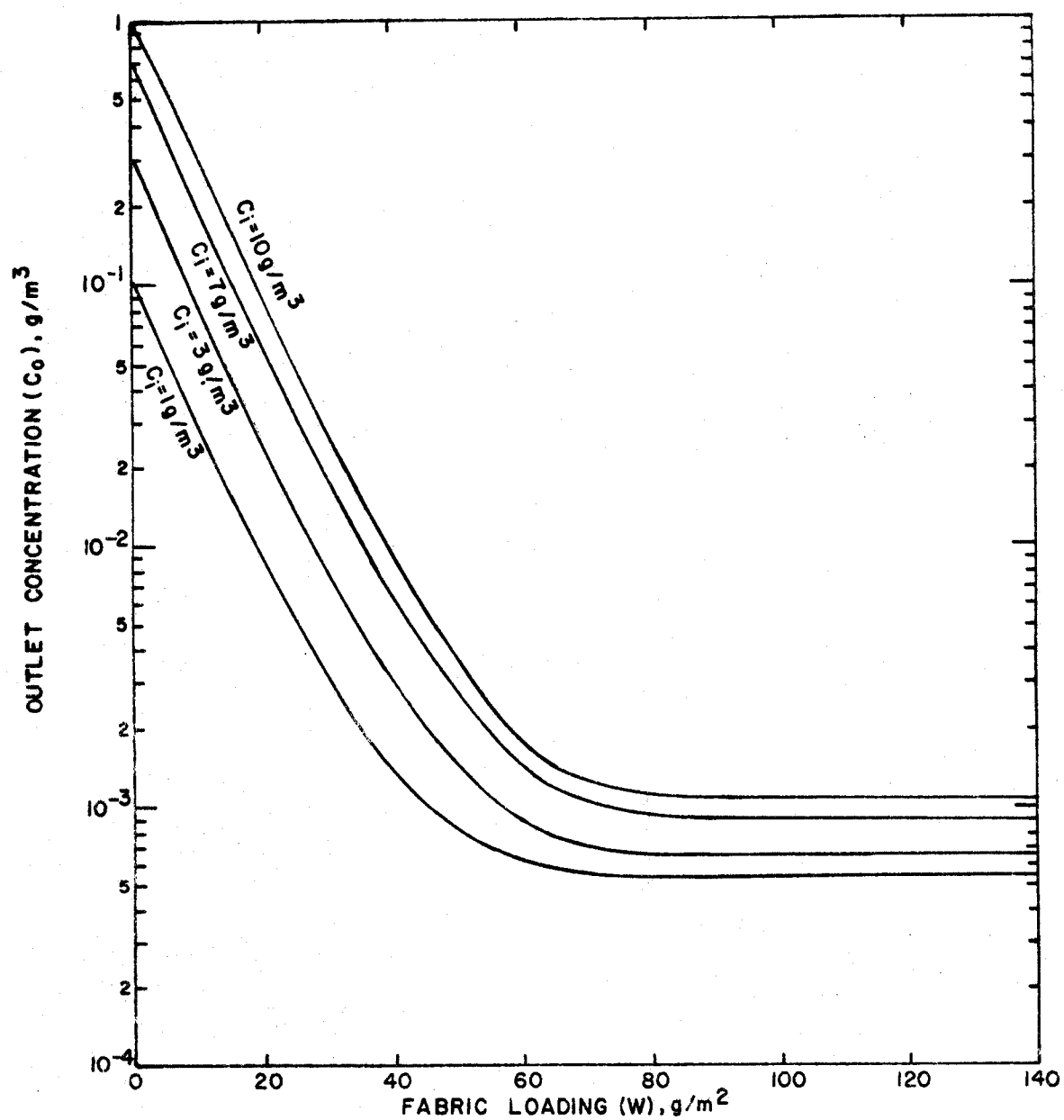


Figure 7. Effect of inlet concentration on predicted outlet concentrations at a face velocity of 0.61 m/min. GCA fly ash and Sunbury fabric.

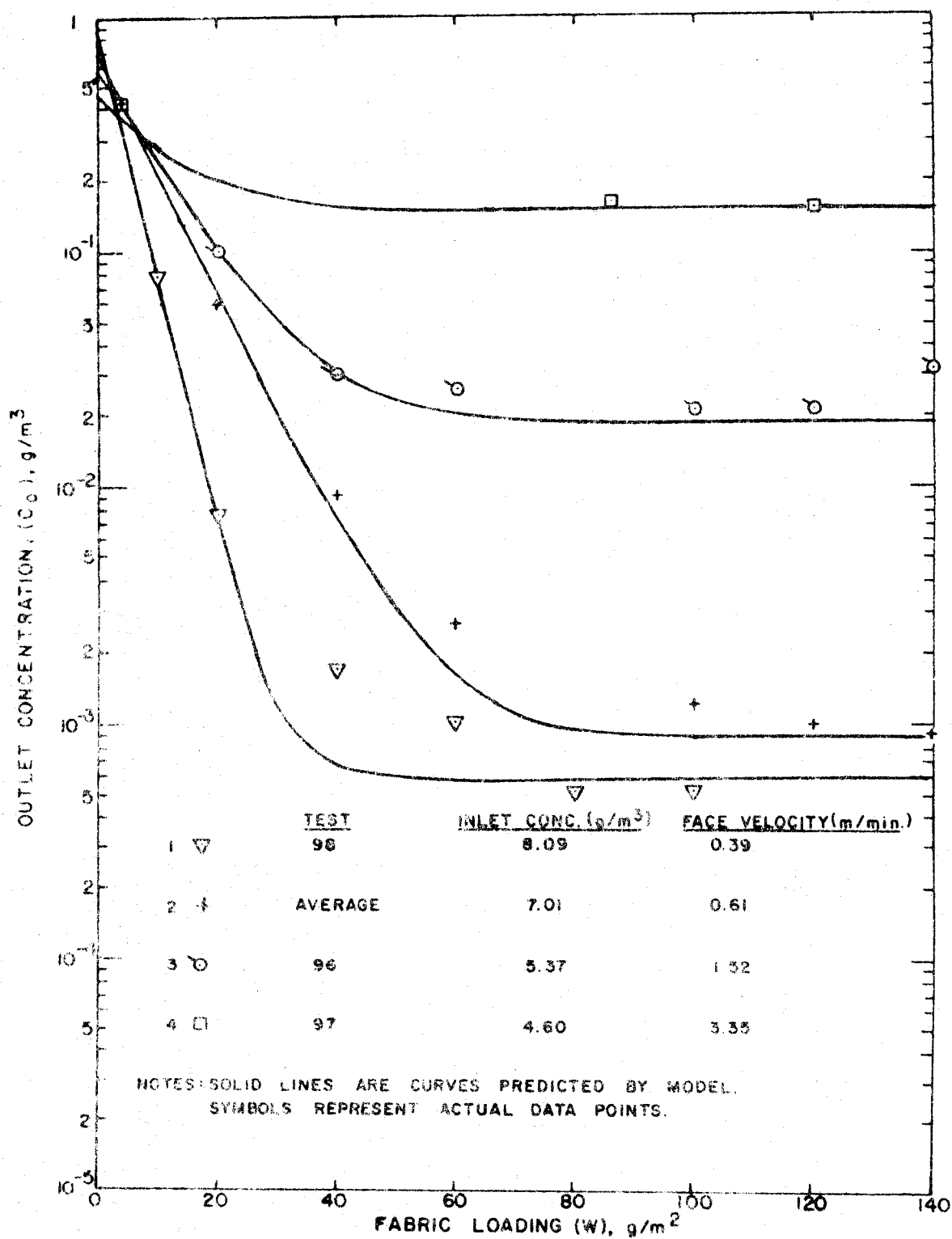


Figure 8. Predicted and observed outlet concentrations for bench scale tests. GCA fly ash and Sunbury fabric.



### SECTION 3

#### MODEL CAPABILITY

In the previous sections, the basic filtration equations and the iterative approach for treating multicompartment systems have been reviewed. The following discussion is intended to demonstrate how closely the predictive model describes the overall fly ash filtration processes for utility applications. The only major constraints for the model are that (1) the inlet aerosol should consist of or possess the general physical properties of a coal fly ash and (2) the fabric characteristics be similar to the woven glass media of the types used in the field. Within the above framework, the model is sufficiently flexible to meet the following criteria:

- The model is adaptable to either constant flow or constant pressure conditions.
- The model can accommodate to a continuous cleaning regimen; i.e., the immediate repetition of the cleaning cycle following the sequential cleaning of successive individual compartments, or
- The model can also describe the situation where lengthy filtration intervals are encountered between the cleaning cycles.
- The model can be used with collapse and reverse flow systems and mechanical shaking systems or combinations of the above. It is not intended for use with pulse jet or high velocity reverse jet cleaning systems.
- The model can be used equally well with pressure or time controlled cleaning cycles.
- The model provides estimates of average and point values of filter drag or resistance for the selected set of operating parameters and dust/fabric specifications.
- The model provides estimates of average and point values for penetration and mass effluent concentration for the selected set of operating parameters and dust/fabric specifications.

## SECTION 4

### MODEL APPLICATIONS

In Figure 9, a schematic flow diagram is shown for a filtration system in which the approaching aerosol is distributed among  $I$  separate compartments (each containing several bags) and  $J$  separate filtration regions on each bag. It is assumed for simplification that the performance of each compartment is represented by the behavior of any single bag within the compartment and that there are no concentration gradients in the approaching air stream. Consequently, the model must describe the integrated effect of many parallel flow paths through fabric surface elements bearing different dust loadings. The local performance of each element, resistance- and penetrationwise, is then defined by the equations presented in earlier sections of this paper.

An analysis of field measurements performed at the Nucla, Colorado Power Station<sup>2,4</sup> illustrates how the filtration model can be used to predict system performance characteristics. The data inputs required to model the filtration process are summarized in Table 1. Items 1 through 3 are based upon system design or operating data provided by the manufacturer. The 2-minute minimal time interval, Item 4, was chosen by the model user so that successive stepwise iterations would always indicate the maximum, minimum and average system resistance while any one compartment was off-line for cleaning.

Average face and average reverse flow velocities, Items 5 and 6, respectively, are operating parameters also selected by the filter manufacturer.

Inlet dust concentration and average filtration temperature, Items 7 and 8, are determined mainly by the combustion process and the type of fuel burned. The estimates of effective residual drag ( $S_E$ ), specific resistance coefficient ( $K_2$ ), and residual dust loading ( $W_R$ ) (Items 9, 10 and 11, respectively) are best determined by direct measurement if not already defined in the literature for the dust/fabric combination of interest.

With respect to the operating parameters set forth in Table 1, it was required that the system pressure loss just before fabric cleaning should not exceed a value of  $1160 \text{ N/m}^2$  (4.7 in. water), (Item 12). Given this constraint, the model has been used to determine the frequency of cleaning and the operating ranges for overall system pressure loss and effluent particulate concentrations. One key input parameter, i.e., the fraction of cleaned filtration surface,  $a_c$ , produced when a given compartment (or bag) is cleaned, is presently evaluated outside of the modeling program. The calculations are performed by first estimating  $W_p$  from the maximum allowable pressure,  $P_{\max}$ , by a rearrangement of Equation (1); i.e.,

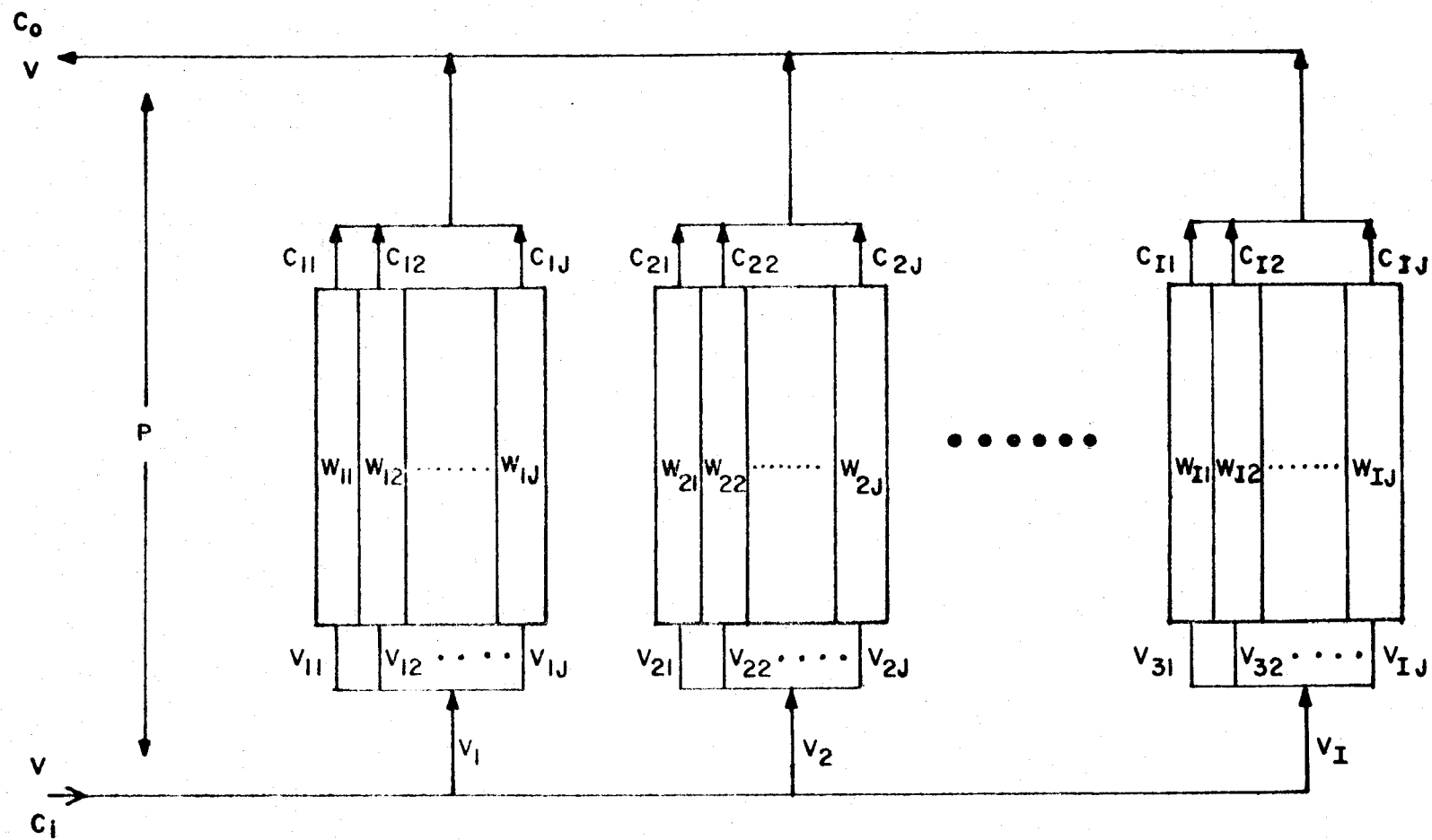


Figure 9. System breakdown for  $I$  bags and  $J$  areas per bag.

TABLE 1. REQUIRED DATA INPUTS FOR SPECIFIC MODEL APPLICATION\*

Item	Variable	Description	Comment
1	Number of compartments	6	System design parameter.
2	Complete cleaning cycle	24 minutes	Time to sequentially clean six compartments.
3	Cleaning time per compartment	4 minutes	Indicates total compartment off-line time.
4	Minimum time increment for iterative computations	2 minutes	Provides data points for maximum, minimum and average resistance and penetration during <u>off-line</u> period for <u>on-line</u> compartments.
5	Average face velocity (v)	0.824 m/min	Based on total flow and total fabric area.
6	Reverse flow velocity ( $V_R$ )	0.0415 m/min	Weighted average velocity over total (4 minutes) cleaning interval.
7	Inlet dust concentration ( $C_i$ )	2.6 g/m <sup>3</sup>	---
8	Temperature	412° K	Average baghouse temperature.
9	Effective (clean) fabric drag ( $S_E$ )	434 N min/m <sup>3</sup>	Based on linear extrapolation of drag versus fabric loading measurements with uniform dust deposit.
10	Specific resistance coefficient ( $K_2$ )	0.76 N min/g·m	Value determined at 0.61 m/min and 25°C.
11	Residual dust loading ( $W_R$ )	50 g/m <sup>2</sup>	Refers to surface loading on freshly <u>cleaned</u> areas only.
12	Cleaned fabric area fraction ( $a_c$ )	0.375	Fraction of <u>cleaned</u> surface exposed when cleaning is initiated with a fabric loading corresponding to a resistance of 1160 N/m <sup>2</sup>

\* Modeling of actual field performance of stoker-fired boilers at Nucla, Colorado, Colorado Ute Electric Association.<sup>2,4</sup>

$$W_P = \left( \frac{P_{\max}}{V} - S_E \right) / K_2 \quad (1a)$$

In Equation (1a),  $W_P$  is the unique (uniformly distributed) fabric loading associated with the maximum allowable pressure loss,  $P_{\max}$ .

The  $a_c$  value may then be computed as indicated below:

$$a_c = 1.51 \times 10^{-8} W_P^{2.52} \quad (8)$$

With the introduction of  $a_c$ , the program is ready to generate a tabular and/or graphical printout that can provide interim, individual compartment, and over-all system performance parameters.

Figure 10 shows the predicted and actual filter resistance characteristics versus operating time, the latter providing a direct measure of fabric dust loading when volume flow rate and inlet dust loading are constant. The good agreement between these curves suggests that the physical concepts used in the model development are a fair expression of the actual system operation. A comparison of selected reference points summarized in Table 2 also illustrates the degree of success attainable with the model.

Figure 11 predicts the changes in overall effluent concentrations that should be expected during periods of filter cleaning and during those periods when all compartments are on line. Although there are no field measurements available to confirm the short term, ~ minutes, predictions for the Nucla baghouse, the weighted average values derived from these curves, agree well with the corresponding field measurements.

TABLE 2. PREDICTED AND MEASURED RESISTANCE CHARACTERISTICS FOR NUCLA FILTER SYSTEM

	Actual		Predicted	
	N/m <sup>2</sup>	in. H <sub>2</sub> O	N/m <sup>2</sup>	in. H <sub>2</sub> O
Maximum resistance during cleaning	1700	6.8	1520	6.1
Initial resistance following cleaning	850	3.4	720	2.9
Maximum resistance just before cleaning*	1160	4.7	1160	4.7
Time between successive cleaning cycles	150 min		188 min	

\* Fixed value for predicted conditions.

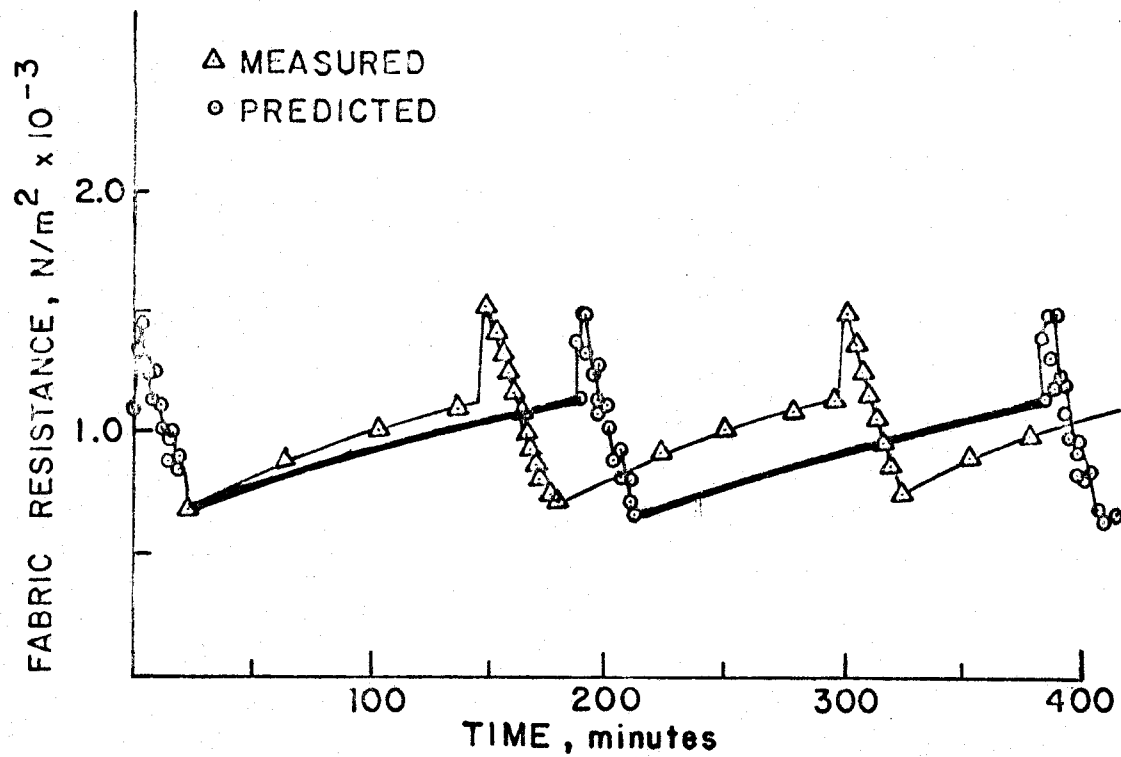


Figure 10. NUCLA baghouse simulation, resistance versus time.

# TEST RUN # 0422 NUCLA BAGHOUSE SIMULATION-LINEAR PENETRATION VS TIME GRAPH

96

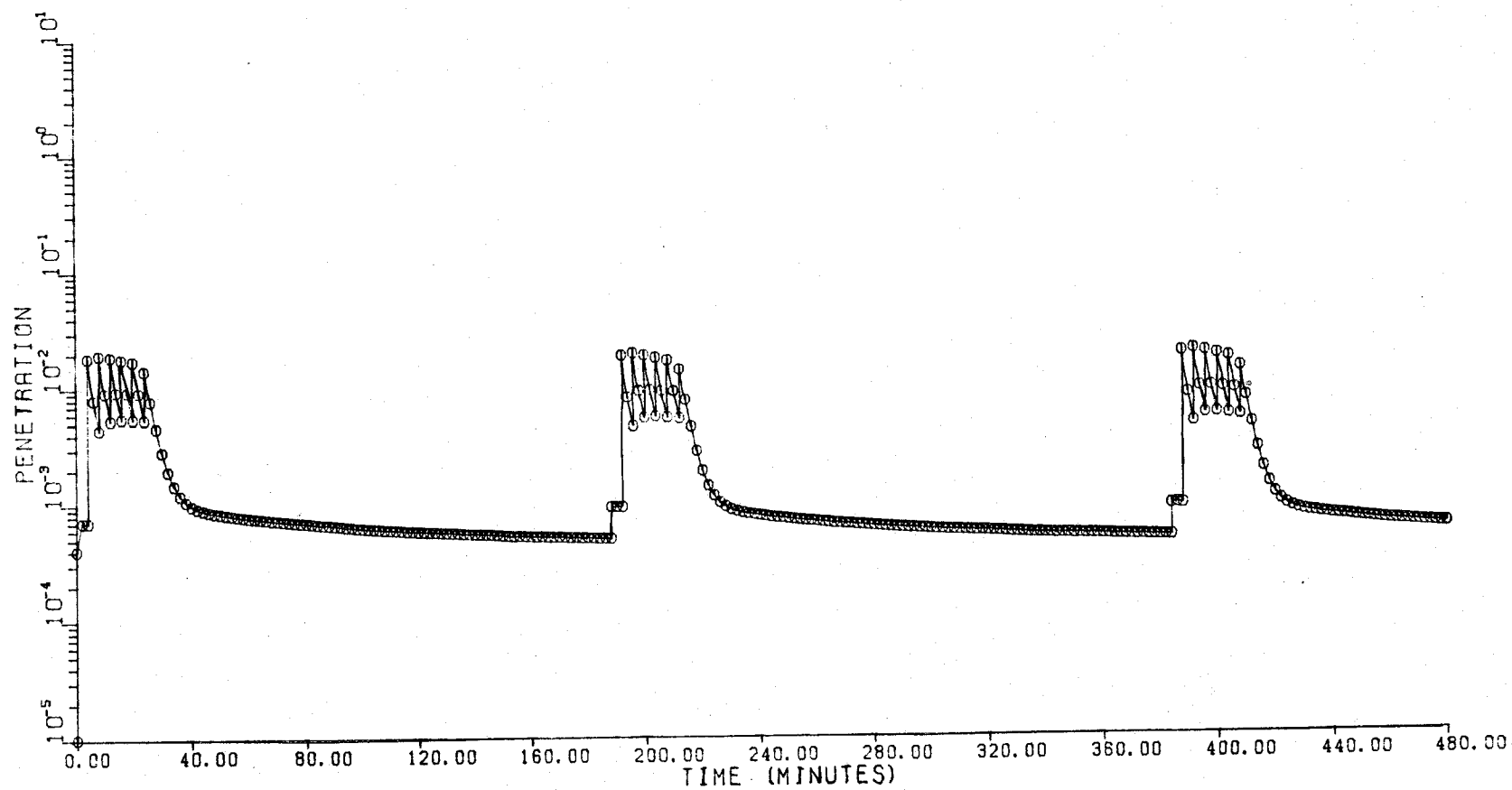


Figure 11. Test run No. 0422 Nucla baghouse simulation - linear penetration versus time graph.

Preliminary model validations were also conducted based upon a combination of field and laboratory tests relating to the fabric filtration equipment at the Sunbury Station of the Pennsylvania Power and Light Company<sup>1,4</sup>. The results for both Sunbury and Nucla modeling operations are compared with actual test observations in Table 3. In view of the early development stage of the model, the overall agreement between actual and predicted values is considered to be highly satisfactory.

The differences between observed and predicted values are attributed to a combination of factors including simplifications in the modeling mathematics and uncertainties in some data inputs. Improvements in model reliability are expected to result from a sensitivity analysis now in progress and the conduct of further field and laboratory measurements.

In the preceeding discussions, the reportings on model structure and its applications represent but a small part of a very extensive study.<sup>4</sup> Although only the linear model is described here, the computer program is also written to accept the condition where use of the true residual drag,  $S_R$ , and a curvilinear drag/fabric loading relationship may afford better estimates of filter system performance. The detailed studies also indicate several techniques whereby the key data inputs can be adjusted to satisfy a broad range of operating conditions.



TABLE 3. MEASURED AND PREDICTED VALUES FOR FILTER SYSTEM PENETRATION AND RESISTANCE, COAL FLY ASH FILTRATION WITH WOVEN GLASS FABRICS

Penetration						
Data source		Testing period	Bag service life	Percent penetration		
Test case	Description			Measured*	Predicted	
				Average†	Linear model Average	Cleaning‡
A	Nucla, Colo.	9/21/74	6 months	0.21	0.19	1.52
B	Sunbury, PA	1/08/75	2 years	0.06	0.20	-
C	Sunbury, PA	3/20/75 to 3/22/75	1.5 days	0.15	0.20	-

Resistance								
Test case	Measured				Predicted			
	Average	Maximum cleaning	Maximum	Minimum	Linear model			
					Average	Maximum cleaning	Maximum	Minimum
A	1030	1700	1160 <sup>§</sup>	850 <sup>§</sup>	972	1521	1160 <sup>§</sup>	720 <sup>§</sup>
B	635	710	710 <sup>#</sup>	560 <sup>#</sup>	620	663	663 <sup>#</sup>	567 <sup>#</sup>

\* Based on field measurements. See References 1 and 2.

† All values listed as average depict overall system performance (penetration and resistance) for combined cleaning and filtering cycles.

‡ All values listed under cleaning describe performance parameter during cleaning only.

<sup>§</sup> Maximum-minimum with Nucla tests indicate resistance immediately before and after cleaning.

<sup>#</sup> Maximum-minimum with Sunbury tests indicate values for envelope curve.

## SECTION 5

### SUMMARY

The mathematical model described here represents a new and very effective technique for predicting average and instantaneous resistance and emission characteristics during the filtration of coal fly ash with woven glass fabrics.

Two basic concepts used in the model design, (1) the quantitative description of the filtration properties of partially cleaned fabric surfaces and (2) the correct description of effluent particle size properties for fabrics in which direct pore or pinhole penetration constitutes the major source of emissions, have played important roles in structuring the predictive equations.

A third factor in the model development was the formulation of explicit functions to describe quantitatively the cleaning process in terms of the method, intensity and frequency of cleaning. By cleaning we refer specifically to the amount of dust removed during the cleaning of any one compartment and the effect of its removal on filter resistance and penetration characteristics.

The success of the model, based upon limited applications to field data, suggests strongly that it be further evaluated. Minor changes in existing compliance type sampling methods and apparatus should provide the key data for resistance/fabric loading relationships that are fundamental to the application of the model. Additionally, such measurements should help to confirm the present observation that electrical charge and/or humidity factors do not appear to play an important role in fly ash filtration with glass fabrics. Application of the concepts presented here and in Reference 4 to other dust/fabric combinations should provide a rational basis for treating heretofore unresolved problems in many field filtration applications.

1. Cass, R.W., and R.M. Bradway. Fractional Efficiency of a Utility Boiler Baghouse: Sunbury Steam-Electric Station. GCA/Technology Division, Bedford, Massachusetts. Control Systems Laboratory, U.S. Environmental Protection Agency, Research Triangle Park, N.C. Report No. EPA-600/2-76-077a (NTIS No. PB253-943/AS). March 1976.
2. Bradway, R.M., and R.W. Cass. Fractional Efficiency of a Utility Boiler Baghouse - Nucla Generating Plant. GCA/Technology Division, Bedford, Mass. Control Systems Laboratory, U.S. Environmental Protection Agency, Research Triangle Park, N.C. Report No. EPA-600/12-75-013a (NTIS No. PB246-641/AS). August 1975.
3. Billings, C.E., and J.E. Wilder. Handbook of Fabric Filter Technology, Volume I, Fabric Filter Systems Study: GCA/Technology Division. EPA No. APTD 0690 (NTIS No. PB-200-648). December 1970.
4. Dennis, R., et al. Filtration Model for Coal Fly Ash with Glass Fabrics. Industrial Environmental Research Laboratory, U.S. Environmental Protection Agency, Research Triangle Park, N.C. Report No. EPA-600/7-77-084. August 1977.
5. Dennis, R., R.W. Cass, and R.R. Hall. Dust Dislodgement from Woven Fabrics Versus Filter Performance. APCA Paper 77-32.3. Presented at the 70th APCA Annual Meeting, Toronto, Ontario, Canada. June 20-24, 1977.
6. Dennis, R., and J.E. Wilder. Fabric Filter Cleaning Studies. GCA/Technology Division, Bedford, Mass. Control Systems Laboratory, Research Triangle Park, N.C. Report No. EPA-650/2-75-009. January 1975.
7. Leith, D., and M.W. First. Particle Collection by Pulse-Jet Fabric Filter. Presented at 68th Annual APCA Meeting, Boston. 1975.
8. Ensor, D.S., R.G. Hooper, and R.W. Scheck. Determination of the Fractional Efficiency, Opacity Characteristics, and Engineering Aspects of a Fabric Filter Operating on a Utility Boiler. Final Report. Meteorology Research Inc., Altadena, California. EPRI-FP-297. November 1976.
9. Robinson, J.W., R.E. Harrington, and P.W. Spaite. A New Method for Analysis of Multicompartment Fabric Filtration. Atmos Environ. 1:499-508, 1967.
10. Walsh, G.W., and P.W. Spaite. An Analysis of Mechanical Shaking in Air Filtration. J Air Pollut Control Assoc. 12:57, 1962.
11. Löffler, F. Investigating Adhesive Forces Between Solid Particles and Fiber Surfaces. Staub (English Translation). 26:10. June 1966.
12. Corn, M. The Adhesion of Solid Particles to Solid Surface. A Review, J Air Pollut Control Assoc. 11:523, 1961.
13. Zimon, A.D. Adhesion of Dust and Powder. Plenum Press, New York, 1969. p. 112.

A PILOT PLANT STUDY OF VARIOUS FILTER MEDIA  
APPLIED TO A REFUSE BOILER

By  
JOHN C. MYCOCK

Paper Presented At  
Fabric Filter Symposium  
Tucson, Arizona  
December 5, 1977

Sponsored By  
Federal Environmental Protection Agency  
Industrial Environmental Research Laboratory

### Acknowledgements

This program was sponsored by the Federal Environmental Protection Agency with Nashville Thermal Transfer as the prime contractor and Enviro-Systems and Research, Inc. as the major subcontractor.

The author wishes to acknowledge the vital role played by each of the participants.

This project has been funded at least in part with Federal funds from the Environmental Protection Agency under Contract Number R80-4223. (1) The content of this publication does not necessarily reflect the views or policies of the U.S. Environmental Protection Agency, nor does mention of trade names, commercial products or organizations imply endorsement by the U.S. Government.

### Abstract

A pilot scale investigation was conducted to determine the techno-economic feasibility of applying fabric filter dust collectors to solid refuse-fired boilers. The pilot facility, installed on a slip stream of a 135,000 lb/hr. boiler, was sized to handle a 9,000 ACFM at an air-to-cloth ratio of 6 to 1. Filter media evaluated included PTFE laminate on a woven backing, woven glass and felted glass.

Overall efficiencies greater than 99.8% were achieved with all three types of filter media tested when operating at air-to-cloth ratios of 6 to 1 or less and having an inlet loading of 0.5 gr/DSCF. For the brief exposure period encountered during the performance testing, all three of the bag materials tested indicated no wear problems.

The pressure drops obtained for the three filter media were within the commercially acceptable range.

The installed, operating and annualized costs for fabric filters were developed and compared with the economics of wet scrubbing and electrostatic precipitation. This analysis indicated that the annualized costs of the electrostatic precipitator and the fabric filter are very close.

In June 1976, an EPA sponsored pilot scale investigation was initiated. The purpose of the study was to determine the techno-economic feasibility of applying fabric filter dust collectors to a refuse-fired boiler. Included in the program was the screening of a variety of filter media. These included Gore-Tex (a PTFE laminate on a PTFE woven backing), supplied by W.L. Gore and Associates, Inc., a woven glass bag (22½ oz. with Q78 finish), supplied by Globe Albany Filtration and an experimental needled felt glass bag supplied by the Huyck Corporation.

The test program was conducted on an existing fabric filter (baghouse) system that is presently installed on the slip stream of a refuse boiler owned and operated by the Nashville Thermal Transfer Corporation (NTTC), a public authority of the State of Tennessee. By burning approximately 25% of the city's daily output of refuse, this plant can supply steam and chilled water to a number of downtown buildings, including the State Capitol.

An experimental program was conducted by NTTC in 1975 for the purpose of establishing methods of controlling pollution from refuse-fired boilers. Enviro-Systems & Research was selected to participate in this program and provided NTTC with a two (2) module Enviro-Clean RA-1 rectangular dust collector to be used as a vehicle for filter media screening. A second baghouse, an Ess Tee pulse jet type was also tested. Only a very preliminary screening of filter media was included in this original program which was terminated due to monetary considerations, but data obtained indicated that a fabric filter dust collector was capable of achieving excellent dust collection efficiencies; therefore the EPA funded program was instituted to confirm and validate this data.

The Enviro-Systems & Research baghouse is designed to contain a total of 1660 square feet of cloth. The house is subdivided into twelve (12) separate cells, each cell having twelve (12) bags.

The operation of the baghouse is as follows: the dirty gases enter one end of the unit, pass through the tapered duct, into the classifier, then through the bags. The classifier forces the dirty gases to change direction 90°, then 180°. This quick directional change forces the larger and heavier

particles out of the flow so that they will fall directly into the hopper. Dirty gases enter the classifier through a central duct tapered to feed the same quantity of gas into each cell. The gases are forced through the fabric filter into the center of the bags. The cleaned gases are drawn up and out through the center of the filtering bag into a center exit plenum via an open damper in the cell above the tube sheet (to which the bags are locked on top and bottom via snap rings).

As solid matter collects on the outside of the filter bag, it builds a cake or crust which begins to restrict the flow of gases. The bags are cleaned one cell at a time by closing off the cell damper. Clean air enters through the damper, is forced down the filter bag (opposite the normal flow direction), and expands the bag with such a shock that the "cake" is cracked and particulate matter falls off the bag and into the hopper. Damper systems and control panel arrangements allow for variations in main gas volume, reverse air volume, duration of cleaning and frequency of cleaning.

The pilot plant was originally installed on one of the NTTC boilers in September 1975. The slip stream is a 16 inch duct approximately 250 feet long with numerous turns. This duct is covered with 1½ inch metal-skinned insulation to decrease heat loss. The outlet and reverse air duct were also insulated. A temperature profile (Figure 2) shows a maximum temperature of 350° F in the inlet duct while the maximum at the outlet was 180° F. Figure 3 is a photograph of the plant.

An inlet profile was obtained at the beginning of the ES&R program and again during the testing of the needled glass fabric. Tables 1 and 2 list these results. Although chloride and flouride concentrations could result in increased bag deterioration, we found no evidence of this during the program.

Rigorous sampling indicated that changes in the inlet loading had no significant effect on outlet loading. Therefore, an average inlet concentration was calculated from data obtained during concentrated testing efforts in March of 1977 and used as the basis for all total mass and fractional efficiencies.



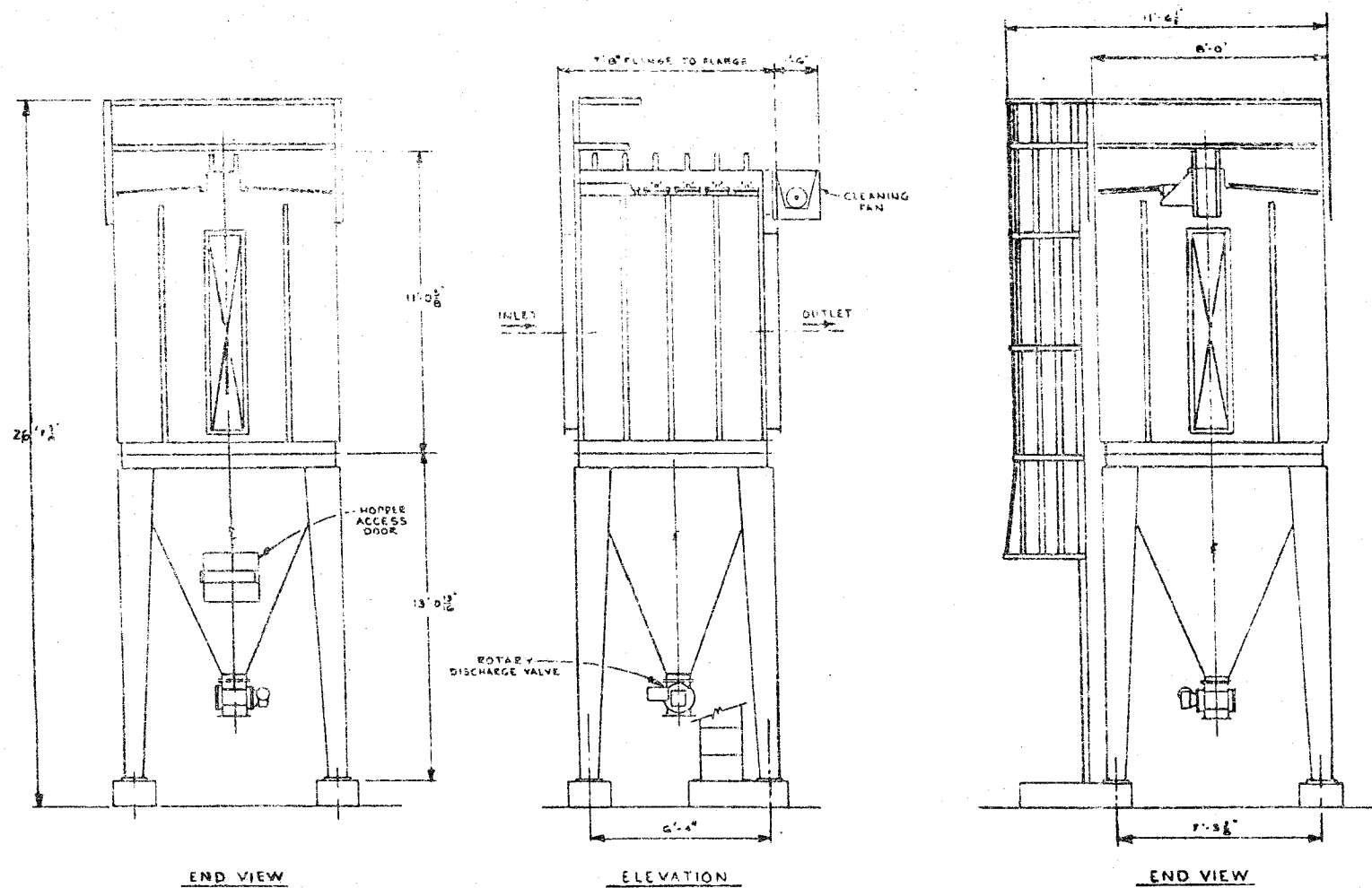


Figure 1

Schematic Diagram of the Enviro-Clean RA-1 Dust Collector Model 144-RA1-5-104

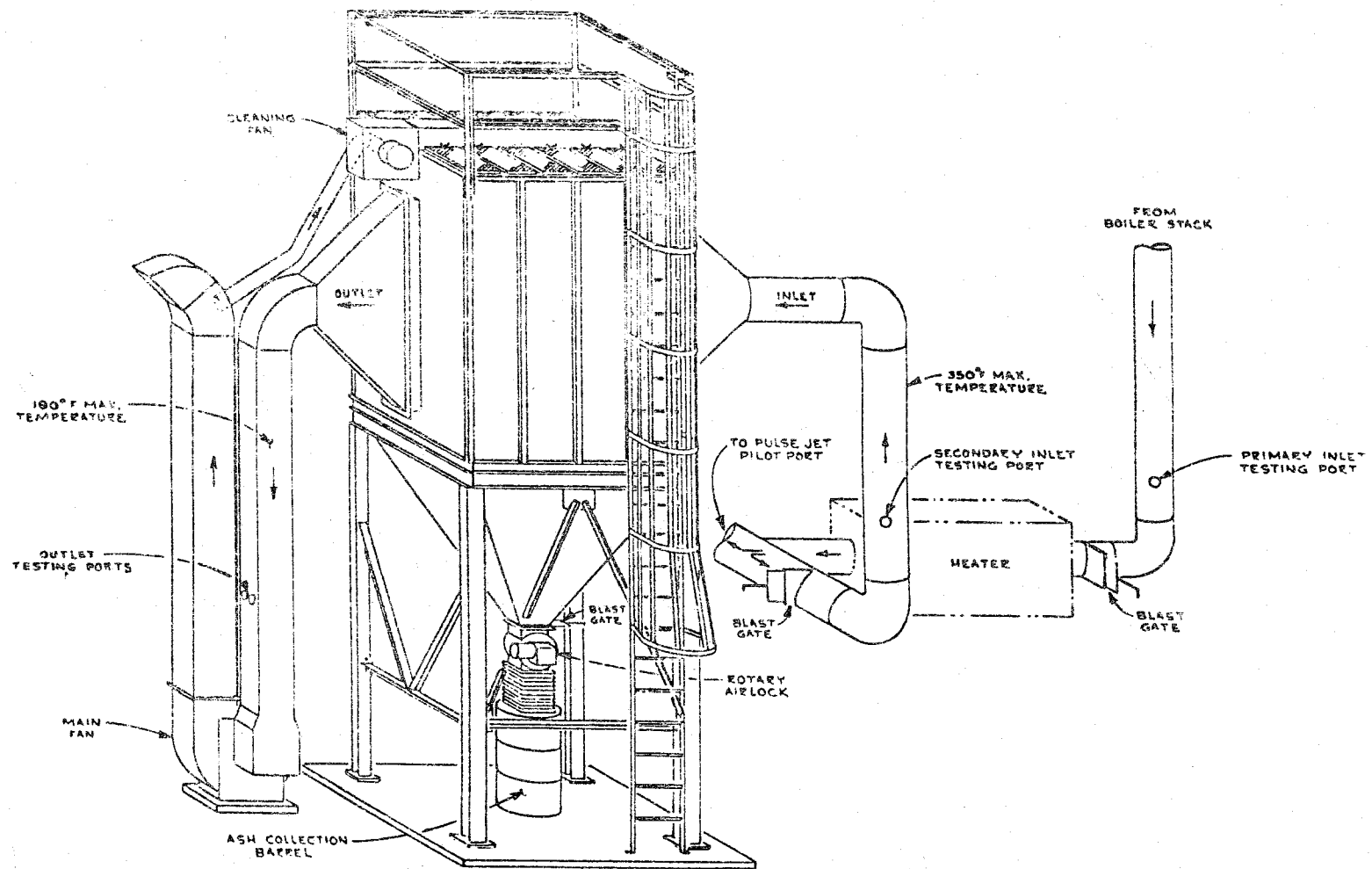


Figure 2

Temperature Profile for the Enviro-Systems Baghouse

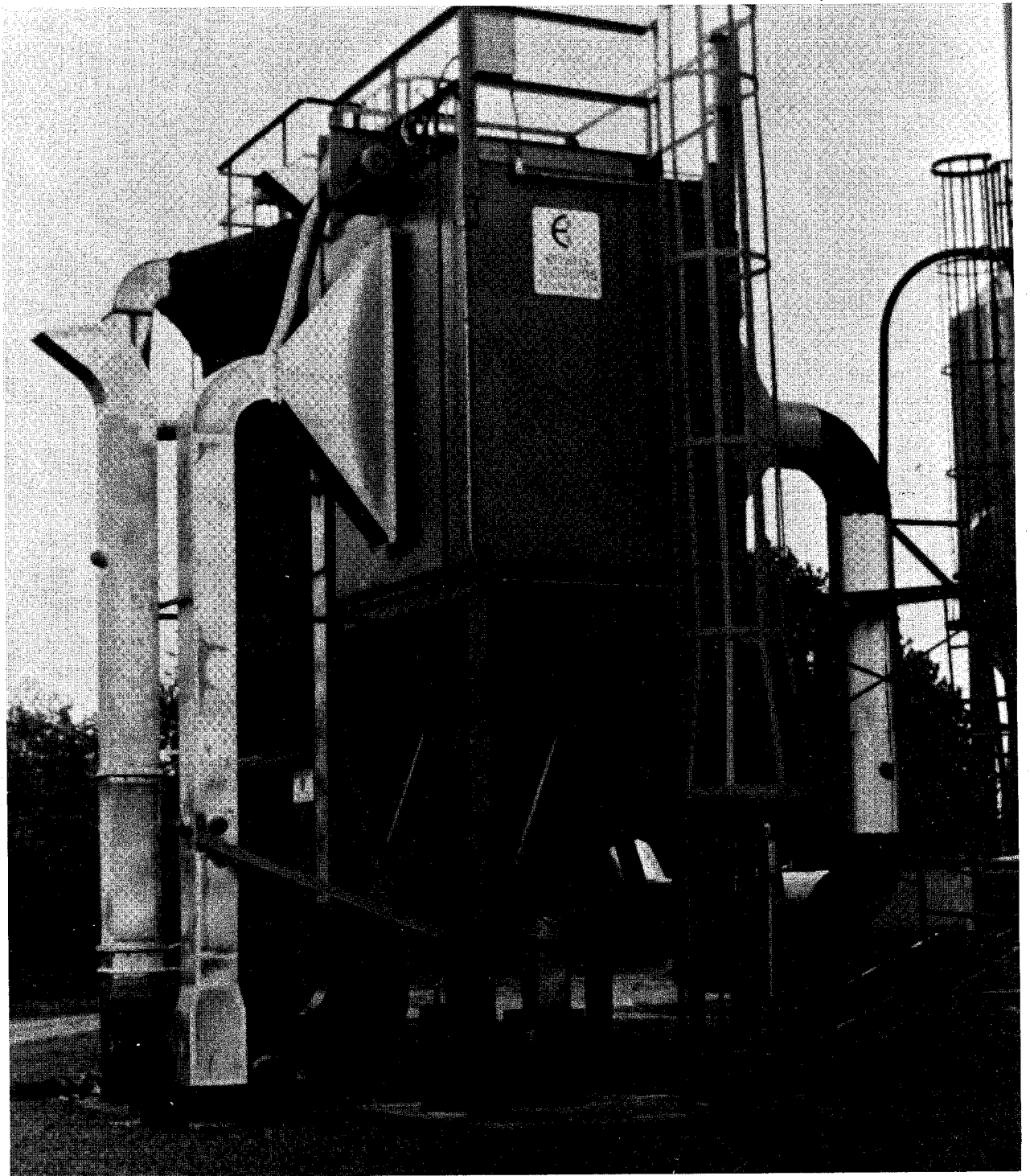


Figure 3. Fabric Filter Pilot Plant Installed at Nashville Thermal Transfer Corp.

TABLE 1  
NASHVILLE THERMAL TRANSFER  
Baghouse Inlet Gas Stream Profile

<u>Test Data</u>	<u>1</u>	<u>Run Number</u> <u>2</u>	<u>3</u>
Date	7/29/76	7/30/76	7/30/76
Gas Temperature (avg. °F)	411	443	410
Stack Rate (SCFMD)	1583	1581	1520
Flue Gas Composition			
H <sub>2</sub> O (%)	15.94	16.03	18.68
O <sub>2</sub> (%)	7.1	7.1	7.1
CO (%)	-	-	-
CO <sub>2</sub> (%)	12.9	12.9	12.9
Particulate Concentration (Grains/SCFD)	0.72	1.38	1.76
Isokinetic Rate (%)	109.16	109.3	94.3
Cl (ppm)	84.1	83.7	68.04
F (ppm)	7.09	0.8	0.61

TABLE 2  
INLET EMISSION PROFILE

Date	11/20/76
Stack Temp. (Avg. °F)	360°F
Stack Rate (SCFMD)	2252.2
Stack Rate (ACFM)	3826.6
Flue Gas Composition	
H <sub>2</sub> O (%)	7%
O <sub>2</sub> (%)	10.88 %
CO <sub>2</sub> (%)	7.25 %
Metered Gas Volume (SCFD)	21.90
Particulate Concentration (Grains/SCFD)	1.1634
Emission Rates (lb/Hr)	22.46
Isokinetic Rate (%)	101.2%
F (ppm)	0.2

Figure 4 shows the average inlet particle size distribution.

#### Needled Glass Felt

Outlet particulate concentrations obtained when varying the apparent velocity or more commonly - the air-to-cloth ratio (A/C ratio) for the glass felt are provided in Table 3. As is evident in this table, the needled glass felt proved to be an extremely efficient filter media for this application at all A/C ratios studied.

Outlet particle size distribution for air-to-cloth ratios of 3.2, 6.4 and 8.7 to 1 is graphically displayed in Figure 5. In ascending order, the percentages of fabric penetration of particles less than three (3) microns are 50%, 41% and 34% respectively.

#### Woven Glass

The woven glass bags were employed at air-to-cloth ratios of 2.75, 4.2 and 6.7. Figure 6 shows the particle size distribution for the A/C ratios. The curves also indicate that as the air-to-cloth ratio is increased, the percentage of sub-micron particles (when compared to total emissions) also increases.

Average outlet concentrations and relative cumulative percentages are shown in Table 4. Although not quite as efficient as the other fabrics tested, woven glass proved more than satisfactory to meet present code requirements.

#### PTFE Laminate

The PTFE laminate was employed at air-to-cloth ratios of 4.2, 5.4 and 6.0 and once again the outlet particulate concentrations and particle size distributions were determined. Particle size data is shown in Figure 7. For the lowest air-to-cloth ratio the penetration of sub-micron particles is 41% of total particulate penetration. Outlet concentration and cumulative percentages are listed in Table 5. While there seems to be no clear correlation between filtration velocity and outlet dust concentration, it is

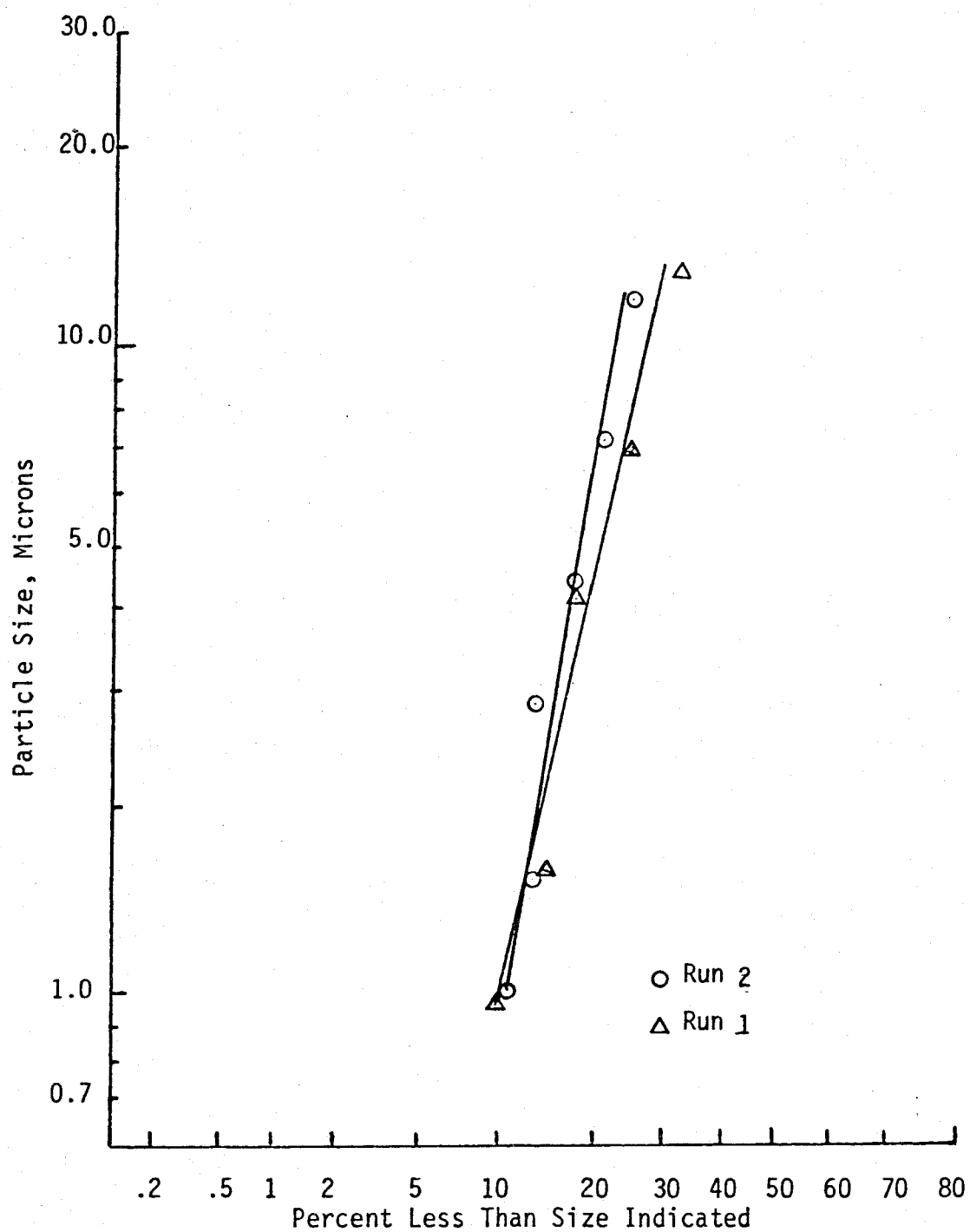


Figure 4

Inlet Particle Size Distribution for Two  
Brinks Impactor Runs  
(3/33/77)

TABLE 3  
OUTLET CONCENTRATION AND CUMULATIVE %

<u>Air-to-Cloth 3.2/1</u>			<u>Huyck Bags</u> <u>Air-to-Cloth 6.4/1</u>			<u>Air-to-cloth 8.7/1</u>		
Avg. (1) Part. Diam. <u>Microns</u>	Avg. (2) Outlet Conc. <u>gr/SCFD</u>	<u>Cum % (3)</u>	Avg. Part. Diam. <u>Microns</u>	Avg. Outlet Conc. <u>gr/SCFD</u>	<u>Cum %</u>	Avg. Part. Diam. <u>Microns</u>	Avg. Outlet Conc. <u>gr/SCFD</u>	<u>Cum %</u>
9.33	.0001834	100.00%	9.33	.0001770	100.00%	9.33	.0005394	100.00%
6.23	.0000657	68.04	6.23	.0000502	59.02	6.23	.0002472	63.31
4.20	.0000391	56.6	4.20	.0000592	47.43	4.20	.0002162	46.49
2.77	.0000459	49.79	2.77	.0000207	33.76	2.77	.0001229	31.78
1.33	.0000744	41.8	1.33	.0000154	28.99	1.33	.0000849	23.42
0.80	.0000286	28.85	0.80	.0000302	25.54	0.80	.0000697	17.64
0.57	.0000434	23.87	0.57	.0000155	18.57	0.57	.0000338	12.9
0.30	.0000455	16.31	0.30	.0000156	15.0	0.30	.0000485	10.6
0.30	<u>.0000482</u>	8.39	0.30	<u>.0000494</u>	11.40	0.30	<u>.0001073</u>	7.30
TOTAL	.0005742		TOTAL	.0004332		TOTAL	.0014699	

(1) Corrected for Stack Temperature

(2) gr/SCFD - Grains Per Standard Cubic Foot Dry (Standard - 70°F, 29.92" Hg)

(3) Percent of Total Outlet Concentration Less Than Size Indicated



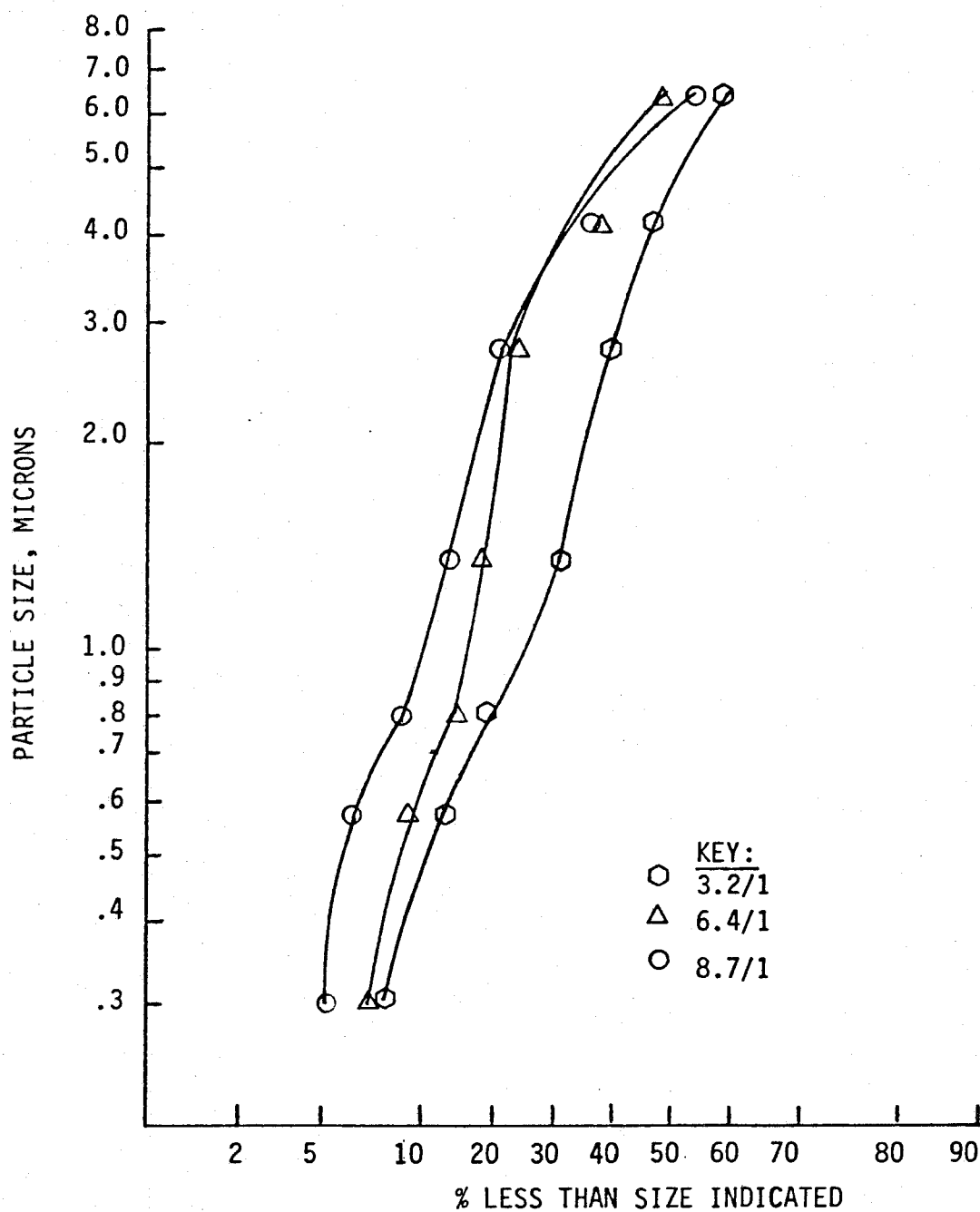


Figure 5  
Outlet Particle Size Distribution  
(Huyck Experimental Bags - April 1977)

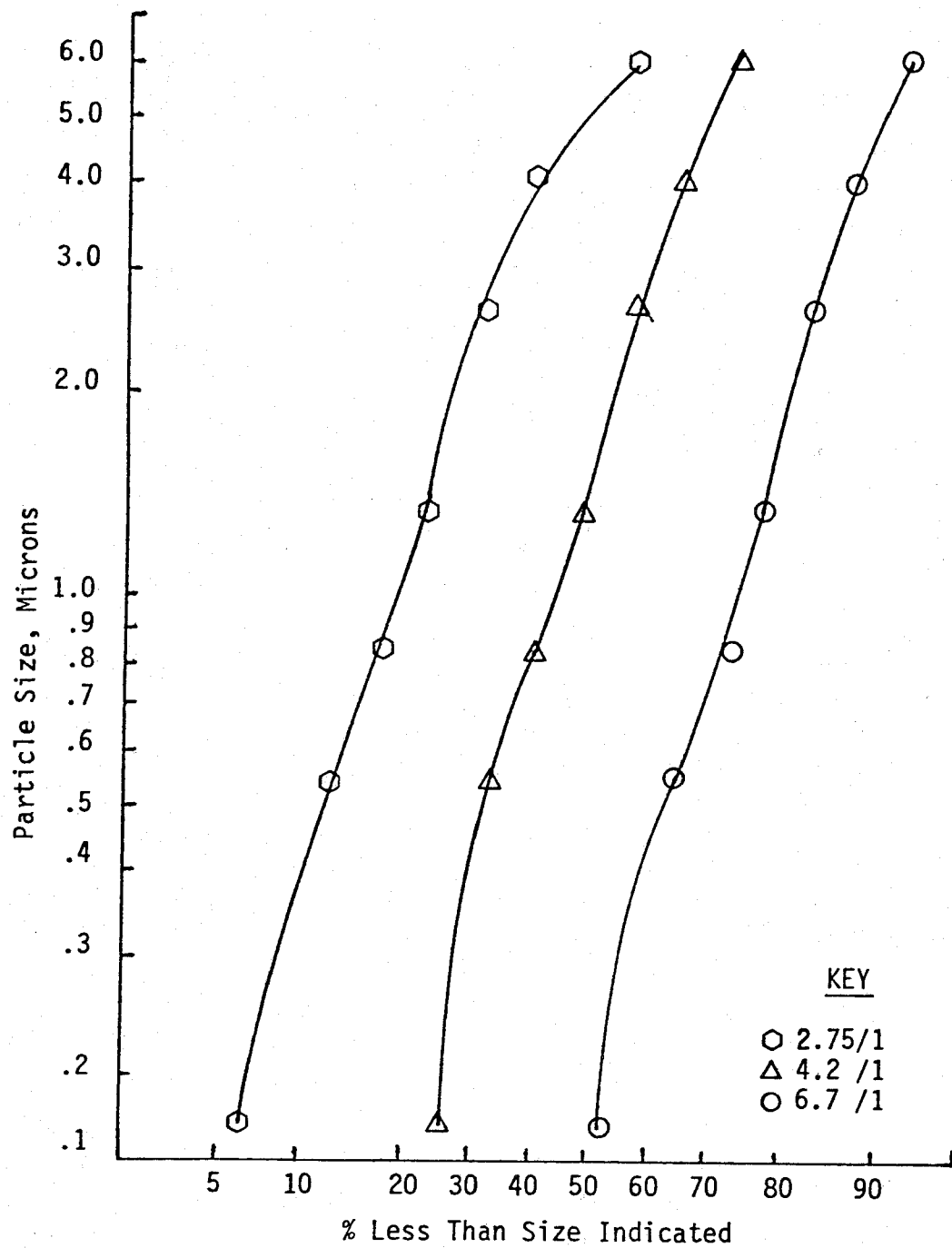


Figure 6  
Outlet Particle Size Distribution, Globe Albany

TABLE 4  
Outlet Concentration and Cumulative %

Globe Albany Bags

<u>Air-to-cloth 2.75/1</u>			<u>Air-to-cloth 4.2/1</u>			<u>Air-to-cloth 6.7/1</u>		
Avg. (1) Part. Diam. Microns	Avg. (2) Outlet Conc. gr/SCFD	(3) Cum%	Avg. Part. Diam. Microns	Avg. Outlet Conc. gr/SCFD	Cum%	Avg. Part. Diam. Microns	Avg. Outlet Conc. gr/SCFD	Cum%
8.85	.0003446	100.00%	78.85	.0001936	100.00%	78.85	.0001936	100.00%
6.03	.0001473	57.09	6.03	.0000647	73.23	6.03	.0000415	91.63
4.10	.0000631	38.75	4.10	.0000536	64.28	4.10	.0000411	87.33
2.63	.0000625	30.89	2.63	.0000618	56.87	2.63	.0000506	83.07
1.33	.0000417	23.11	1.33	.0000601	48.32	1.33	.0000456	77.83
0.84	.0000431	17.92	0.84	.0000558	40.01	0.84	.0000828	73.01
0.54	.0000515	12.55	0.54	.0000482	32.29	0.54	.0001134	64.44
0.17	.0000493	6.14	0.17	.0001009	25.62	0.17	.0002527	52.69
0.17	---		0.17	.0000843	11.66	0.17	.0002563	26.53
TOTAL	.0008031		TOTAL	.0007230		TOTAL	.0009659	

(1) Corrected for Stack Temperature

(2) gr/SCFD - Grains Per Standard Cubic Foot Dry (Standard - 70°F, 29.92" Hg)

(3) Percent of Total Outlet Concentration Less Than Size Indicated

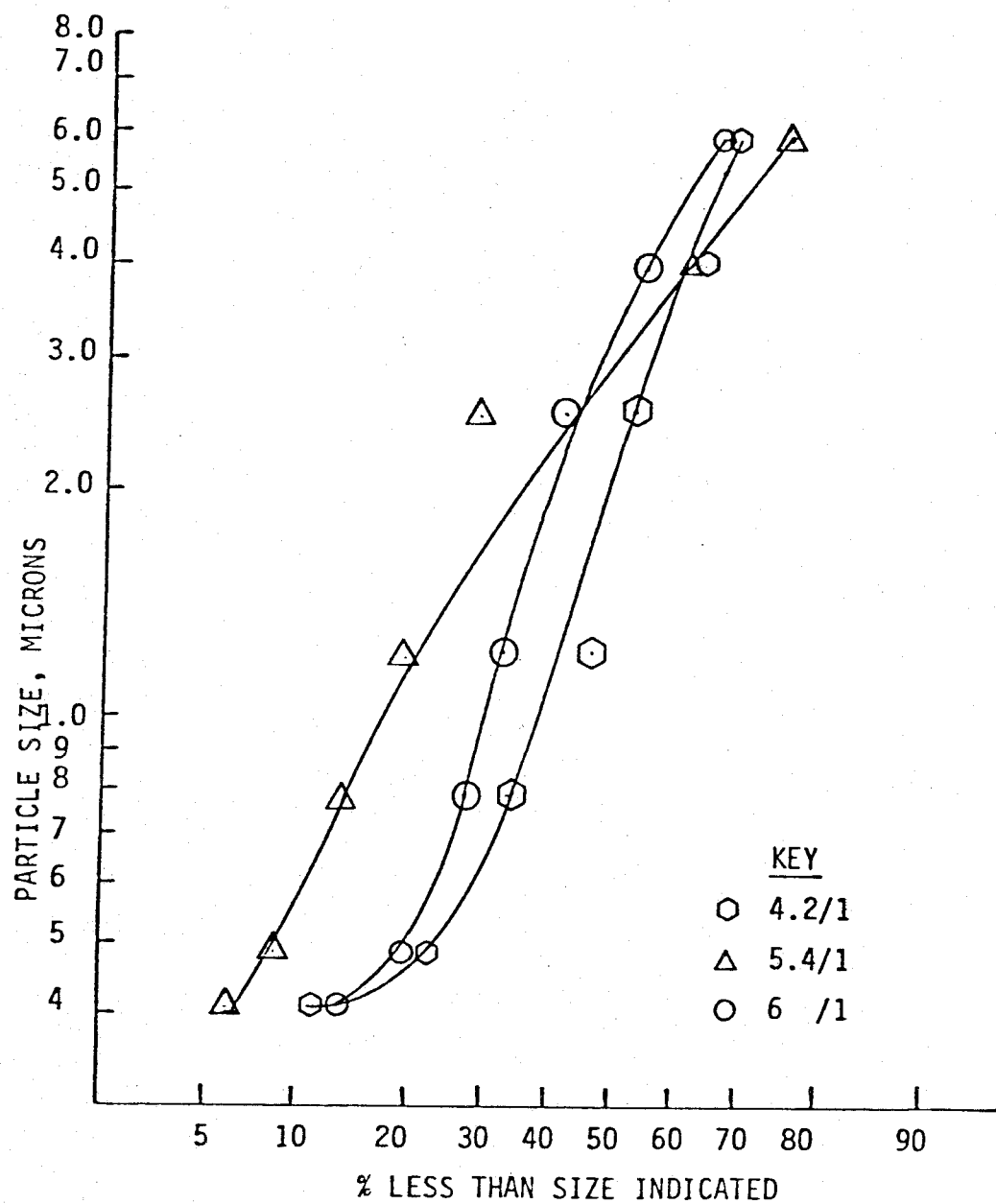


Figure 7  
Outlet Particle Size Distribution for Gore-Tex Fabric

TABLE 5

Outlet Concentration and Cumulative %Gore-Tex Bags  
March 1977Air-to-cloth 4.2/1

Avg. Part. Diam. Microns	Avg. Outlet Conc. gr/SCFD	Cum.%
8.4	.0001760	100.00%
5.7	.0000235	67.28
3.9	.0000512	62.92
2.5	.0000372	53.42
1.2	.0000666	46.52
0.77	.0000637	34.16
0.48	.0000581	22.34
0.41	.0000221	11.56
0.41	<u>.0000402</u>	7.46
TOTAL	.0005388	

Air-to-cloth 5.4/1

Avg. Part. Diam. Microns	Avg. Outlet Conc. gr/SCFD	Cum.%
8.4	.0001628	100.00%
5.7	.0000961	75.71
3.9	.0002230	61.42
2.5	.0000564	28.27
1.2	.0000423	19.93
0.77	.0000333	13.64
0.48	.0000179	8.74
0.41	.0000179	6.08
0.41	<u>.0000230</u>	3.42
TOTAL	<u>.0006727</u>	

Air-to-cloth 6/1

Avg. Part. Diam. Microns	Avg. Outlet Conc. gr/SCFD	Cum.%
8.4	.0001703	100.00%
5.7	.0000605	66.75
3.9	.0000688	54.94
2.5	.0000461	41.51
1.2	.0000251	32.51
0.77	.0000346	27.61
0.48	.0000374	20.86
0.41	.0000213	13.56
0.41	<u>.0000482</u>	9.40
TOTAL	.0005123	

1) Corrected for Stack Temperature

2) The outlet concentration for the air-to-cloth ratio of 5.4 was not an average of two values  
gr/SCFD - Grains Per Standard Cubic Foot Dry (Standard - 70° F, 29.92" Hg)

3) Percent of Total Outlet Concentration Less Than Size Indicated

evident that the PTFE laminate is extremely efficient at the three air-to-cloth levels studied.

As shown in Figure 8, for air-to-cloth ratios of approximately 3 and 6 to 1 the felted glass showed the lowest dust concentrations and the woven glass media the highest. However, as I had stated before, the woven glass media was considered more than satisfactory to meet present code requirements for this application.

### Economic Considerations

The economics of applying fabric filters to the refuse-fired boilers were evaluated and comparative costs for an electrostatic precipitator (ESP) and wet scrubber were developed. Installed costs were calculated for a fabric filter dust collector sized to handle 140,000 acfm at 460° F. The costs were developed for four (4) filter media: woven glass, PTFE laminate, needled glass felt, and Teflon felt (style 2663). Air-to-cloth ratios considered were 2.9, 5.8, 8.9 and 11.3 Table 6 shows the costs were developed from actual bag manufacturer quotes obtained during 1976.

The installed costs for an electrostatic precipitator capable of handling 140,000 ACFM at 98.5% efficiency were also developed. This cost was developed by adding the flange-to-flange cost (supplied by a leading ESP manufacturer) plus 70% of the purchase price for erection cost (the same figure was used in the fabric filter case), plus 5% of the purchase price for fans.

A graphical comparison of the installed costs for the four bag materials versus the installed costs of the electrostatic precipitator is shown in Figure 9. At air-to-cloth ratios of 5.8/1 or greater, the installed costs of the fabric filter (for all bags considered) was lower than the electrostatic precipitator.

Installed costs for a wet scrubber capable of handling 140,000 ACFM with 99% efficiency and a pressure drop of 30" W.G. were derived by doubling the figure of \$316,000 for 70,000 ACFM given in the article "Performance and Cost Comparison between Fabric Filters and Alternate Particulate Control Techniques"<sup>2</sup> and adding 12% for escalation.

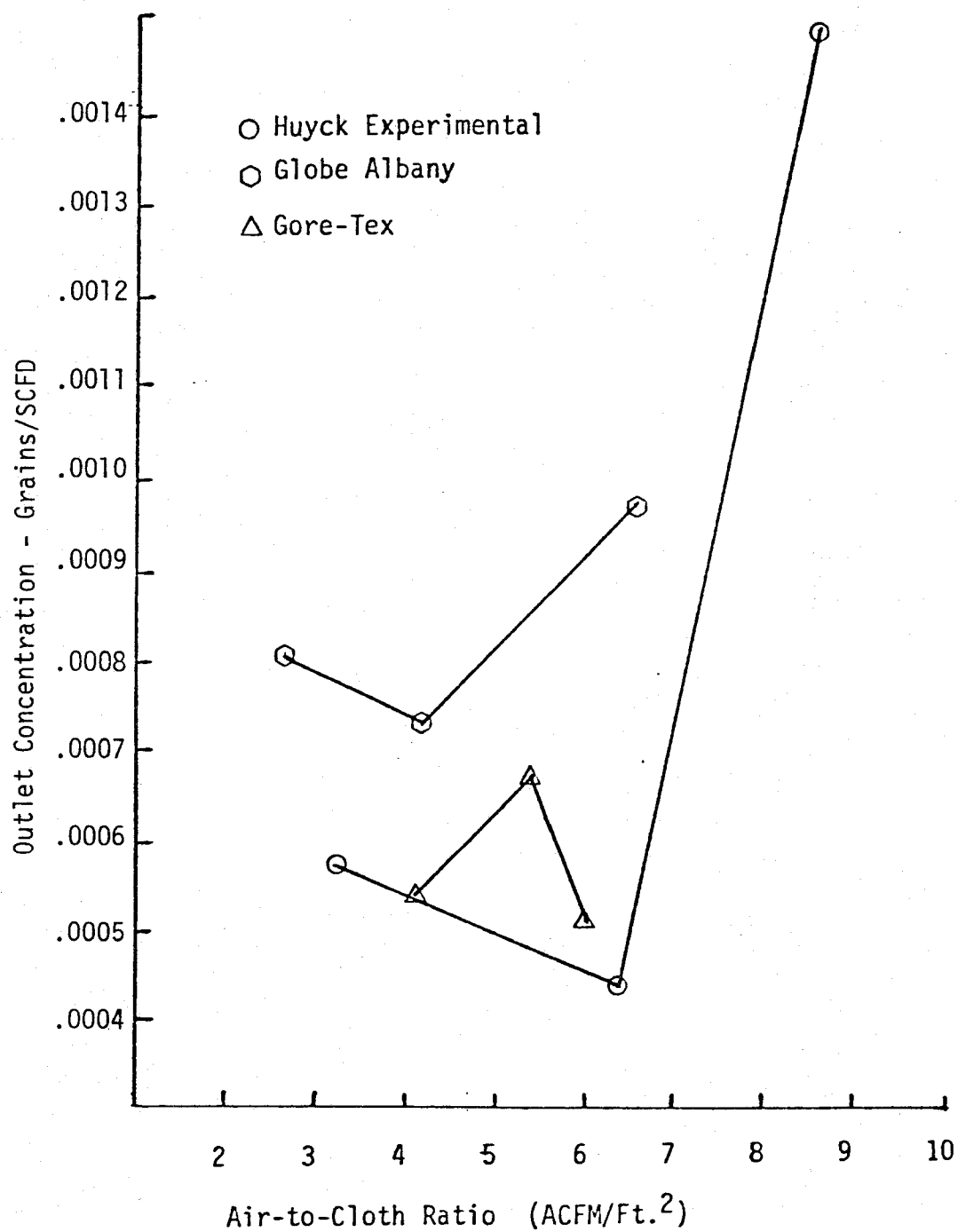


Figure 8

Comparison of Three (3) Fabrics for Outlet Concentration  
vs. Air-to-Cloth Ratio

TABLE 6  
Bag Cost as Percent of Installed Cost

	<u>Installed Cost</u>	<u>Bag Cost</u>	<u>% of Installed Cost for Bags</u>
Globe Albany (\$17.25/bag)			
2.9	817,260	74,520	9.1
5.8	421,750	37,260	8.8
8.9	316,734	24,840	7.8
11.3	271,837	19,872	7.3
Huyck(\$32.40/bag)			
2.9	928,522	139,968	15.1
5.8	477,381	69,984	14.7
8.9	353,821	46,656	13.2
11.3	301,505	37,325	12.4
Gore-Tex/Gore-Tex (\$51.50/bag)			
2.9	1,068,792	222,480	20.8
5.8	547,516	111,240	20.3
8.9	400,578	74,160	18.5
11.3	338,912	59,328	17.5
Teflon Felt (\$68/bag)			
2.9	1,189,968	293,760	24.7
5.8	608,104	146,880	24.1
8.9	440,970	97,920	22.2
11.3	371,226	78,336	21.1



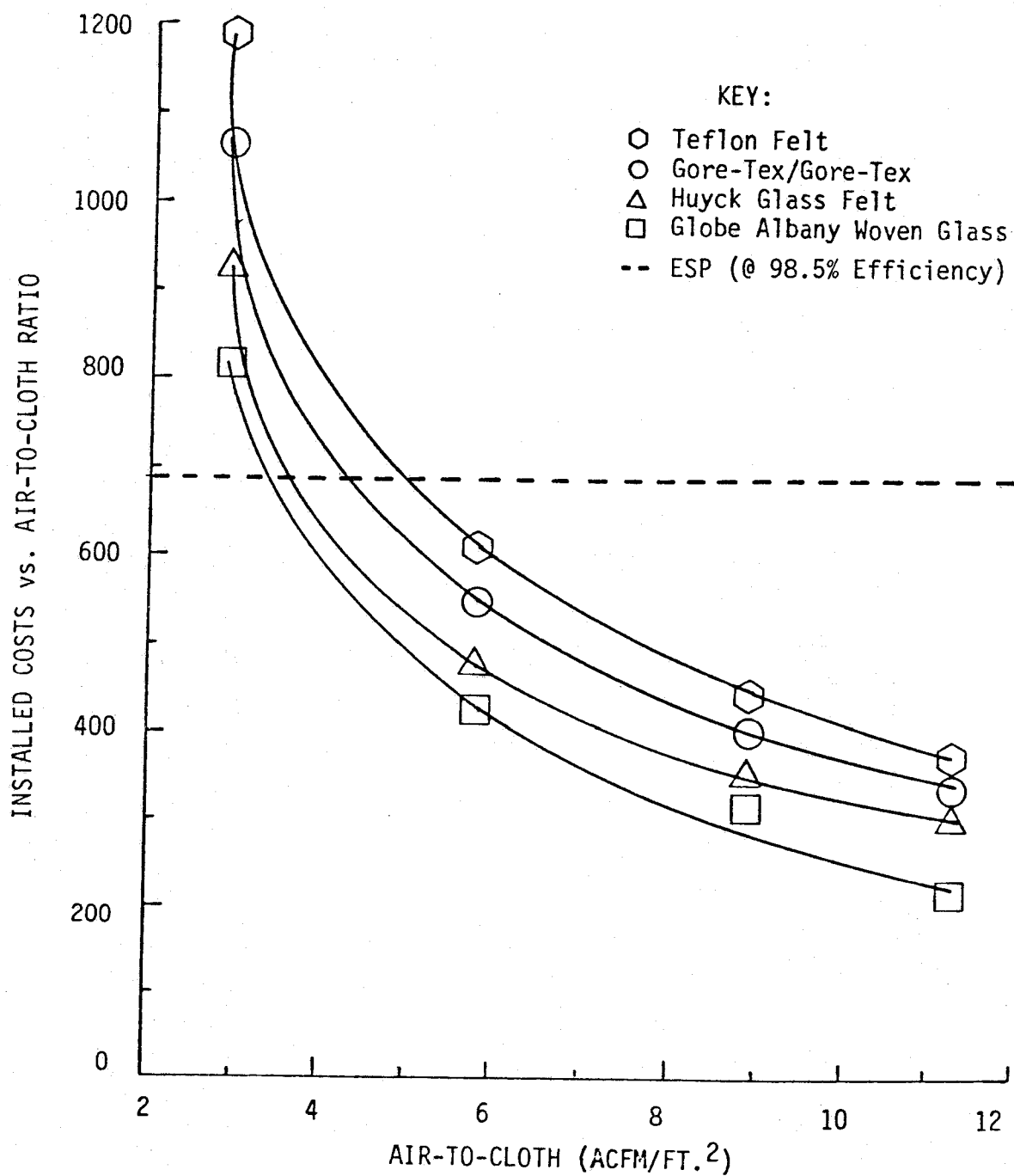


Figure 9

Comparison of Installed Costs for Four (4)  
Filter Media and Electrostatic Precipitators

A comparison of the three methods of particulate control is seen in Figure 10. The fabric filter technique for air-to-cloth ratios of 5.8/1 and greater on all bags considered has the lowest installed cost and the wet scrubber the highest. However, should an air-to-cloth ratio of 2.9/1 be required, fabric filters would be the most expensive and the electrostatic precipitators the least expensive method. Development of the operating and annualized costs for the three control techniques, employed the formulae published by Edmisten and Bunyard.<sup>3</sup>

Operating costs were developed for the fabric filters with two and four year bag life and compared with those of the electrostatic precipitator. Fabric filter costs were based on pressure drops of 6", 7", 10.5" and 12.5" W.G. for air-to-cloth ratios of 2.9, 5.8, 8.9 and 11.3/1 respectively. Precipitator costs were based on a pressure drop of 2" W.G. (all pressure drop values included 1.5" W.G. for drop across the inlet duct) and maintenance costs of 3% of the flange-to-flange price (considered higher than average but used due to the corrosive elements in the gas stream). Electrical rates for both cases were actuals obtained from NTTC. These costs presented in Figures 11 and 12 show the electrostatic precipitator to be less expensive to operate than any of the fabric filter cases considered.

While studying these graphs one must remember that in the formula for calculating annual operating costs for a specific bag life only two variables exist:

1. the number of bags (which decrease with increasing A/C).
2. the pressure drop (which increases with increasing A/C).

It appears that at some point in the increase of the air-to-cloth ratio for a particular bag life, the effect of the increase in pressure drop outweighs the effect of the decrease in number of bags required.

As I had stated previously all bag materials were treated the same with regard to pressure drop. Actual pressure drops obtained during the course of

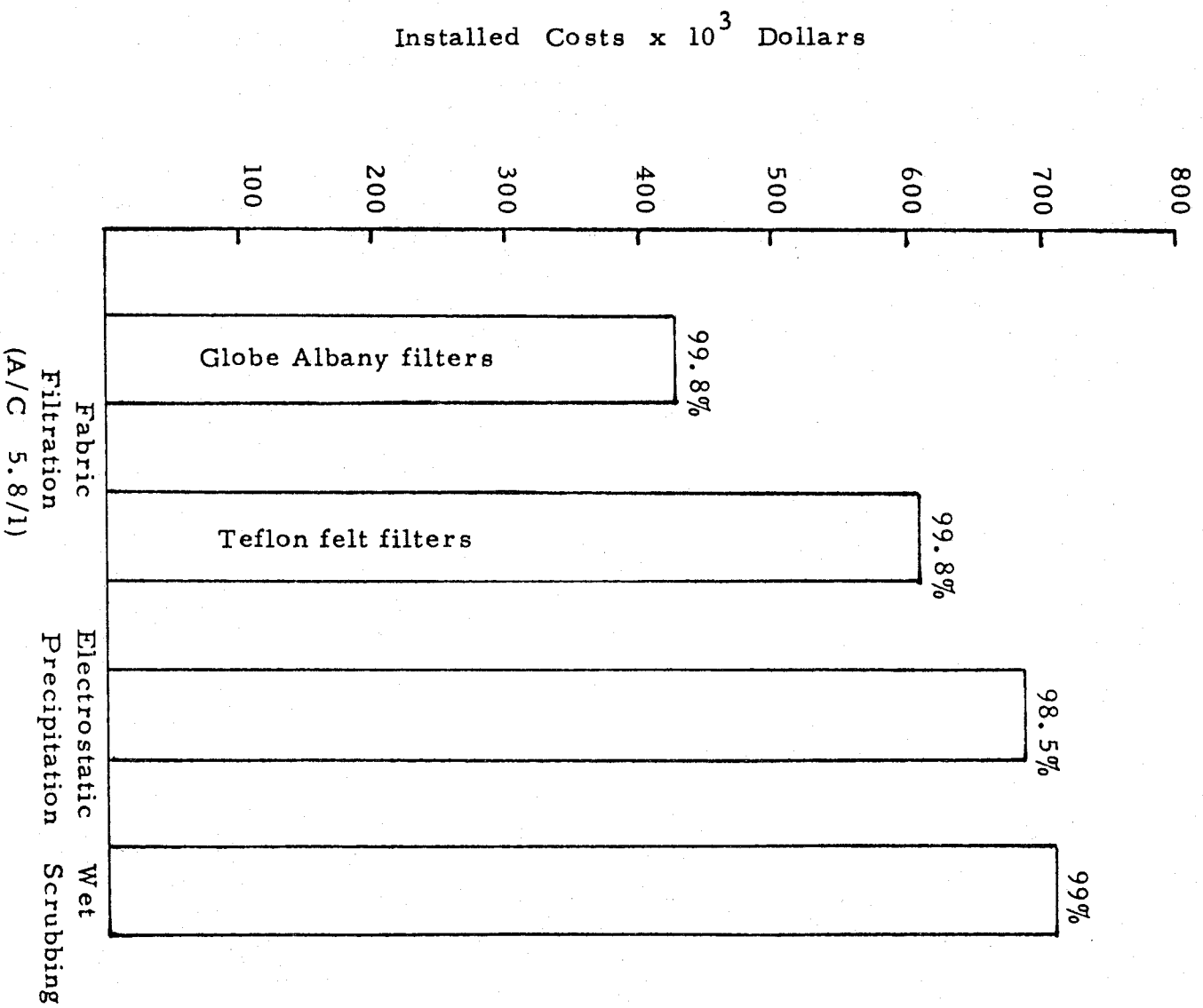


Figure 10

Installed Cost Comparisons for Different Air Pollution  
Control Techniques  
(At Slightly Different Efficiencies)

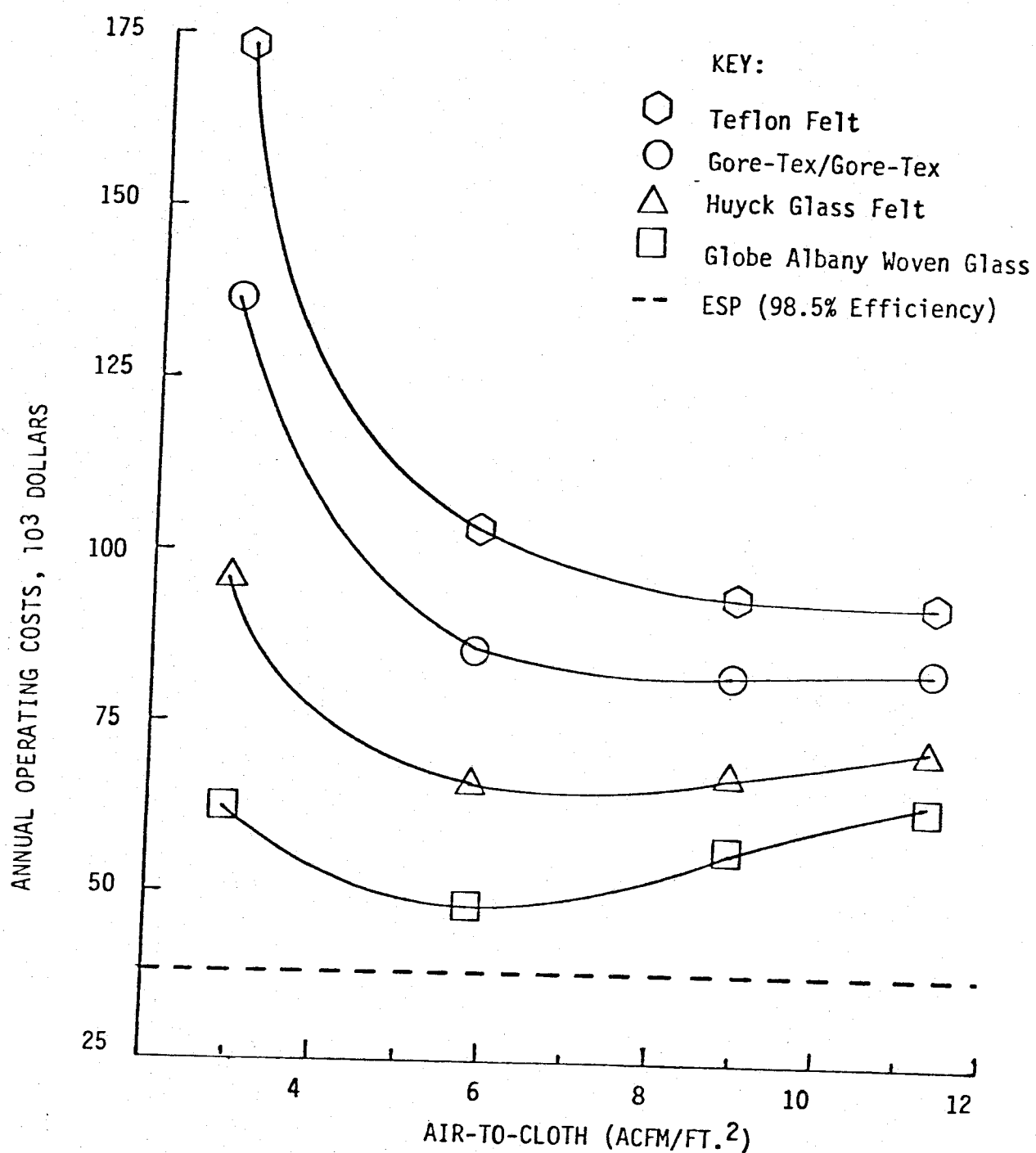


Figure 11

Comparison of Annual Operating Costs of Four (4) Filter Media and ESP Assuming Four Year Bag Life

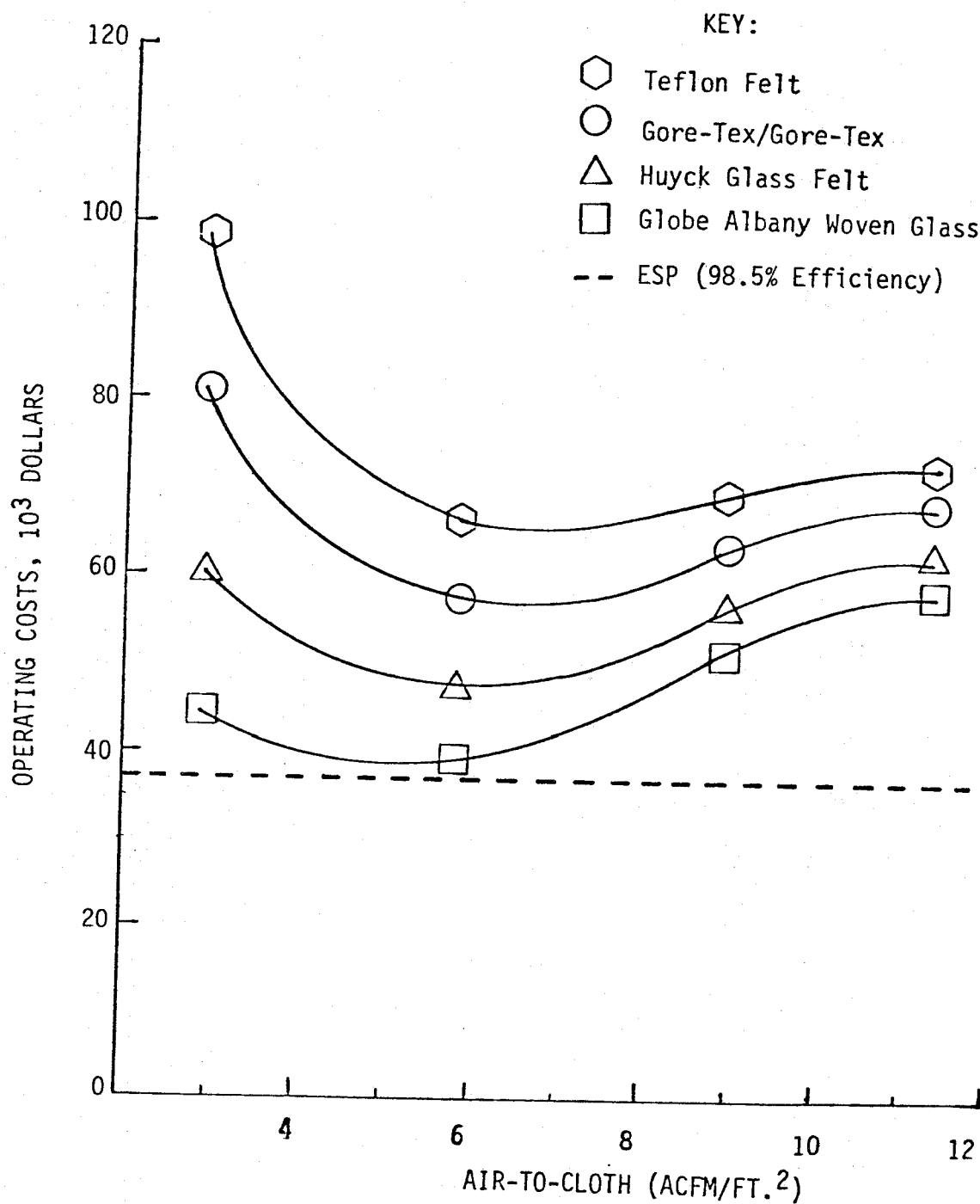


Figure 12

Comparison of Annual Operating Costs of Four (4)  
Filter Media and ESP Assuming Four Year Bag Life

the program, although well within the commercially acceptable range, were not used for this comparison because of the suspected influence of the sub-dew point conditions that plagued us throughout the program.

A comparison of the annual operating costs for the three techniques of control is illustrated in Figure 13. The electrostatic precipitator is seen to be the most economical while the wet scrubber seems the most expensive approach.

The annualized costs or total costs of control were developed from the preceding installed and operating costs. These results shown in Figures 14 and 15 were based on the following assumptions: First, hardware and installation costs are depreciated over fifteen (15) years. Second, the straight line method of depreciation ( $6 \frac{2}{3}\%$  per year) is used. This method has the simplicity of a constant annual write-off. Third, other costs called capital charges, which include interest, taxes, insurance and other miscellaneous costs are assumed equal to the amount of depreciation, or  $6 \frac{2}{3}\%$  of the initial installed costs. Therefore, depreciation plus these other annual charges amount to  $13 \frac{1}{3}\%$  of the installed costs.

As illustrated in Figures 14 and 15, fabric filters, at air-to-cloth levels of 5.8/1 or greater, and electrostatic precipitators are extremely competitive on an annualized costs basis.

Figure 16 shows the comparison of the annualized costs of control for the three techniques studied. Once again the wet scrubber is the most expensive approach, while the costs of the fabric filter and electrostatic precipitator are very close. This being the case, the need to replace bag life and pressure drop assumptions in computations for operating costs with empirical facts is necessary for final selection of the best alternative.

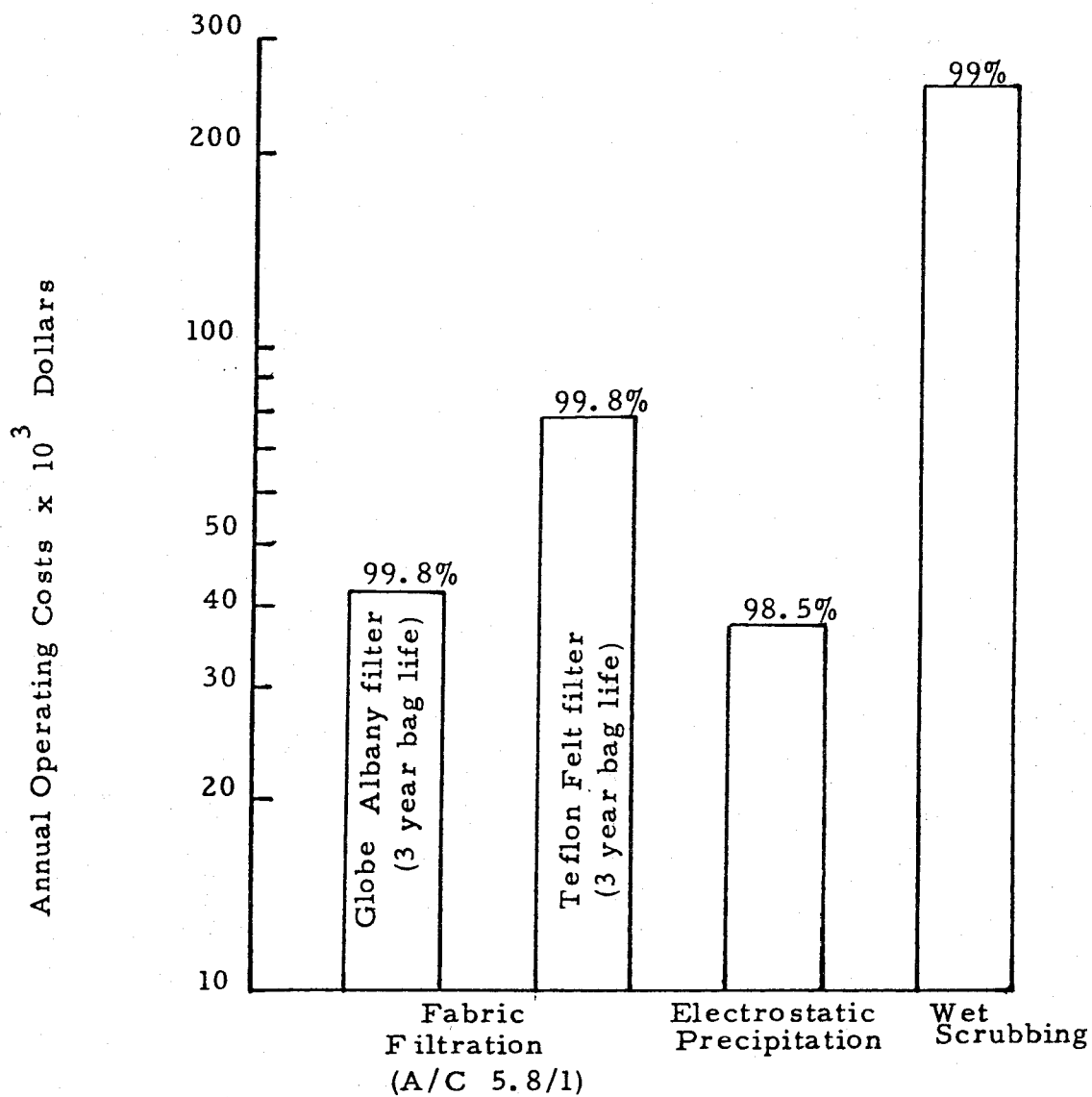


Figure 13

Annual Operating Cost Comparison for Three Air  
Air Pollution Control Techniques

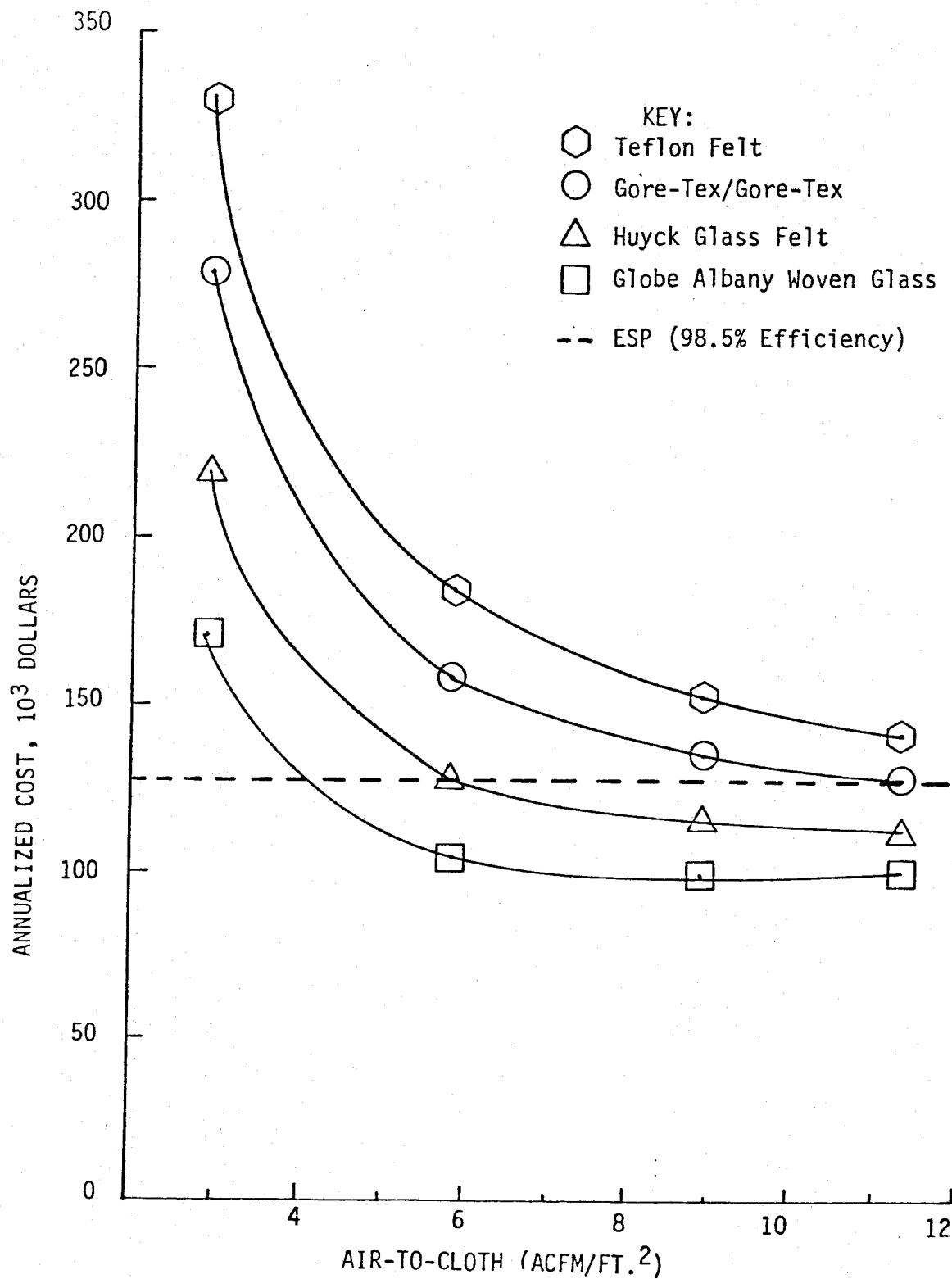


Figure 14

Comparison of Annual Operating Costs of Four (4) Filter Media and ESP Assuming Two Year Bag Life



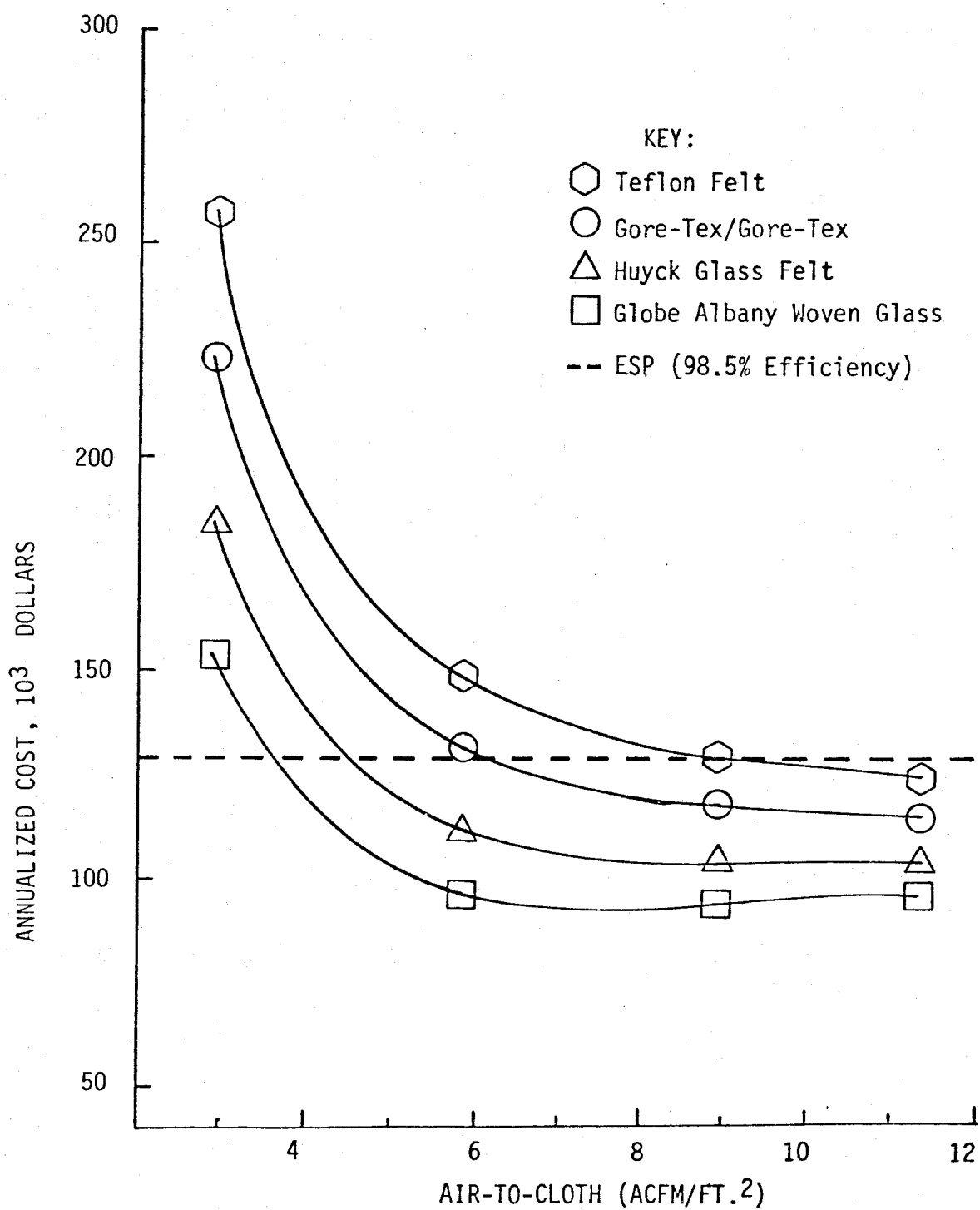


Figure 15

Comparison of Annual Operating Costs of Four (4) Filter Media and ESP Assuming Four Year Bag Life

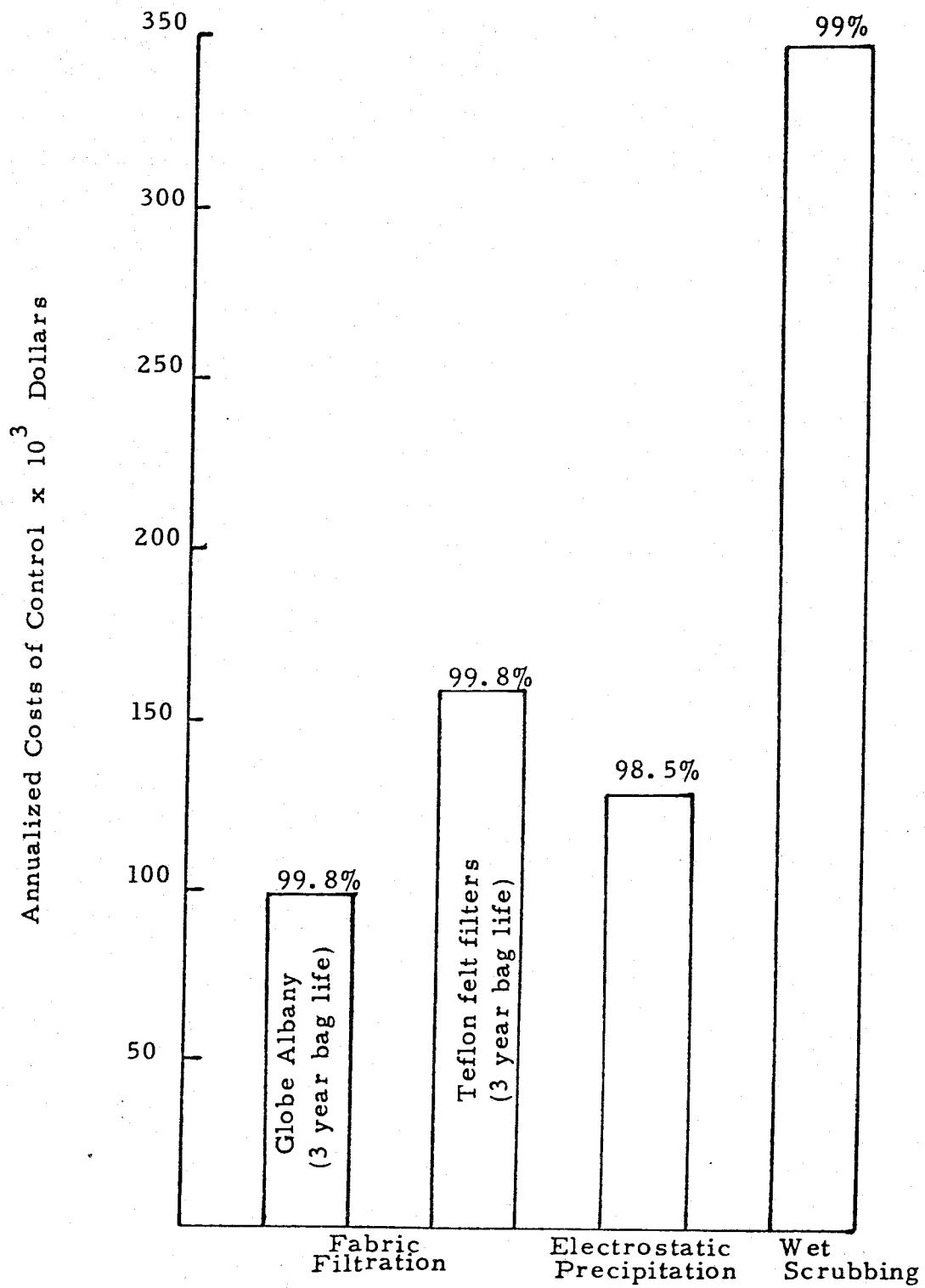


Figure 16

Annualized Cost for the Three Air Pollution Control Techniques

## CONCLUSIONS

The three filter media tested for dust removal capability indicated high level removal over a range of air-to-cloth ratios (apparent filtration velocity). For air-to-cloth ratios of approximately 3 to 1 and 6 to 1 the felted glass media showed the lowest outlet dust concentration and the woven glass media was considered more than satisfactory to meet present code requirements for this application.

No clear correlation between filtration velocity and outlet dust concentration was demonstrated. There may well be such a correlation, however, testing circumstances did not allow for determination of it in this program.

The three filter media for dust removal capability did not show signs of wear or weakening during this test program. It should be noted, however, that total on-stream time was very limited.

The pressure drops obtained for the three filter media were within the commercially acceptable range.

Generalizations regarding the costs of particulate removal devices are inherently dangerous, however, it does appear that of the conventional routes to particulate control, only fabric filters and electrostatic precipitators are suitable to refuse-fired boilers. The economic analysis indicates that the wet scrubber has both higher operating and capital costs (and, therefore, higher total annualized costs) than either the electrostatic precipitator or fabric filter.

In view of this and considering its potential for corrosion, the wet scrubber appears to be an unlikely candidate for this application.

As previously mentioned, the economic analysis indicate that the annualized costs of the electrostatic precipitator and the fabric filter are very close. Final selection of the best alternative can only be made after bag life and pressure drop assumptions have been replaced with empirical facts.

## References

- 1) J.D. McKenna, J.C. Mycock, R.L. Miller, K.D. Brandt, "Applying Fabric Filtration to Refuse Fired Boilers", Report to be published by EPA.
- 2) J.D. McKenna, J.C. Mycock and W.O. Lipscomb, "Performance and Cost Comparisons Between Fabric Filters and Alternate Particulate Control Techniques", JAPCA, V24, N12 December 1974, P1144.
- 3) N.G. Edmisten and F.L. Bunyard, "A Systematic Procedure for Determining the Cost of Controlling Particulate Emissions from Industrial Sources", J. Air Pollution Control Association V20, N7, p.446 (1970).



## FIELD TESTS WITH A MOBILE FABRIC FILTER

Dale L. Harmon  
Particulate Technology Branch  
Industrial Environmental Research Laboratory  
Research Triangle Park, N. C. 27711  
December 1977

### Abstract

In 1973, EPA funded the design and construction of a mobile fabric filter unit, the first of a series of three mobile research units built for the assessment of the collectibility of particulate emissions from industrial sources. The mobile filter unit can be adapted to cleaning by mechanical shaking, pulse jet or low-pressure reverse flow. Cleaning parameters can be varied easily over broad ranges. The paper presents results of tests completed on a brass and bronze foundry, a hot mix asphalt plant, a pulp mill lime recovery kiln, a refuse processing plant the three coalfired boilers. The most recent test was at the Amarillo, Texas Harrington Station generating plant of the Southwestern Public Service Company. Low-sulfur subbituminous coal was burned. Woven Teflon coated fiberglass and woven graphite - and - silicone - coated fiberglass bags were tested in shake and reverse air cleaning modes. Total mass efficiency for all tests ranged from 99.56% to 99.99% with an overall average of 99.87%. Bag blinding problems were encountered with reverse cleaning.

## FIELD TESTS WITH A MOBILE FABRIC FILTER

Dale L. Harmon  
Particulate Technology Branch  
Industrial Environmental Research Laboratory  
Research Triangle Park, N. C. 27711  
December 1977

### INTRODUCTION

The Environmental Protection Agency and predecessor organizations have been involved in development of systems for control of emissions from industrial sources for many years. The EPA R&D program for particulate control is designed to establish engineering design techniques and performance models, and to improve the collection capability and economics of control devices for particulate matter. The objective is the development and demonstration of control technologies capable of effectively removing large fractions of the under 3 micron diameter particles from effluents.

In 1973, EPA funded the design and construction of a mobile fabric filter unit, the first of a series of three mobile research units built for the assessment of the collectibility of particulate emissions from industrial sources. These units house the three types of conventional particulate collectors (fabric filter, wet scrubber and electrostatic precipitator) that are generally used by industry at the present time.

Actual data on particle collection efficiency of conventional particulate collectors is sparse. Actual operating data for the optimization of collection efficiency and cost is not readily available. Design of control equipment is presently based on projections from historical data which has been developed by manufacturers for their own devices and is proprietary. This information is not standardized and cannot be extrapolated to other devices. On-site testing prior to control device selection is seldom attempted and the possibility of alternative devices is poorly defined. The EPA mobile units are highly versatile and will be used to investigate the applicability of these control methods to the control of fine particulate emitted from a wide range of sources. The relative capabilities and limitations of these control devices will be evaluated.

and documented. This information, supplemented by data from other EPA particulate programs, will permit selection by equipment users of collection systems that are technically and economically optimum for specific applications. Operation of the mobile units will be coordinated with other EPA laboratories and regions to provide, when possible, field data on specific problem sources.

#### MOBILE UNIT DESIGN

The original mobile fabric filter unit was built by GCA Corporation for EPA and was mounted on an open 1360 kg (1.5 ton) truck. The equipment could be operated on the truck or could be removed and operated at locations not accessible to the truck. The mobile filter unit can be adapted to cleaning by mechanical shaking, pulse jet or low-pressure reverse flow. Filtration can be conducted at cloth velocities as high as 0.1 m/s (20 fpm) with a pressure differential up to 50 cm (20 in.) of water, and at gas temperatures up to 290°C (550°F). Cleaning parameters can be varied easily over broad ranges. One to seven filter bags of any fabric media, 1.2 to 3 m (4 to 10 ft) long and up to 30 cm (12 in.) in diameter may be used. Gas flows used are from 0.012 to 0.13 m<sup>3</sup>/s (26 to 280 cfm), as determined by cloth velocity, bag size and bag number.

The mobile fabric filter unit just described operated on effluents from a brass and bronze foundry, a hot mix asphalt plant, a coal-fired boiler, a lime kiln and a pulp mill recovery boiler. Operation of the unit from the open truck was found to be extremely inconvenient and detrimental to efficient field testing, so the filter system was installed in a 12 m (40 ft) closed trailer in October 1976. Since then the unit has been used to determine the performance of a fabric filter on the effluent from a cyclone collector used on the St. Louis Refuse Processing Plant and a power plant burning a western subbituminous coal.

The second mobile unit received by EPA was the wet scrubber. This unit, built by the Naval Surface Weapons Center at Dahlgren, Va., was delivered in December 1974. The scrubber unit is in a 12 m (40 ft) trailer and contains a venturi scrubber and a sieve tray scrubber.



Maximum gas flow rate through the scrubbers is  $0.28 \text{ m}^3/\text{s}$  (600 cfm). Maximum L/G ratio is  $0.01 \text{ m}^3/\text{m}^3$  (75 gal./acf). The unit can treat gas at temperatures up to  $480^\circ\text{C}$  ( $900^\circ\text{F}$ ).

The mobile electrostatic precipitator was delivered to EPA in September 1976. This system was also designed and built by the Naval Surface Weapons Center. The mobile ESP facility consists of two separate units mounted in 12 m (40 ft) freight vans. The first unit is the process van which houses a five-section ESP and all auxiliary equipment. Each section of the ESP has a separate power supply which provides up to 50,000 volts and 7 milliamps DC. The precipitator is designed to operate at flow rates up to  $1.4 \text{ m}^3/\text{s}$  (3000 cfm) at temperatures up to  $480^\circ\text{C}$  ( $900^\circ\text{F}$ ). The second unit is a control/laboratory van containing all process controls, monitors and recorders plus provisions for an analytical laboratory and equipment storage.

#### MOBILE FABRIC FILTER FIELD TESTS

##### Tests by GCA/Technology Division

After designing and building the mobile fabric filter for the Environmental Protection Agency, GCA/Technology Division conducted field tests on the following three sources:<sup>1</sup>

- Secondary brass and bronze foundry.
- Hot mix asphalt plant.
- Coal-fired boiler.

Results of these three tests are discussed briefly below:

##### Secondary Brass and Bronze Foundry

The mobile fabric filter system was operated in the pulse jet, mechanical shake, and reverse flow cleaning modes on a secondary brass and bronze foundry. Three pulse cleaning tests using Nomex felt bags were conducted. The only parameter varied was the interval between pulses: two tests were at a 40 second interval and one at a 20 second interval. Data is summarized in Table 1. During test 3, in

which the filter bags were cleaned twice as often, the average pressure drop across the filter was only 13 cm (5 inches) as compared to 23 and 25 cm (9 and 10 inches) for the first two tests. However, increasing the cleaning frequency also doubled the percent penetration.

Four shake cleaning tests using woven Nomex bags were conducted. Bag tension, shaking frequency and amplitude, and filtration velocity were varied. Data is summarized in Table 2. Test 4 was designed to simulate cleaning parameters for a full scale fabric filter which was operating at the test site. The plant had experienced problems with excessive pressure drop across the filter. This problem was evident with the mobile unit during test 4. Very little cleaning was accomplished. After 2 hours operation the pressure drop had increased to 38 cm (15 inches) and even after shaking was only slightly reduced to 33 cm (13 inches). Tests 5, 6, and 7 indicate that increased shaking frequency and amplitude (both contributing to higher bag acceleration) reduced the filter pressure drop and increased filtration capacity but also increased penetration. This information was helpful in analyzing the plant's problem.

Only one reverse flow cleaning test was conducted: it was primarily to shake down the mobile fabric filter system in the reverse flow cleaning mode. Data collected was not sufficient to develop conclusions.

#### Hot Mix Asphalt Plant

Four pulse cleaning tests on a hot mix asphalt plant using Nomex felt bags were conducted. Results of these tests are presented in Table 3. The pressure drop performance of the mobile unit was worse than that of a plant fabric filter system operating on the source tested. The plant filter operated at 5 to 8 cm (2 to 3 inches) pressure drop and had a reported air consumption of 0.5 to 0.8 m<sup>3</sup>/hr/m<sup>3</sup> (8 to 13 ft<sup>3</sup>/min/1000 ft<sup>3</sup>) versus a 28 to 30 cm (11 to 12 inch) pressure drop near the end of the test series and a compressed air consumption of 3 m<sup>3</sup>/hr/m<sup>3</sup> (50 ft<sup>3</sup>/min/1000 ft<sup>3</sup>) for the mobile system. The plant fabric filter operated at a lower filtration velocity (3.3 cm/sec [6.5 ft/min] for the plant filter and 3.7 to 4.1 cm/sec [7.2 to 8 ft/min] for the mobile filter)

which may account for the lower pressure drop, although filter geometry may have also been an important factor. The continuous rise in filter pressure drop throughout the field test may have been caused by moisture problems.

#### Coal-Fired Power Plant (Cyclone-Fired Boiler)

Three shake cleaning tests on a coal-fired power plant with cyclone-fired boilers using woven glass bags were conducted. Results of these tests are presented in Table 4. Pressure drop across the mobile fabric filter averaged about 13.7 cm (5.4 inches) after 20 hours of testing at a filtration velocity of 1.4 cm/sec (2.7 fpm). Total mass efficiency averaged 99.66%.

#### Tests by Monsanto Research Corporation

Following completion of the three tests described above, operation of the mobile filter was transferred to Monsanto Research Corporation (MRC) under a contract with EPA's Industrial Environmental Research Laboratory at Research Triangle Park (IERL-RTP) to maintain and operate various IERL-RTP field and laboratory test facilities. The following tests were completed by MRC:

#### Coal-Fired Power Plant (Anthracite Coal)

The mobile fabric filter was operated at the Shamokin Dam, Pennsylvania, generating station of Pennsylvania Power and Light Company.<sup>2</sup> This station was unusual in two respects: it had a full-scale fabric filter operating and it burned a mixture of anthracite silt and petroleum coke. An extensive test was conducted with the mobile filter using three bag types and three cleaning modes over a range of values of air/cloth ratio, filtration time, and pulse interval. Operating conditions for the tests are given in Table 5. Total particulate collection efficiency and penetration results are given in Table 6. Fractional efficiency measurements were also made for each run.

Based on collection efficiency of particles 5  $\mu$ m and less in size, cleaning mode/bag type combinations can be ranked in descending order of collection efficiency as follows:

- 1) Reverse clean - Nomex felt bag
- 2) Reverse clean - glass bag
- 3) Shake clean - Nomex felt bag
- 4) Shake clean - Nomex woven bag
- 5) Pulse clean - Nomex felt bag

This ranking is based on the data at the operating conditions given in Table 5 and does not necessarily describe optimum performance achievable for each cleaning mode/bag type combination.

#### Pulp Mill Lime Recovery Kiln

The mobile fabric filter was operated at the Weyerhaeuser Corporation's pulp mill in Plymouth, North Carolina, on a lime recovery kiln.<sup>3</sup> Two cleaning modes and two fabric types were used in this test program. Operating conditions are given in Table 7. Total particulate collection efficiency and penetration results are given in Table 8. Fractional efficiency results are given in Table 9. Overall, integrated mass collection efficiency was 99.98%. Overall averages of mean fractional efficiencies by size range were as follows:

<u>Size, <math>\mu</math>m</u>	<u>Efficiency, %</u>	<u>Penetration, %</u>
1-3	99.815	0.185
4-6	99.814	0.186
7-10	99.918	0.082

Bag pressure drop ( $\Delta P$ ) data is summarized as average values in Table 10. The results show marked differences in bag  $\Delta P$  both within and between cleaning mode/bag groups. The variation within groups is in the direction expected in response to changing test conditions. A comparison of results between cleaning modes clearly shows shake mode operating at a significantly lower  $\Delta P$ . In other words, shake appears to provide

considerably more efficient cleaning than reverse flow.

On the basis of collection efficiency, it appears that a high level of control of lime recovery kiln emissions can be attained by a fabric filter. However, operating problems during this test program, caused by the high moisture content in the flue gas which resulted in condensation and much deposition on occasion, discourages the use of a fabric filter in this application.

#### Refuse Processing Plant

The mobile fabric filter was operated at the City of St. Louis Refuse Processing Plant on the plant's air density separator cyclone exhaust. The plant receives raw domestic solid waste which is shredded in a hammermill. The shredded waste is conveyed in an air classifier which separates heavier particles from lighter ones by gravitational settling and vertical pneumatic conveyance. The lighter fraction from the air classifier is separated from its carrier air stream in a cyclone where the coarse matter settles out and is collected to be burned in a local power plant. The cyclone separator air is exhausted to the atmosphere. It is these emissions to which the test was directed.

Only the pulse cleaning mode was used for this test with Dacron polyester felted bags and one set of cleaning parameters. It was necessary to run three 6-hour days in order to collect enough material at the filter outlet to weigh for mass and fractional particulate efficiency measurements. Total mass penetration was 0.05%. The corresponding mass efficiency was 99.95%.

#### Coal-Fired Power Plant (Subbituminous Coal)

The mobile fabric filter was operated at the Amarillo, Texas, Harrington Station generating plant of the Southwestern Public Service Company from May to July 1977. Harrington Station is the first coal-fired electric generating plant in the Southwestern Public Service Company system. Unit 1, a 350 MW pulverized coal-fired boiler, went on line in August 1976. It burns low-sulfur subbituminous coal transported by train from Wyoming. Harrington Station Unit 2, almost identical to

Unit 1, is under construction and is scheduled to go on line in 1978. Unit 2 will employ a fabric filter designed by Wheelabrator-Frye for particulate removal. Unit 3 is planned for 1980 and will also have a fabric filter.

EPA has funded a contract with Southwestern Public Service to conduct an exhaustive 1 year test program on the Unit 2 fabric filter to determine the performance of a fabric filter on a large coal-fired boiler burning low-sulfur coal. The demonstration is expected to show that fabric filters are cost effective and show superior performance for collecting particulates from large utility boilers. Options to extend the demonstration and pilot plant work beyond the 1 year base period are included in the contract.

The objectives of the mobile fabric filter test program at the Harrington Station were:

- 1) To develop filter operating performance data for input to the design of the full scale filter and development of the test program.
- 2) To provide data to compare fabric filter operation and particulate collection capability for boilers burning low-sulfur western coal with those for boilers burning high-sulfur eastern coal.

Two bag materials were tested: woven Teflon-coated fiber glass and woven graphite-and-silicone-coated fiber glass. The bag materials were tested in shake and reverse air cleaning modes. Operating conditions for the tests are given in Table 11. Bags were tested at an air-to-cloth ratio of 0.0155 m/s (3.05 fpm). This ratio was chosen to approximate that planned for the Unit 2 and Unit 3 fabric filters at Harrington Station. Bags were cleaned when the bag pressure drop reached 10.2 cm (4 inches).

Shake cleaning parameters were: frequency - 6.9 cps, amplitude 2.22 cm (0.875 inches), and duration - 10 sec. These parameters gave a shaker arm acceleration of 4.3 g's and 138 shakes (2 per cycle) per cleaning. Bag tension was not measured, but was estimated at 0.45 - 0.91 kg (1-2 lb). A delay of 1 min was used between filtration and shaking and a 2 min delay between shaking and filtration to allow dislodged dust to settle. Average filtration time with the Teflon/glass shake bags was 219 min, and with the graphite/glass bags was 181 min.

For the reverse air cleaning tests, the reverse air-to-cloth ratio was initially set at 0.0102 m/s (2 fpm). During fabric filter operation, however, bag blinding was observed with this reverse air flow rate. The reverse air-to-cloth ratio was ultimately increased to 0.0269 m/s (5.3 fpm), the maximum available from the reverse air fan at the selected operating conditions. Several time combinations were attempted to help reduce blinding. The combination settled upon was: first delay - minimum (5 sec), with reverse air fan on; reverse air time - 30 sec; second delay - 1 min, with reverse air fan shut off at about 30 sec. Filtration times with the Teflon/glass reverse air bags were 20-30 min. The filtration times with the graphite/glass bags using reverse air cleaning were so short that these bags were tested using alternating shake and reverse air cleaning. After shaking, filtration times were 30-60 min; after reverse air cleaning, filtration times were 10-28 min with an average of 17 min.

In all cases, new bags were conditioned a minimum of 24 hours prior to sampling. Gas temperature in the slipstream probe was usually between 180 and 200°C (350 and 390°F) during sampling. Heat loss through the inlet duct caused a temperature drop of 27-32°C (80-90°F) to the inlet sampling section. The temperature dropped another 27-32°C as the gas passed through the bag compartment to the outlet sampling section. Gas pressure in the slipstream probe was between 25 and 43 cm (10 and 17 inches) vacuum. Pressure drop in the inlet duct to the inlet sampling section was 2.5 to 4 cm (1 to 1.5 inches). Bag compartment pressure drop was usually a maximum of 10.2 cm (4 inches) except during bag cake resistance tests.

A summary of shake cleaning pressure drop results is shown in Table 12. Data from the Teflon/glass shake bags on June 9 are questionable due to low flow rate during the last few hours of operation. Average filtration time for the other 2 days of particulate sampling was 3 hrs, 39 min. Average effective residual bag  $\Delta P$  for the last 2 days was 38 mm (1.5 inches) and the average terminal bag  $\Delta P$  was 107 mm (4.2 inches).

The graphite/glass shake bag average filtration time was 3 hrs, 1 min. Average effective residual bag  $\Delta P$  was 44 mm (1.7 inches) and the average terminal bag  $\Delta P$  was 103 mm (4.1 inches).

The filtration times were shorter and residual pressure drops higher with the graphite/glass bags. These results indicate higher particulate filtration efficiency and less cake removal during cleaning. The average boiler load was slightly higher during sampling of the graphite/glass bags: an average of 336 MW for the 3 days compared to 331 MW for the last 2 days with the Teflon/glass bags. The small difference in boiler load is not believed responsible for the difference in results.

A summary of the reverse cleaning pressure drop results for the Teflon glass bags is presented in Table 13. Bag blinding problems were encountered. In an effort to get better bag cleaning and extend filtration time the bags were sometimes cleaned 2 or 3 times before filtration was resumed. Some additional cleaning was accomplished, but not enough to extend the time between cleans to more than 30 min. Even with multiple cleanings, the filtration times grew shorter as operation continued. Extending the delay or reverse air durations did not improve cleaning. The reverse air flow was 1.7 times the forward rate.

To determine the cause for bag blinding, several factors were investigated. First, the bags were observed during cleaning. The bags collapsed well as the reverse air damper opened at the start of the first delay and stayed collapsed until the manual reverse air gate valve was closed during the second delay. The reverse air fan caused no additional collapse because the negative system pressure pulled in reverse air without the fan running. As filtration resumed, the bags



inflated. When collapsed, the bags had an hourglass shape between the spreader rings. The bags did not collapse to the point where the reverse air flow was choked off due to the bags closing up completely.

Dust cake removal was observed through the bag compartment hopper window. During the first delay, there was a large quantity of fallout immediately when the reverse air gate valve opened. Most visible particles were large flakes. A fairly large portion exited the hopper entrance into the inlet duct. After the initial puff, flakes settled slowly toward the dust collection can, with a portion pulled out through the hopper entrance. When the reverse air fan came on, there was a small quantity of flaky dust as the fan started--much less than during the first delay. Flakes again settled slowly. During the second delay, a few flakes were dislodged at the start. Flakes continued settling for most of the duration. As filtration was resumed, a puff of dust entered the hopper. Much of the dust was pulled up into the bags, but did not appear to be enough to make much difference in the bag cake or pressure drop. The puff was probably due to the forward air reentraining particles that settled in the inlet duct during bag cleaning.

The reverse air temperature was at least the same as the bag compartment outlet temperature at the start of cleaning and rose about 35°C as reverse flow continued. The reverse air moisture content, measured with the wet bulb method, was found to be 2 percent by volume less than the filtration gas moisture content. Condensation on the bags was therefore a doubtful cause of bag blinding.

The bags never completely relaxed during the delay between cleaning and the resumption of filtration. This was due to leakage through the reverse air gate valve. To stop reverse air leakage, the manual gate valve was also shut about halfway through the second delay, but bag cleaning was not improved.

On the second day of sampling the Teflon/glass reverse air bags, the bags were cleaned by shaking prior to sampling. The first filtration time was approximately 2 hours, but decreased to about 25 min when operation was stopped at the end of the test.

The pressure drop results for the graphite/glass reverse air bags are shown in Table 14. During bag conditioning, blinding was even more severe than with the Teflon/glass reverse air bags. After only 10 hours of operation (having started with new bags), filtration time had decreased to less than 4 min. and residual bag  $\Delta P$  rose to 81 mm (3.2 inches).

For particulate sampling, it was decided to use reverse air cleaning until the time between cleans decreased to 30 min or less, then shake the bags and resume reverse air cleaning. The result, as shown in Table 14, was that only every other cleaning was with reverse air. Even after shake cleaning, filtration times were much shorter than when using shake cleaning alone.

Table 15 presents the results of sampling for total mass concentrations. Penetration of both Teflon/glass bag types was higher than that of the graphite/glass bags. Penetration was about the same for both cleaning modes with the graphite/glass bags, possibly influenced by the alternating reverse air and shake cleaning employed with the reverse air bags.

Figure 1 presents mass penetration versus particle size curves for the four fabric/cleaning mode combinations tested. All four penetration curves exhibit minima. The minimum penetrations of the shake-type bags occur at larger particle sizes than those of the reverse-air-type bags. With both the shake and reverse air bags, the minimum penetrations were at smaller sizes with the graphite/glass bag material. The maxima for the two reverse air curves at about 4  $\mu m$  may not be real. It is suspected that characteristics of the impactors produced or magnified these results. It is possible that the penetrations actually continue to increase above 4  $\mu m$ . The graphite/glass shaken bags had the lowest penetrations in the particle size range measured.

Plans are underway to operate the mobile fabric filter at a site burning eastern high sulfur coal using the same fabric/cleaning mode combination as used at Harrington Station so a more direct comparison of fabric filter performance on high sulfur and low sulfur coal can be presented.

## SUMMARY

The original objective in building the mobile fabric filter, wet scrubber and electrostatic precipitator units was to operate all three units on the same source to compare the relative capabilities and limitations of the control methods on a given source. In practice the units, more frequently, have been used individually to answer specific control problems. The fabric filter unit has been operated on eight field sources including three utility boilers. A second mobile unit was operated at only two of these sources. It is anticipated that these mobile units will find wide application in the future to meet the original objective as well as to answer specific control problems.

Table 1. BRASS AND BRONZE FOUNDRY PULSE CLEANING TEST RESULTS

Parameter	Test Number		
	1	2	3
Inlet dust concentration, g/m <sup>3</sup> (grains/scf)	3.89 (1.7)	3.89 (1.7)	3.89 (1.7)
Inlet particle size, $\mu$ m (mass median)	0.5	0.5	0.5
Avg. filter pressure drop, cm water (inches)	25 (10)	23 (9)	13 (5)
Outlet dust concentration, g/m <sup>3</sup> (grains/scf)	0.0032(0.0014)	0.0030(0.0013)	0.0064(0.0028)
Interval between pulses, sec	40	40	20
Penetration, %	0.081	0.078	0.15
Efficiency, %	99.919	99.922	99.85

Table 2. BRASS AND BRONZE FOUNDRY SHAKE CLEANING TEST RESULTS

Parameter	Test Number			
	4	5	6	7
Cleaning Parameters				
Amplitude, cm (inches)	0.95(3/8)	2.2(7/8)	2.2(7/8)	2.2(7/8)
Frequency, cps	3-6	6	8	6
Tension, grams (pounds)	2270(5)	908(2)	454(1)	454(1)
Filtration velocity, cm/sec (fpm)	1.5(3)	1.5(3)	1.5(3)	1.3(2.5)
Maximum pressure drop, cm water (inches)	38(15)	33(13)	30(12)	18(7)
Average penetration, %	0.08	0.14	0.16	0.05
Average outlet dust concentration, g/m <sup>3</sup> (grains/scf)	0.0011 (0.0005)	0.0027 (0.0012)	0.020 (0.0087)	0.00069 (0.0003)

Table 3. HOT MIX ASPHALT PLANT PULSE CLEANING TEST RESULTS

Parameter	Test Number			
	1	2	3	4
Filtration velocity, cm/sec (fpm)	4.1 (8)	4.1 (8)	3.8(7.5)	3.7(7.5)
Avg. filter pressure drop, cm water (inches)	11.7(4.6)	14.2(5.6)	18.8(7.4)	26.9(10.6)
Inlet particle size, $\mu\text{m}$ (mass median)	12-15	12-15	12-15	12-15
Inlet dust concentration, $\text{g/m}^3$ (grains/scf)	34.1(14.9)	35.5(15.5)	35.0(15.3)	36.9(16.3)
Outlet dust concentration, " "	0.066 (0.029)	0.034 (0.015)	0.039 (0.017)	0.08 (0.03)
Avg. penetration, %	0.18	0.10	0.13	0.23
Avg. efficiency, %	99.82	99.90	99.87	99.7

Table 4. COAL-FIRED POWER PLANT (CYCLONE-FIRED BOILER) SHAKE CLEANING TEST RESULTS

Parameter	Test Number		
	1	2	3
Filtration velocity, cm/sec (fpm)	1.4 (2.7)	1.4 (2.7)	1.4 (2.7)
Avg. filter pressure drop, cm water (inches)	12.2 (4.8)	13.2 (5.2)	13.7 (5.4)
Inlet particle size, $\mu\text{m}$ (mass median)	5	5	5
Inlet dust concentration, $\text{g/m}^3$ (grains/scf)	1.6 (0.7)	1.6 (0.7)	1.6 (0.7)
Outlet dust concentration, $\text{g/m}^3$ (grains/scf)	0.009(0.004)	0.004(0.0016)	0.005(0.002)
Avg. penetration, %	0.57	0.23	0.34
Avg. efficiency, %	99.43	99.77	99.66

Table 5. OPERATING CONDITIONS FOR COAL-FIRED POWER  
PLANT (ANTHRACITE COAL) TESTS

Shake Mode	
Filtration period	20 min.
1st pause	10 sec
Cleaning period	10 sec
2nd pause	30 sec
Shake frequency	7 cps
Amplitude	2.22 cm
Shaker-arm acceleration	4.4 g's
Bag tension	0.682 kg
A/C	0.010, 0.015, 0.020 m/s
Pulse Mode	
Pulse interval	1, 2, 3 min
Pulse duration	0.10 sec
Pulse jet pressure	$4.14 \times 10^5$ Pa
A/C	0.020, 0.031 (max.) m/s
Reverse Mode	
Filtration period	30, 40, 50 min
1st pause	30 sec
Cleaning period	20 sec
2nd pause	30 sec
Bag tension	0.682 kg
A/C	0.010, 0.015, 0.020 m/s
Reverse flow air rate	$0.045 \text{ m}^3/\text{s}$

Table 6. COAL-FIRED POWER PLANT (ANTHRACITE COAL) MASS EFFICIENCY TEST RESULTS

Run <sup>a</sup>	Mass Loading, mg/m <sup>3</sup>		Col. Eff. %	Penetration %
	In	Out		
S-G-2-20	2 503	93	96.30	3.70
S-G-3-20	3 108	1	99.97	0.03
S-G-4-20	4 030	207	94.88	5.12
Average	3 213	100	97.05	2.95
S-WN-2-20	5 828	14	99.76	0.24
S-WN-3-20	1 246	1	99.89	0.11
S-WN-4-20	1 898	53	97.23	2.77
Average	2 991	23	98.96	1.04
S-FN-2-20	4 456	1	99.71	0.28
S-FN-3-20	4 818	1	99.98	0.02
S-FN-4-20	5 299	1	99.98	0.02
Average	4 862	1	99.89	0.11
P-FN-4-1	3 858	2	99.94	0.06
P-FN-6.2-1	7 855	35	99.56	0.44
P-FN-6.2-2	6 069	119	98.03	1.97
P-FN-6.2-3	7 525	77	98.97	1.03
Average	6 325	58	99.13	0.88
R-G-2-30	3 616	21	99.42	0.58
R-G-3-30	3 197	9	99.73	0.27
R-G-4-30	3 075	8	99.74	0.26
R-G-4-40	1 509	--	---	--
R-G-4-30	1 960	--	---	--
Average	2 672	13	99.63	0.37

(more)

Table 6. (Cont'd) COAL-FIRED POWER PLANT (ANTHRACITE COAL)  
MASS EFFICIENCY TEST RESULTS

Run <sup>a</sup>	Mass Loading, mg/m <sup>3</sup>		Col. Eff. %	Penetration %
	In	Out		
R-FN-2-30	3 902	1	99.99	0.01
R-FN-3-30	4 122	5	99.88	0.12
R-FN-4-30	4 282	1	99.99	0.01
R-FN-3-40	3 833	--	---	--
R-FN-3-50	4 889	3	99.95	0.05
R-FN-3-30	2 352	1	99.95	0.05
Average	3 896	2	99.95	0.05
Average	3 969	31	99.18	0.82

<sup>a</sup>Run Code

Example: S-G-2-20

First letter = Cleaning Mode: S - Shake

P - Pulse

R - Reverse

Second letter = Bag Type: G - Glass

WN - Woven Nomex

FN - Felted Nomex

First Number = A/C Ratio, fpm ( $\times 5.08 \times 10^{-3} = \text{m/sec}$ )

Second Number = Filtration Period, min, for shake and reverse

= Pulse Interval, sec, for pulse



Table 7. OPERATING CONDITIONS FOR PULP MILL LIME RECOVERY KILN TESTS

Shake Mode	
Filtration period	30, 50 min
First pause	30 s
Cleaning period	5 s
Second pause	30 s
Shake frequency	7 cps
Amplitude	22.2 mm (0.875 in.)
Shaker-arm acceleration	43.1 m/s <sup>2</sup> (4.4 g's)
Bag tension	0.68 kg (1.5 lb)
A/C	0.015, 0.025 m/s (3, 5 fpm)
Reverse Mode	
Filtration period	30, 50 min
First pause	30 s
Cleaning period	5, 20, 40 s
Second pause	30 s
Bag tension	0.68 kg (1.5 lb)
A/C	0.015, 0.025 m/s (3, 5 fpm)
R.F. air temperature	113°C (235°F)
R.F. air flow	4.5 x 10 <sup>-2</sup> m <sup>3</sup> /s (95 acfm)

Table 8. PULP MILL LIME RECOVERY KILN MASS EFFICIENCY TEST RESULTS

Run <sup>a</sup>	Grain Loading, g/m <sup>3</sup> (gr/sdcf)		Collection Efficiency, %	Penetration, %
	In	Out		
S-WN-3-30-5	8.65(3.78)	0.00291(0.00127)	99.97	0.0336
	8.65(3.78)	0.00318(0.00139)	99.96	0.0368
S-WN-3-50-5	7.83(3.42)	0.000191(0.0000835)	99.99	0.00244
	2.79(1.22)	0.000149(0.0000649)	99.99	0.00532
S-WN-5-30-5	2.33(1.02)	0.000359(0.000157)	99.98	0.0154
	4.39(1.92)	0.00130(0.000569)	99.97	0.0300
Average	5.77(2.52)	0.00135(0.000589)	99.98	0.0233
S-FN-3-30-5	6.86(3.00)	0.000613(0.000268)	99.99	0.00893
	6.86(3.00)	0.000897(0.000392)	99.99	0.0130
S-FN-3-50-5	0.597(0.261)	0.000831(0.000363)	99.86	0.139
	0.309(0.135)	0.000570(0.000249)	99.82	0.184
S-FN-5-30-5	4.35(1.90)	0.00220(0.000963)	99.95	0.0507
	8.21(3.59)	0.00563(0.00246)	99.93	0.0685
Average	4.53(1.98)	0.00179(0.000783)	99.96	0.0395
R-WN-3-30-5	11.2(4.91)	0.00102(0.000444)	99.99	0.00904
	8.58(3.75)	0.00281(0.00123)	99.97	0.0328
R-WN-3-30-20	6.80(2.97)	0.00110(0.000482)	99.98	0.0162
	5.95(2.60)	0.00105(0.000459)	99.98	0.0176
R-WN-5-30-5	24.9(10.9)	0.00118(0.000516)	99.99	0.00471
	5.84(2.55)	0.00113(0.000492)	99.98	0.0193
R-WN-3-50-5	5.88(2.57)	0.000755(0.000330)	99.98	0.0128
	5.95(2.60)	0.00146(0.000638)	99.97	0.0245
Average	9.40(4.11)	0.00131(0.000574)	99.99	0.0140
R-FN-3-30-20	8.56(3.74)	0.000931(0.000407)	99.99	0.0109
	4.97(2.17)	0.00112(0.000490)	99.98	0.0226
R-FN-3-50-40	6.80(2.97)	0.000490(0.000214)	99.99	0.00721
	9.15(4.00)	0.00166(0.000726)	99.98	0.0182
R-FN-3-30-40	13.9(6.08)	0.00166(0.000726)	99.99	0.0119
	7.94(3.47)	0.00180(0.000788)	99.98	0.0227
Average	8.56(3.74)	0.00128(0.000559)	99.99	0.0149
Average	7.24 (3.17)	0.00142 (0.000622)	99.98	0.0222

<sup>a</sup>Run Code - Example: S-WN-3-30-5

First Letter - cleaning mode (Shake - S, Reverse - R)

Second Set of Letters - fabric type (Woven Nomex - WN, Felted Nomex - FN)

First Number - A/C ratio, fpm ( $\times 5.08 \times 10^{-3}$  = m/sec)

Second Number - filtration period, min

Third Number - cleaning period, sec

Table 9. PULP MILL LIME RECOVERY KILN FRACTIONAL EFFICIENCY TEST RESULTS

Run <sup>a</sup>	Mass Median Diameter, $\mu\text{m}$		Fractional Efficiency <sup>b</sup>		Mean Fractional Efficiency		
	In	Out	Min.	Max.	1 - 3 $\mu\text{m}$	4 - 6 $\mu\text{m}$	7 - 10 $\mu\text{m}$
S-WN-3-30-5	7.7	3.6	99.61 @3	99.99 @10	99.66	99.85	99.97
	7.7	1.1	99.28 @3	99.99 @10	99.46	99.81	99.99
S-WN-3-50-5	7.5	0.46	<sup>c</sup>	<sup>c</sup>	<sup>c</sup>	<sup>c</sup>	<sup>c</sup>
	7.4	0.45	<sup>c</sup>	<sup>c</sup>	<sup>c</sup>	<sup>c</sup>	<sup>c</sup>
S-WN-5-30-5	7.4	0.5	<sup>c</sup>	<sup>c</sup>	<sup>c</sup>	<sup>c</sup>	<sup>c</sup>
	8.3	0.7	<sup>c</sup>	<sup>c</sup>	<sup>c</sup>	<sup>c</sup>	<sup>c</sup>
S-FN-3-30-5	7.7	0.5	99.89 @1	99.99 @10	99.91	99.99	99.99
	7.6	0.5	99.51 @1	99.99 @ 8	99.73	<sup>a</sup>	99.98
S-FN-3-50-5	0.4	2.8	99.80 @6	99.86 @10	99.84	99.81	99.84
	1.2	0.6	99.21 @4	99.99 @ 8	99.46	99.52	99.98
S-FN-5-30-5	8.2	10.0	99.84 @6	99.99 @ 3	99.99	99.86	99.90
	8.2	5.7	99.20 @3	99.95 @10	99.38	99.54	99.90
R-WN-3-30-5	7.8	4.5	99.87 @3	99.99 @10	99.92	99.96	99.99
	7.8	3.2	99.08 @4	99.98 @10	99.50	99.55	99.96
R-WN-3-30-20	7.6	3.8	99.89 @4	99.99 @10	99.95	99.93	99.99
	7.5	4.7	99.92 @3	99.99 @10	99.93	99.96	99.99
R-WN-3-50-5	7.3	7.1	99.97 @4	99.99 @10	99.98	99.98	99.99
	7.2	5.9	99.97 @5	99.98 @10	99.99	99.98	99.98
R-WN-5-30-5	8.4	7.0	99.67 @5	99.96 @1,10	99.92	99.71	99.90
	8.2	9.6	<sup>c</sup>	<sup>c</sup>	<sup>c</sup>	<sup>c</sup>	<sup>c</sup>
R-FN-3-30-20	7.8	4.8	99.97 @4	99.99 @ 8	99.98	99.98	99.99
	7.6	4.9	99.85 @4	99.99 @ 8	99.95	99.88	99.99
R-FN-3-30-40	7.7	2.3	99.80 @3	99.99 @10	99.87	99.93	99.99
	7.6	3.5	97.15 @4	99.99 @10	99.76	98.94	99.98
R-FN-3-50-40							
R-FN-3-50-40	8.0	3.2	99.95 @7	99.99 @ 1	99.99	99.96	99.96
	8.0	1.9	97.90 @4	99.99 @10	99.89	99.12	99.99

<sup>a</sup> See Table 8 for code explanation<sup>b</sup> Number after @ is particle size,  $\mu\text{m}$ , at which minimum or maximum collection efficiency occurs<sup>c</sup> Test conditions which had apparent fraction efficiencies > 100%

Table 10. PRESSURE DROP RESULTS OF PULP MILL LIME RECOVERY KILN TESTS

Run <sup>a</sup>	$\Delta P_e^b$	$\Delta P_r^c$	$S_e^d$	$S_r^e$	$K^f$
S-WN-3-30-5	0.60(2.4)	1.00(4.0)	40.2(0.82)	65.1(1.33)	39,400(33.9)
S-WN-3-50-5	0.52(2.1)	0.95(3.8)	34.8(0.71)	61.7(1.26)	25,100(21.6)
S-WN-5-30-5	1.44(5.8)	1.94(7.8)	56.8(1.16)	75.9(1.55)	18,300(15.7)
S-FN-3-30-5	0.17(0.7)	0.40(1.6)	11.3(0.23)	26.0(0.53)	29,400(25.3)
S-FN-3-50-5	0.32(1.3)	0.70(2.8)	21.1(0.43)	45.6(0.93)	29,400(25.3)
S-FN-5-30-5	0.67(2.7)	1.29(5.2)	26.9(0.55)	50.9(1.04)	28,700(24.7)
R-WN-3-30-5	0.65(2.6)	1.17(4.7)	42.1(0.86)	76.4(1.56)	32,900(28.3)
R-WN-3-30-20	0.90(3.6)	1.19(4.8)	58.8(1.20)	78.4(1.60)	18,700(16.1)
R-WN-3-50-5	0.85(3.4)	1.37(5.5)	55.4(1.13)	89.6(1.83)	19,800(17.0)
R-WN-5-30-5	1.84(7.4)	2.44(9.8)	72.5(1.48)	96.0(1.96)	13,700(11.8)
R-FN-3-30-20	1.54(6.2)	2.07(8.3)	99.4(2.03)	135.2(2.76)	35,100(30.2)
R-FN-3-30-40	1.94(7.8)	2.31(9.3)	128.4(2.62)	153.8(3.14)	25,100(21.6)
R-FN-3-50-40	1.97(7.9)	2.44(9.8)	129.3(2.64)	159.2(3.25)	19,100(16.4)

<sup>a</sup> See Table 8 for code explanation

<sup>b</sup> = Effective pressure drop, kPa (in. w.c.)

<sup>c</sup> = Residual pressure drop, kPa (in. w.c.)

<sup>d</sup> = Effective drag =  $\Delta P_e/U$ , kPa/m/s (in. w.c./fpm)

<sup>e</sup> = Residual drag =  $\Delta P_r/U$ , kPa/m/s (in. w.c./fpm)

<sup>f</sup> = Cake specific resistance, kPa/m/s  $\cdot$  kg  $\cdot$  m<sup>2</sup> (in. w.c./fpm-lb-ft<sup>2</sup>)

Table 11. OPERATING CONDITIONS FOR COAL-FIRED POWER PLANT  
(SUBBITUMINOUS COAL) TESTS

Shake Mode				
	Teflon/Glass Bags		Graphite/Glass Bags	
	Range	Avg	Range	Avg
Filtration period, min	166-290	219	152-225	181
1st pause, min	1		1	
Cleaning period, sec	10		10	
2nd pause, min	2		2	
Shake frequency, cps	6.9		6.9	
Amplitude, cm	2.22		2.22	
Shaker-arm acceleration, g's	4.3		4.3	
Bag tension, kg	0.45-0.91		0.45-0.91	
A/C, m/s	0.0155		0.0155	
Reverse Mode				
	Teflon/Glass Bags		Graphite/Glass Bags	
	Range	Avg	Range	Avg
Filtration period, min	20-30	23	10-28	17
1st pause, sec	5		5	
Cleaning period, sec	30		30	
2nd pause, sec	60		60	
A/C, m/s	0.0155		0.0155	
Reverse air A/C, m/s	0.0102-0.0269		0.0102-0.0269	

<sup>a</sup> Alternate shake and reverse air cleaning--data reported is for reverse air only

Table 12. PRESSURE DROP RESULTS OF COAL-FIRED POWER PLANT  
(SUBBITUMINOUS COAL) SHAKE CLEANING TESTS

Date (1977)	Fabric Type	Filtration Time (hr:min)	Residual Bag $\Delta P$ (mm H <sub>2</sub> O)	Effective Residual $\Delta P$ (mm H <sub>2</sub> O)	Terminal Bag $\Delta P$ (mm H <sub>2</sub> O)
6-9	Teflon/Glass	4:50	14(43) <sup>a</sup>	33	74 <sup>b</sup>
		2:46	18	32	58 <sup>b</sup>
6-11	Teflon/Glass	3:31	30(97)	41	104
		3:45	23	36	109
6-13	Teflon/Glass	3:36	25(66)	36	102
		3:45	28	38	112
Avg <sup>c</sup>	Teflon Glass	3:39	27	38	107
6-22	Graphite/Glass	3:45	30(53)	34	102
		2:47	33	42	102
		2:32	20	46	102
6-23	Graphite/Glass	2:52	30(119)	46	104
		2:53	28	48	108
		2:46	33	43	102
		3:07	32	48	102
6-24	Graphite/Glass	3:05	32(112)	43	102
		2:59	30	43	103
		3:05	36	46	102
		3:25	38	43	103
Avg	Graphite/Glass	3:01	31	44	103

<sup>a</sup> Previous terminal bag  $\Delta P$  (mm H<sub>2</sub>O)

<sup>b</sup> Shut down due to low flow rate

<sup>c</sup> Data for 6-9-77 not included because of unreliability

Table 13. PRESSURE DROP RESULTS OF COAL-FIRED POWER PLANT  
(SUBBITUMINOUS COAL) REVERSE CLEANING TESTS  
(TEFLON/GLASS BAGS)

Date	Filtration Time, Min	No. of Clean Cycles	Residual Bag $\Delta P$ (mm H <sub>2</sub> O)	Effective Residual $\Delta P$ (mm H <sub>2</sub> O)	Terminal $\Delta P$ (mm H <sub>2</sub> )
7-15-77	19	2	61	84	108
	15	2	64	84	102
	21	2	64	89	102
	14	1	66	94	104
	14	1	69	94	107
	14	1	69	89	102
	16	1	69	94	102
	15	2	71	91	102
	19	2	58	89	103
	25	2	64	91	100
	12	2	67	94	102
	25	2	64	91	100
	17	1	74	97	102
	28	3	65	90	110
	20	3	66	89	107
	17	3	64	89	102
	21	1	64	84	102
	16	1	69	91	100
	9	1	74	91	102
	13	1	74	90	102
	15	3	66	94	102
	15	3	66	91	102
	26	1	18	36	102
7-16-77	58	1	44	79	102
	53	1	48	76	102
	37	1	56	90	102
	29	1	76	91	102
	24	1	61	94	102
	24	1	61	89	100
	40	3	52	84	102
	28	1	61	85	102
	29	1	61	91	102
	24	1	61	89	102
Average	23	-	63	88	103

Table 14. PRESSURE DROP RESULTS OF COAL-FIRED POWER PLANT  
(SUBBITUMINOUS COAL) REVERSE CLEANING TESTS  
(GRAPHITE/GLASS BAGS)

Date	Filtration Time, Min	Cleaning Mode	Residual Bag $\Delta P$ (mm H <sub>2</sub> O)	Effective Residual $\Delta P$ (mm H <sub>2</sub> O)	Terminal Bag $\Delta P$ (mm H <sub>2</sub> O)
7-19-77	44	Shake	23	61	102
	76	Shake	28	66	89
	17	Rev. air	58	86	102
	64	Shake	29	74	102
	16	Rev. air	66	91	102
	31	Shake	38	81	102
	17	Rev. air	67	88	102
	34	Shake	34	81	102
	16	Rev. air	66	84	102
	55	Shake	25	71	102
	13	Rev. air	-	-	102
	17	Rev. air	74	91	102
	55	Shake	25	71	102
	10	Rev. air	70	91	102
	109	Shake	18	53	102
	28	Rev. air	61	88	99
	78	Shake	20	55	100



Table 15. COAL-FIRED POWER PLANT (SUBBITUMINOUS COAL)  
MASS EFFICIENCY TEST RESULTS

Run <sup>a</sup>	Mass Loading, mg/m <sup>3</sup>		Collection Efficiency, %	Penetration, %
	In	Out		
S-T-6-9	368	1.63	99.56	0.44
S-T-6-11	4830	5.45	99.89	0.11
S-T-6-13	1450	4.31	99.70	0.30
Average	2216	3.80	99.83	0.17
S-G-6-22	3940	1.74	99.96	0.04
S-G-6-23	3590	2.18	99.94	0.06
S-G-6-24	5130	1.15	99.98	0.02
Average	4220	1.69	99.96	0.04
R-T-7-15	3530	4.44	99.87	0.13
R-T-7-16	3600	2.38	99.93	0.07
Average	3570	3.41	99.90	0.10
R-G-7-19	3690	1.05	99.97	0.03

<sup>a</sup>Run Code

Example: S-T-6-9

First Letter = Cleaning Mode: S - Shake  
R - Reverse

Second Letter = Bag Type: T - Teflon/glass  
G - Graphite/glass

First Number = Month of Test

Second Number = Day of Test

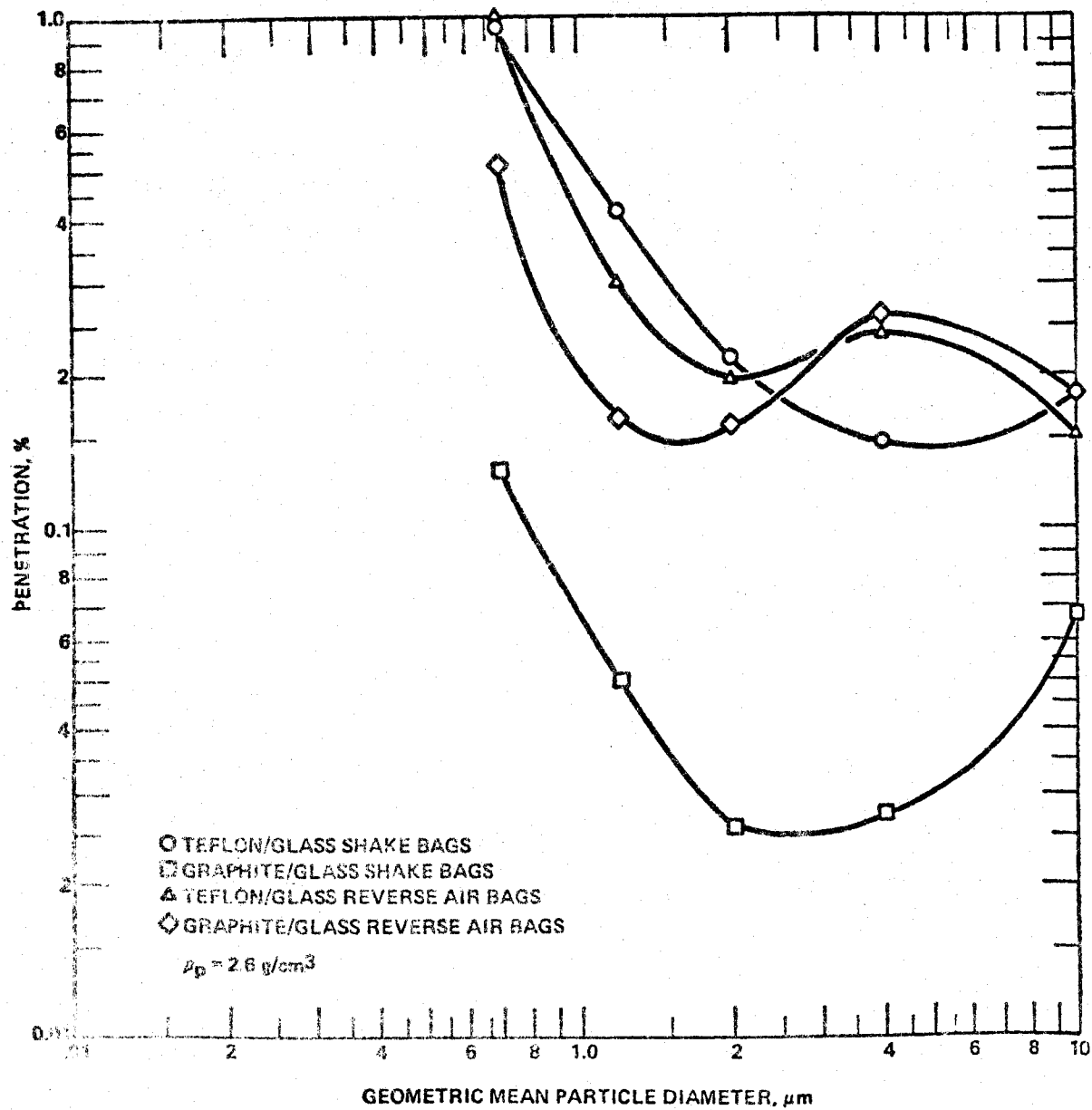


Figure 1. Average mass penetration vs geometric mean particle diameter.

## References

1. Hall, R. H. and Dennis, R., "Mobile Fabric Filter System Design and Field Test Results," EPA-650/2-75-059, (NTIS No. PB 246-287/AS), July 1975.
2. Opferkoch, R. E., "Particulate Control Mobile Test Units: First Year's Operation," EPA-600/2-76-042, (NTIS No. PB 251-722/AS), February 1976.
3. Zanders, D. L., "Particulate Control Mobile Test Units: Second Year's Operation," EPA-600/2-77-042, (NTIS No. PB 264-067/AS), January 1977.

AUSTRALIAN EXPERIENCE, FILTRATION OF  
FLYASH FROM VERY LOW SULFUR COALS

THIRD SYMPOSIUM ON FABRIC FILTERS  
FOR PARTICLE COLLECTION  
DOUBLETREE INN TUCSON, ARIZONA  
December 5-6, 1977

By  
A. C. LEUTBECHER  
MARKETING MANAGER, FABRIC FILTERS  
WESTERN PRECIPITATION DIVISION  
Los Angeles, California

## BIOGRAPHICAL NOTE

DEL LEUTBECHER is a graduate from Cleveland State University (1967) with a B.S. degree in Engineering Science. He has also attended Graduate School at Northern Illinois University, majoring in marketing. Del has eight years sales and marketing experience in the air pollution control field, specifically involved with scrubbers and bag filters, and presently is Marketing Manager, Fabric Filters for Western Precipitation Division of JOY Manufacturing in Los Angeles, California.

## AUSTRALIAN EXPERIENCE, FILTRATION OF FLYASH FROM VERY LOW SULFUR COALS.

---

### Abstract

This paper examines the Australian experience in applying fabric filters to coal fired boilers. Consequences of burning very low sulfur coal (0.3%-0.4%) are highlighted. Specific examples of shaker, reverse air and pulse jet cleaning mechanisms are discussed and experience with acrylic filtration media is detailed.

As can be seen by Fig. 1, Australian coal is quite different from that mined in the United States. U. S. coals classified as low sulfur generally run .7%-1.0% sulfur content. Coals with sulfur contents on the order of 0.6% to 0.7% are considered "high sulfur" varieties in Australia. Low sulfur coal is defined as containing approximately 0.3% sulfur. Given this extremely low sulfur content and the mild Australian climate, air heater gas outlet temperatures on efficient boilers can run as low as 220<sup>0</sup>F. At these conditions flyash is highly resistive and precipitator performance has been unsatisfactory. As an analogous situation opened the door to baghouse application for flyash collection in the United States, so, too, are the Australians turning to fabric filtration.

The single factor making the Australian experience so unique is low gas inlet temperatures to the baghouse. Inlet temperatures in the 250°F to 300°F range are not uncommon. This phenomenon of low inlet temperatures makes possible the use of synthetic fibers such as acrylic for filtration media.

The Electricity Commission of New South Wales has taken the technical lead in baghouse applications in Australia. A listing of experience to date is shown in Figure 2. This paper will discuss some of these installations in detail.

The first significant installation was commissioned in May of 1972 at the Tallawarra Power Station. This shaker type filter was installed on a pulverized fuel boiler and designed to handle 80,000 ACFM of flue gas at 270°F. The intent upon successful operation of this pilot unit was to retrofit the entire station with baghouses, amounting to four 30 MW boilers in Section "A" and two 100 MW boilers in Section "B". Specific design details of this pilot are shown in Fig. 3A. As can be seen, pilot experience was very good with pressure drop maintained at 3" W. C. and efficiency at 99.9%. This was accomplished at a gross filter ratio of 2.23/1 with a cleaning cycle initiated every thirty minutes. Based upon successful experience a 500,000 ACFM full scale baghouse was commissioned at Section "A" in September of 1974, and four 170,000 ACFM units at Section "B"

during the period March 1975 to March 1976. Design details are shown in Fig. 3B. Operating experience has been consistent with that of the original pilot unit.

Several comments are worthy of mention with regard to the fabric material utilized. Polyester bag material was judged to be unsuitable due to hydrolysis and subsequent acid attack. Although steps were taken to prevent moisture ingress, the possibility of accidental wetting such as economizer leaks cannot be excluded. In addition, high moisture conditions as occur during soot blowing have caused polyester hydrolysis. Acrylic fibers have demonstrated resistance to hydrolysis and acid attack. Acrylic fiber is, however, temperature sensitive and will support combustion. Necessary steps must be taken to prevent heating acrylic fiber in excess of 260<sup>0</sup>F by using air dilution and/or water sprays. As protection against air heater failure, bypass is recommended. Finally, care must be taken during operation and maintenance to avoid a dangerous fire as bags burn fairly readily. A full water spray or CO<sub>2</sub> fire protection system is recommended.

The specific bag recommended by the Commission is Draylon T, 12 oz/sq yd, 2X2 twill with a permability of 25-33.

As previously mentioned, there are three pulse jet installations in Australia at Wangi Station Units 4, 5 and 6. They are essentially identical installations as shown in Fig. 4.



Of the units tested, efficiencies have been in excess of 99.5%, however, problems have been reported. Pressure drop has averaged 5" W.C. This is primarily due to the high filter ratio and the Commission is recommending 3.5 - 4.0 ratios to conserve pressure drop and maximize bag life. The acrylic bags have experienced an embrittlement problem. It has been theorized that the cold, compressed cleaning air has caused localized condensation of flue gas and subsequent acid attack. Bag bleeding and visible puffing during cleaning have also been reported. The acrylic bags used were 18 oz/square yard needled felt with a permeability of 25 CFM/square foot/ $\frac{1}{2}$ " W.G.

The final pilot installation to be discussed is the reverse air cleaned baghouse pilot unit at Wangi Station Unit 5. Design conditions for this baghouse are shown in Fig. 5. As shown, this unit has four compartments of six bags each for a total of twenty-four bags. The bags are 8-inch diameter by 22-foot long Menardi 601T fiberglass with 10% Teflon B finish. Material is 9.5 oz/sq. yd., 3 X 1 twill with a permeability of 75.

The baghouse is designed so that one compartment is always off line in the cleaning mode. When a section is dampered off for cleaning it automatically goes into a 75 second null period. The collapse period is adjustable over a wide range, however, it currently is set very short (5-8 seconds) with the intention of providing more residual dust cake for acid dew

point protection. After collapse, the compartment goes into a second null period. This second null period can be quite long as all four compartments are never on line at once.

Overall, the unit has performed extremely well. Even with the short collapse period, pressure drop is maintained between 2-3" W.C. Efficiencies are very high. After 400 hours of service, outlet emissions were less than .006 gr/acf. The most recent test in October of this year was inconclusive in that emission levels were so low measurement was impractical. After some 3500 hours of operation, including 70 starts and stops (140 dew point excursions) the bags show no signs of wear or deterioration.

In summary, it is fair to say that since 1972 the technical experience with baghouses on very low sulfur coal burning boilers has been good. This paper has focused on two inter-related variables: cleaning mechanism and type of bag material. With regard to type of cleaning mechanism, the experience has been most favorable with the reverse air cleaned baghouse in terms of low pressure drop and projected bag life, with the shaker a close second. The pulse jet experience has not been good, however, some design modifications would give more favorable results.

The question of whether to use acrylic or glass bags is really the central issue as once this selection is made the cleaning mechanism follows logically. Acrylic bags have shown to be suitable at temperatures of 260<sup>0</sup>F and below. We can expect that with acrylic bags some type gas cooling will be required as well as an emergency bypass and a fire protection system. This auxiliary equipment may substantially change the economic balance, especially at shaker ratios of 3.0 and lower in favor of reverse air cleaning with glass bags. Glass bags with their higher temperature capability of 500<sup>0</sup>F are not as susceptible to temperature variations as may be found in Australia and do not present the fire hazard.

## TYPICAL COAL ANALYSIS

### U. S. LOW SULFUR WESTERN

<u>MOIST %</u>	<u>FIXED CARBON %</u>	<u>VOLATILE %</u>	<u>ASH %</u>	<u>SULFUR %</u>
8-10	40-50	35-40	7-14	.6-.9

### AUSTRALIAN LOW SULFUR

<u>MOIST %</u>	<u>FIXED CARBON %</u>	<u>VOLATILE %</u>	<u>ASH %</u>	<u>SULFUR %</u>
1-3	60-70	20-30	8-12	0.3-0.5

Fig. 1

ECNSW FABRIC FILTER INSTALLATIONS

Mo/Yr in Service	Station/ Boiler	Gas Flow ACFM	Nom. Gas Tempera- ture	Gross Ratio	Fabric Type	Cleanin Mechan- ism
May 1972	Tallawarra 4	80,000	290	2.23	Acrylic	Shake
Sept 1974	Tallawarra 1-4	500,000	290	2.10	Acrylic	Shake
March 1975	Tallawarra 6B	170,000	270	2.4	Acrylic	Shake
Aug 1975	Tallawarra 6A	170,000	270	2.4	Acrylic	Shake
Dec 1975	Wangi 4	320,000	260	6.8	Acrylic	Pulse
Jan 1976	Tallawarra 5A	170,000	270	2.4	Acrylic	Shake
Mar 1976	Tallawarra 5B	170,000	270	2.4	Acrylic	Shake
April 1976	Wangi 5	320,000	260	6.8	Acrylic	Pulse
June 1976	Wangi 1A	130,000	300	3.5	Acrylic	Shake
	Wangi 1B	130,000	300	3.5	Acrylic	Shake
	Wangi 6	320,000	260	6.8	Acrylic	Pulse
	Wangi 2A	130,000	300	3.5	Acrylic	Shake
	Wangi 2B	130,000	300	3.5	Acrylic	Shake
	Wangi 3A	130,000	300	3.5	Acrylic	Shake
July 1976	Wangi 3B	130,000	300	3.5	Acrylic	Shake
Oct 1976	Wangi 5	1,900	270	2.29	Glass	R/A

Fig. 2

ECNSW TALLAWARRA STATION

SECTION A PILOT UNIT

Gas Volume	80,000 ACFM
Gas Temperature	270 <sup>0</sup> F
Dust Loading	13 gr/cubic foot
Particle Size	4% less than 2.5 microns
Gas Cooling	Air dilution/water spray
Gross Filter Ratio	2.23/1
Net Filter Ratio	2.98/1 (one out for cleaning)
Number of Bags	330/compartment (1320 total)
Bag Size	6½" dia X 16'-6" long
Bag Material	Acrylic, Polyester
Cleaning Mechanism	Shaker

OPERATIONAL RESULTS

Pressure Drop	3" W.C. Flange to Flange
Outlet Emission	Less than .004 gr/ft <sup>3</sup> (99.9%)
Polyester Bag Life	400 hrs rapid deterioration
Acrylic Bag Life	Good, no acid attack after 14,000 hrs/340 starts

Fig. 3A

ECNSW TALLAWARRA STATION

SECTION A and B FULL SCALE

DESIGN VARIABLE	SECTION A	SECTION B
Gas Volume	500,000	170,000 ea.
Gas Temperature	290	270
Gross Filter Ratio	2.1	2.4/1
Number of Bags	7,200	2,880
Bag Size	6½" X 16'-6"	6½" X 16'-6"
Bag Material	Acrylic	Acrylic
Cleaning Mechanism	Shaker	Shaker

Fig. 3B

ECNSW WANGI STATION

UNITS 4, 5, 6

PULSE JET FILTERS

Gas Volume	160,000 ACFM
Gas Temperature	260 <sup>0</sup> F
Dust Loading	10 gr/cubic foot
Median Particle Size	12 microns
Gas Cooling	Air Dilution
Filter Ratio	6.68/1
Number of Bags	2,016
Bag Size	4½" dia X 10'-0" long
BAG Material	Draylon T Acrylic
Cleaning Mechanism	Pulse Jet

Fig. 4



ECNSW WANGI STATION

UNIT 5 PC BOILER

REVERSE AIR BAGHOUSE

DESIGN CONDITIONS

Gas Volume	1900 ACFM
Gas Temperature	260-270°F
Dust Loading	5-6 gr/acf
Avg. Moisture	4.67%
Median Particle Size	2 microns
Gas Cooling	none
Net Filter Ratio	2.29/1 (one out)
Number of Bags	24 (4 compartments)
Bag Size	8" Dia by 22'-0" long
Bag Material	(Menardi 601T glass) (with 10% Teflon B finish)
Cleaning Mechanism	Reverse Air

OPERATIONAL RESULTS

Pressure Drop	2½-3"
Outlet Emission	.005 gr/acf max.
Bag Life	3500 hrs - no visible deterioration (70 starts)

Fig. 5

DEMONSTRATION OF A HIGH VELOCITY FABRIC FILTRATION  
SYSTEM USED TO CONTROL FLY ASH EMISSIONS

By

John D. McKenna

and

Kathryn D. Brandt

Presented At

The Third Symposium on Fabric Filters for  
Particle Collection

Tucson, Arizona

December 5-6, 1977

## ABSTRACT

As a follow-up to a pilot plant study, a full scale investigation of applying high velocity fabric filtration to coal-fired boiler fly ash control was conducted. Two filter systems were separately applied to two 60,000 lb./hr. coal fired boilers. Performance evaluations conducted over the course of a year included total mass removal efficiency and fractional efficiencies. One filtration system employed Teflon felt as the filter media while the second system employed Gore-Tex, a PTFE laminate on PTFE woven backing. During the course of the year a limited number of glass felt and woven glass bags were introduced into the house containing Gore-Tex.

Performance results and economic evaluation indicate this method of fly ash control to be an attractive alternate to electrostatic precipitation.

## INTRODUCTION

In 1973 Enviro-Systems & Research, Inc. was awarded an EPA contract. The purpose of this contract was to determine the technical and economic feasibility of employing fabric filter dust collectors for fly ash emission control, particularly as applied to industrial boilers. Initially the program was jointly funded by the EPA, Kerr Finishing Division of Fabrics-America and ES&R, Inc.<sup>(1)</sup> The Kerr Plant located in Concord, North Carolina, served as the host site for the program and ES&R manufactured and installed the pilot facility. The pilot plant program provided short term performance data including dust removal efficiencies and pressure drops for a number of filter media.<sup>(2)</sup> This data and a preliminary economic analysis indicated that long term bag life and performance studies were warranted. EPA thus decided to award a contract for the full scale demonstration of this approach to fly ash control. The initial demonstration contract awarded to Fabrics-America with ES&R as the major sub-contractor called for ES&R to design, fabricate, install and then operate the two fabric filter units for a period of one year. Contract options called for subsequent additional long term operation of the units in order to test other filter media and also to evaluate the device as an sulfur oxide removal system.

## KERR - THE HOST SITE

The Kerr Finishing Division of FabricsAmerica is a textile dye and finishing plant located in the textile belt of central North Carolina.

Kerr's normal production schedule is three shifts per day, five days per week with 450-500 employees. Plant capabilities include processes to bleach, mercerize, dye, nap, finish and sanforize both cotton and synthetic fabrics, as well as cutting and preparing corduroy.

Two Babcock & Wilcox steam boilers are in operation at the Kerr facilities. Each has a design capacity of sixty thousand pounds of steam per hour and both are equipped with spreader stokers. Each boiler has a two-hour peaking capacity of seventy thousand pounds per hour. The design efficiency of these units is 82 percent. Based on the above parameters, the heat input for these units is 73.2 million BTU/hr. each. Both boilers are equipped with fans for supplying draft and unit number two, the unit tapped for the pilot plant stream, has overfire steam injection for better combustion control. In January, 1973, emission tests had been conducted on these boilers. The particulate emission rates were found to be approximately 130 pounds/hour versus an allowable of about 25 pounds/hour. Gas volumes were determined to be about 35,000 ACFM at a temperature of about 355° F. Thus the grain loading measured was about 0.4 grains per ACFM. Orsat analysis indicated 9.5% CO<sub>2</sub>, 10% O<sub>2</sub>, 0% CO and 80.5% N<sub>2</sub>. Coal analysis indicated the percent sulfur to be about 0.6%.

## THE HIGH VELOCITY FILTER

A schematic of the fabric filter dust collector is shown in Figure 1. As shown, the unit is about 10 feet wide by 27 feet high. It is of modular construction and the length increases as the number of modules increase. Each module consists of two thirty-six bag cells as shown in Figure 2. Each additional module adds 3 feet 4 inches to the length of the house. One baghouse may contain as many as fifteen modules and thus house 1,080 bags with a total of 12,400 square feet of filter media.

The bags are 5 inches in diameter and 104 inches long, giving each bag 11.5 square feet of cloth. The bags are set into the tube sheet by the use of two snap rings incorporated into the bag itself. The snap rings lock in place,

# General Arrangement SD-10

Not For Construction Purposes

## Pyramid Hopper

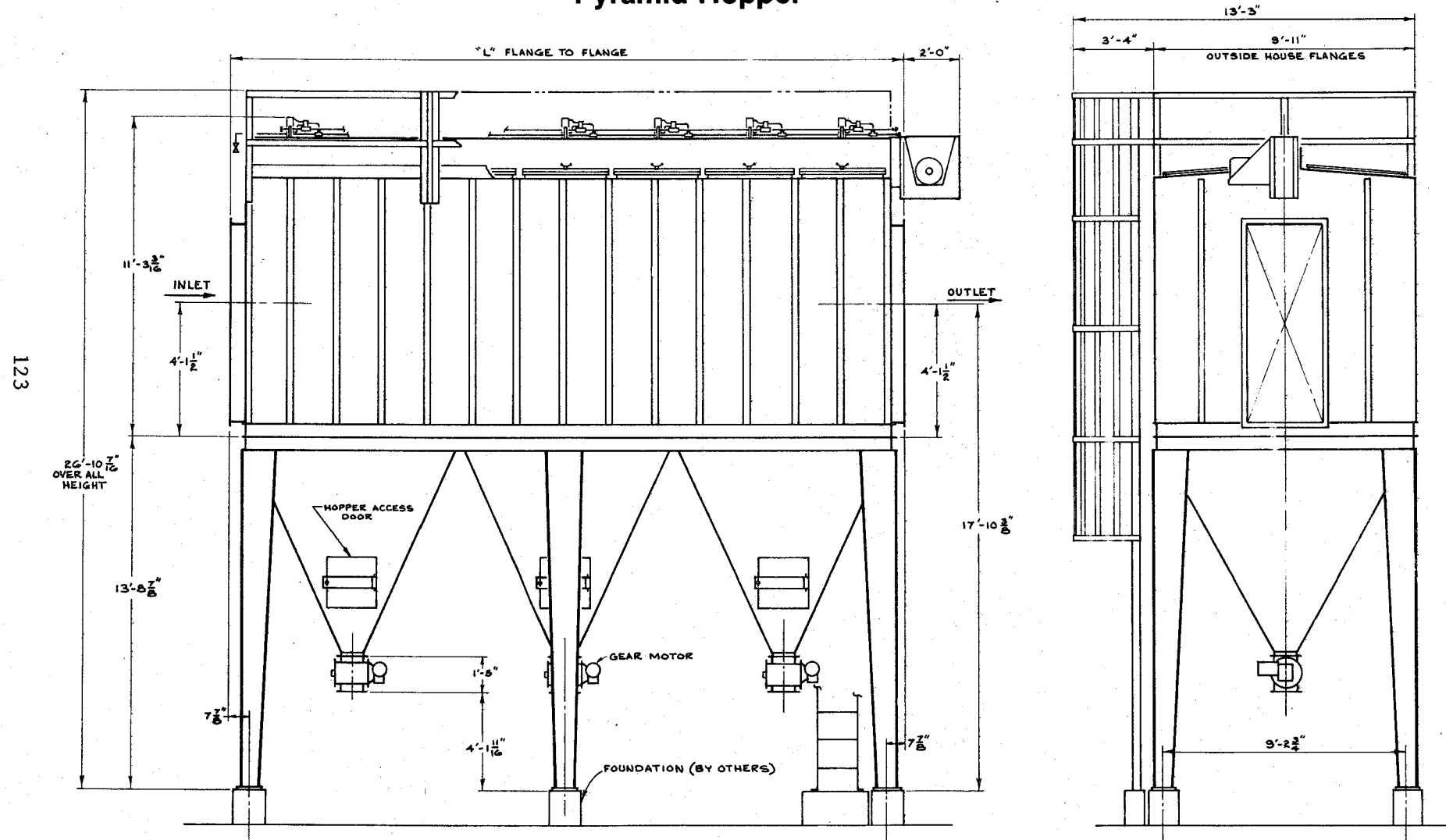


Figure 1

SD-10 General Arrangement With Pyramid Hoppers

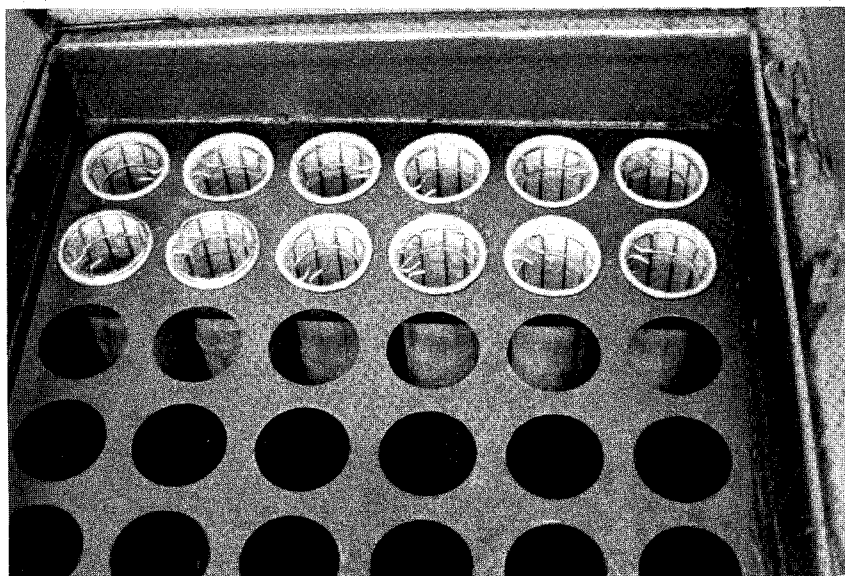


Figure 2  
Fabric Filter Module Cell

one above and one below the tube sheet. A cage is set inside the bag and keeps the bag from collapsing. The dust laden gas enters one end of the unit, as shown in Figure 3, passes through the tapered duct, into the classifier, and then through the bags. The classifier forces the dirty gases to change direction 90°, then 180°. This quick directional change forces the larger and heavier particles out of the flow so that they fall directly into the hopper. The gas flows through the fabric filter into the center of the bags (Figure 4), leaving the particulate on the outer surface of the bags where it is removed periodically during the cleaning cycle. The clean gas then flows up and out through the center of the filtering bag into a center exit plenum via an open damper in the cell above the tube sheet. The bags are cleaned one cell (36 bags) at a time by activating the pneumatic cell damper. See Figures 5 and 6. When the damper is in the up position, the flow is through the bags from the dirty side to the center plenum or clean side. When the damper is dropped to the down position, the flow is from the cleaning gas plenum through the bags to the dirty side or hopper.

The cleaning system employs a unique hybrid method referred to as the Shock-Drag Cleaning System, designed to prolong bag life by minimizing distortion of the fibers.

During the cleaning cycle, clean gas enters the cell through the pneumatic damper. The clean gas is forced down the filter bag, opposite to the normal flow direction. The bag expands with a shock (Figure 5) so that the cake is cracked and the particulate falls off the bag into the hopper. After the shock has expanded the filter bag and broken off the cake, the clean air continues to flow providing a drag (Figure 6) which pushes and pulls the dust particles away from the fabric. The smaller particles are thus forced out of the fabric and fall into the hopper for removal from the unit. Damper system and control panel arrangements allow for variations in main gas volume, reverse-air volume, duration of cleaning and frequency of cleaning.

#### THE PILOT PLANT

In the summer of 1973 a pilot scale investigation was initiated with the purpose of determining the techno-economic feasibility of applying a fabric filter dust collector to coal-fired industrial boilers. The pilot facility,



STEP 1 - THE CLASSIFIER

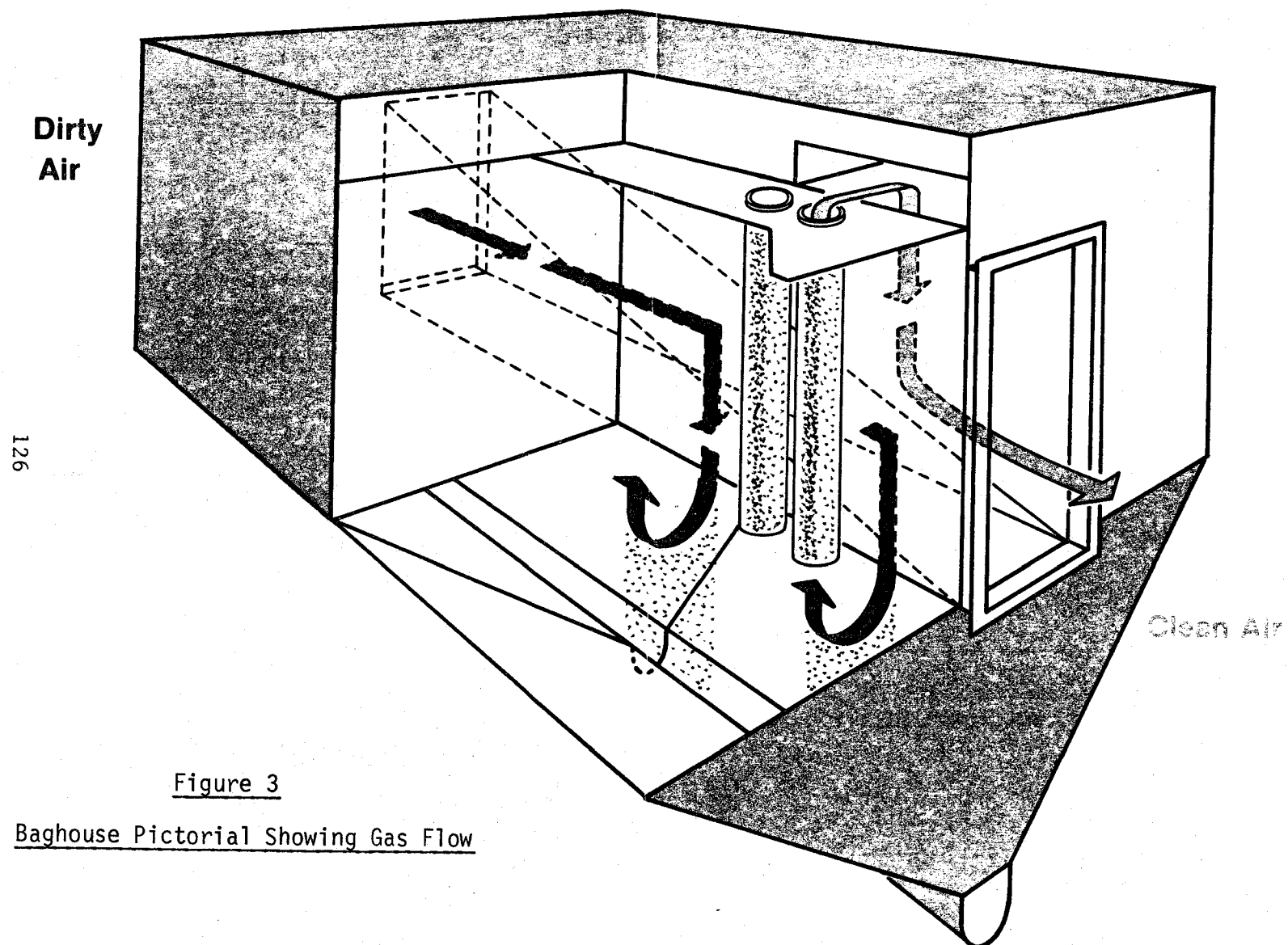


Figure 3

Baghouse Pictorial Showing Gas Flow

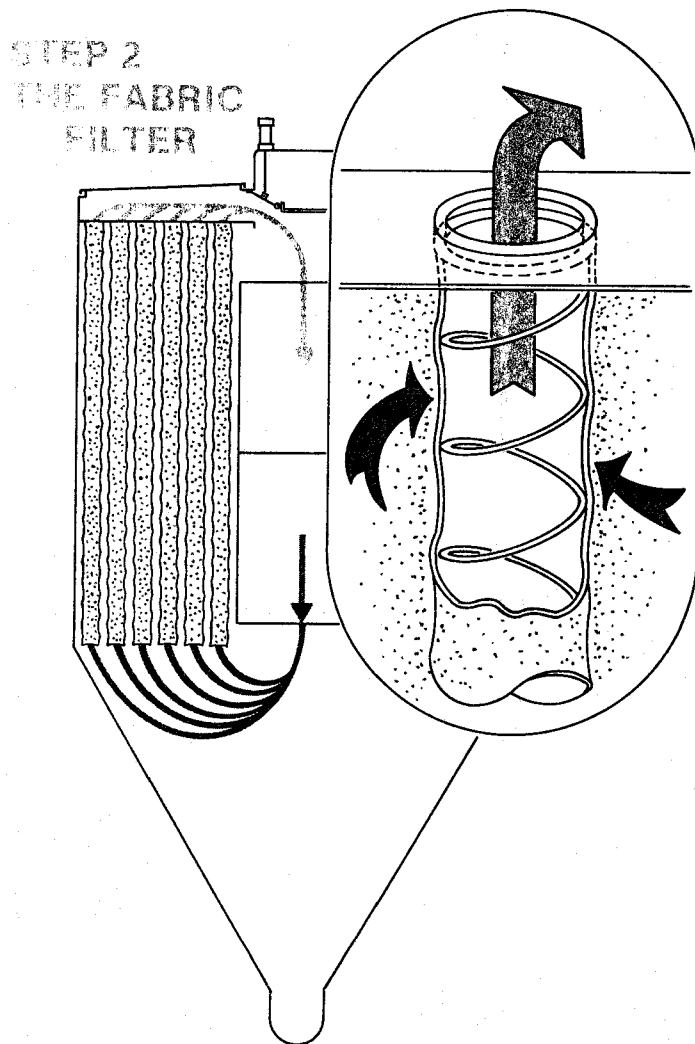


Figure 4

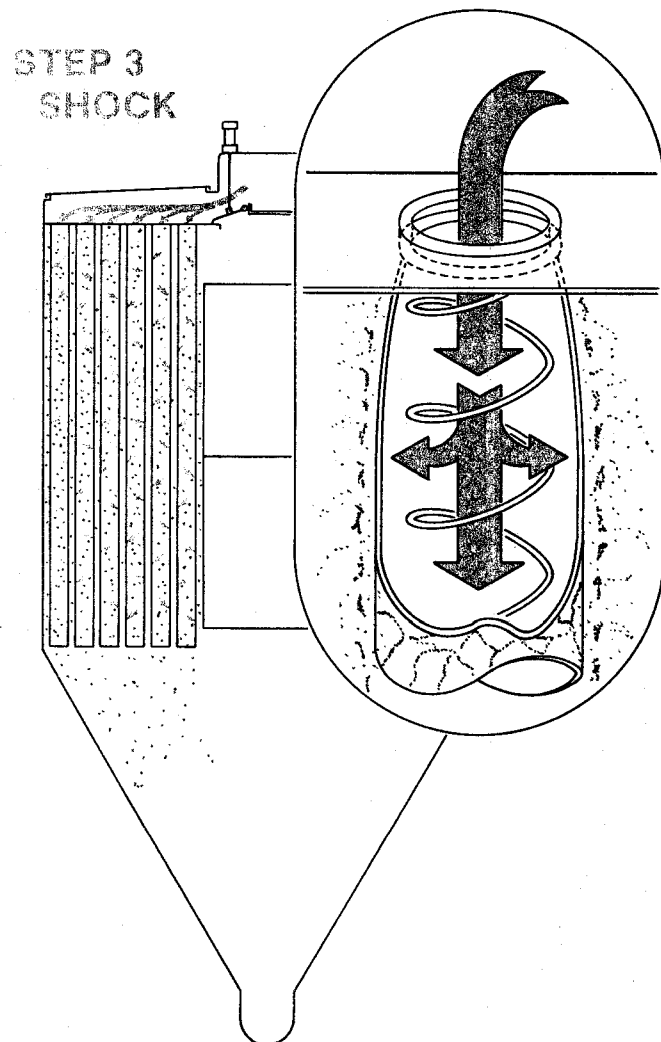


Figure 5

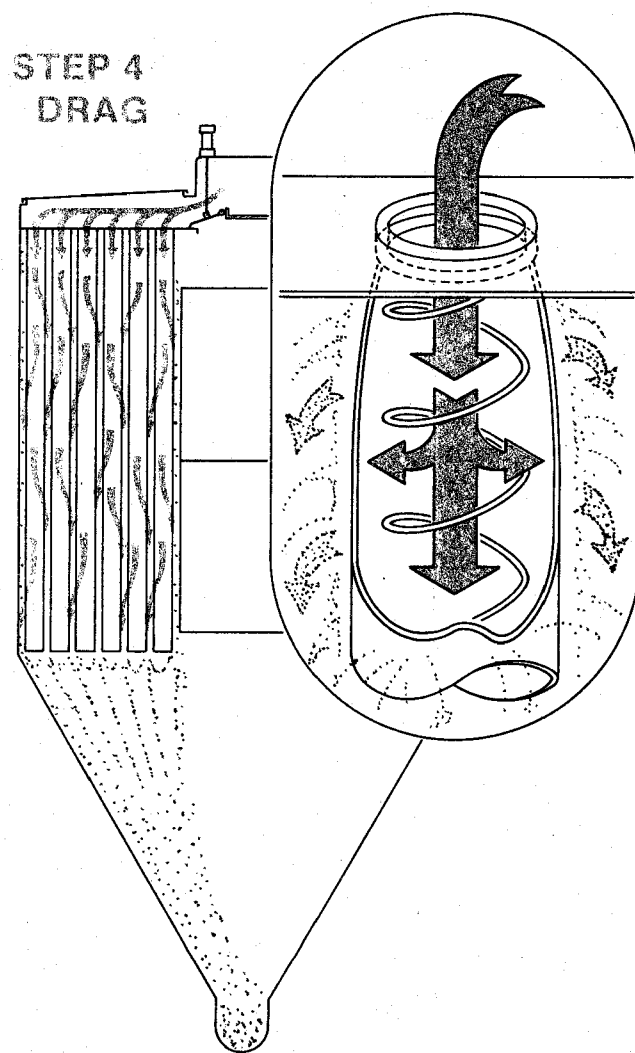


Figure 6

installed on a slip stream of Kerr's number two boiler, was to handle 11,000 acfm when operating at an air-to-cloth ratio of 6/1. Figure 7 shows the pilot facility. This prototype facility was actually a two module commercial size unit containing five inch diameter 104 inch long bags. Thus, future scale up problems were minimized.

The filter media evaluated were Nomex<sup>(R)</sup> felt, Teflon<sup>(R)</sup> felt (2 styles), Gore-Tex<sup>(R)</sup> and Dralon-T<sup>(R)</sup>. Fractional efficiency was determined using an Andersen inertial impactor for the four filter media at three A/C levels. The effect of cleaning gas volume on outlet loading and pressure drop across the bags were evaluated. In addition, studies of the effect of cleaning frequency and duration were conducted. The overall technical conclusion was that all four media tested could achieve outlet loadings meeting state code requirements regardless of the air-to-cloth ratio (apparent velocity). As the air-to-cloth ratio increased, both the pressure drop and the outlet loadings increased. See Figures 8 and 9.

Installed, operating and annualized costs were determined as shown in Figures 10, 11 and 12. These costs were developed from the operating characteristics obtained plus assumptions regarding bag life. They were then compared with precipitator costs developed for the same site. See Figure 13. This pilot plant program and economic analysis led to the conclusion that fabric filter dust collectors are suitable for control of fly ash from stoker fed coal fired industrial boilers in terms of both dust removal efficiency and operating pressure drop. The main question left unanswered was what bag life is achievable with continuous service. If two year bag life could be achieved, even with Teflon felt -- the most expensive bags, fabric filters appear economically more attractive than electrostatic precipitators for industrial coal fired boiler applications.

Of the four filter media tested, Teflon felt and Gore-Tex were selected as the first to be tested for bag life. The Dralon-T was not included initially because of the maximum temperature limitation of about 280° F and the Nomex was omitted because lab analysis of bags used in the pilot program indicated deterioration of the fiber due to acid attack. Of the two recommended for bag life studies, Teflon felt had no indication of any potential life problems while

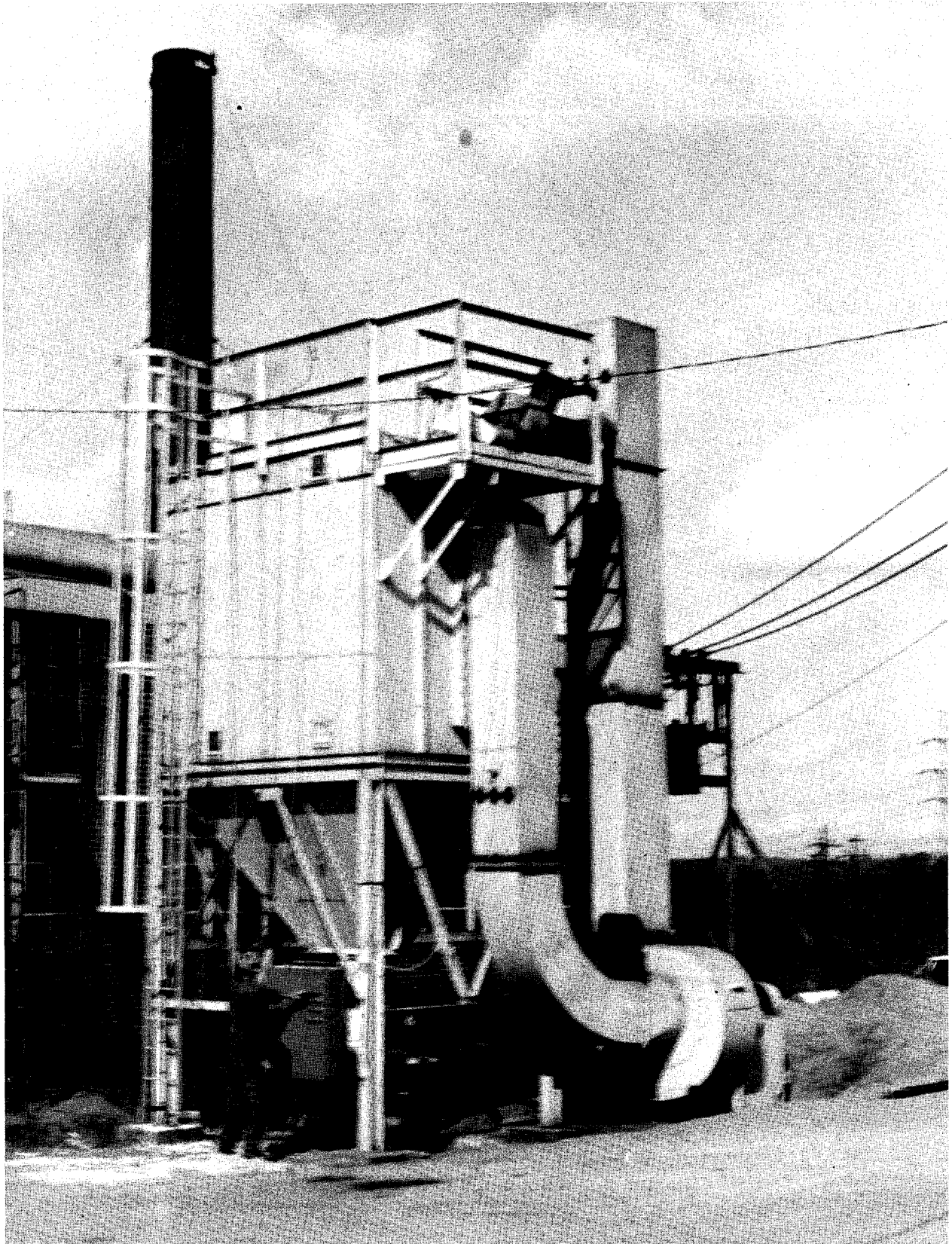


Figure 7   Kerr Pilot Plant Photo

Figure 8  
Outlet Concentration  
vs.  
Air-to-Cloth Ratio for Various Bag Materials

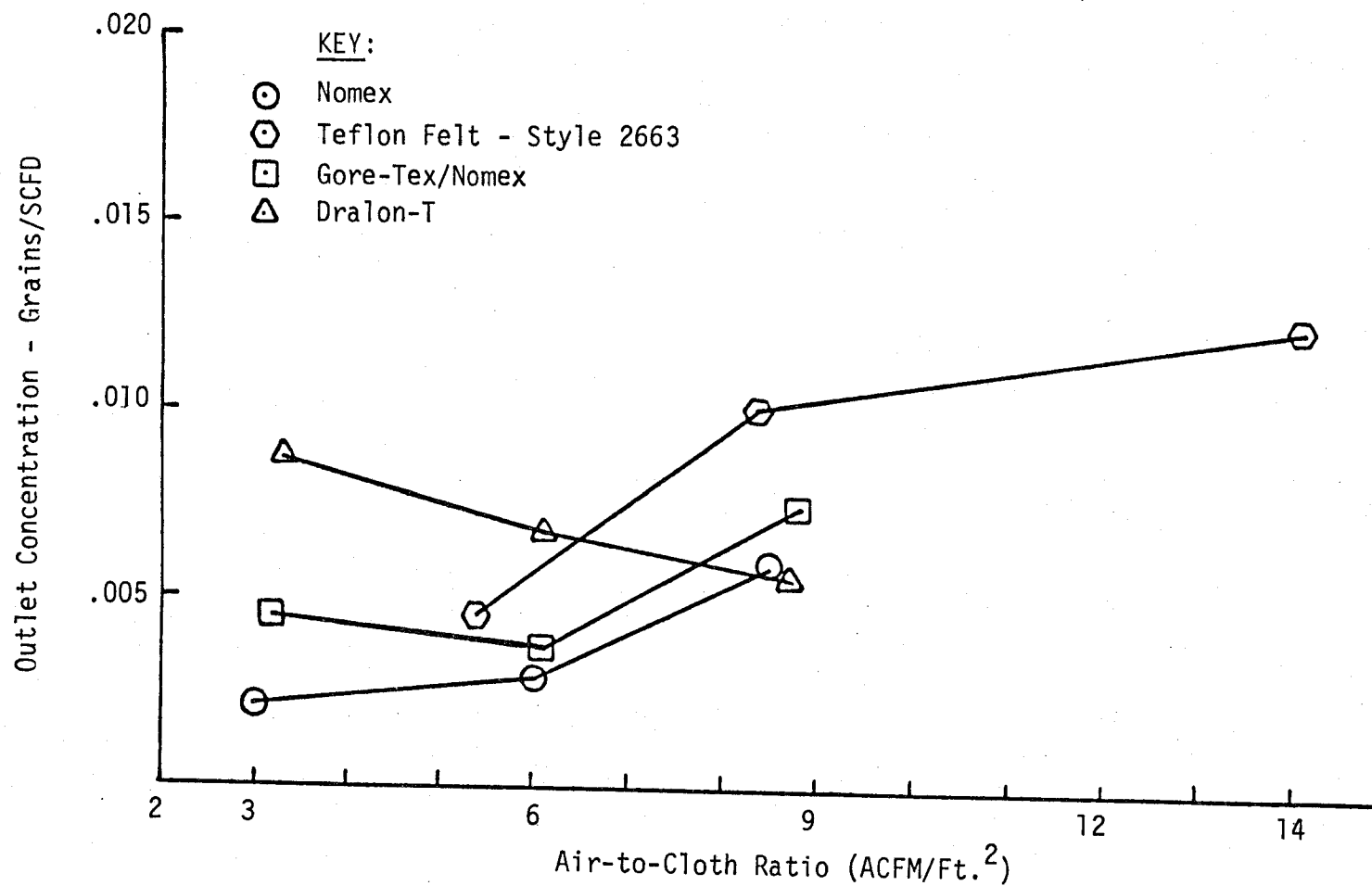


Figure 9  
Comparison of Operating Pressures for Various  
Bag Materials

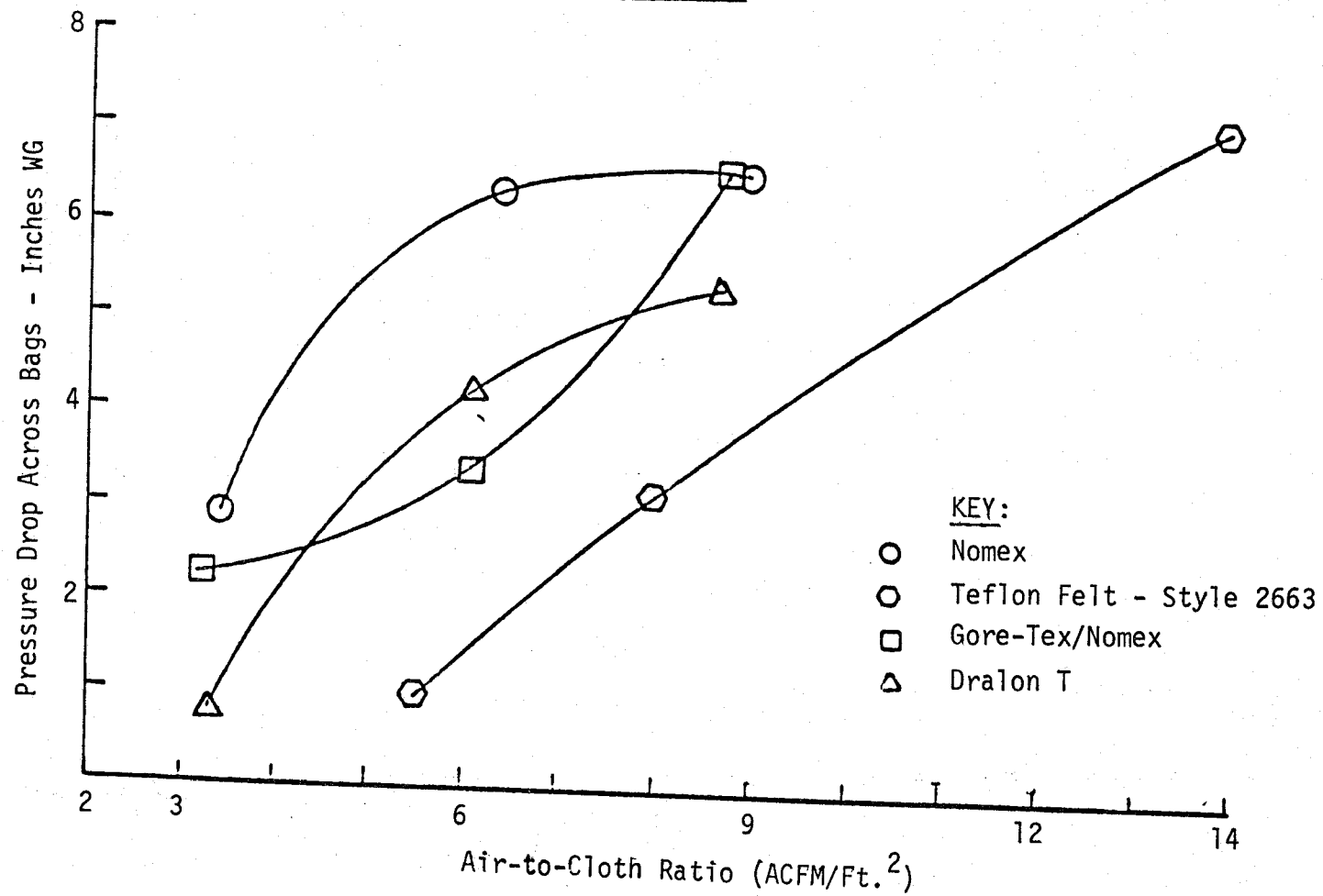




Figure 10

Installed Costs vs. Air-to-Cloth Ratio

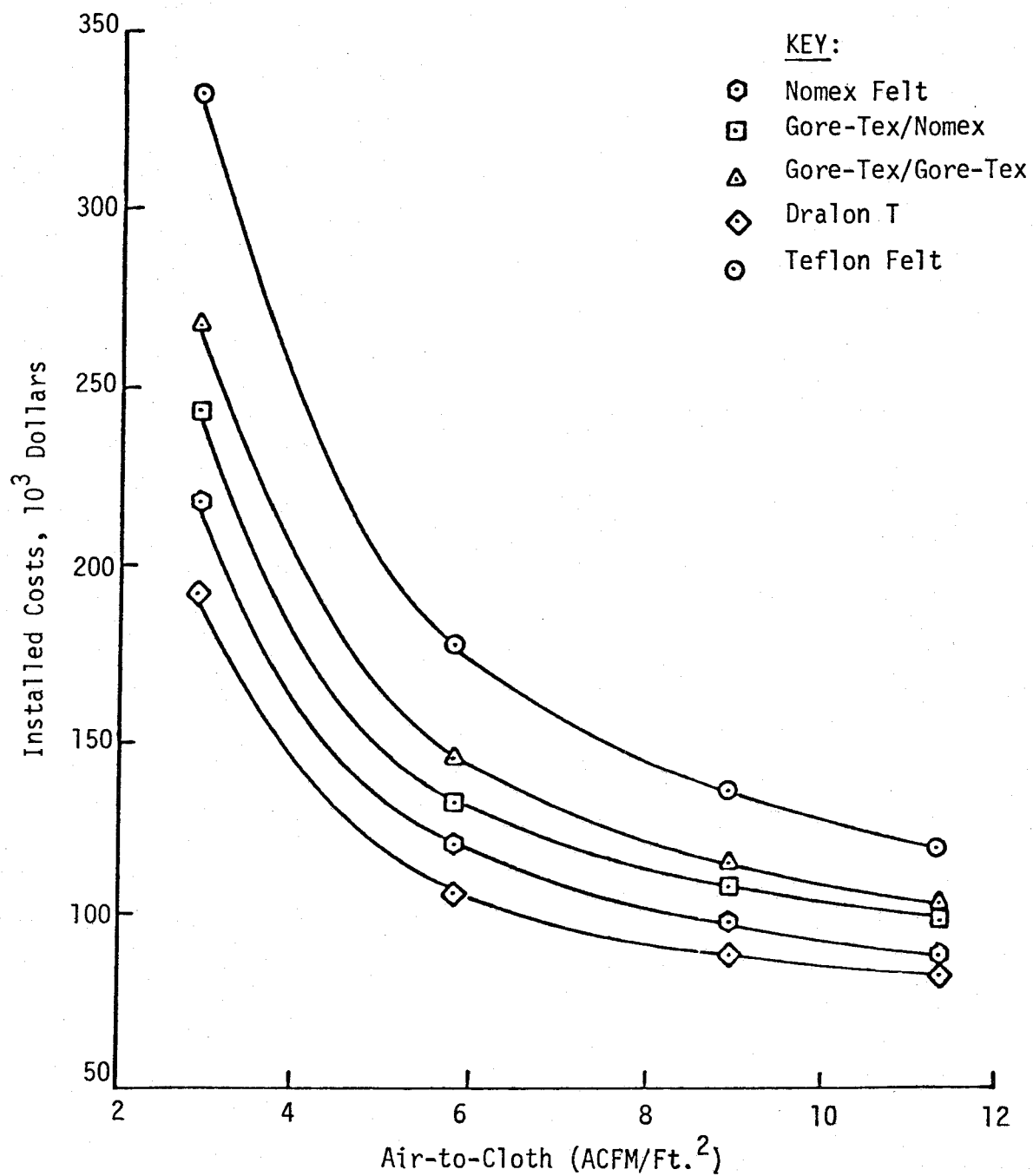


Figure 11  
Operating Costs vs. Air-to-Cloth Ratio

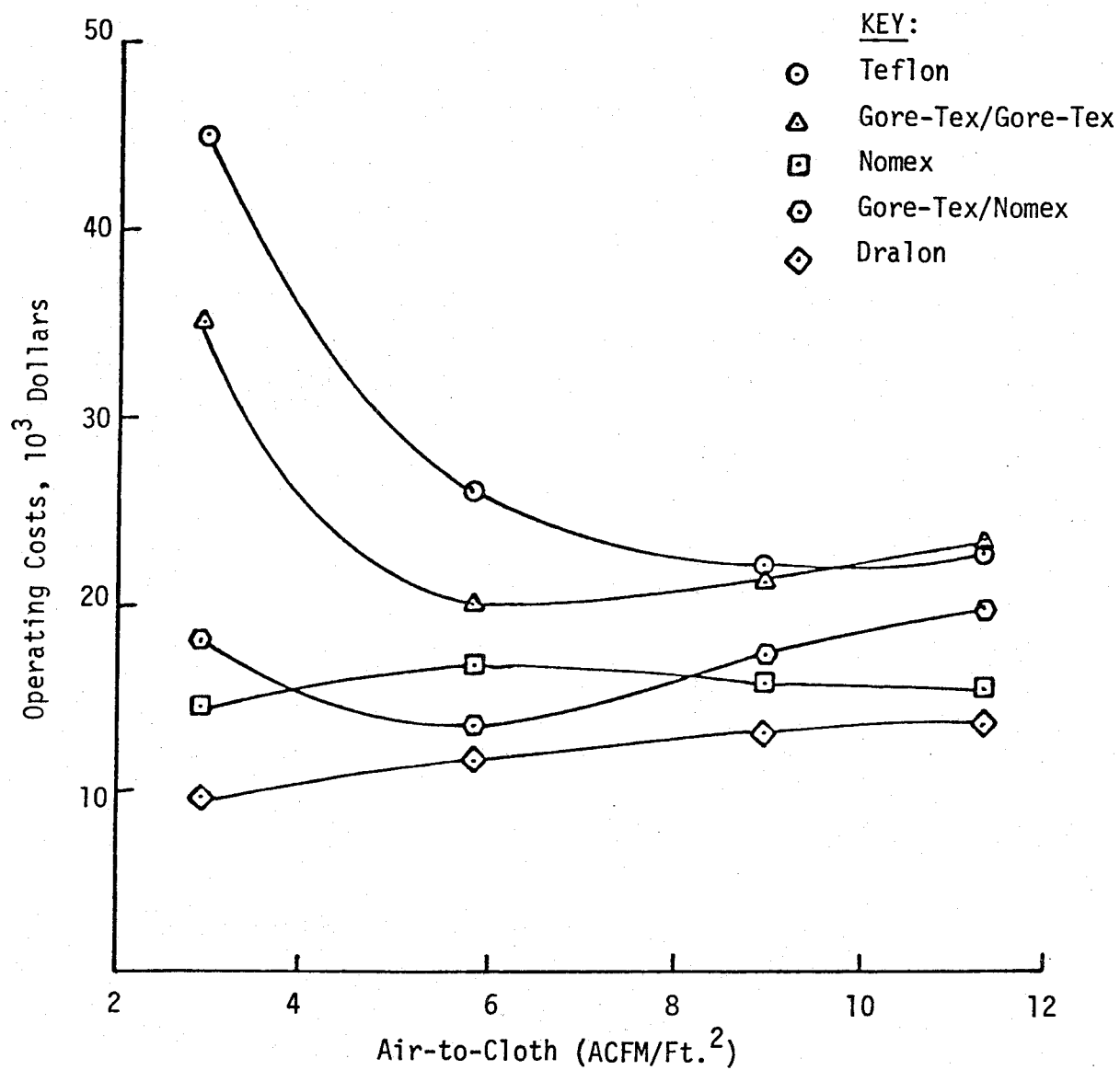


Figure 12

Teflon Felt

Annual Operating Cost vs. Air-to-Cloth Ratio  
for Different Bag Life Assumptions

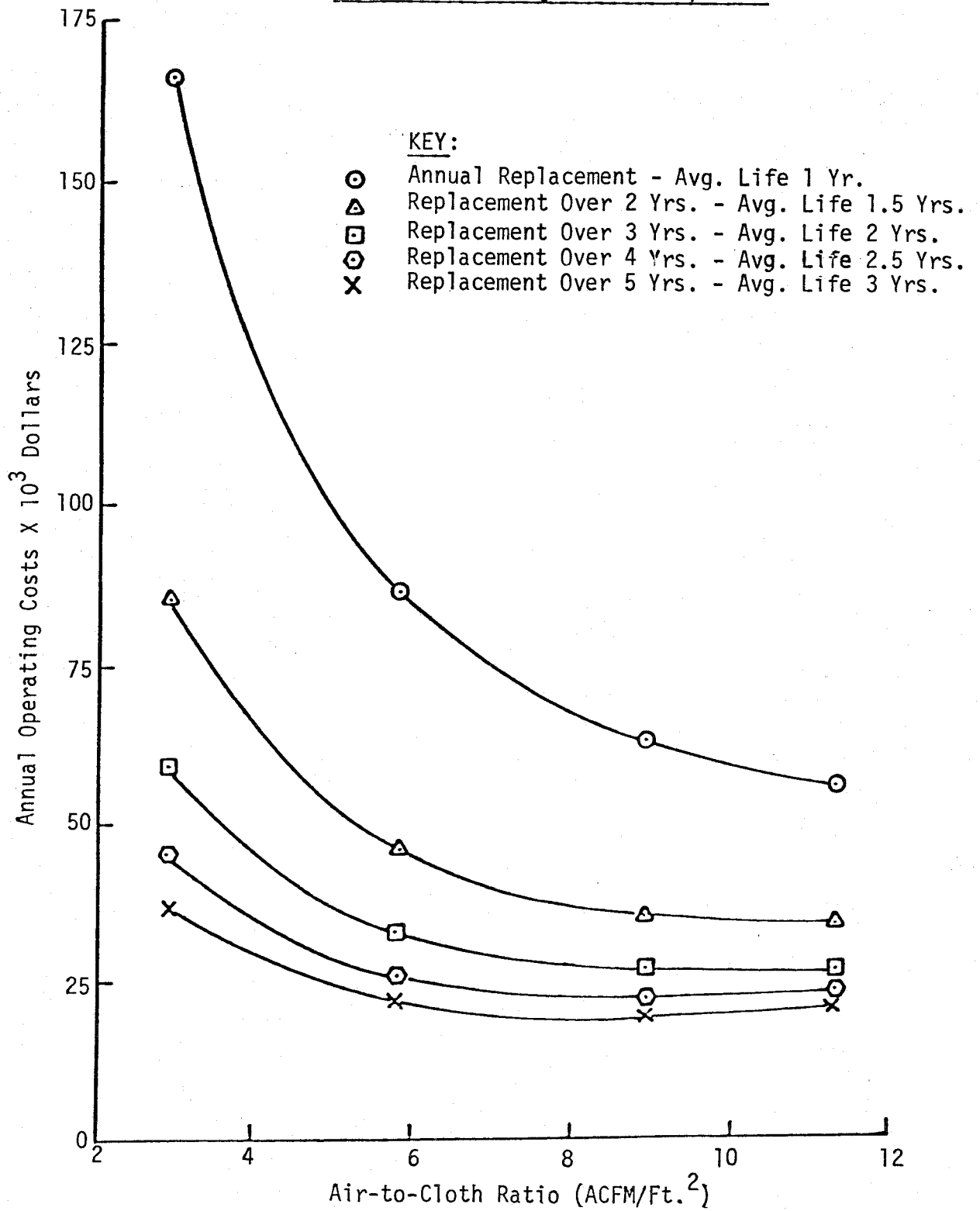
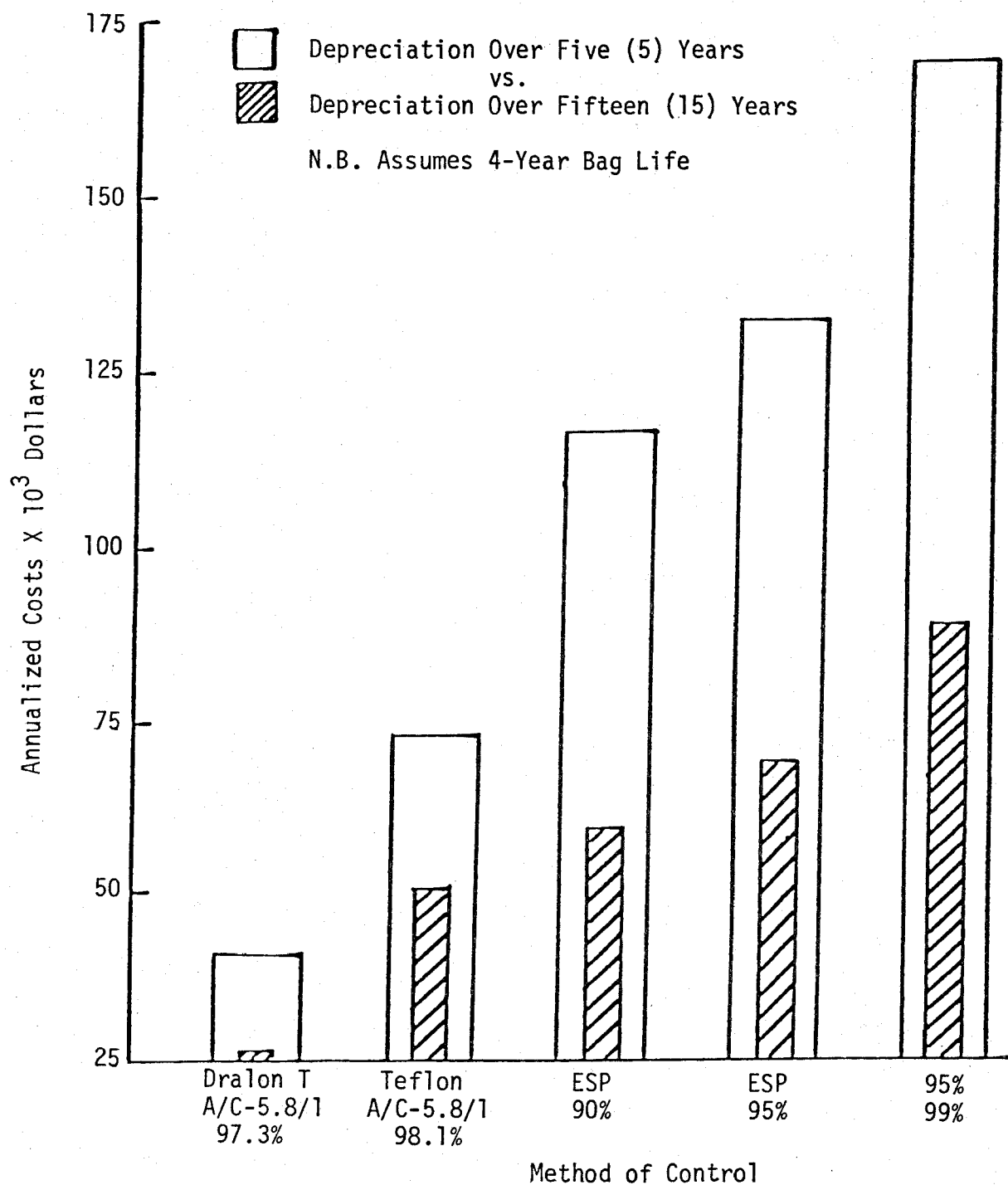


Figure 13

Annualized Cost Comparison



Gore-Tex had torn in a matter of days when used with a spiral cage. This problem was overcome by use of a rigid cage.

### FULL SCALE OPERATION

In 1976, two full scale fabric filter dust collection systems were designed, fabricated and installed on each of the two 60,000 lb/hr Kerr boilers in Concord, North Carolina. In December of 1976, both dust collectors were brought on stream under an EPA Demonstration Program (Contract No. 68-02-2148) with FabricsAmerica being the prime contractor and ES&R the major subcontractor. Figure 14 is an artist rendition of the full scale baghouse. ES&R was contracted to provide a turn-key system. This contract included system design, fabrication of ductwork and baghouses, supply and installation of all system components, start-up and testing of the units for a minimum of one year. The system was designed to include features accommodating the planned test program. Long straight duct runs were provided at both the inlet and outlet, platform and stair access to all major test ports, a sophisticated separate control house and a penthouse over both fabric filter dust collection systems were provided. The penthouse covers the outlet test ports, thus allowing testing in inclement weather at the points where the major share of the testing is to be done.

Each unit was constructed of a 10 gauge mild steel house and 3/16" mild steel hoppers. Pyramid hoppers were chosen to eliminate potential problems with screw conveying of the collected fly ash. Two inches of Fiberglas insulation with a sheet metal skin overlay was installed on both house and hopper at the factory. Houses and hoppers were shipped from Roanoke, Virginia to Concord, North Carolina by truck. Figure 15 shows one house leaving the factory. Figures 16 and 17 show one of the houses being lifted onto its hopper. Figure 18 shows the system with all major hardware elements complete. The common penthouse is shown covering both baghouses and in the foreground the control house is seen. The dust collection system control panel within the control house is shown in Figure 19. A system schematic is provided in Figure 20. As is shown in this figure, the dust collection system is brought on line by closing a boiler stack damper and opening a system inlet damper, the flue gas then passes into the inlet duct, down by an auxiliary gas fired heater into a center baghouse inlet plenum, the dust laden gas then enters the hopper turns

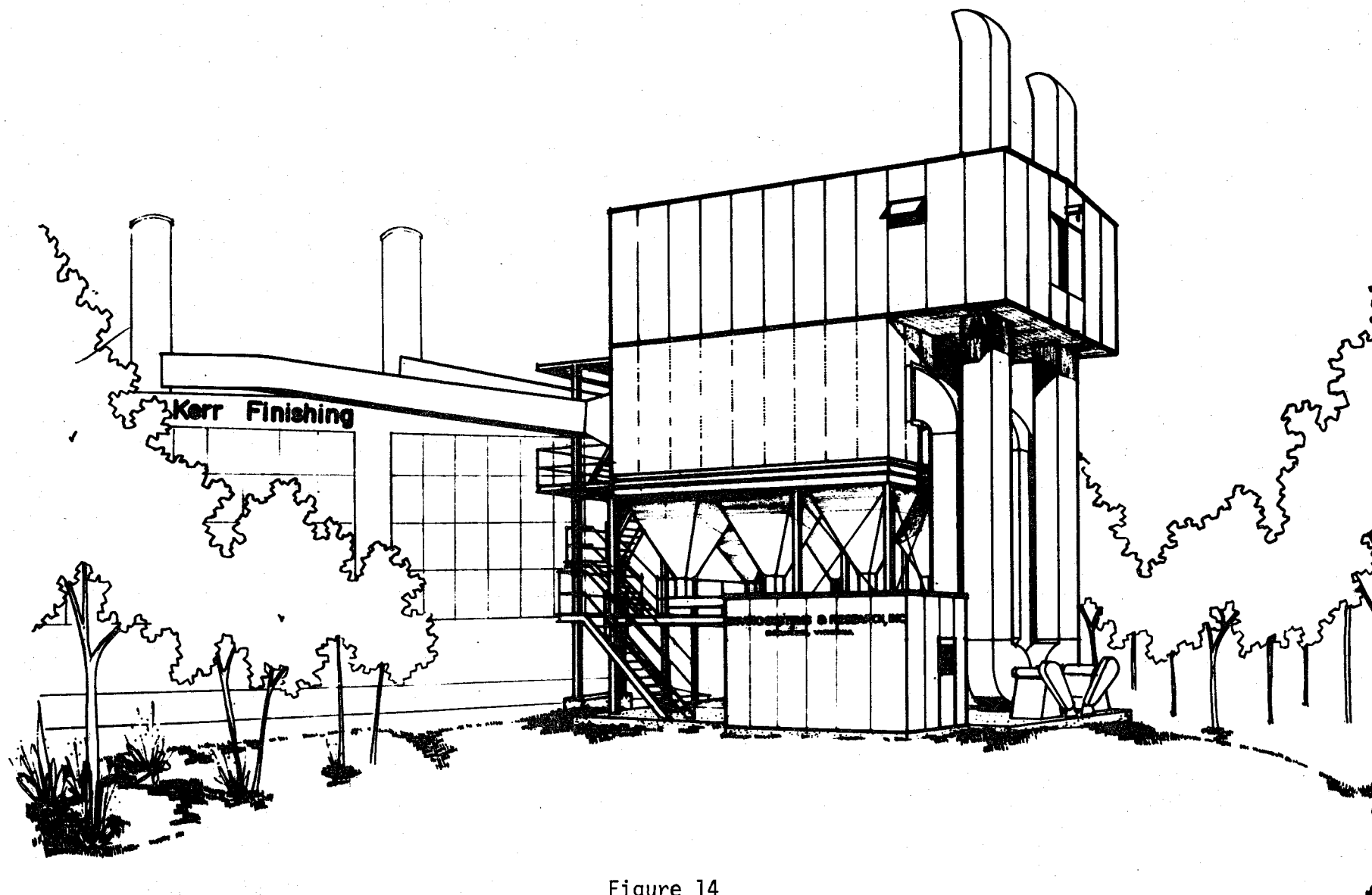


Figure 14

**EPA DEMONSTRATION OF THE ENVIRO-SYSTEMS FABRIC FILTER SYSTEM  
AT KERR FINISHING DIV. FABRICSAMERICA, CONCORD, NORTH CAROLINA**

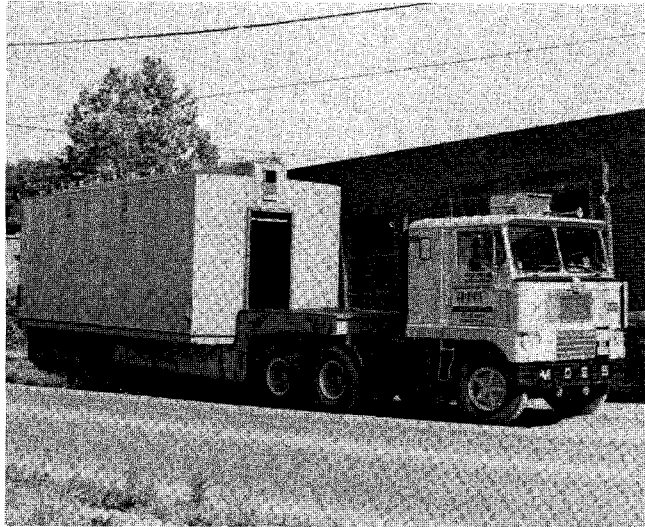


Figure 15

One House On Truck

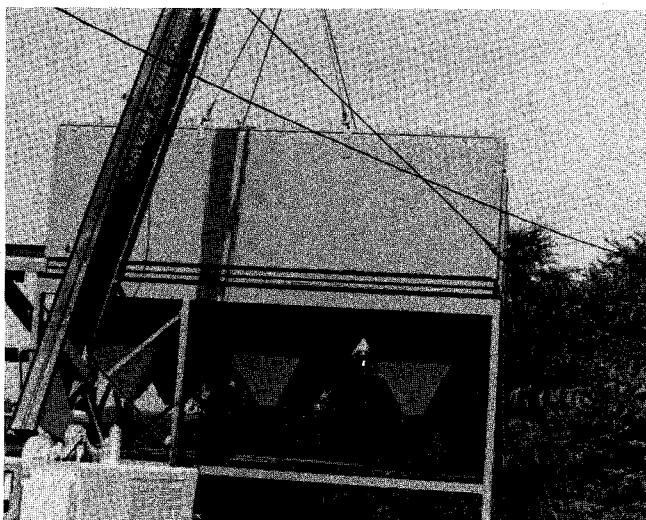


Figure 16

House Being Lifted Onto Hopper - Far View



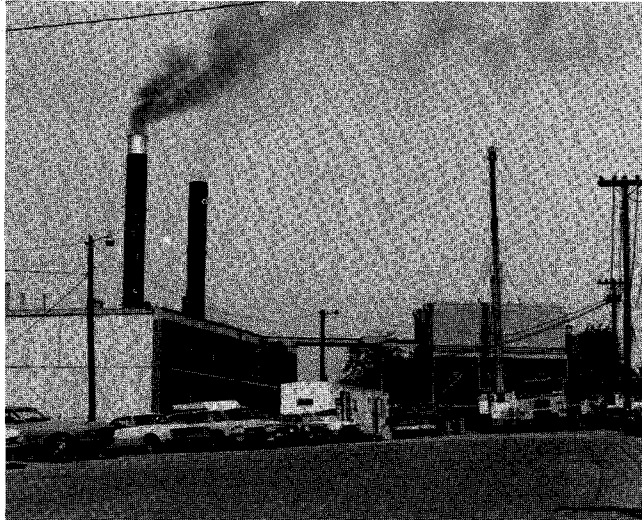


Figure 17

House Being Lifted Onto Hopper - Near View

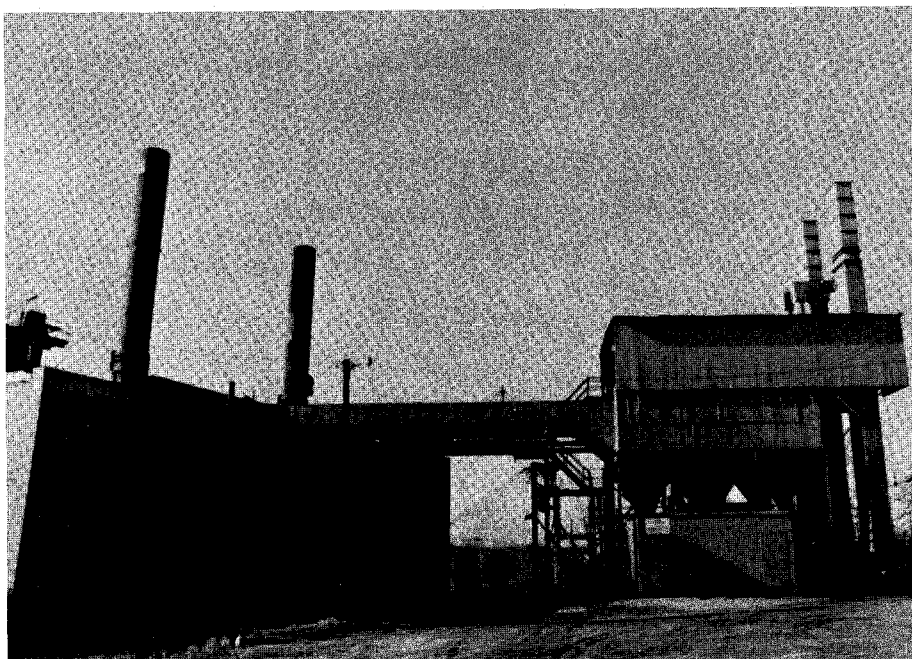
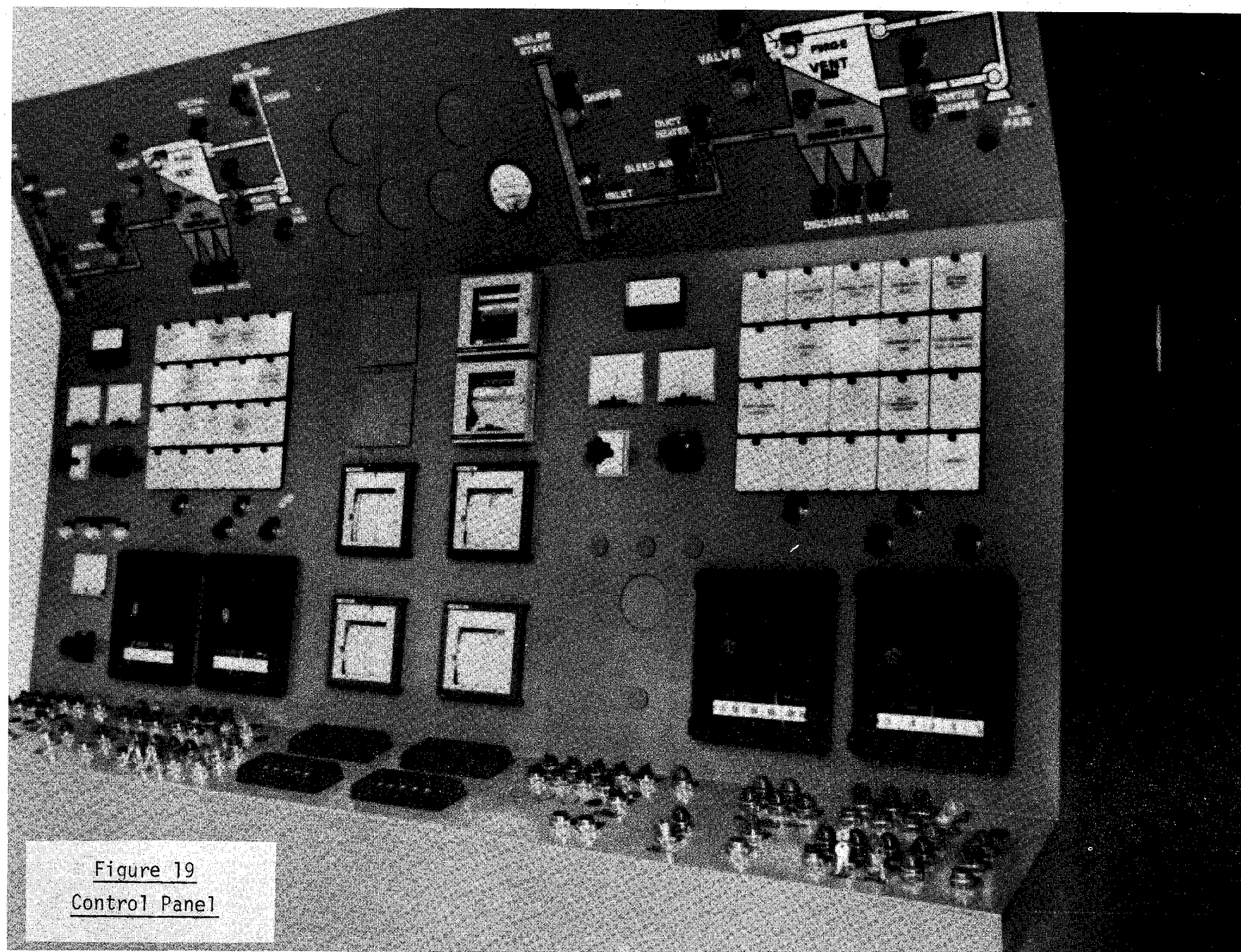


Figure 18  
Completed System



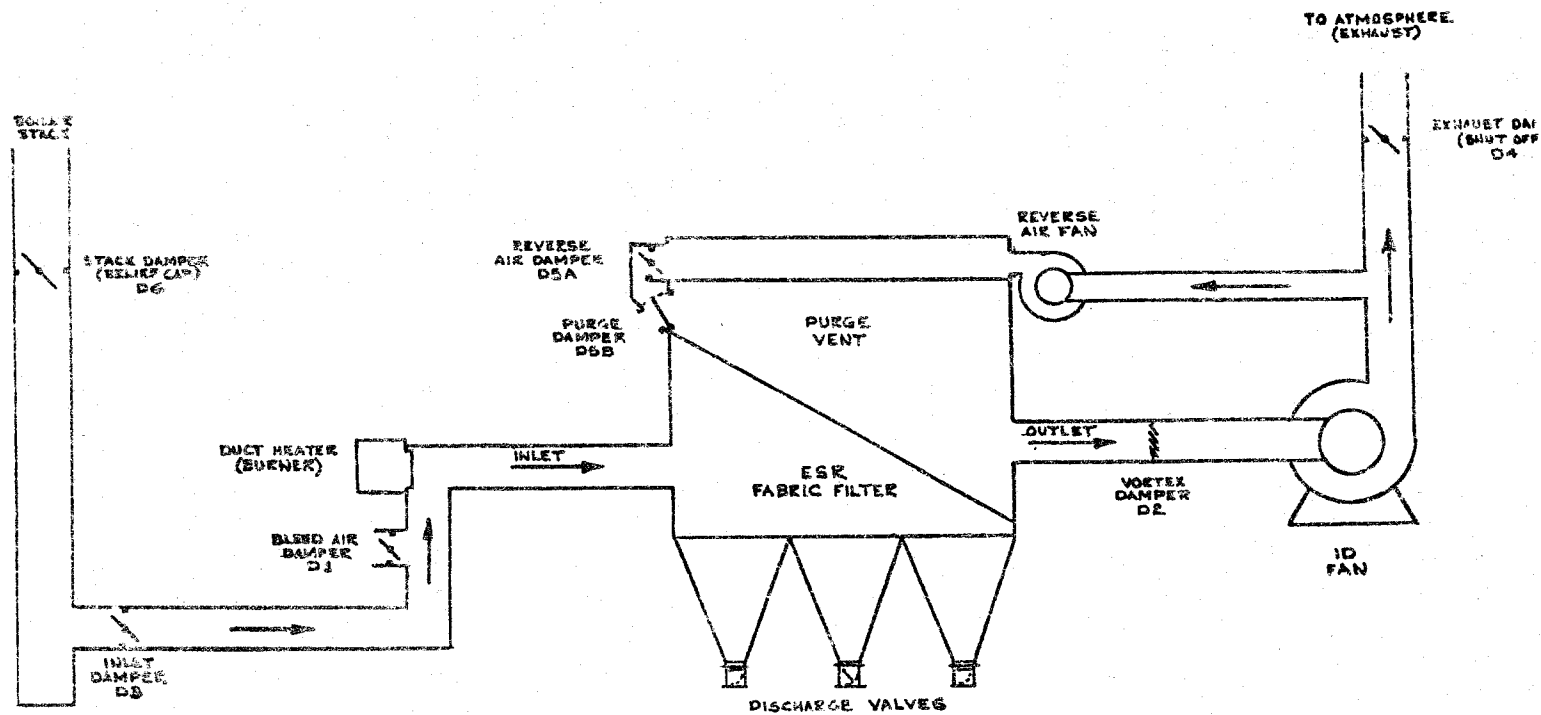


Figure 20

Fabric Filter Schematic

and comes up to the filter bags. Once it passes thru the filter media, the now clean gas passes into the exit plenum thru the exit duct, a vortex damper and out the main system fan to the dust collection system stack. A portion of the cleaned flue gas is drawn from the stack by a separate smaller cleaning fan and returned to the system to be used in backflushing the bags during cleaning. The auxiliary heater can be employed to preheat the house prior to baghouse start-up and it can also be employed to purge the house at shut-down. The vortex damper is employed to maintain a predetermined pressure at the boiler stack in an attempt to prevent the dust collection system pressure drop fluctuations from influencing the boiler operation. The control system includes automatic preheat, start-up and purge mode and operation of the vortex is also automated. The system is arranged so that the entire operation of both baghouses is controlled from the console located in the control house. When set up for automatic operation, either baghouse can be started and stopped from controls located in the boiler house, however, provision was included on the control house console for locking-out the boiler house start function. Alarms and an automatic shut-down have been included for the functions shown on Table 1. A number of temperatures and pressures are permanently recorded. These include the inlet and outlet temperature of each house and the pressure drop across each house and main fan. One of the two houses is equipped with an inlet and outlet transmissometer.

The two houses are identical in terms of the basic hardware. Each house contains eighteen (18) cells with thirty-six (36) 5" dia. X 8' 8" long bags in each cell, thus both houses contain a total of 7,440 square feet of cloth. Initially, House No. 1 contained 648 Teflon felt bags and House No. 2 contained 648 Gore-Tex bags. During the first year of operation one cell (36 bags) of Gore-Tex was replaced by an experimental felted glass media and subsequently a second cell of Gore-Tex bags was replaced by a 26 oz. woven glass media.

#### DEMONSTRATION PROGRAM PURPOSE AND OBJECTIVES

The purpose of the demonstration program is the testing of a full scale demonstration fabric filter system installed on an industrial size coal fired stoker boiler. The baghouse system will be operated and tested over the duration of the program to determine general operating parameters, bag life data and economic factors necessary for making techno-economic evaluations.

Table 1  
Alarms and Shut-Down Functions

<u>Function</u>	<u>Alarm Only</u>	<u>Alarm &amp; Shut-Down</u>
Bag Cleaning on Manual	X	
Boiler House Stop		X
Control House Stop		X
System Fan Below 1400 RPM		X
RA Fan Off	X	
Hopper Full	X	
Heater Off	X	
Pneumatic Air Low	X	
Stack Pressure Out of Range		X
Phase Monitor Tripped	X	
Inlet or Outlet Temp. High		X
Dryer Off	X	
Alarm Horns Off	X	

The objectives of the program are to demonstrate the feasibility of applying fabric filtration to industrial size coal fired stoker boilers and to accomplish the following:

Obtain operating data that would be generally useful for application engineering.

Obtain operating data and bag life data necessary in making techno-economic evaluations.

Determination of the efficiency of removal for specific particle size ranges as a function of filter media on-stream duration.

Determination of filter media property changes as a function of bag on-stream duration.

An economic evaluation comparing capital, operating and annualized costs of baghouses for the filter media tested.

#### RESULTS: COMPARISON OF FULL SCALE AND PILOT UNITS

The data gathered at this time indicates similarity between full scale and pilot plant operations. The outlet particle sizing achieved with Andersen inertial impactors seem to approximate the results obtained with the pilot study for Teflon felt; however, demonstration tests at only one air-to-cloth ratio have been obtained. Outlet grain loading values for Teflon felt acquired via Andersen impactor confirm pilot plant results although four values from late August 1977 were higher. Andersen outlet grain loadings calculated for the Gore-Tex bags showed results higher and lower than the pilot plant value of 0.004 grains/SCF but all values were below 0.01 gr/SCF. The pressure drop across the house is somewhat higher for the full scale plant than for the pilot plant; however, the relative position of the pressure drop curves for different bag materials is very close to the pilot operation. One factor contributing to the higher pressure drop may be the removal of the cyclones which were present during the pilot plant studies. Another consideration is the limited on-stream time of the pilot plant operation.

Hardware problems encountered during the testing program included compressed air in-line freezing during the extreme cold of January and February, 1977, and rapid deterioration of silicone rubber gasketing material employed around the dampers and hatch covers. All gasketing material was replaced with asbestos gasketing. Debugging of the system controls was extensive and plugging of the boiler stack pressure tap with moisture and ash required subsequent installation of a continuous compressed air purge system.

High pressure drop across both houses appeared to be the result of boiler start-up through the baghouses, plus a number dew point excursions occurring when the controls were being debugged. In view of the heavy dust pearls on the surface of the bags it was decided to manually vacuum each bag. After vacuuming the houses were brought on stream and the pressure drops were reduced to acceptable levels. In the case of the Teflon felt the pressure drop across the bags returned to the original clean bag level. Lab permeability analysis confirmed this. Subsequent to bringing the houses on stream, failure of the Gore-Tex bags occurred. At the end of the first year of operation about ten percent of the Gore-Tex bags had failed; no bag failures or obvious signs of deterioration had occurred with the Teflon felt bags. The failure of the Gore-Tex bags generally was in the form of either a small round hole, one inch or less in diameter, or a tear about 1/8 to 1/4 inch wide and one to six inches long. Occasionally a bag would be found totally shredded. One possibility is that the impact of the PTFE membrane on the tube sheet during installation and removal initiates the failure. Another contributing factor may be the stress occurring as the bags shrink on the rigid cage when going through the temperature elevation at start-up each week.

#### CURRENT COSTS

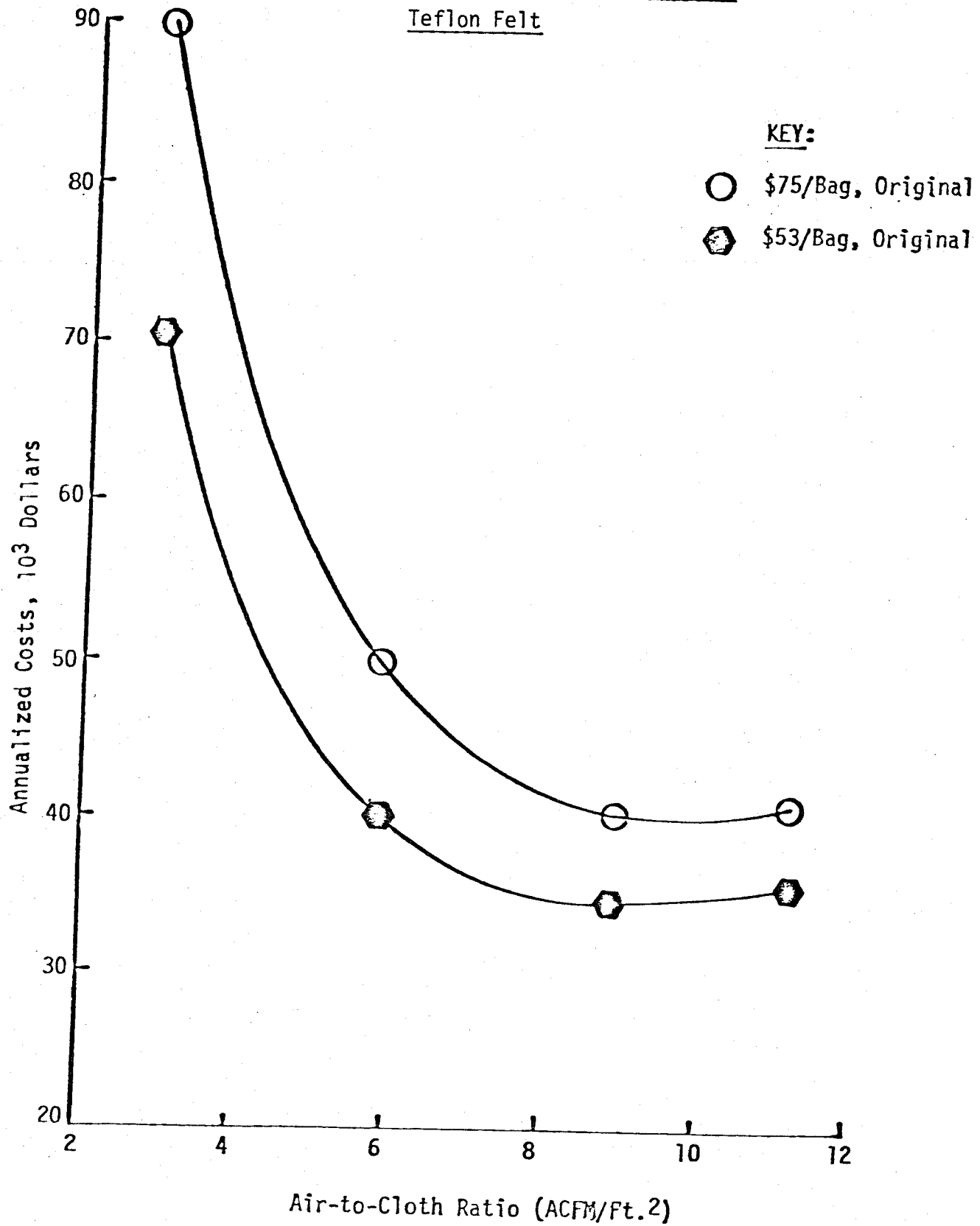
Overall, the economic evaluation executed during the pilot plant program remains valid. For the 70,000 ACFM case, a baghouse outfitted with Teflon felt and assuming a two-year bag life continues to be a more economically attractive alternative than an electrostatic precipitator. During 1977 a major price reduction for Teflon felt occurred. The installed price was reduced from \$75 per bag (5" dia. X 8' 8" long) to \$53 per bag. The impact of this price reduction on annualized cost is shown in Figure 21. This brings the Teflon felt



Figure 21

Total Annualized Cost vs. Air-to-Cloth Ratio

Teflon Felt



alternative in line with the cost of Gore-Tex, as can be seen by reviewing the pilot study annualized cost comparison, shown in Figure 22, with the current comparison, shown in Figure 23.

#### FUTURE PLANS

EPA has at this time elected to exercise two of the three proposed options, thus the two demonstration units will continue to be operated and tested throughout 1978 and 1979. House No. 1 will continue to be operated with Teflon felt as the filter media. The program plan calls for replacement of the Gore-Tex with a series of other filter media, thus obtaining cost, life and performance data on a variety of candidate media considered potentially suitable for fly ash control applications. The initial candidate materials include both woven and felted glass.

Figure 22

Annualized Costs vs. Air-to-Cloth Ratio

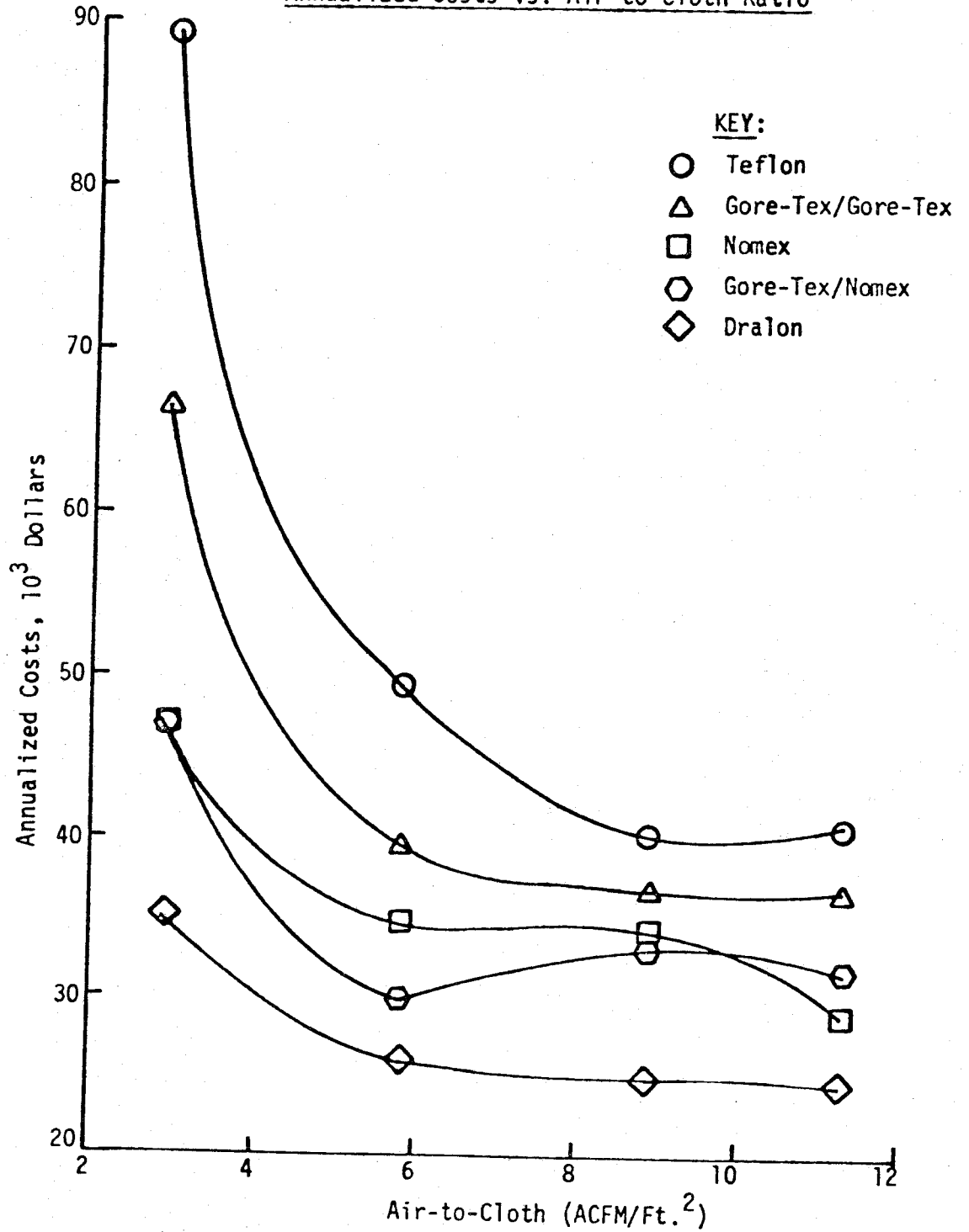
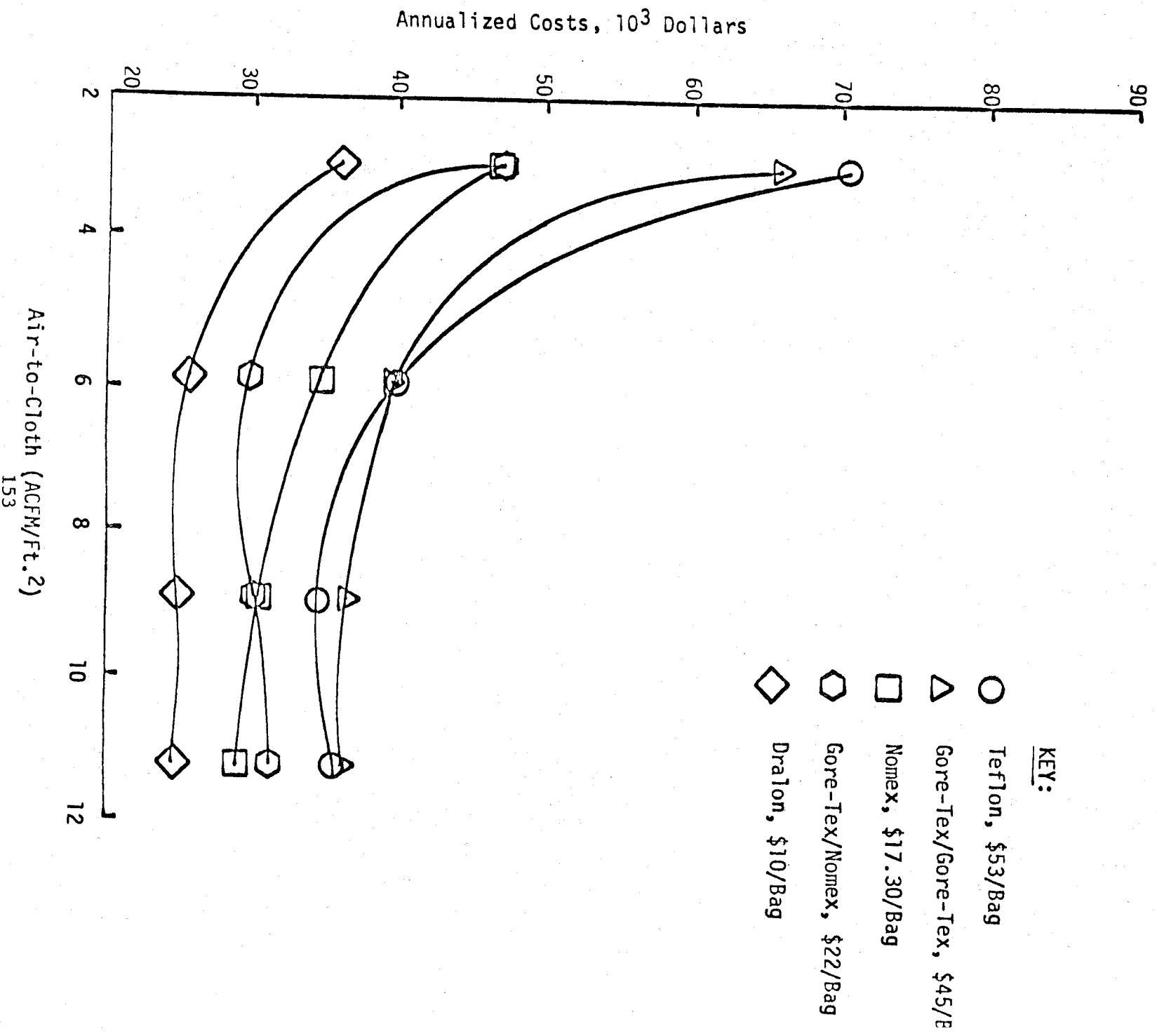


Figure 23

Annualized Costs vs. Air-to-Cloth Ratio



## REFERENCES

- (1) J. D. McKenna, "Applying Fabric Filtration to Coal Fired Industrial Boilers - A Preliminary Pilot Scale Investigation", July - 1974, EPA 650/2-74-058.
- (2) J. D. McKenna, J. C. Mycock, and W. O. Lipscomb, "Applying Fabric Filtration to Coal Fired Industrial Boilers - A Pilot Scale Investigation", August - 1975, NTIS PB-245 186.

## BAGHOUSE PERFORMANCE ON A SMALL ELECTRIC ARC FURNACE

by

Robert M. Bradway  
GCA/Technology Division

### ABSTRACT

This paper presents the results of an evaluation of a fabric filter system controlling emissions from either one or two 30-ton electric arc furnaces producing a high-strength, low-alloy specialty steel. The evaluation involved measuring the system's total mass collection efficiency and apparent fractional collection efficiency. Testing involved 8 sampling days with one furnace operating, and 2 days with two furnaces. Baghouse influent and effluent streams were sampled with total mass samplers, inertial impactors, a condensation nuclei counter (CNC), and an optical dust counter. Total mass tests showed baghouse mean mass efficiency to be 97.9 percent with one furnace operating, and 98.7 percent with two furnaces. Mean outlet mass concentrations for one- and two-furnace operation were 0.0014 and 0.0019 grains/dscf, respectively. Influent impactor tests showed considerable size distribution differences as a function of the phase of the process: the greatest concentrations for the particles sized occurred during the first melt. Effluent impactor size distribution tests suggested agglomeration.

## INTRODUCTION

The work reported in this paper presents one phase of a program whose purpose was to characterize the performance of several industrial size fabric filter systems. The fabric filter tested at the Marathon LeTourneau Company in Longview, Texas cleaned the emissions of either one or two 30-ton electric arc furnaces which produce a high strength, low-alloy specialty steel. Each furnace is fitted with a side draft hood and a canopy hood which is used only during charging and pouring. The hoods are ducted through a spark arrester to a 10-compartment American Air Filter baghouse which utilizes Dacron<sup>TM</sup> bags.

The performance of the fabric filter was characterized by determination of the particulate removal efficiency as a function of total mass and particle size. The apparent fractional efficiency, defined as the measured change in the particulate concentrations as a function of particle size that results from the filtration process, was determined by upstream and downstream sampling using inertial cascade impactors. The baghouse influent and effluent streams were also monitored with a condensation nuclei counter to determine variations in submicron particle concentrations as a function of the process and the cleaning cycle.

## MARATHON LETOURNEAU STEEL MILL

The steel mill at Marathon LeTourneau produces high strength, low alloy, specialty steel in two electric arc furnaces of 30 tons each, nominal capacity. The furnaces are 10,000 kVA swing roof top charged units with individual combination side-draft and canopy hooding. The side-draft hoods operate while the furnace roof is in place and the canopy hoods operate when the roof is removed for charging and tapping. The furnaces use the basic steel making process with cold number one oil-free scrap. The furnaces must be back charged once to reach holding capacity, and the double slag method of refining is used. Additions of fluorspar are commonly made for slag conditioning and oxygen lancing is used to lower the carbon content of the melt.

The furnace hoods are ducted to a 10-compartment American Air Filter baghouse installed in 1973. Photographs of the baghouse are presented in Figures 1 and 2. The baghouse has a cloth area of 52,778<sup>2</sup> which results in an air-to-cloth ratio of 3.22:1 at the design flow of 170,000 acfm at 150°F. The net air-to-cloth ratio increases to 3.58:1 with one compartment off-line for cleaning. The cleaning cycle is actuated by timer such that there is no delay time between cycles. Each baghouse compartment contains 288 Dacron<sup>TM</sup> filter tubes which are 5 inches in diameter by 14 feet long.

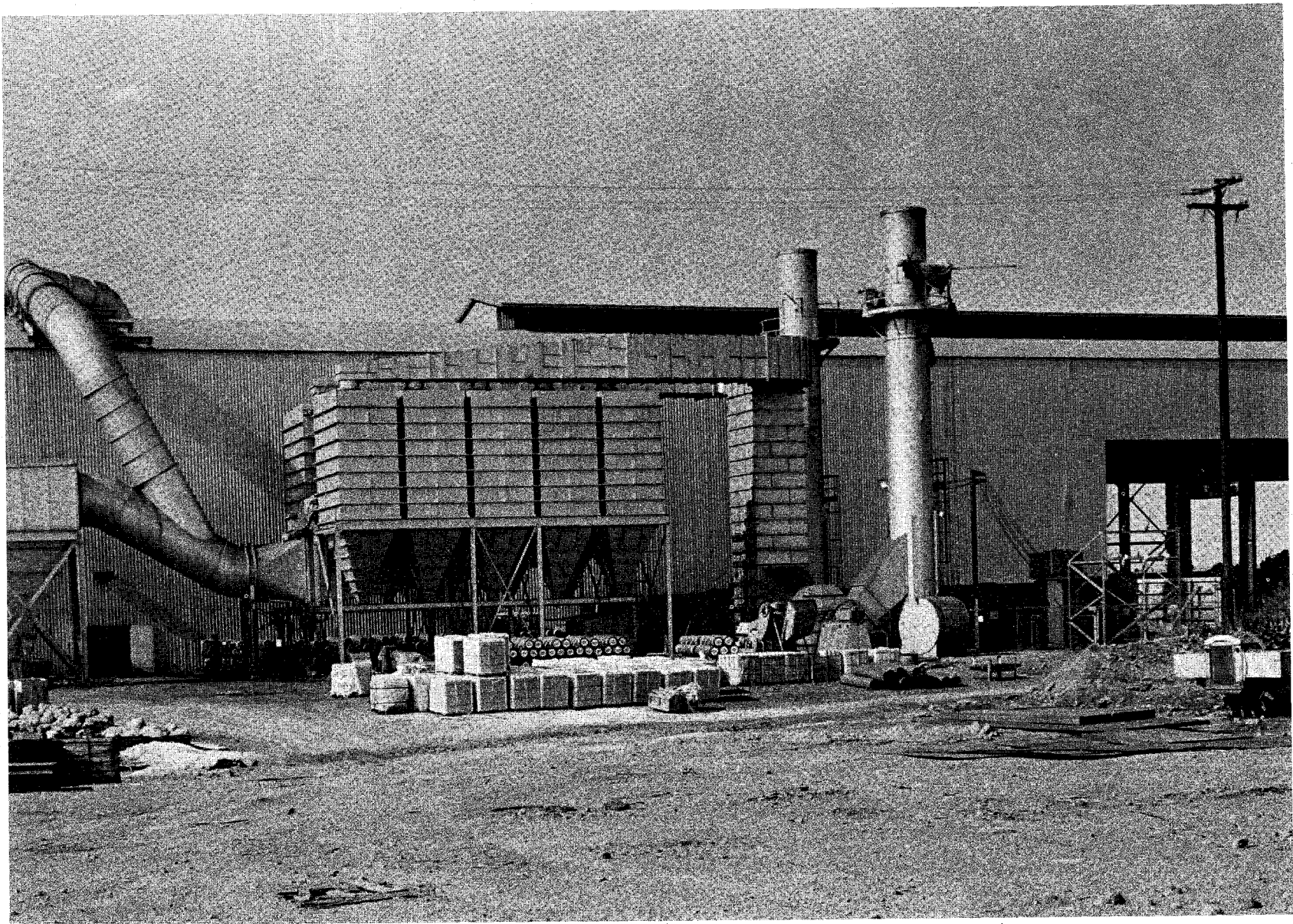


Figure 1. Photograph of side of fabric filter.



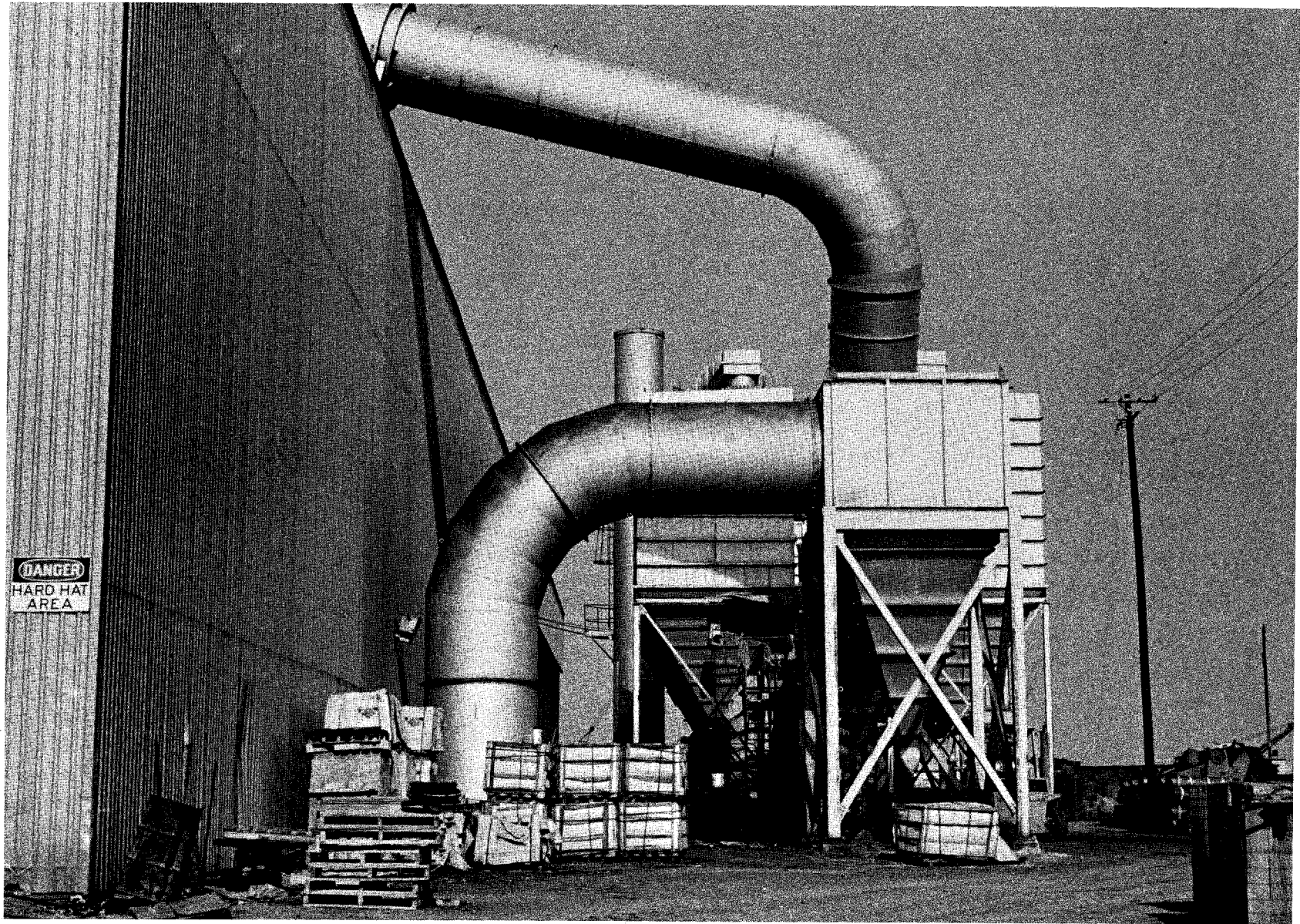


Figure 2. Photograph of end of fabric filter.

## RESULTS

The primary purpose of the sampling program at Marathon LeTourneau was to define the total and fractional particulate penetration through a fabric filter cleaning the emissions from an electric arc furnace. The secondary reason for testing was to determine the effect of approximately doubling the particulate loading to the baghouse on the total and fractional penetration. In addition, the baghouse inlet and outlet submicrometer particle concentrations were measured as a function of the process cycle and the baghouse cleaning cycle to determine if periods of high penetration are a function of the process cycle, the cleaning cycle or both. Finally, the inlet particle size distributions were measured as a function of the process cycle.

### Total Mass Measurements

The baghouse inlet and outlet average particulate mass concentrations and the resulting efficiency penetration results are presented in Table 1. Examination of the table shows that the inlet concentrations for the test days during which there were two furnaces in operation were approximately twice that of the runs in which there was only one furnace in operation.

TABLE 1. AVERAGE RESULTS OF TOTAL MASS MEASUREMENTS

Tests	Concentration, gr/dscf		Efficiency, percent	Penetration, percent
	Inlet	Outlet		
All	0.0824	0.0015	98.18	1.82
Two furnaces	0.1472	0.0019	98.71	1.29
One furnace	0.0662	0.0014	97.94	2.06

The mass penetration and the total mass sample outlet concentration statistics show that the penetration is lower even though the outlet concentration is higher (40 percent) with the two furnaces in operation indicating the baghouse particulate removal efficiency varies with inlet grain loading. Thus the baghouse dampens changes in the outlet concentration or emission rate caused by variations in the inlet concentration.

The particle size distribution data was not such a straightforward task as the total mass measurements, however. The duration of the inlet impactor sampling to collect a weighable sample on each stage without overloading was quite variable due to differences in the mass concentration as a function of the process cycle. Figure 3 illustrates in a somewhat simplistic way what happens to the mass concentration as a function of the process cycle for one micrometer particle. Other curves were constructed for two, four, six, eight

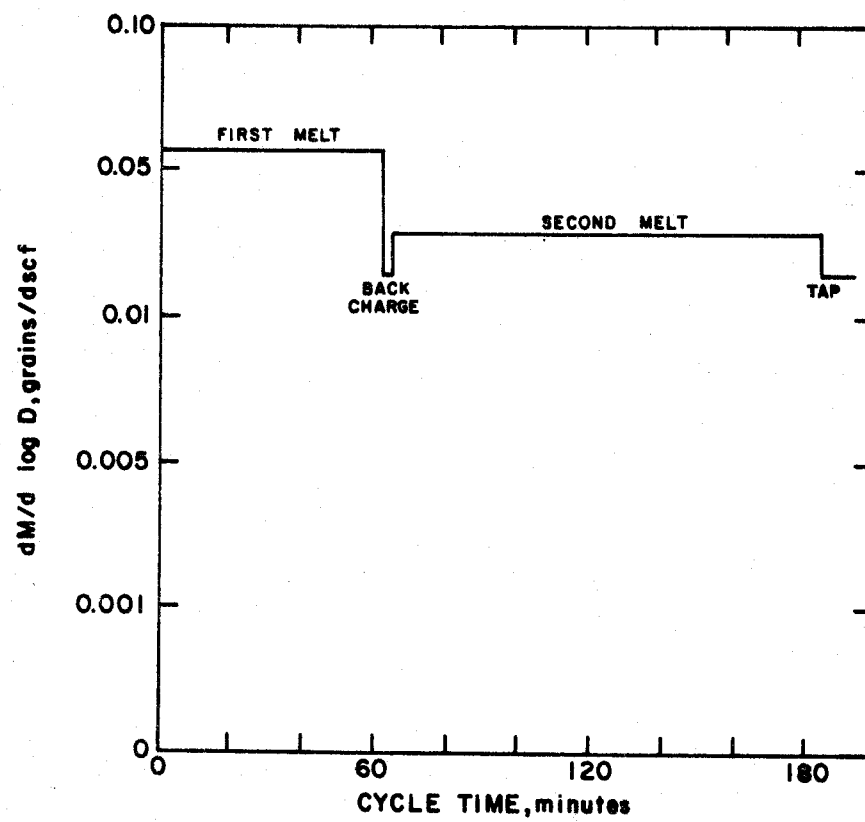


Figure 3. Concentration versus process cycle for 10  $\mu\text{m}$  particles.

and ten micrometer particles and all showed the same pattern. The concentration is highest during the first melt, drops dramatically during back charging, increases somewhat during the second melt and then decreases again during tap.

Because of the large temporal changes in concentration, it was important that we sample during phases of the cycle. Figure 4 shows the sequence of inlet impactor measurements that were taken, showing that nearly every part of the process cycle was sampled. These results were the time averaged and composited to construct a single curve for the inlet particle size distribution with our furnace in operation and another for two furnaces in operation. These curves are shown in Figure 5. It can be seen from these curves that highest inlet concentration occurs at about two micrometers and that two furnace operation roughly doubles the concentration over the entire size range covered by the impactors.

The measurement of the outlet particle size distribution was more straightforward. Because of the very low concentrations, however, outlet impactors were run for 9 to 15 hours each day so that a weighable amount of particulate could be collected on each stage.

The results of the outlet impactor runs are summarized in Figure 6. As can be seen, the grain loadings are very low but the particle size of maximum concentration is 4 micrometers. This is compared to a maximum concentration at 2  $\mu\text{m}$  at the inlet, a phenomenon discussed yesterday by Dick Dennis.

By comparing the inlet and outlet size distribution curves, one can construct a fractional efficiency curve for the baghouse, as shown in Figure 7. Although we generally do not like to describe baghouse collection performance in terms of fractional efficiency because many of the outlet particles do not directly penetrate the filter, it is a conventional method of describing collector performance. These curves show a minimum at about 1  $\mu\text{m}$ , a maximum at about 6  $\mu\text{m}$  and then a dropoff to 10  $\mu\text{m}$ .

Inlet and outlet measurements were also made in the submicrometer particles with a condensation nuclei counter. These measurements showed collection efficiencies of 99.23 to 99.86 percent for particles over the range of 0.0025  $\mu\text{m}$  to about 0.5  $\mu\text{m}$ . This device, when used on the outlet gas stream, very consistently showed peaks in the small particle concentration immediately after a compartment was cleaned.

In summary, the baghouse evaluated controlled the emissions to an outlet concentration of 0.0015 gr/dscf. This is  $3\frac{1}{2}$  times below the allowable concentration. The baghouse studied also was shown to efficiently collect particles over a very broad range of particle sizes.

This project has been funded at least in part with Federal funds from the Environmental Protection Agency under Contract No. 68-02-1438, Task 4. The contents of this publication does not necessarily reflect the view or policies of the U.S. Environmental Protection Agency, nor does mention of trade names, commercial products, or organizations imply endorsement by the U.S. Government.

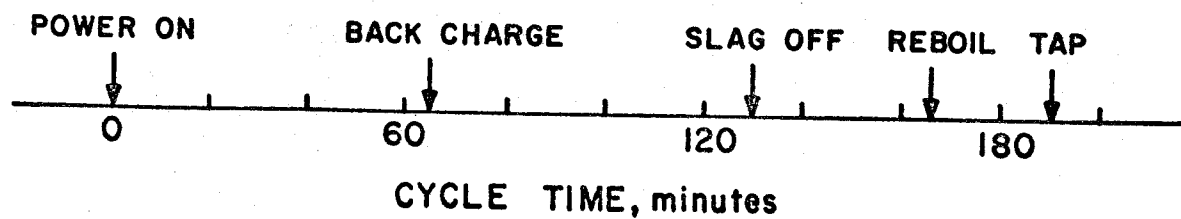
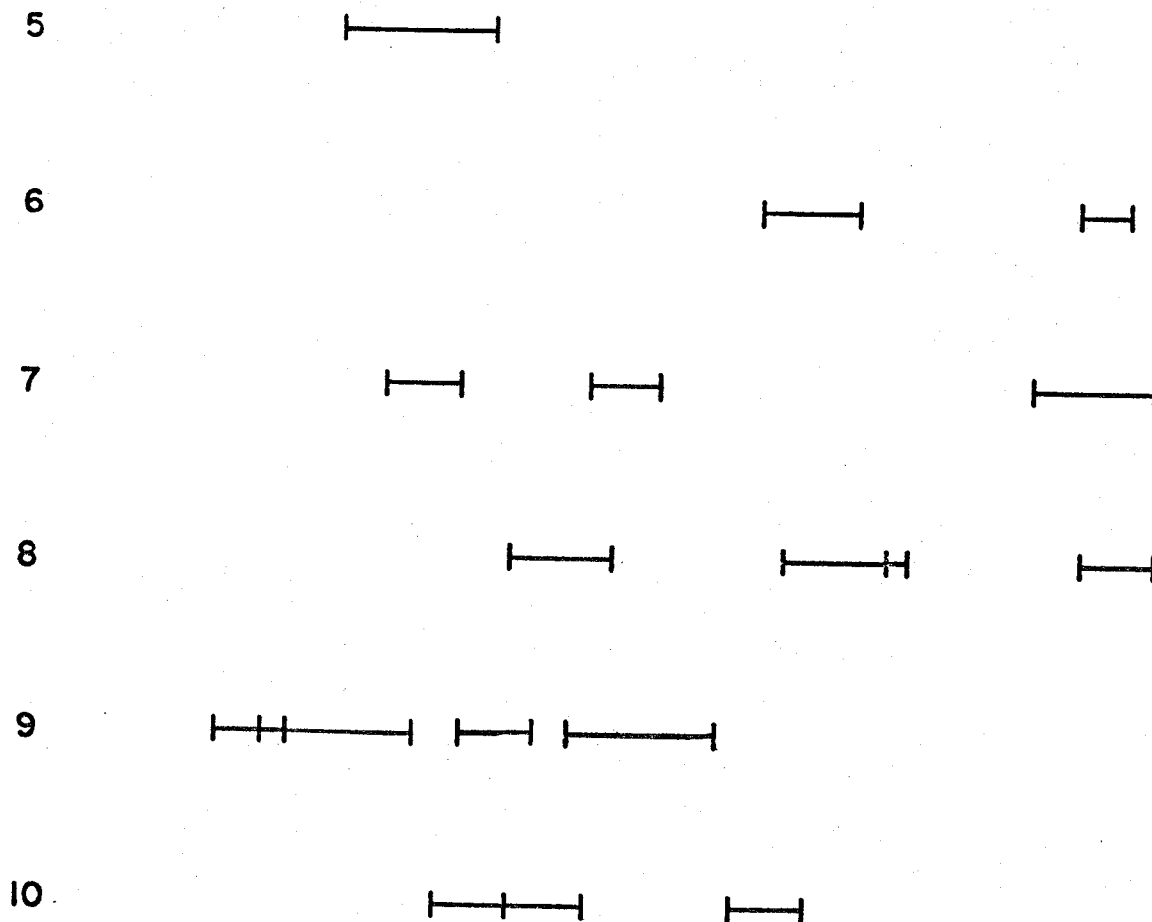
INLET  
RUN NO.

Figure 4. Time in process cycle at which inlet samples were collected.

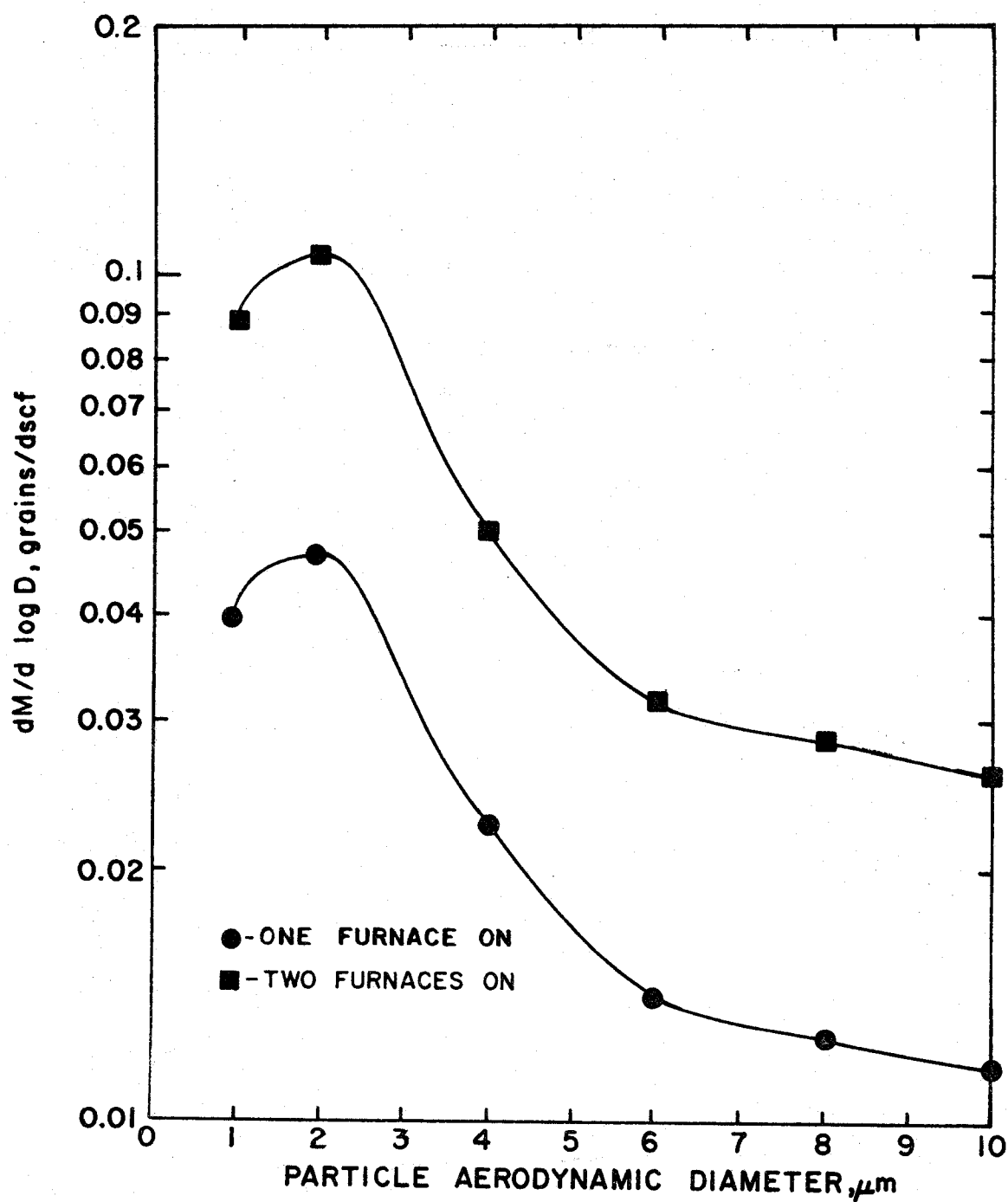


Figure 5. Composited differential size distribution curves of baghouse inlet aerosol.

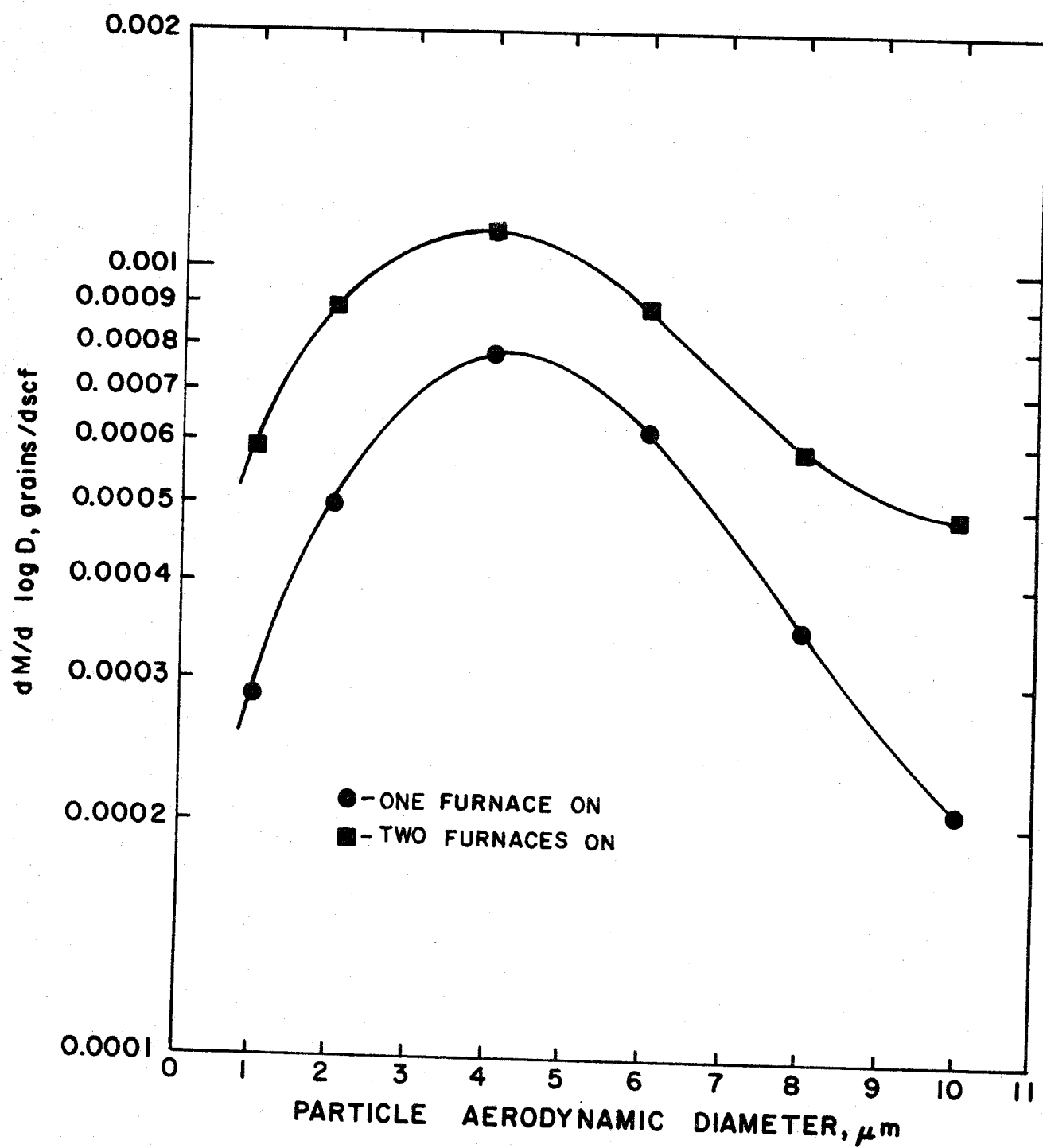


Figure 6. Average outlet differential size distribution curves.

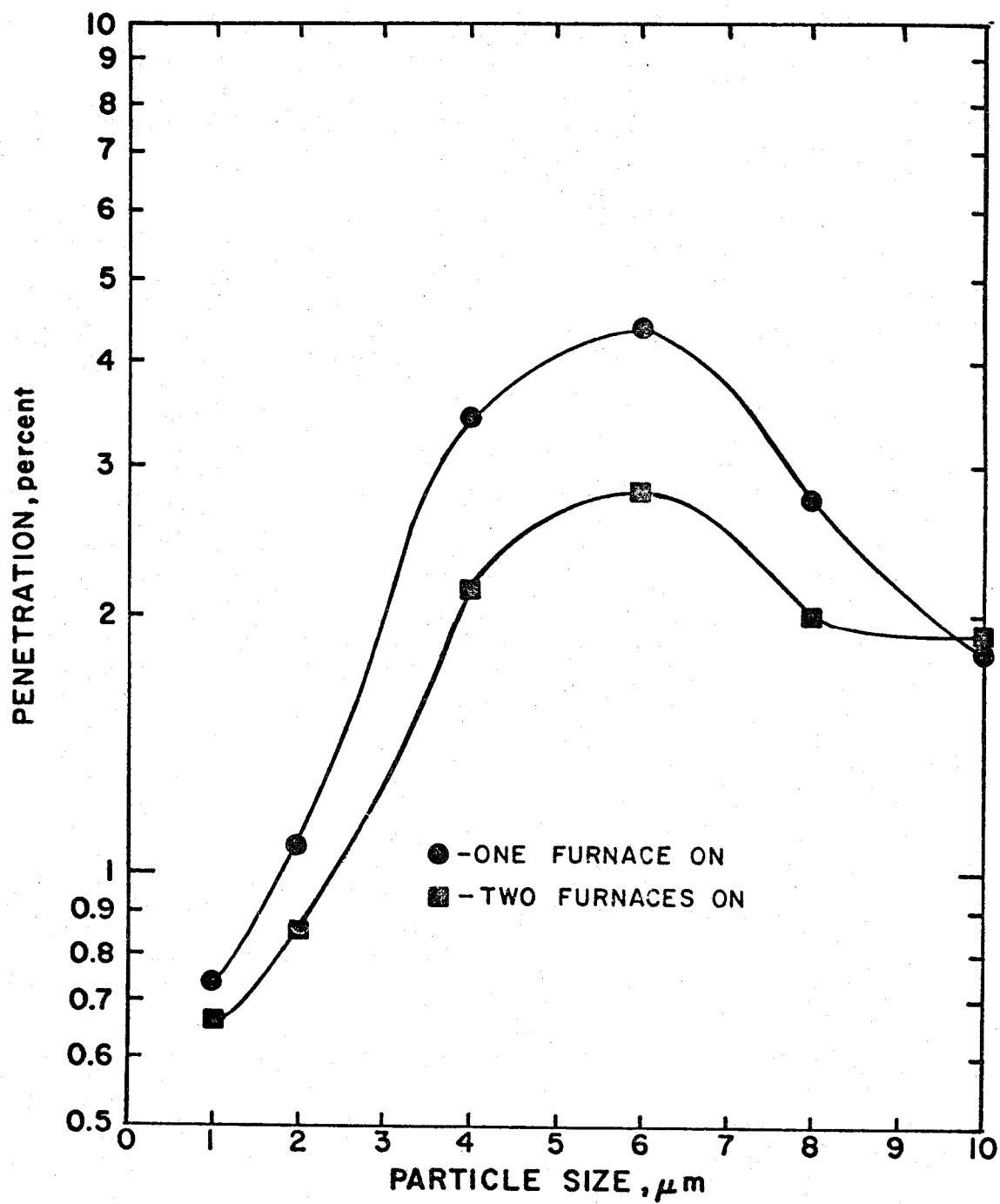


Figure 7. Fabric filter fractional penetration curves.





## FUME CONTROL AT SMALL SMELTERS

Knowlton J. Caplan

### ABSTRACT

In general, fabric filters are successfully applied to fume control in small smelters. Special considerations need to be provided for hot gases, possible presence of acid (especially  $\text{SO}_2$ ), high dew points, and sometimes for fire prevention. Efficiencies are adequate for present emission standards and a clear stack is usually obtained. Air-to-cloth ratios are usually quite conservative because the permeability of the dust cake is quite low. The dust is somewhat, but not exceedingly, difficult to handle. A table is provided summarizing the performance of 15 fabric filters in small smelters processing lead, brass, and copper.

## FUME CONTROL AT SMALL SMELTERS

By Knowlton J. Caplan\*

Presented at 3rd EPA Symposium on Fabric Filters for Particle Collection, December 6, 1977, Tucson, Arizona

### INTRODUCTION

The term "small smelters" covers a very heterogeneous and poorly described segment of U.S. industry. Almost all small smelters are secondary smelters, that is, the raw material for the process is recycled scrap. Obviously, such industries provide a highly useful economic and environmental function. Apparently these industries are not represented as such by any trade association, although they may be members of other trade associations related to the end uses of their product. In a recent study on economic impact of proposed government regulations on the lead industry, it proved impossible to closely define or accurately count the number of secondary lead smelters.

With such a heterogeneous definition of the subject, this paper will only cover part of it, that part which is represented in our direct experience. This paper is not a comprehensive literature survey, but rather a description of general operating characteristics of the industry as related to fume control.

### INDUSTRY CHARACTERISTICS

#### Secondary Lead Smelters

Secondary lead smelters are generally centered around a local supply of scrapped automobile batteries and those batteries are the main source of feed material to the plant. Other forms of lead scrap are handled incidentally. Such secondary smelters may be associated with a battery manufacturing plant which consumes the lead produced, or may be independent, producing pig lead. Although a process does exist for charging the drained batteries, case and all, into a melting furnace, that process is not widely used and most plants operate by "breaking" the batteries. A mechanical saw or guillotine is used to cut the case open, the lead bearing plates are dumped out of the case, allowed to dry in piles on the floor, and handled by front end loader for manipulating the stock piles and charging the furnace. Various mechanized schemes

---

\* President, Industrial Health Engineering Associates, Inc., Minneapolis, Minnesota.

have been proposed and tried without notable success. Obviously this method of bulk handling is dusty and presents a difficult occupational health problem, but the dust concentrations are usually below present emission standards and even if they were not, the particle size is relatively coarse and collection would not be difficult.

The major sources of fume in the secondary lead smelter are either a blast furnace resembling a foundry cupola or a reverberatory furnace, and the associated refining kettles. These will be described later.

### Secondary Copper Smelters

Recycled copper can be recovered by wet chemical methods or by smelting. The copper scrap going to a smelter is much more heterogeneous than is the case with the lead industry. The scrap contains many other metals besides copper and many alloying elements for copper, so that the metals separation and refining process is much more complicated. The same smelter may also receive other non-ferrous scrap materials involving semi-precious or precious metals. As far as the copper scrap is concerned, it is even less homogeneous than the lead battery scrap and is handled by front end loader in bulk, with the associated hygiene problems. The first process evolving fume is the charging of the material to a blast furnace; from there on the melting process resembles in its process steps a primary copper smelter, with the major exception that the sulfur content is low and evolution of SO<sub>2</sub> is not too significant a problem.

Fabric filters are used for fume collection from the blast furnace, converter and other associated fume sources. Our experience in this particular problem is limited in that the severe depression of the copper market has delayed our projects in this area.

### Brass Recovery

It is our impression that most brass is recycled by brass foundries or other brass producers, rather than attempting to smelt the brass to a marketable grade. Brass melting in brass foundries is usually conducted in crucible furnaces or in tilting melting furnaces using scrap brass of known composition as part of the charge. The emission from crucible furnaces is quite low, unless oily scrap is used. The emission from direct fired melting furnaces

is higher, and causes potential problems of baghouse fires either from carryover of sparks or from finely divided metallics (especially zinc) that may be generated by the reducing atmosphere and collected in the baghouse. As far as we know, brass is either smelted for its copper content in a copper smelter or directly used in the foundry and there are no "brass smelters" as such.

### Secondary Aluminum Smelting

We have no experience with this particular industrial function other than the typical problems associated with aluminum melting as practiced in light metal foundries. The major problem associated with fume in such operations arises from the use of chlorine as a scavenging gas in the melt, which produces a copious aluminum chloride fume. Treatment of this source has been extensively described in literature.

### FABRIC FILTER APPLICATION TO SMELTERS

Table I presents a summary of data available to us concerning the general operating parameters of fabric filters in small smelters. Much of the data is missing, as is obvious, since the information was collected incidentally to other work which may have been on the baghouse itself or only indirectly related. Some information from AP-40 has been included for the sake of completeness.

Most notable among the missing data is particle size information. Although scientifically this is regrettable, for practical application it is not too important. All the systems are handling a fine metallurgical fume which would be expected to, and does, have a mass median aerodynamic diameter of 1 micron or less. Of greater practical importance is that the fume is "difficult"; that is, the permeability of the accumulated filter cake is low. The dust is also, in general, somewhat difficult to handle, somewhat sticky, etc., as distinguished from a free flowing granular material.

It will be noted that all the filters except one (which is troublesome) are operating at quite modest air-to-cloth ratios for the type of filter involved. Differential pressures across the fabric are, with the same exception, in the normally expected range even though accurate data may not be available due to the large variations in operating conditions for some filters.

Efficiencies are usually in the range of 98 to 99% on a weight basis, the stack is usually visually clear, and the outlet grain loading is usually comfortably below the present emission standard for primary lead smelters. The reason for the efficiency being somewhat below the 99.9 weight percent that can usually be expected for a fabric filter is not clear. The duty conditions are rather severe, involving high temperatures and chemical attack on the fabric. Furthermore, the baghouses are usually quite large so that, in view of the high temperatures and noxious conditions, finding and fixing small mechanical leakages through the fabric is difficult and is not actively pursued as long as the emissions are satisfactory.

The hot gases from the furnaces may be cooled to suitable baghouse temperatures by any of the classical methods. If acid is present, the most favorable design would be to use radiant coolers to avoid introduction of additional water vapor. When water sprays are used, they are usually used only for partial cooling, the remainder being by dilution in order to avoid too high a dew point.

If acid gases are present in significant quantity or if water spray cooling is used, the hoppers of the fabric filter should be kept above the dew point. This requires provisions over and above that required to keep the main housing above the dew point. With material collected in the hopper, the collected layer of dust provides an insulating effect so that the metal temperature may be far below the gas temperature. However, the vapors will still migrate through the bed of dust, condensing on the cold metal walls and forming a cake or mud.

Blast furnaces or cupola type furnaces can be operated under significant draft so that there is no escape of fume from the furnace itself. There is, of course, fume evolved from the pouring of the metal or the tapping of slag which should be controlled from a hygiene point of view. The air from such hoods is usually only 100 - 150°F and is an economical source for dilution air since it also requires filtration.

Reverb furnaces on the other hand are typically operated at a few hundredths of an inch water gage draft in order to conserve fuel. Such furnaces tend to be somewhat leaky and loss of the draft will result in leakage of fume from the furnace itself or from various operating ports. In some primary smelters, very elaborate, fast-acting control systems are installed to regulate the furnace

draft in accordance with operating conditions, the opening of charge ports, etc. Such elaborate controls are usually not found in secondary smelters. External hygiene control hoods may be located over the charge ports, metal and slag taps, and again, this contaminant-laden air provides a source of dilution air for cooling the furnace gas on an economic basis. Such hygiene hoods do not, however, provide for maintenance of adequate furnace draft to prevent leakage from the furnace itself.

### FIRES IN METALLURGICAL BAGHOUSES

Fires are not uncommon in metallurgical baghouses. They usually but not always occur in the hopper of the baghouse. However, the circumstances under which they occur are highly variable, and immediate investigations following a fire usually lack the application of scientific expertise. As far as we know, no concerted research has been done on the subject.

Fires occurring in the hopper are almost always caused by the presence of finely divided unoxidized metallics of a pyrophoric nature. The presence of metallic zinc is probably the most common source of such fires, and the presence of metallic lead probably the second most common source.

Prevention of fires in baghouse hoppers has been most successfully accomplished by the addition of an inexpensive diluent material. The most common diluent is agricultural lime, it serving obviously as a diluent to the combustible materials and also, if a fire does start, heat will be absorbed in dehydrating of the lime thus furnishing an additional cooling effect. Some installations have used various carbonates such as soda ash or ground limestone, the theory being that the heat of the fire will release carbon dioxide which will tend to smother the fire. This latter action probably would not be effective for a fire in the bags since the filtering air flow would rather quickly flush the blanket of carbon dioxide away from the combustion area.

There is an empirical test called a "burning test" which is applied to controlling fires in metallurgical baghouses. In general the test consists of taking a shallow pan full of the collected dust and attempting to light it at one end by ordinary means such as a match or a burning paper towel. The time of burning from one end to the other of the pan is then measured, and

if it is less than some specified value, the diluent is added to the duct entering the baghouse so as to mix with, dilute, etc., the combustible dust. The test is strictly empirical and the parameters need to be developed for each individual plant or baghouse situation.

One plant used a pan one-half inch deep, 2 inches wide, and 6 inches long. In this case, the burning was not actually timed; if the dust burned at all, the diluent was added. The diluent was hydrated lime (agricultural lime) and was added in amounts varying from 5% to 20% of the total dust load.

In another plant the test pan was 1 inch deep, 3 inches wide and 9 inches long. If the length of time required to burn from one end to the other was greater than 2 minutes, it was judged acceptable; if less than 2 minutes, agricultural lime was added to the flue.

Fires starting on the bags rather than in the hopper are usually blamed on the carryover of sparks although there are some indications that these fires also are sometimes started by metallics. In one interesting case, the bags of a reverse pulse filter with bottom inlet caught fire at the top of the bags and there was no fire in the hopper. Because at times sparks had been observed in the flue, the fire was blamed on sparks. It is difficult to understand how such sparks would preferentially migrate to the top of the bags. Another possible explanation would be that the reverse pulse air, having more energy and physically agitating the dust cake more at the top of the bags than further down, may have started the fire in the metallics present. In any case, the provision of a spark trap such as a cyclone or a spray chamber would prevent fires from sparks if they cannot otherwise be prevented. If both sparks and unoxidized zinc or lead are present, both types of precautions may be required.

#### DUST HANDLING

The handling of recovered dust in most secondary smelters is a difficult problem because such plants usually do not have a multiplicity of processes and options for disposal of such material. The material may also have a significant monetary value. Its disposal by means other than to the process would be an obvious problem in solid waste disposal.



The dust is usually somewhat difficult to handle. It does not flow readily from hoppers, etc., unless special provisions are made. The dust should be capable of conveyance by pneumatic conveying, but some operators have experienced difficulty with this operation due, in our opinion, to inadequately designed systems. Screw conveyors work, but they must be enclosed and dust control applied. Belt conveyors or other dusting type of material handling equipment is to be avoided.

The dust is usually significantly different in metallic composition to the parent material and metallurgical considerations may govern the point in the process to which it is returned, or even if it is to be returned. Leaving aside the metallurgical considerations, dust returned in that form to a blast furnace or cupola is mostly re-entrained and immediately reappears in the baghouse, constituting a circulating dust load. The circulating dust load may be an operating advantage if such recirculation accumulates unwanted impurities so that a bleed-off or programmed disposal of the dust can be made. Otherwise, the dust will be recovered more efficiently by returning it to a different type of furnace such as a reverberatory furnace. Most secondary smelters do not indulge in pugging or briquetting of dust to reduce its loss in the furnace.

#### SUMMARY

In general, fabric filters are successfully applied to fume control in small smelters. Special considerations need to be provided for hot gases, possible presence of acid (especially  $\text{SO}_2$ ), high dew points, and sometimes for fire prevention. Efficiencies are adequate for present emission standards and a clear stack is usually obtained. Air-to-cloth ratios are usually quite conservative because the permeability of the dust cake is quite low. The dust is somewhat, but not exceedingly, difficult to handle.

TABLE I  
"Fume Control in Small Smelters", by R. J. Caplan  
Third Symposium on Fabric Filters, Tucson, Dec. 1977

Process Description	Filter Type	Temp. °F	A/C Ratio lb air/lb dust	AP in. H <sub>2</sub> O	Inlet gr/acf	Efficiency %	Outlet gr/acf	Particle Size μm	Cooling	SO <sub>2</sub> ppm	Acid Dew Point °F	Bag Life Mos.	Remarks
Lead smelter, mostly battery scrap, blast and 1 reverb furnace	Shaker 4 Section Orlon	130	1.4	6.5	1.7	---	---	---	Waterpin & dilution	---	---	---	Only 1 reverb in use at any one time
Lead smelter, mostly battery scrap, reverb and 2 blast furnaces	Reverso Glass, still- flow cone treated (collapse)	450	1.5	1.5-5.0	5.5	90.85	0.003	---	Waterpin	130	375	14	
Lead smelter, mostly battery scrap, blast furnace	Reverso Orlon felt 40 psig	250	5.7	6.5	1.3	>98.5	<0.02	800 > 43 μm	Waterpin & dilution	4000	240 (est.)	12	
Lead smelter, mostly battery scrap, reverb furnace	Shaker Dacron	330	1.0	---	1.4	99.0	0.013	(2)	Dilution	1040	---	---	Sparks (Ref. 1)
Lead smelter, mostly battery scrap, blast furnace	Saw Collector	175	1.0	---	2.1	98.3	0.035	(2)	Dilution	30	---	---	Sparks (Ref. 1)
Lead smelter, charge and tap scrap, blast & reverb furnaces	High pres- sure re- verb filter w/3001 bag	---	5.4	16.5	0.04	---	---	---	None	---	---	16-24	
Lead smelter, refining kettle hoods	-do- 17 oz. Tudex (woven)	---	8.1	15	0.02	---	---	---	None	---	---	---	Fires, cause uncertain
Brass crucible melting (gas fired)	Shaker Orlon	---	2.5	---	0.031	93.7	0.002	---	---	---	---	---	(Ref. 1)
Brass crucible melting (gas fired)	Shaker Orlon	---	2.5	---	0.012	96.2	0.0005	---	---	---	---	---	(Ref. 1)
Brass crucible melting (electric)	Shaker Orlon	---	2.8	---	0.22	96.0	0.008	---	---	---	---	---	(Ref. 1)
Brass induction tilt furnace	Shaker Orlon	---	1.6	1.8-4.0	---	---	---	---	Water sprays	---	---	---	No mention of fires (Ref. 1)
Copper smelter, electric arc "reverb" furnace	Shaker ---	170	1.6	---	---	---	---	---	Dilution	---	---	---	
Copper smelter, blast furnace	Shaker ---	---	1.5	5-6.5	---	---	---	---	Dilution & water sprays	---	---	---	
Copper smelter, converter	Shaker Glass	350	0.9	---	---	---	---	---	Dilution & water sprays	1200	---	---	
Brass foundry, tilt melting furnace	Reverso Homax pulse	190	3.6	6	2.5	---	---	---	Dilution	---	---	---	Fires, sparks and molten

(1) "Air Pollution Engineering Manual", 2nd Ed. EPA Publ. AP-40, May 1973

(2) 3 to 3 μm 13.3%  
1 to 2 μm 45.2%  
2 to 1 μm 19.1%  
1 to 0.5 μm 14.0%  
4 to 16 μm 8.4%  
Method of sizing  
not stated.





FULLER  
COMPANY

FABRIC FILTERS IN THE CEMENT INDUSTRY

N. D. PHILLIPS  
SENIOR PROJECT ENGINEER

AND

W. C. BRUMAGIN  
CHIEF PRODUCT ENGINEER

DUST PRODUCTS DIVISION  
FULLER COMPANY

FOR PRESENTATION AT  
THIRD SYMPOSIUM ON FABRIC FILTERS  
FOR PARTICLE COLLECTION  
DECEMBER 5-6, 1977  
TUCSON, ARIZONA

## INTRODUCTION

Over the last 20 years, cement producers have been under considerable pressure to reduce their contributions to the air pollution problem of the nation. In fact, dust collection equipment has been used for a very long time in cement plants, much longer than the last twenty (20) years. This has been primarily due to the nature of the materials used in the process and the materials produced, as well as, the two initial reasons why any plant will consider installation of dust collection equipment. The first being recovery of a product that already has an investment in it and is usable in the end product of the plant. The second being the elimination of air-borne dust within the plant facilities, thereby extending the life of mechanical equipment in the plant and reducing housekeeping expenses in the facility. For these reasons, 30 or 40 years ago, it was common to see dust collection equipment within the plant venting material handling facilities, drying facilities, pyroprocessing equipment, and milling equipment.

There have been two distinct processes used in the manufacture of cement that differ primarily in the treatment of the raw material before pyroprocessing. The wet process in earlier times being the most common, required little in the way of dust collection equipment, until after the raw feed had been dried, calcined and clinkered. The dry process plant, has always required dust collection equipment in greater degree, because of the crushing, drying, milling, and blending of dry, relatively fine materials. With the advent of the energy crisis, dry plants in the United States are becoming more popular, therefore, cement plants will be equipped with dry filtration dust collection equipment to a greater degree in the future.

In the late 1950's, good neighborliness and the move to improve the quality of our environment, caused cement manufacturers to look at replacing their mechanical separation equipment and electrostatic precipitators with more efficient devices. In the late 1950's, fabric filters began to be applied to the waste gases from long dry kilns, the initial small suspension preheater kilns, and somewhat later than that, to long wet process kilns. This came about largely because of an increase in production of fiberglass fabrics and early improvements in treating fiberglass fabrics with lubricants to prolong their service life. This development gave cement manufacturers the best available filtration efficiency of the time and allowed them to use a piece of equipment that could guarantee extremely high efficiency regardless of production rate. Prior to this time, plants recovered a substantial amount of material from the air stream before it ever got to the final discharge. The installation of higher efficiency filtration equipment, required today by EPA, required in some cases by local law in earlier days, gave cement manufacturers two ad-

ditional benefits. The first, a better rapport with local neighbors, the second being a cleaner plant environment. In early days, it was not uncommon to see roofs of the plant facilities with 6 to 8" of dust all over them, causing in some cases structural damage, in others replacement of roofs at more frequently than normal intervals.

Today, we break up application of dust collection equipment into two distinct categories. The first is application of the equipment to parts of the process that are largely housekeeping in nature. Examples would be ventilation of material handling equipment, crushing, storage and withdrawal facilities of both raw and finished materials, etc. The second category is application of equipment to the process train and process gas itself. Examples here are drying, milling, burning (kiln), material cooling (clinker coolers), and others.

There are eight (8) basic processes in cement plants which require dust collection equipment:

- 1) material handling
- 2) storage and silos
- 3) crushing
- 4) drying
- 5) milling
- 6) burning (kiln)
- 7) alkali bypass
- 8) cooler (clinker)

In some cases, the air streams from several of these can be combined to form one combination gas stream handled by a single piece of equipment. We will discuss each of these separate areas to point out the potential problems for design and operation of the dust collection equipment.

### Duct System Design

An important part of dust ventilation systems is the design of the ducts.

The design of the duct system used for collecting the vent air streams and fugitive dust from the material handling equipment or any of the other equipment to be discussed in this paper can follow either of two general methods of design; each would be used for different purposes.

The first would be a self-cleaning duct system. This duct system would be designed with a maximum velocity of about 2000 feet per minute. Because of these low velocities, material may settle out in the pipes, hence all pipe runs must have a minimum slope of 45° with no horizontal runs whatsoever. This design approach should be considered when handling extremely abrasive material in order to reduce wear on pipe-lines. It should also be considered where there is large inherent variation in the

volume within the system, whereby material handling velocities cannot be guaranteed for a conventional high velocity vent system.

This type of duct system is expensive to install. This system is limited to short horizontal distances where the dust collector is located as close as possible to the sources being vented. Self-cleaning systems also present support problems, particularly, at the apex of runs where the ductwork must go to a 90° bend and back down to filtration equipment.

The advantage of the self-cleaning system is that it provides the lowest operating static pressure and thus the lowest fan energy requirement; a consideration that must be kept in mind today.

The other general method of designing a vent system would be to use conventional high velocity ventilation techniques. The design velocities for this system would be between 3500 and 4000 feet per minute. These velocities must be maintained to prevent any settling of dust in any long horizontal runs. This system can be used on any materials, but abrasive materials, such as clinker dust or sand will present wear problems; and the duct system must therefore be designed to allow for wear at the elbows and any intersections or transition points.

There are some cases in these various material venting systems in which the material may be hot and moist, and the collected air and dust could present a caking problem. Insulation of the ductwork and dust collector or the admission of supplementary warm air might be required.

#### I. Material Handling

Since a cement plant is required to move large quantities of dry materials as either raw feed or finished product, many belt conveyors and bucket elevators are used. At each of the transfer points onto or off the belt or from the bucket, some dry dust emission is produced. The air volume that must be handled is definitely related to the height of the material fall. The further the material falls, the bigger the ventilation problem. Also at transfer points, there is a tendency for the stream of material to drag air in at the upper end of the transfer. The air migrates to the lower transfer housing, backing up at the discharge of the lower transfer housing, and causing dusting primarily at this point. For this reason, the primary ventilation volume should be removed from the lower portion of any transfer housing.

If too high an air velocity of the vent air is used, excessive dust is transported from the point of transfer rather than removing only the amount of dust and air that is generated. Generally, the dryer and finer the material

that is being conveyed, the more fugitive dust that is generated at the transfer points. Belt conveyors require less energy than pneumatic conveying, but have the potential of greater fugitive dust production.

Either small shaker collectors or high ratio pulse type collectors are used for these collection points.

## II. Storage and Silos

Silos are filled by bucket elevators, belts, or pneumatic conveying. At the discharge points of bucket elevators, the material is flung from the buckets. The volume of air to be removed is dependent upon the cross sectional area of the housing and its height.

The volume of air to be ventilated from a silo depends upon any one or combination of:

1. Width and speed of belt conveyor
2. Size of bucket elevator
3. Air volume capacity of pneumatic conveying system

(A surge factor should be included when sizing the fan and filter).

The first two systems generally require the lowest volume of air and the least amount of dust to be collected. A pneumatic conveying system requires the largest volume of air and generates more dust to be collected.

Silo venting also applies to the homogenizing (blending) silos for raw feed in dry process plants. The air volume is determined by the air supply required for blending.

Either intermittent or continuous collectors of the shaker or pulse type can be used.

## III. Crushing

The crushers used in a cement plant are generally selected on the basis of the type of stone being used to supply raw material for the product, as well as, the size required for further processing after the crusher. Commonly, hammermills or impactors are applied to limestone today, and in many existing plants, the combination of jaw crushers, gyratory crushers, and cone crushers have been used. The fugitive dust problem in crushing operations increases as the amount of energy increases in the crushing operation. The hammermill creates the most serious dusting problem as it is really analogous to a large fan, thereby creating motion of an air stream by itself. The hammermill has extremely high



tip velocities, thus imparting considerable kinetic energy to the stone being crushed which has to be "killed" below the crusher and hopefully before the stone reaches the material handling system below. This is not true with the other methods of crushing where air flow is induced primarily due to the flow of stone by gravity thru the other crusher designs.

In all cases in the crushing operation, it is preferable to do all of the venting down below the crushers, either in chutes or in the material handling system below the chutes. The design of the plant can help to reduce a fugitive dusting problem if rock boxes are included underneath the crushers to kill the motion of the moving material before it reaches the material handling system. A rock box is a trap, usually formed of concrete that extends the full width and length of the crusher discharge opening. In the bottom of this rock box there is a smaller opening, allowing the passage of material to the subsequent operations downstream. The crushed stone is allowed to fill up and seek its natural angle of repose and thus any additional stone falling from the crusher must impact on the entrapped stone before it can reach the opening in the rock box passing the material on to the conveying system.

It should be noted that when a crusher is operating with a choke of material ahead of it, there is usually no dusting on the top side of the crusher; however, when the choke is no longer ahead of the hammermill, some minor dusting can occur at the feed opening to a hammermill.

Most crushers are fed with either front end loaders or dump trucks. At the time that the crusher is fed with a load of material, dusting occurs at the initial dump of the quarried material into the feed hopper for the crusher. Ventilation of a condition like this has not been usually attempted as vast quantities of air are required to adequately prevent fugitive dust from getting into the ambient air away from the crusher. Conventionally, feed points of crushers should be enclosed and usually have been enclosed with a small building, open on one side to accept front end loaders and dump trucks.

Primary crushers usually reduce the quarry-size rock to less than four inch size, normally, about one inch.

Secondary crushers, generally of the hammermill type, reduce the rock to 1/4" x 0. As long as the feed and product are dry, there is no particular problem with dust collection on this installation.

Since these facilities usually require large air volumes, high ratio pulse type collectors are the best selection.

#### IV. Drying

Drying of raw feed can be accomplished in a separately fired rotary dryer, a rotary dryer utilizing some waste kiln gases, or in a combination dryer-crusher operation. The main concern for handling the off-gases from a dryer or crusher/dryer operation is insulation to prevent any dewpoint occurrence in the collector system. If the off-gases are at least 100° above the projected water dewpoint of the system, with proper insulation there should be no particular problem.

Depending upon the gas temperature, the collector could be either a glass bag reverse air cleaned unit, or a synthetic bag pulse type collector. Care should be taken in the choice of fabric on drying operations. Potential hydrolysis or chemical attack of fabric may occur.

#### V. Milling

In a cement plant, ball mills are used to grind finished cement to the size distribution required for the specific type of cement being produced. The ball mill and the separator are the two main items of process equipment in any milling circuit whether it be a finished cement circuit or a raw feed circuit in a dry process cement plant. Classification of the mill product is done in an air separator where the fines are separated from the coarse material using principles of Stokes's Law. The fines are discharged to the outer cone of the separator and separated by centrifugal action, and the coarse product is returned to the milling circuit from the inner cone of the separator.

In a finished cement circuit, there is a difference in the fineness of grinding for different types of cement, and therefore there is a difference in the size distribution as well as the amount of material. Masonry cement and Type III cement are ground to the finest size distribution. It is often necessary to cool the cement before it is transported to storage silos. This cooling can be done in the ball mill by introducing water along with a grinding aid; it may be done by introducing substantial quantities of cooling air into the air separator, or independent cement coolers may be used downstream of the air separator. Cement coolers usually operate under the principle of cooling the cement with water either by an indirect heat transfer coil within the cooler or by allowing a continuous flow of water on the outer shell of a tank containing aerated finished cement.

On the raw feed circuit of a dry cement plant, drying of the raw materials may occur in the mill, or by introducing preheated air into the air separator to flash dry the material.

Dust collection in a milling circuit for raw feed or cement can normally be classified as application of process type dust collectors. Generally, two dust collectors are used, one to vent the mill along with all the other ancillary ventilation points that occur at both the feed end and the discharge of the mill and material handling equipment downstream of the mill. In cases where either drying or cooling occurs in the separator, an independent dust collector is applied on this portion of the mill circuit. There are two reasons to apply a separate dust collector here, one being to take advantage of a fan energy saving as drying and cooling circuits and separators generally operate at low static pressures; two, if this circuit was applied to one general ventilation system for the entire mill room, there can be interaction between the mill and the separator air volumes that can potentially cause control problems of the milling process itself.

The air streams coming from the ball mills and from the separators contain great quantities of material; with the exception of a roller mill circuit, these two areas are the highest grain load encountered in a cement plant. Since most of the material is very fine, the dust collector catch represents a substantial quantity of the finished product in the circuit.

There are several things to be very careful of in application of dust collectors in this area. The extreme amount of material caught from the air stream requires careful choice of the material handling system within the collection equipment. Introduction of moisture into the mill, must be made known, as this could affect the choice of the filtering equipment as well as its size. If drying is to occur either in a mill or in a separator, this must be made apparent as this also could affect the choice of fabric applied as well as the size of the equipment installed.

Both shaker and pulse type collectors have been successfully applied in this system.

## VI. Burning - Kilns

For venting the burning or calcining equipment, kiln, different problems are involved in the three types of processes wet process, dry process, and preheater process.

Wet Process - In the wet process kiln, since the feed material is a slurry or wet cake, the off-gases will contain as much as 35% by volume moisture producing a high dewpoint temperature, in the order of 165°F but with dry bulb temperatures of about 500°F. The prime problem in venting this gas stream is the necessary insulation required for the system to prevent condensation which produces extreme corrosion on the housing and potential blinding of the dust cake on the filter bags.

Glass bag reverse air units with adequate insulation have been successfully used for this type of process.

Long Dry Kiln - The off-gases from a long dry kiln are usually at a temperature of 750 to 1000°F and require cooling prior to entering the baghouse. Depending on the alkali content of the waste kiln gases, a cyclone may be incorporated at the kiln discharge to collect the coarser fraction for refiring into the kiln with the raw feed or by the insufflation technique. If the dust is high in alkali content, then the fines, which contain the larger percentage of alkali can be wasted. If the alkali content is low, then the total waste dust stream can be collected in the fabric filter and returned to the kiln for firing. Some cooling in the case of the cyclone equipment is obtained, but, generally, the cooling is accomplished by water sprays in the discharge end of the kiln.

Water Spray Towers or Air-to-Air Heat Exchangers can be utilized for cooling of the kiln gases, however, this is not usually done.

Since the moisture level content of these gases is not of great concern, generally, uninsulated pressure type baghouses are used, however, fully insulated suction type houses are also employed. Both types use glass bags and reverse air cleaning.

Preheater Kiln - Since the waste gases from the preheater kiln are used for warming the incoming raw feed, the off-gas temperatures are lower than for the long dry kiln and temperature control is usually accomplished by a bleed-air damper. The exit gas temperatures are normally 650°F, when the preheater is operated at rated capacity. Tempering with air brings the gas stream down to 500-550°F allowing application of glass fabric filters.

One variation which can be used with preheater kilns is an air-swept in-line roller mill used for grinding the rock, from the secondary crusher size, plus clay, iron ore or other additives, to the size necessary for raw feed. The ground material goes directly to the homogenizing silos.

Generally, the in-line roller mill is used as a raw mill and drying operation, since sufficient heat is available in the kiln gases. The dust collection problem associated with this operation is to insure adequate insulation to prevent possible water dewpoint conditions in the fabric collector. Of course, another design consideration must be for handling the hot gases when the roller mill must be bypassed for periods of maintenance or emergency outages. This is generally accomplished with a multi-fan installation so that normally one fan provides the pressure drop re-

quirements of the mill while it is in operation and a separate fan provides drop for the collector alone.

The off-gas from the mill circuit quite often goes thru a set of cyclones to collect the majority of the milled material, however, this does not always have to be the case and the baghouse can handle the total dust load. All of the dust collected is then supplied as raw feed to the preheater. If the raw feed contains sufficient alkali content that some of the dust must be wasted, this is usually handled in the alkali bypass system.

Fabric collectors for kilns have all been glass bag reverse air cleaned units, of either pressure or suction design. Proper fabric selection depends on the type of kiln and type of feed material being calcined.

#### VII. Alkali Bypass, Preheater Kilns

In order to control the alkali content of the finished clinker, when the alkali content of the raw feed is too high, a small proportion of the kiln gases are vented at the kiln exit prior to the preheater and are cooled and collected in a separate fabric filter. Since the gas stream leaving the kiln prior to the preheater is in the 1800°F temperature range, the gases must be quickly quenched by either, or a combination of, air-quenching and water spray cooling to reduce the gas temperature to 500 to 550°F for collection in the fabric filter.

Reverse air cleaned glass bag units are used for this system.

#### VIII. Clinker Cooler

The clinker cooler's main purpose, of course, is to cool the clinker quickly enough by air-quenching to set the chemical properties of the clinker. Another important function of the clinker cooler is to recover sufficient heat in the air stream to assist the combustion and burning of the cement rock. Additional heat is also utilized for the pulverized coal circuit or additional drying operations which might be utilized at the plant.

There is always excess waste hot air from the clinker which must be vented. The main problem in handling this waste hot air stream to a fabric filter is the temperature control required during the flushes which occur from the kiln. The temperature can vary from less than 300°F to 800 or 1000°F. Cooling of this waste stream can be accomplished in either of two ways:

1. Water sprays in the cooler onto the clinker bed plus the addition of large quantities of dilution

air to the vent stream to reduce the temperature of the gases sufficient to be handled by the fabric filter.

2. Air-to-air heat exchangers in which the hot gases are cooled to the control temperature by passing them thru a tubular heat exchanger cooled from the outside by a secondary stream of ambient air moved by separate low pressure fans. This technique can produce large volumes of relatively warm air which might be useful for warming buildings during the wintertime.

No particular problem is involved in the fabric filters for the clinker coolers as long as the temperature control and the surge volumes are adequately provided for. Both Nomex bags, 425° maximum temperature, and glass bags, 550° limit, have been successfully utilized. High ratio pulse type collectors use Nomex felt bags at the 425°F limit, while glass bags are used in reverse air cleaned collectors.

### CONCLUSION

As a reference to define the amount of material to be handled, cement plants producing 1000 ton per day of finished product require a supply of about 1500 ton per day of raw feed materials. Plants are operating at 3000 TPD production and others being built with capacities up to 7000 TPD. These, usually dry materials must be handled and conveyed many times through the different processes. Today plants operate at 99.9998% material efficiency. This means more saleable product from the raw materials.

Federal E.P.A. emission regulations of 0.3 lb/ton from kilns and 0.1 lb/ton from clinker coolers are easily met with fabric filters when design consideration of the process conditions and proper selection of filter media are made. Test data shows kiln emissions to be 0.013 to 0.035 grains/SCFD (.1 to .25 lb/ton) and cooler emissions to be 0.0012 to 0.015 grains/SCFD (.011 to .061 lb/ton) for a variety of plants.

All of the miscellaneous sources are regulated by opacity, but with proper fabric no visible emissions occur.



NEW APPLICATIONS FOR FABRIC FILTERS

R. L. Adams

Wheelabrator-Frye Inc.  
Pittsburgh, Pa.

December 1977



## NEW APPLICATIONS FOR FABRIC FILTERS

Requirements for improved filtration efficiencies have led to the use of fabric filtration in many areas that a few years ago were considered the domain of high-efficiency cyclones and low-energy wet scrubbers. This paper will review a few of these new applications for fabric filters. It is recognized that almost any so-called "new" applications will have been tried somewhere at some time in the past. However, we believe that the applications discussed herein represent major future potential for fabric filtration and that developments over the past year or so in these areas have been significant.

It should be noted that three of the five applications to be discussed employ coated fabric filters. It is this area that provides great potential for expanding the use of the fabric filtration in the future. The applications which are discussed in this paper represent only a few of the many potential uses for coated fabric filters. Expanding research and development activity in this field will uncover many more in the near future.

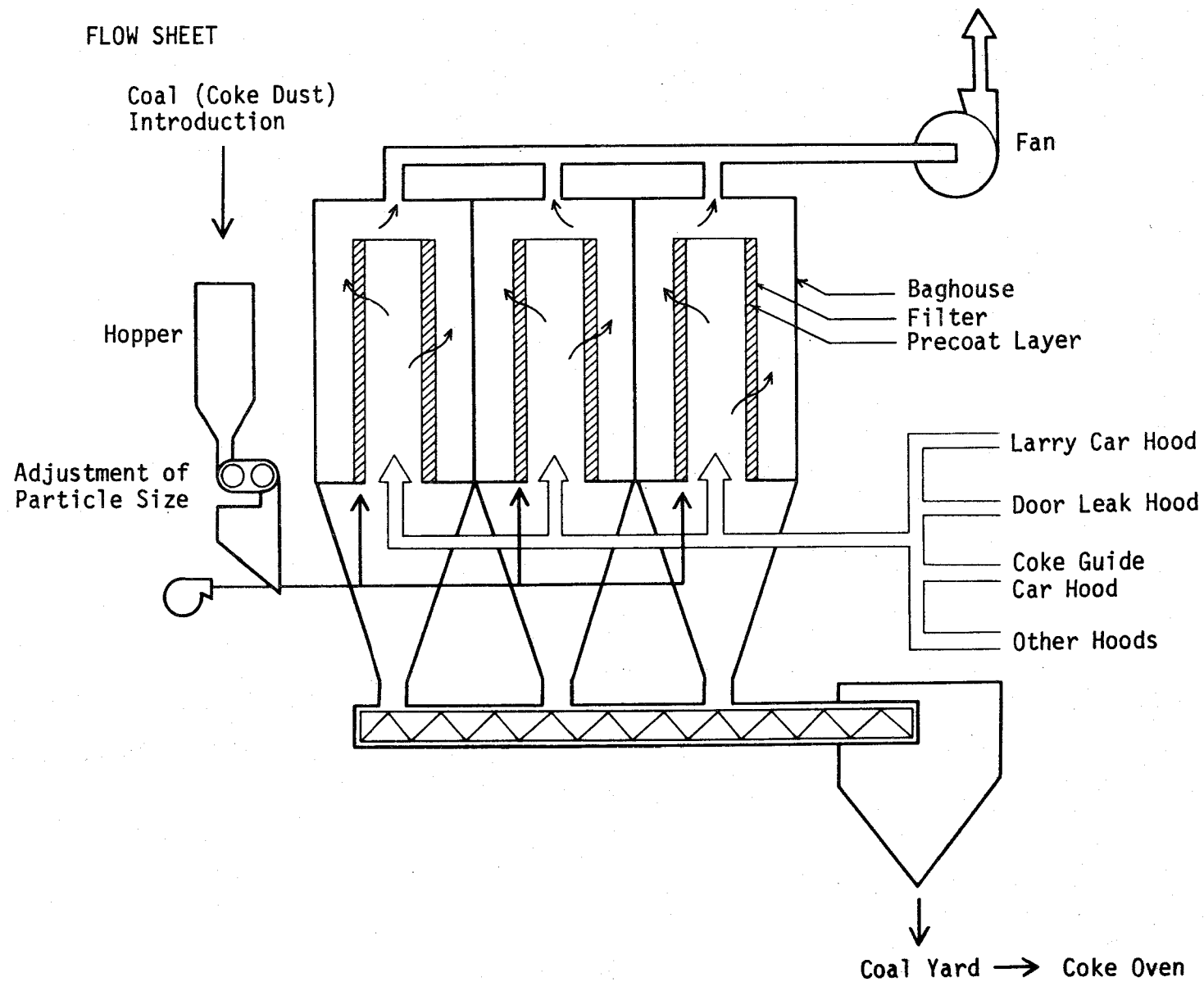
We have chosen for discussion five new applications. These are: 1) coke oven emission sources, 2) coke oven combustion stacks, 3) sinter machine windboxes, 4) galvanizing lines and 5)  $\text{SO}_2$  removal. We would like to give a brief review of the current state of the art in each of these areas. In some cases, the work has been done on only a pilot scale in other cases full-scale production units are in operation.

### Coke Oven Emission Controls

A unique application of a fabric filter for coke oven emission control has recently been disclosed by the Taisei Corporation, Tokyo, Japan. This process is covered by United States Patent 4,010,013. The process utilizes a coated fabric filter called the PRECO Filter to remove particulate and tars from charging, pushing and other coking side operations. It has not been applied to coke oven combustion stacks and these will be discussed in another section of this paper.

Figure 1 shows a typical flow sheet for the process. Coal or coke is passed through a pulverizer and injected onto the filter bags. Coke oven gas ventilation sources are then ducted to the filter. The fabric filter utilized

FIGURE 1



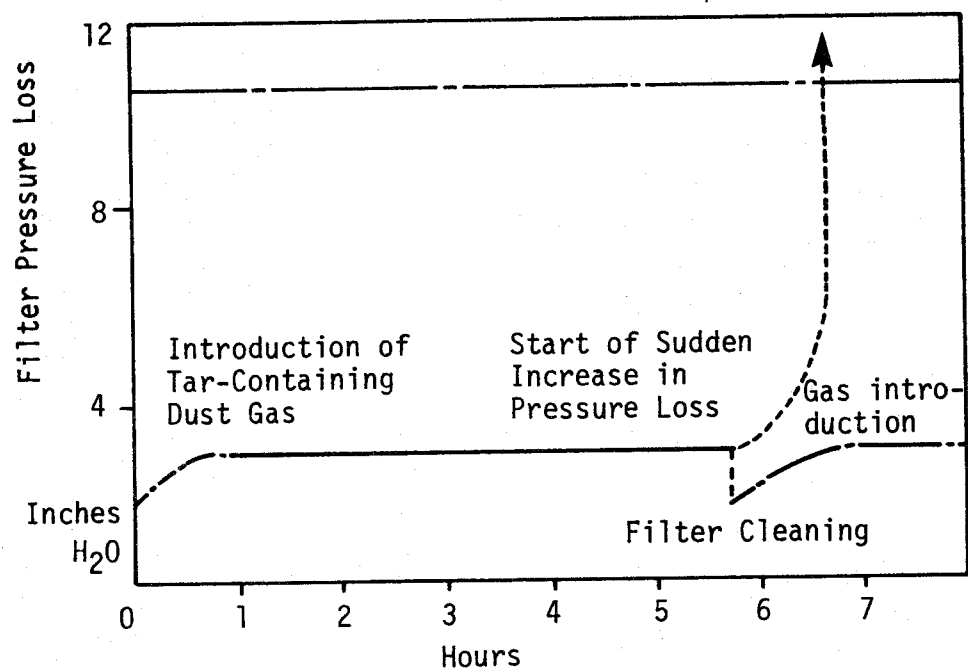
in this application is a standard filter equipped with polyester filter fabric and bag cleaning is accomplished by mechanical shaking. The protective coating of coal or coke dust effectively prevents the adhesion of the tar to the fabric. It also serves as a filter aid in that it contributes considerably to the filtration efficiency of the unit.

Operation of the unit is somewhat different than operation of a standard fabric filter. Figure 2 shows a typical filter pressure loss curve for this operation. It can be seen that after an extended period of operation, breakthrough on the filter aid material is anticipated and substantial increases in pressure drop may be encountered. The operating goal, therefore, is to begin cleaning of the filter prior to this time to keep operation on the flat part of the curve. This has been successfully accomplished in a full-scale facility operating at Tokyo Gas Company.

Figure 3 shows the extremely high removal efficiencies that have been obtained in both pilot and full-scale operation. At the filtration temperatures employed, the tars exist in a condensed state as liquid aerosols and can be effectively removed by the coal or coke precoat layer. The collected material from the process is returned to the coal yard, mixed with coal, and sent to the coke oven for reuse.

FIGURE 3  
COKE OVEN EXHAUST  
TAR REMOVAL EFFICIENCY

Precoating Material	Temperature °F	Tar Concentration Grains/Cu. Ft.		Removal Efficiency %
		Inlet	Outlet	
Coke	104	0.083	0.00006	99.93
		0.015	0.00001	99.93
Pulverized Coal	104	0.049	0.0001	99.79
		0.169	0.0005	99.70
Pulverized Coal	248	0.264	0.00009	99.97
		0.084	0.00003	99.99
		0.223	0.000009	99.99



TYPICAL FILTER PRESSURE LOSS CURVE

FIGURE 2

We believe that the Taisei PRECO Filter represents a very new and novel application for fabric filters. The fact that the coating material is the raw material for the ovens and that the collected material may be returned to the ovens is significant. We would expect to see application of this type of filter in the United States in the future.

#### Coke Oven Combustion Stacks

In many of the older coke ovens, leaks exist between the coking side and the combustion side of the oven due to deterioration of the bricks. Therefore, contaminants such as hydrocarbons and tars leak into the combustion side of the oven where they are partially burned to produce a finely divided form of carbon black along with condensibles. This leakage is generally intermittent in nature but as the air pollution codes become more stringent, control of this source is now being required in some areas.

Early this year, a pilot fabric filter was operated at a major steel mill. During operation of the pilot unit, the oven was fired with both coke oven gas and blast furnace gas. During firing of coke oven gas, the filter was operated both with a precoat of limestone and without a precoat. Performance with regard to filtration of solid particulate is given in Figure 4. It should be noted that the average outlet concentration on solid particulate when using the coated baghouse was 55% less than when using a noncoated baghouse.

FIGURE 4

#### COKE OVEN PILOT UNIT

<u>Solid Particulate gr./DSCF</u>	<u>Blast Furnace Gas (noncoated)</u>	<u>Coke Oven Gas (precoated)</u>	<u>Coke Oven Gas (noncoated)</u>
<u>Inlet</u>			
(max.)	0.1173	0.0958	0.0841
(min.)	0.0101	0.0219	0.0077
(avg.)	0.0585	0.0657	0.0312
<u>Outlet</u>			
(max.)	0.0048	0.006	0.0096
(min.)	0.0007	0.0014	0.0096
(avg.)	0.0023	0.0035	0.0056

Performance of the unit with regard to condensibles and sulphuric acid is given in Figure 5.

FIGURE 5

COKE OVEN PILOT UNIT

<u>Condensibles gr./SDCF</u>	<u>Blast Furnace Gas (noncoated)</u>	<u>Coke Oven Gas (precoated)</u>	<u>Coke Oven Gas (noncoated)</u>
<u>Ether Fraction</u>			
<u>Inlet</u>			
(max.)	0.0041	0.0035	0.0081
(min.)	0.0014	0.0005	0.0000
(avg.)	0.0024	0.0015	0.0028
<u>Outlet</u>			
(max.)	0.0017	0.0027	0.0046
(min.)	0.0003	0.0003	0.0000
(avg.)	0.0011	0.0013	0.0018
<u>Water Fraction</u>			
<u>Inlet</u>			
(max.)	0.1791	0.0973	0.2366
(min.)	0.0225	0.0574	0.0503
(avg.)	0.0868	0.0685	0.1322
<u>Outlet</u>			
(max.)	0.0762	0.0973	0.1356
(min.)	0.0077	0.0312	0.0122
(avg.)	0.0289	0.0422	0.0724
<u>H<sub>2</sub>SO<sub>4</sub></u>			
<u>Inlet</u>			
(max.)	0.1323	0.0486	0.1636
(min.)	0.0166	0.0363	0.0244
(avg.)	0.0669	0.0432	0.0978
<u>Outlet</u>			
(max.)	0.0528	0.0392	0.0728
(min.)	0.0047	0.0232	0.0260
(avg.)	0.0185	0.0282	0.0529

An examination of the data shows that the average ether fraction condensibles were 27% lower when using the coated fabric filter and that the outlet concentration of the water fraction condensibles was 42% less when using the coated fabric filter. In both cases, either with the use or without the use of the precoat, stack opacity was less than 5%. The portion of the water fraction of the condensibles due to sulphuric acid is also given in Figure 5. Since this fraction would not occur in those ovens firing sulphur-free gases, the sulphuric acid fraction may be deducted from the water fraction condensibles to give a true picture of the effectiveness of the fabric filter.

Due to the extremely light grain loading, high air-to-cloth ratios were utilized. Air-to-cloth ratios ranged from 3.0 to 3.5 to 1 when utilizing a coated fabric filter and 2.5 to 3.0 to 1 when using the noncoated fabric filter. The pressure drop using a coated fabric filter was approximately 25% lower when using the noncoated fabric filter at the same air-to-cloth ratio. In either case, bag cleaning was carried out only once every 24 hours.

The first commercial unit using a fabric filter in this application is now being built. We believe that this too represents a major extension of fabric filters into an area previously considered to be outside of the boundaries of good fabric filter application.

#### Galvanizing Line Control

There have been infrequent attempts over the years to apply fabric filters to fume generated from galvanizing lines. Some of these have met with limited success and, therefore, strictly speaking this is not a new application. However, to our knowledge, a pulse-jet filter has not been used for this service in the United States. We would like to review the successful application of this type filter to a galvanizing line. The unit has been in operation since June 1977. It was installed after operation of a pilot unit for ten weeks.

Figure 6 gives both the design and the actual measured operating conditions of the unit. It should be noted that while the actual operating air-to-cloth ratio is approximately 20% greater than design, pressure drop is in the design range. The design features of this unit are shown in Figure 7. Since start-up, operation of the unit has been generally satisfactory. However, it is essential that the unit be kept completely dry. The collected material is

FIGURE 6  
GALVANIZING LINE  
FABRIC FILTER OPERATING CONDITIONS

	Design	Actual
Gas Volume (ACFM)	14,000	16,964
Gas Temperature (°F)	250 (max.)	187
Total Cloth Area (sq. ft.)	5,040	5,040
Air-to-cloth Ratio	2.78 to 1	3.37 to 1
Pressure Loss (in. w.g.)	6"	6"
Inlet Grain Load (gr./ACF)	4	2.5

FIGURE 7  
GALVANIZING LINE  
FABRIC FILTER DESIGN FEATURES

Standard Pulse Jet  
Two Modules  
16 oz. Dacron Siliconized Finish  
Stainless Steel Cages  
On-line Pulsing  
Completely Insulated  
Material Collected --  
Zinc Chloride  
Aluminum Chloride  
Ammonium Chloride  
Elemental Zinc

hygroscopic and readily absorbs moisture from the atmosphere. While the material is light and fluffy in the dry state, the particles tend to agglomerate as they take on moisture and become very sticky.

Almost all of the operating problems encountered with this unit have been due to the nature of the collected material. Upon first start-up of the equipment, insulation of the system was not adequate and the collected material



tended to get wet. Once the defects in the insulation system were corrected, there have been no more problems in this area. The other areas where difficulties have been encountered are in the ductwork leading to the collector where the material tends to fall out or to stick on elbows and other impact surfaces. There has also been some difficulty in removing the material from the hopper. As long as the rotary valves are operated continuously, the material flows freely. If, however, the rotary valves are shut down for any extended period, and plant operations seem to accomplish this in spite of all instructions to the contrary, the material tends to build up and bridge in the hoppers. Even though the vanes of the rotary valves are teflon coated, the material also tends to stick to the vanes if hopper storage is attempted.

This unit shows that a pulse-jet filter operating at a relatively low air-to-cloth ratio represents an excellent means for controlling galvanizing line fume. We would recommend, however, that each galvanizing line be studied as there are individual differences which may dictate the type of equipment to be employed. It is necessary to use proper operating precautions with this type of equipment to preclude moisture in the system and subsequent problems.

#### Sinter Machine Windbox Ventilation

Fabric filters have been used for many years to ventilate the discharge end of sinter machines in the steel industry. In addition, we are aware of at least one installation utilizing a woven fabric filter to ventilate the sinter machine windbox. However, within the past year, a pulse-jet type filter for windbox ventilation has been installed and we would like to review briefly the design and operation of this unit.

The design data is given in Figure 8. These design parameters were set after extensive pilot testing of a pulse-jet collector. Operation over the first year has generally been satisfactory but some of the parameters that have adversely affected operation should be reviewed.

## FIGURE 8

### SINTER MACHINE WINDBOX FABRIC FILTER

Gas Volume - 200,000 ACFM  
Gas Temperature - 260°F  
Inlet Load - 0.5 gr./ACF Solid Particulate  
              - 0.02 gr./ACF Condensible Hydrocarbons  
Filter - 14-module Pulse Jet  
Cloth Area - 35,630 sq. ft.  
Air-to-cloth - 5.6 to 1  
Fabric - 16 oz. Dacron Felt ICR Finish  
Pressure Drop - 4.5" to 6" w.g.

Extensive operating experience indicates that the most important parameter affecting operation of the baghouse is the amount of oil being introduced onto the sinter strands. As you know, this oil is not completely burned and carries over into the filtration system in the form of oil vapor and, as it is cooled, in the form condensed liquid aerosols. As long as there is sufficient dry filter cake on the bags, the effect of the condensed oils is minimal. However, since the grain loading can be light at times from the operation of the sinter machine, the dust cake on the bags will be light and in that case a large quantity of condensed oils can cause increased pressure drop in the fabric filter.

While this unit has not been tested, the discharge stack has remained optically clear. It is expected that performance tests will be performed in January. However, there would appear to be little or no problem with condensibles passing through the baghouse and later condensing at the discharge of the stack.

In spite of the successful operation of this baghouse, we would strongly recommend that most sinter line windboxes be piloted for an extended period of time to encounter all expected operating conditions of the sinter machine prior to installation of the baghouse. In addition to the problem of condensibles noted above, we have also seen a pilot installation where solids such as zinc ammonium sulphate pass through the baghouse as a vapor at filtration temperatures and later desublime into a solid at the discharge stack. Presence of these materials is almost impossible to predict from observing sinter machine operation and charging

practices; therefore, a pilot unit is recommended to determine the adequacy of a fabric filter for this application.

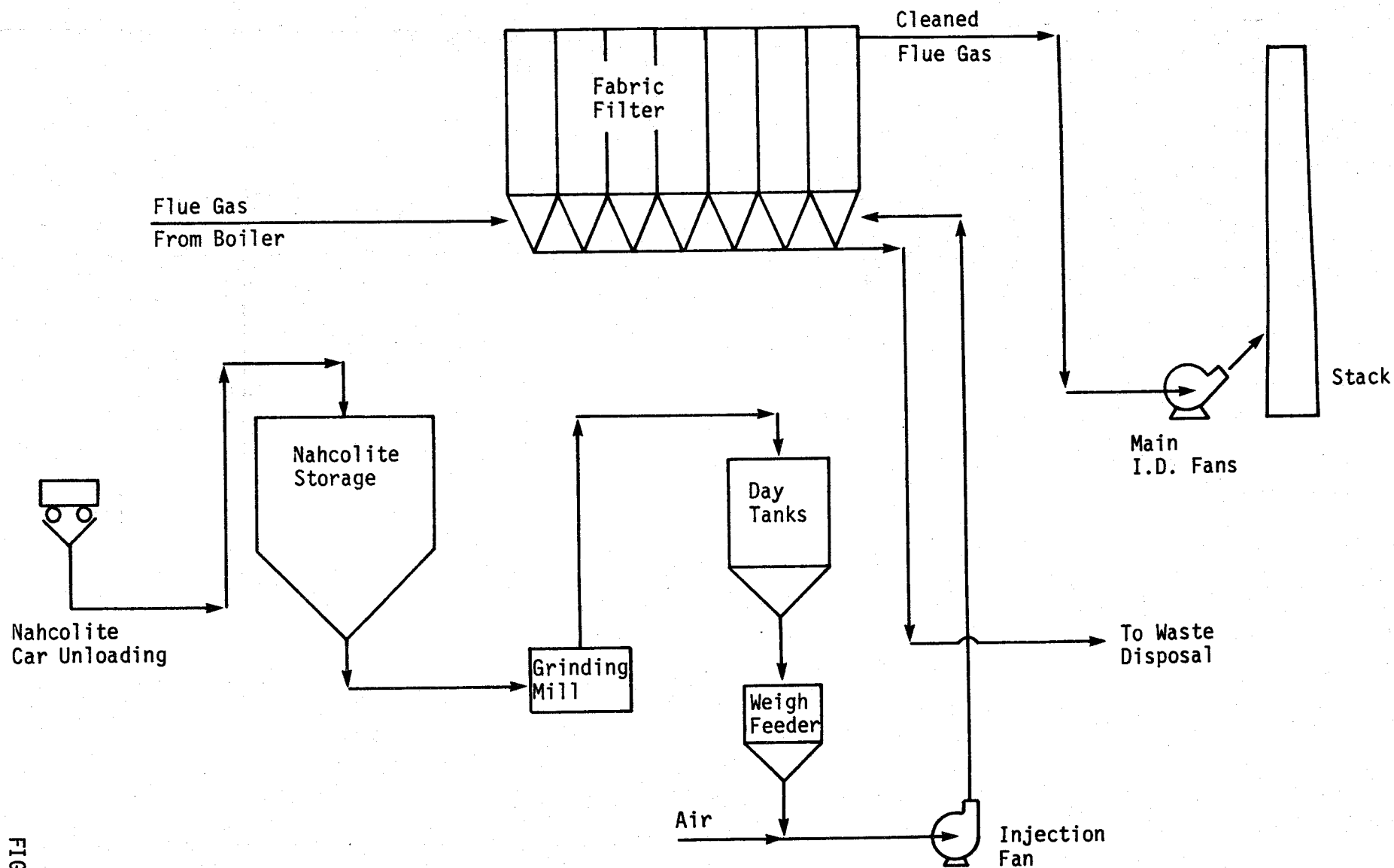
### SO<sub>2</sub> Removal

Another novel application for a fabric filter is its use to remove gaseous contaminants. Proper selection of an additive material allows for chemical reaction with certain gaseous contaminants as the gases pass, at low velocity, through the filter cake. One example of this technology is the use of a fabric filter with the additive Nahcolite, a naturally occurring sodium bicarbonate, for removal of sulphur dioxide from boiler flue gas.

Figure 9 shows a typical design of this type of system. The flue gases from the boiler containing both particulate and sulphur dioxide are conveyed to the fabric filter in a conventional manner. A solids additive system is utilized to air convey the reactant material into the filter and to utilize this material to form part of the filter cake and act as a reactant. It is also possible to feed the reactant into the flue gas stream from the boiler prior to its entry into the fabric filter.

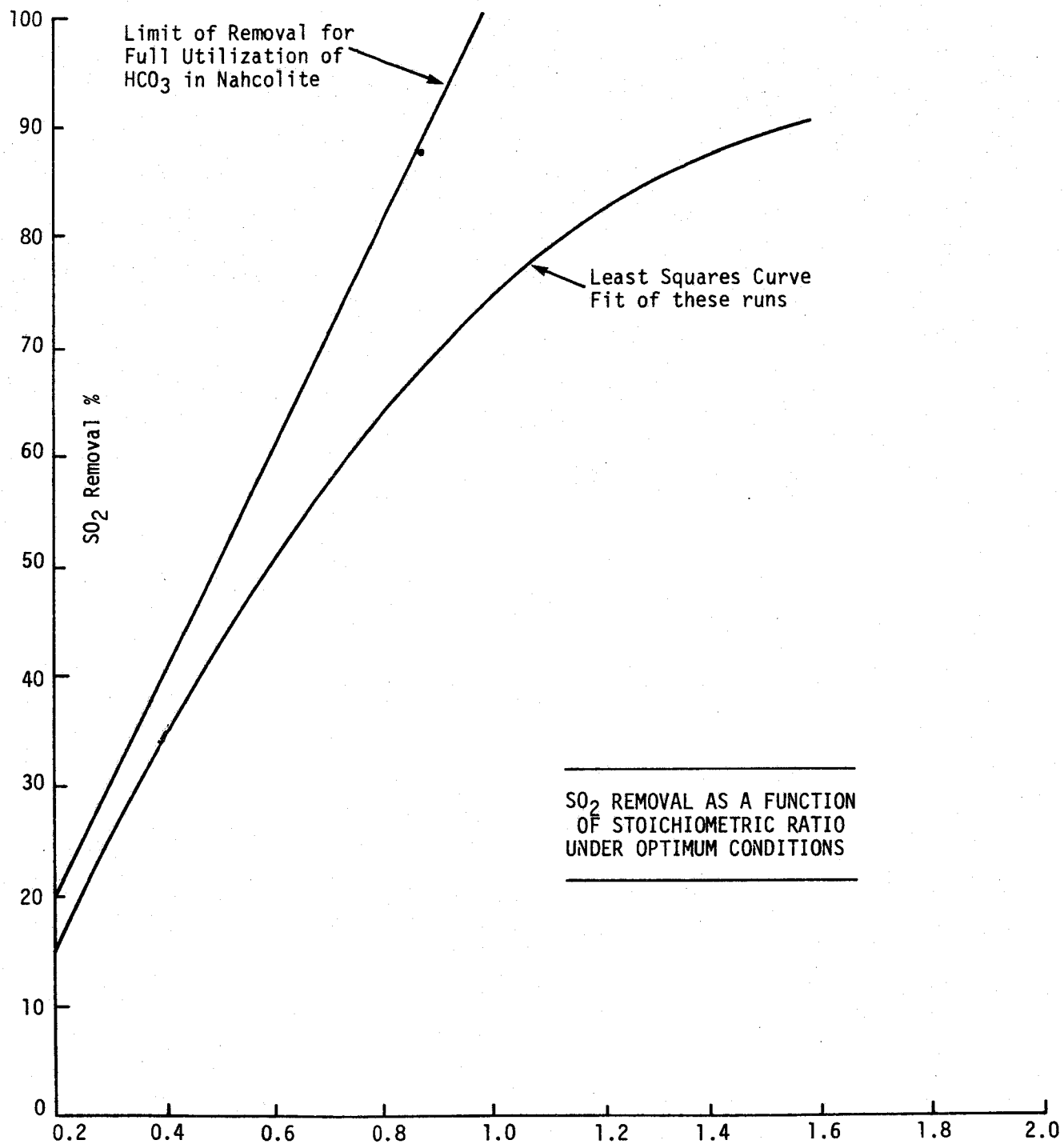
This "dry scrubbing" system is capable of removing up to 90% of the SO<sub>2</sub> contained in the inlet gas stream. Figure 10 shows SO<sub>2</sub> removal as a function of the stoichiometric ratio of Nahcolite fed into the fabric filter. The curve shown is under optimum feeding conditions. It should be noted that at a one-to-one stoichiometric ratio approximately 73% of the SO<sub>2</sub> in the inlet gas stream can be removed. In addition, of course, the fabric filter will remove solid particulates with efficiencies in excess of 99%. Particulate removal efficiency in the pilot unit of 99.7% was not considered typical since the pilot unit was operated in a manner which required that the bags be completely cleaned at the end of each test cycle in order to check material balances. As a result of this operating procedure, the filter cake was essentially destroyed each time the bags were cleaned and this resulted in some inefficiency at the start of each cycle with regard to particulate removal. This would not occur in an operating unit since filter cake would be retained during each cleaning cycle.

It may be of interest to examine some estimated costs for the fabric filter-Nahcolite system. These costs are given in Figure 11. The basis of the costs is a 500 megawatt unit handling 1.5% sulphur coal with SO<sub>2</sub> reduction



FABRIC FILTER - NAHCOLITE SYSTEM

FIGURE 10  
202



consistent with present EPA requirements limiting SO<sub>2</sub> emissions to 1.2 lbs. per million Btu's. It can be seen that this system is estimated to be highly competitive with present day SO<sub>2</sub>-particulate removal systems. It should be noted that a source of Nahcolite material is not yet available and the future of this process hinges upon commitments to begin mining operations by those who hold Nahcolite reserves.

FIGURE 11  
FABRIC FILTER-NAHCOLITE SYSTEM  
COSTS

Estimated Capital Costs	\$23,100,000
	\$46.20/kw
Annual Operating Costs	
Capital Charges @ 14.9%	\$ 3,442,000
Raw Material	3,003,000
Disposal	1,010,000
Labor, Maintenance, Utilities & Misc.	1,963,000
	<u>\$ 9,418,000/year</u>
	2.69 mils/kwh

Conclusion

Examination of the above five applications shows in a general way the directions of expansion for fabric filter technology. These five applications certainly do not represent the only new applications for fabric filters but were chosen because we believe that they do show the current general directions of technology expansion. With the increasing efficiency requirements and with requirements for fine particulate control, which we believe are forthcoming, we feel that the scope of application of fabric filters will be continually broadened in the future.



Effect of Modified Cleaning Pulses  
on Pulse Jet Filter Performance

by

David Leith, Melvin W. First and Dwight D. Gibson

Harvard University  
School of Public Health  
Department of Environmental Health Sciences  
665 Huntington Avenue  
Boston, Massachusetts 02115

Abstract

Dust seepage through a pulse-jet filter can be minimized by gradually reducing air pressure at the end of the cleaning pulse instead of using the usual square wave pattern. This allows the pulsed bags to return gently to their rigid supporting cages and avoids driving dust trapped in the fabric into the cleaned gas stream. Pulse modification by this method is especially effective at high filtration velocity but requires 27% more compressed air than normal. Pressure drop is unaffected.

Increased relative humidity was associated with higher pressure drop but lower dust penetration. Higher humidity should cause stronger bonds between the dust deposit and its substrate. This may bring about a thicker dust deposit and thereby cause increased pressure drop as observed. More tightly bound particles should be less likely to seep through the fabric, thereby reducing penetration as was also found.



## Introduction

An attractive feature of pulse-jet filters is their ability to operate at higher filtration velocities (air to cloth ratios) than do filters cleaned by other means. To increase filtration velocity further is a tempting goal as the resultant decrease in installed cost can often more than compensate for the increased operating cost caused by higher pressure drop across the fabric.<sup>1</sup> The filtration velocity associated with least annualized cost increases as the number of operating hours per year decreases, so that for a process operated one shift per day or less, relatively high velocities (100 mm/s) at relatively high pressure drops ( $\sim 250$  mm water) may be appropriate.<sup>1</sup>

However, as filtration velocity increases penetration increases as well for both pulse-jet cleaned filters<sup>2,3</sup> and for filters cleaned by other means,<sup>4-7</sup> and in some cases the penetration increase may become unacceptable. Although data are few, bag life may decrease as well at high filtration velocities.<sup>8</sup>

In a conventional cleaning pulse, compressed air enters the bag rapidly and pushes the bag outward, away from its supporting cage. Upon approaching full inflation, the bag decelerates rapidly to a state of metastable rest, during which residual pulse air flows through the fabric and flushes out dust loosened by this deceleration.

At the end of a conventional pulse, the backflow of pulse air stops and normal filtration resumes. The bag accelerates

back toward its supporting cage and hits it smartly causing a rapid deceleration analogous to that observed as the bag snaps open. This causes additional dust agglomerates and particles to become loosened. These, together with the agglomerates and particles that were loosened but not blown free by the cleaning phase of the pulse, may now be flushed through the bag to the cleaned air side by the filtration gas. Dust penetration by this mechanism has been called seepage.<sup>3</sup>

Effective cleaning requires interaction between the cleaning pulse and the fabric. The bag must be flexible enough to inflate rapidly as the pulse begins. It should not stretch radially so that the bag may decelerate rapidly as it reaches full inflation. However, these same qualities, flexibility and radial distortion resistance, will also allow the bag to return to its cage rapidly as filtration resumes and this aggravates seepage.

Recently it was shown that almost all the dust that penetrates through a pulse-jet filter does so by seepage, and that seepage increases with increasing filtration velocity.<sup>3</sup> This occurs for several reasons. First, higher filtration velocity increases the fraction of dust feed by a cleaning pulse that redeposits on the bags, and decreases the fraction of freed dust that falls to the hopper.<sup>9</sup> This causes a thicker dust deposit to build up, with more dust available to seep through. Second, higher filtration velocity drives the cleaned fabric back to its cage faster, causing it to hit with greater impact.

This drives through more dust.

Dennis and Wilder<sup>10</sup> placed a 1.7 liter damping tank after the outlet of the pulse valve in their single bag, pilot pulse-jet filter and studied the effect of this tank on both penetration and pressure drop. They found that for filtration velocities between 30 and 50 mm/s, penetration was reduced by a factor of about five when damped pulses were used; however, pressure drop increased about 20%. Some of the air released by a cleaning pulse was taken up momentarily by the tank, and the transient reverse pressure gradient across the bag was somewhat reduced. For this reason, bag cleaning was less effective; the greater residual dust holding was thought to account for the higher pressure drop found. Reduced fabric stretching and reduced transient pressure gradients across the bag were thought to account for the reduced penetration.

Ideally, a cleaning pulse should: (1) inflate the bag quickly so that it will decelerate rapidly when it snaps fully open, (2) provide time after inflation for pulse air to flow through the bag and flush loosened dust into the housing, and (3) return the fabric to its cage support gently to prevent seepage and excessive fabric wear. A conventional cleaning pulse of sufficient duration produced by a conventional pulse-jet solenoid valve should satisfy the first two objectives, but does not satisfy the last. Dennis and Wilder's damped pulses<sup>10</sup> should satisfy the last two objectives but not the first.

To satisfy all three objectives simultaneously, conven-

tional cleaning pulses were modified in a way that retained rapid air delivery to each bag at the pulse beginning but that gently returned the bag to its cage. Modified pulses described here began normally but at the pulse end, pressure trailed off gradually allowing each pulsed bag to deflate gradually and return gently to its cage.

### Experiments

To test the effectiveness of modified cleaning pulses, a three bag pilot filter fitted with polyester felt bags 2.44 m tall and 114 mm in diameter was used.<sup>9</sup> A schematic drawing of the apparatus is given in Figure 1. The test dust was fly ash with cumulative size distribution by count given in Figure 2. Mass concentrations of fly ash upstream and downstream of the fabric filter were found by sampling isokinetically, onto glass fiber papers.

Cleaning pulses, either conventional or modified, were delivered sequentially to each bag once per minute. The valve arrangement for the pulse-air manifold is shown schematically in Figure 3. Compressed air entered through a regulator which controlled pressure at 6.8 atmospheres gauge and passed into a reservoir from which it flowed through a normally open solenoid valve, A, into a 1.6 L pulse air chamber. This chamber could be fitted with an extension which doubled its volume. Chamber pressure was measured on a Bourdon gauge and by a transducer connected to an oscilloscope.

The volumes of compressed air used for a conventional

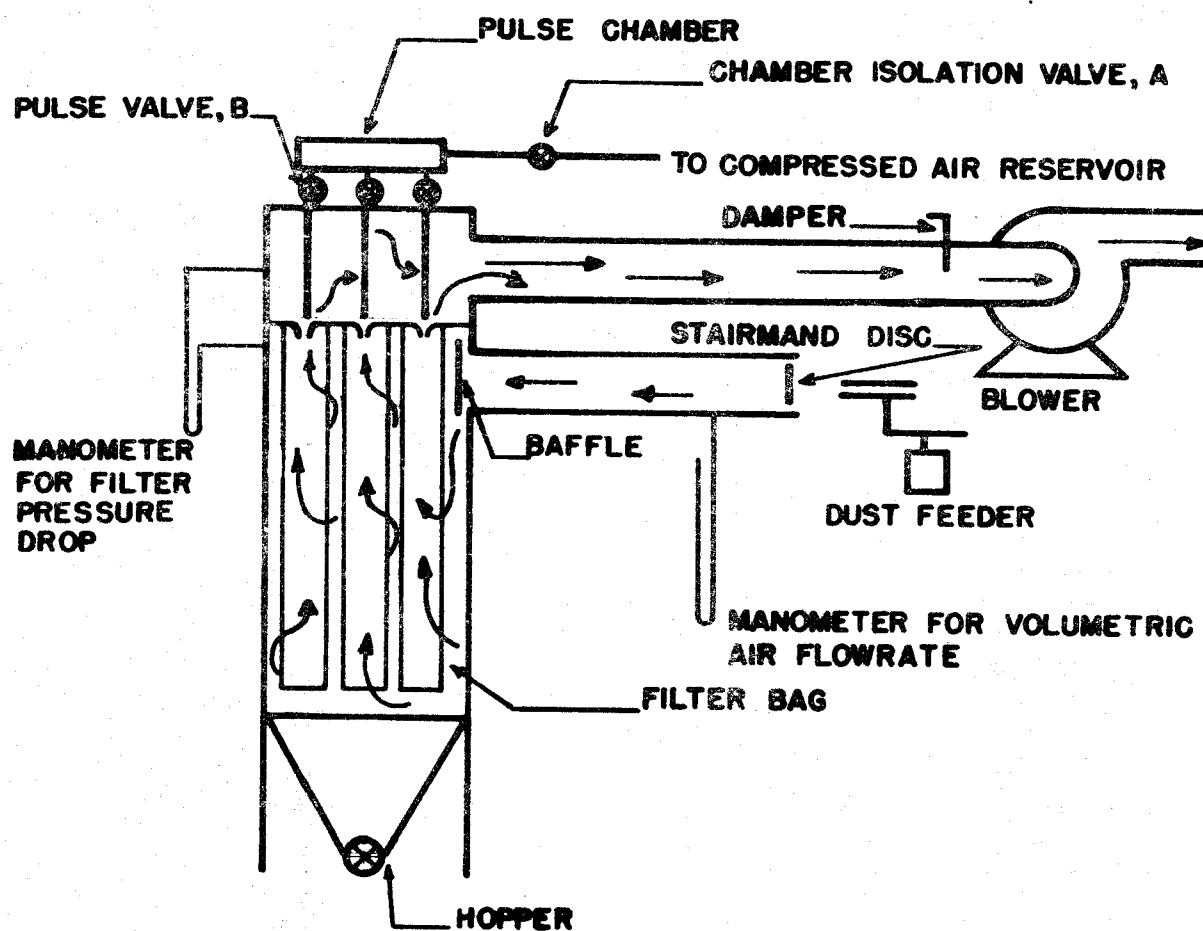


FIGURE 1. Schematic drawing of fabric filter apparatus used.

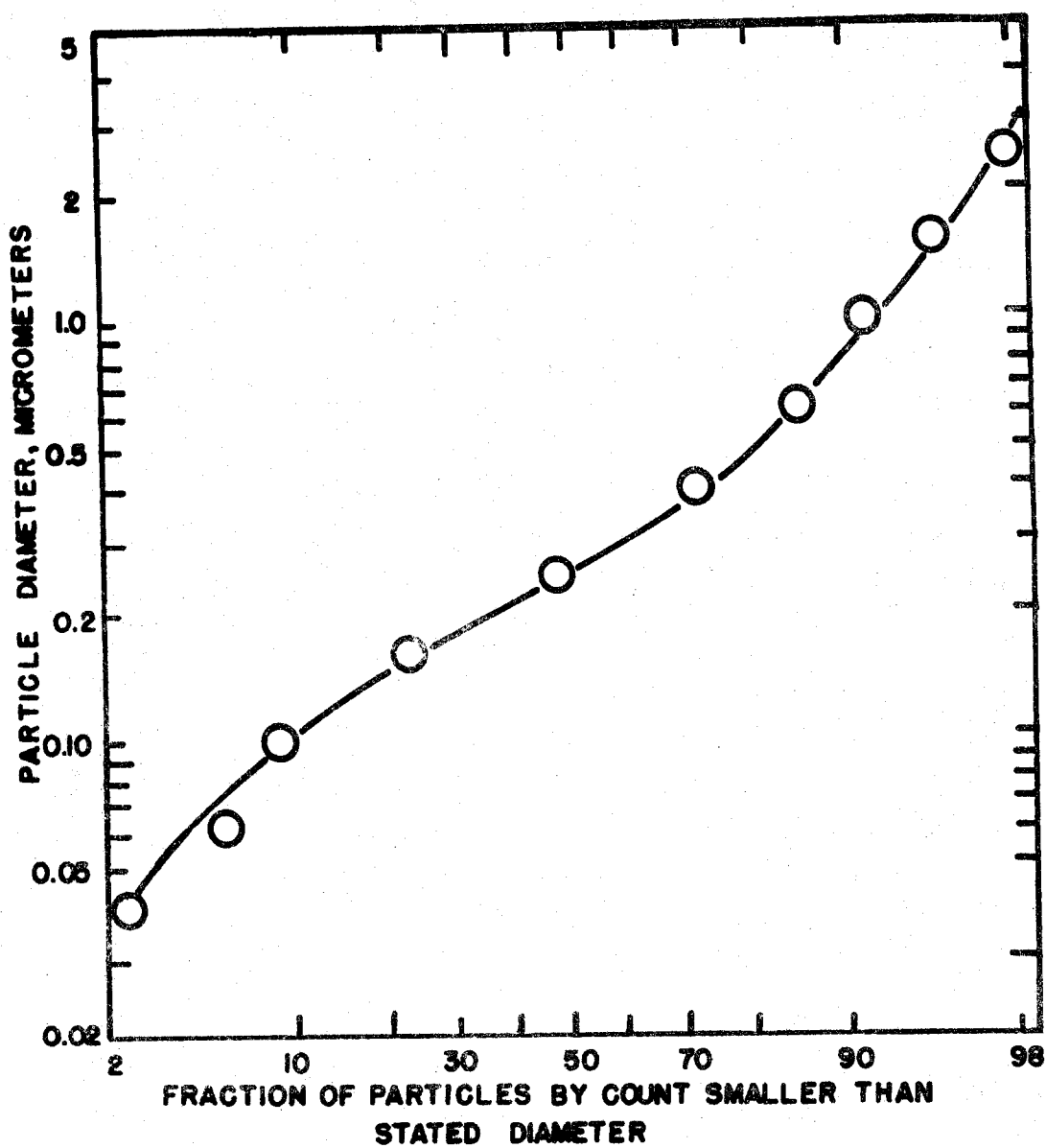


FIGURE 2. Cumulative size distribution by count for fly ash.

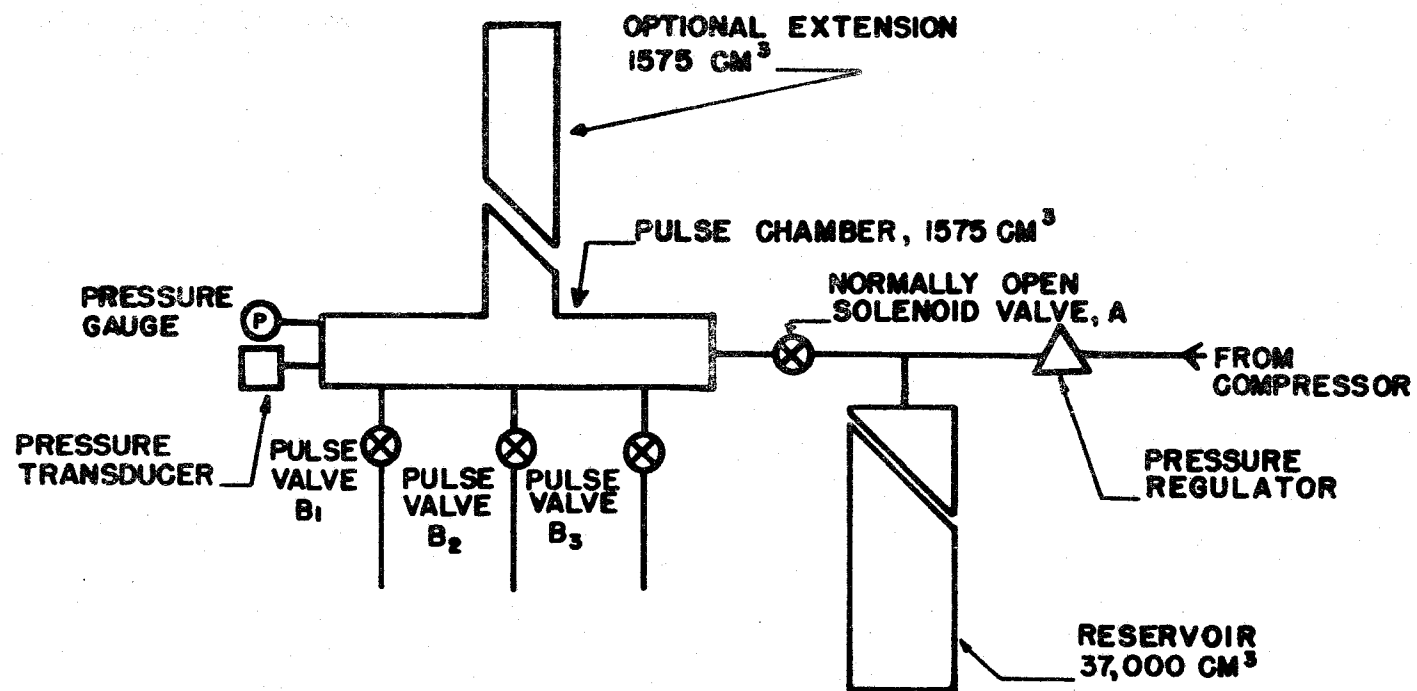


FIGURE 3. Valve arrangement for pulse-air manifold.

pulse, a modified pulse, and a modified pulse with chamber extension were measured by connecting the outlet from each pulse to a spirometer. The volume of compressed air per pulse was found to be 8.6 liters for a conventional pulse, 10.9 liters for a modified pulse, and 20.7 liters for a modified pulse with extended chamber volume, all measured at ambient pressure.

For conventional pulse operation the appropriate pulse valve,  $B_1$ ,  $B_2$ , or  $B_3$ , Figure 3, received an electrical signal to "open" for 75 milliseconds. A photograph of the relationship between chamber pressure and time for a conventional pulse as shown on the oscilloscope is given in Figure 4. It shows that pulse valve  $B_1$  began to open about 20 ms after receiving an electrical impulse. Although the electrical on-time was set at 75 ms, the valve continued to pass air for about 220 ms. This occurred because the pneumatic valve took about 150 ms to build up enough air pressure behind its diaphragm to close, although once closure began it was rapid. Pressure vs. time traces for valves  $B_1$ ,  $B_2$ , and  $B_3$ , were virtually identical.

To generate a modified cleaning pulse, one of the pulse valves ( $B_1$ ,  $B_2$ , or  $B_3$ ) was opened and 240 ms later solenoid valve A, Figure 3, was closed causing pressure in the chamber to drop as air bled from it to the pulsed bag. This gradual reduction in pulse pressure allowed the bag to move back to its supporting cage gently. After about 560 ms, the pulse valve closed and pressure within the chamber stabilized. Some time later, solenoid A was reopened, refilling the chamber with



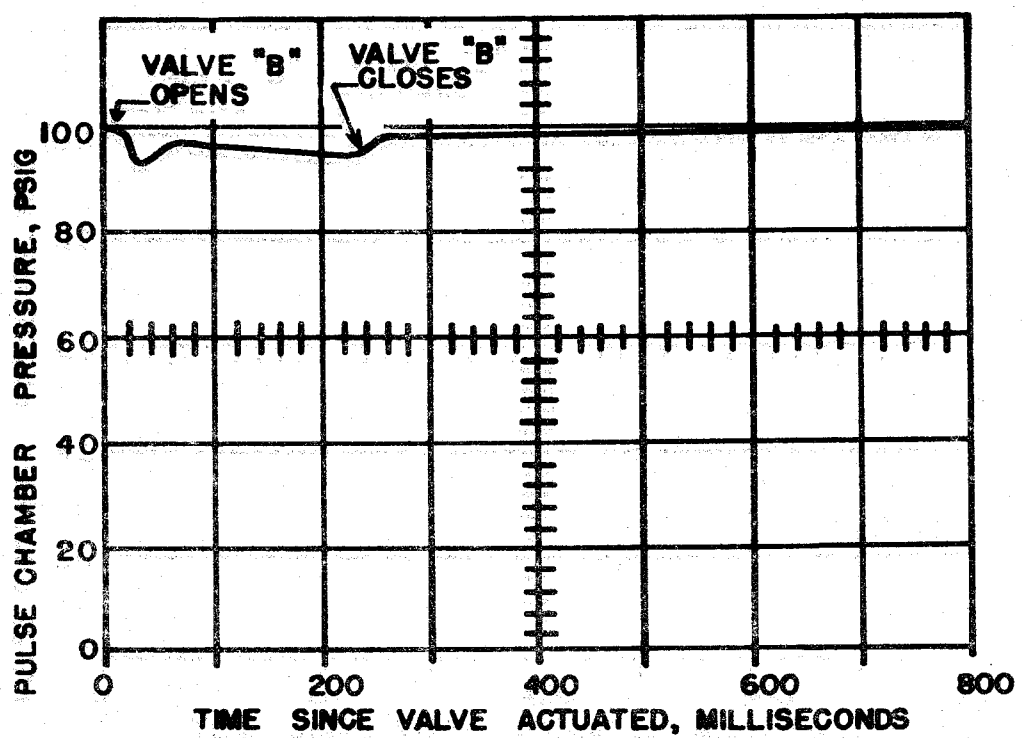


FIGURE 4. Photograph tracing of oscilloscope display: pulse pressure vs. time for normal pulse.

compressed air for the next pulse. A photograph of the oscilloscope pressure-time trace for a modified pulse is given in Figure 5.

The declining portion of the pressure-time relationship for the modified pulse, and by inference the speed with which the bag returns to its cage, are determined by the pulse valve flow characteristics and the volume of the chamber. To determine the effect of chamber size on filter performance, its volume was doubled by adding an extension. The pressure-time trace for this arrangement is given in the oscilloscope photo shown in Figure 6.

The effects of pulse modification on dust penetration and filter resistance were determined for a range of operating conditions. Before taking data the fabric filter was operated at constant conditions until the bags reached pressure drop equilibrium. This process took some hours; the length of time necessary depended upon the degree to which experimental conditions differed from test to test. Tests were run at filtration velocities of 50, 75, 100, 125 and 150 mm/s, using both conventional and modified pulses, and for normal and extended chamber volumes, so that twenty different operating and cleaning situations could be studied. All tests were replicated and run in random order with approximately the same inlet dust mass flux  $0.33 \text{ kg/m}^2/\text{hr}$ , so that the amount of dust fed between pulses would be the same regardless of filtration velocity.

Increased relative humidity has been shown to reduce both

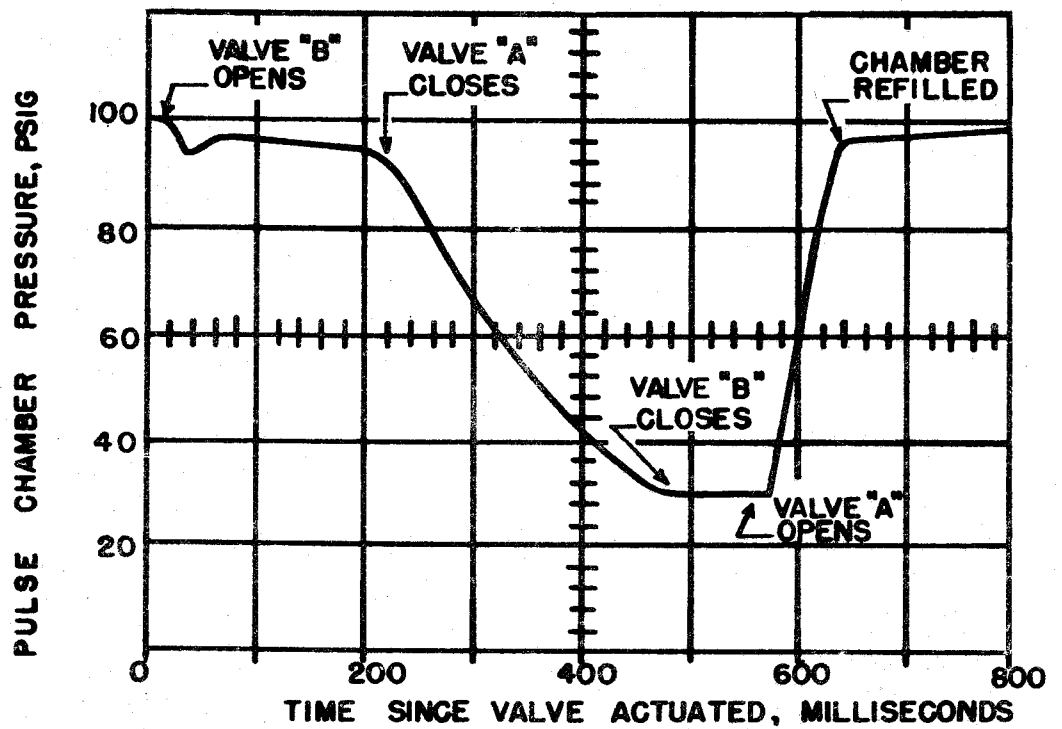


FIGURE 5. Photograph tracing of oscilloscope display: pulse pressure vs. time for modified pulse.

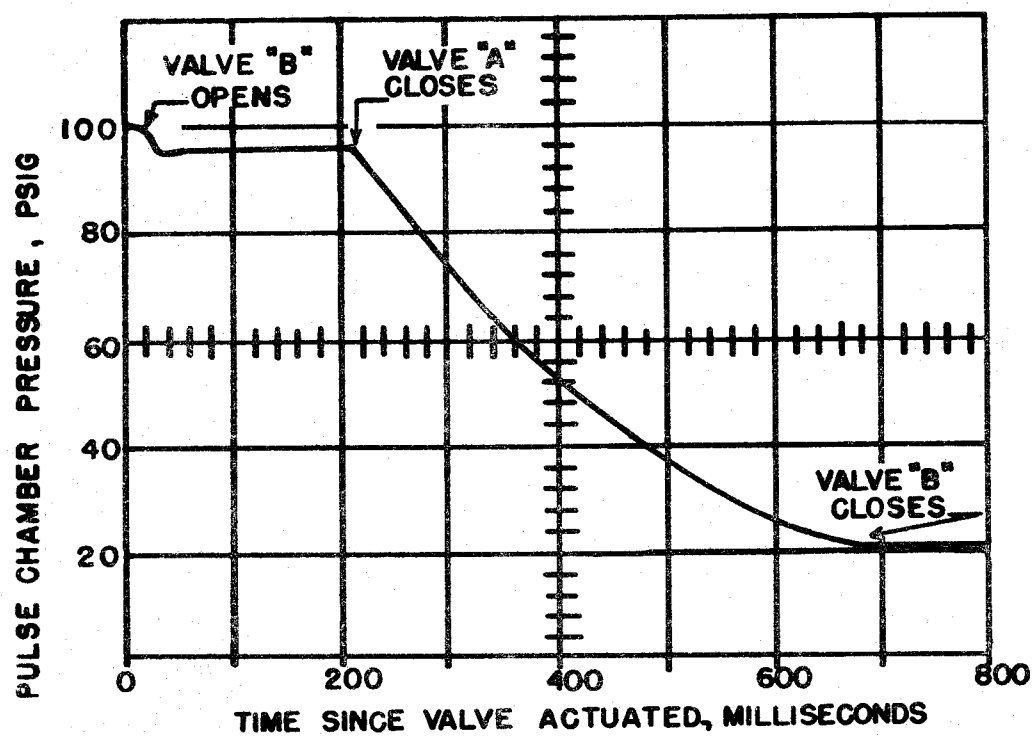


FIGURE 6. Photograph tracing of oscilloscope display: pulse pressure vs. time for modified pulse with twice normal chamber volume.

pressure drop and penetration in a woven fabric filter cleaned by shaking the bags.<sup>11</sup> Bench scale tests on Nomex and Dacron felts also show a decrease in pressure drop with increased humidity.<sup>12</sup> Although it was not possible to control the humidity of the air passing through the present apparatus, relative humidity was measured for each test. Because replicates were taken, the data could be sorted into "higher" and "lower" relative humidities for each replicated experimental condition. The variation in relative humidity between replicates ranged from less than 1% to 32%.

### Results

Table 1 shows the fractional mass penetration, equilibrium pressure drop in mm water column, and per cent relative humidity measured for each test.

Figure 7 is a plot of penetration against filtration velocity with pulse type as parameter. An analysis of variance performed on the data after taking logarithms showed that penetration increased significantly with increased filtration velocity. However, at all velocities tested penetration was significantly lower with modified pulses than with conventional pulses. The penetration reduction due to pulse modification is increasingly effective as velocity increased. Pulse chamber volume within the range studied had no significant effect on penetration for either normal or modified pulses. Penetration is plotted against filtration velocity with relative humidity as parameter in Figure 8. The penetration increase with increasing velocity

Table 1.

Fractional Mass Penetration/Pressure Drop, MM Water Gauge/% Relative Humidity

Filtration Velocity cm/s	Relative Humidity H/L	Normal Pulses		Modified Pulses	
		Std. Pulse Volume	2 x Std. Volume	Std. Pulse Volume	2 x Std. Volume
5	Lower	0.011/35 mm/38%	0.008/35 mm/38%	0.007/35 mm/33%	0.000/75 mm/59%
	Higher	0.006/65 mm/48%	0.005/65 mm/54%	0.007/65 mm/44%	0.001/70 mm/59%
7.5	Lower	0.011/82.5 mm/38%	0.014/75 mm/33%	0.007/103 mm/52%	0.009/70 mm/49%
	Higher	0.012/225 mm/60%	0.011/97.5 mm/50%	0.007/275 mm/56%	0.007/180 mm/56%
10	Lower	0.016/80 mm/43%	0.023/115 mm/36%	0.033/150 mm/29%	0.032/160 mm/26%
	Higher	0.027/260 mm/53%	0.019/145 mm/51%	0.003/230 mm/67%	0.007/300 mm/62%
12.5	Lower	0.029/160 mm/52%	0.083/400 mm/40%	0.041/150 mm/38%	0.040/195 mm/37%
	Higher	0.005/500 mm/62%	0.003/385 mm/64%	0.005/465 mm/64%	0.009/280 mm/69%
15	Lower	0.178/680 mm/49%	0.072/475 mm/51%	0.048/250 mm/55%	0.035/625 mm/37%
	Higher	0.006/385 mm/70%	0.027/615 mm/60%	0.036/685 mm/58%	0.033/695 mm/43%

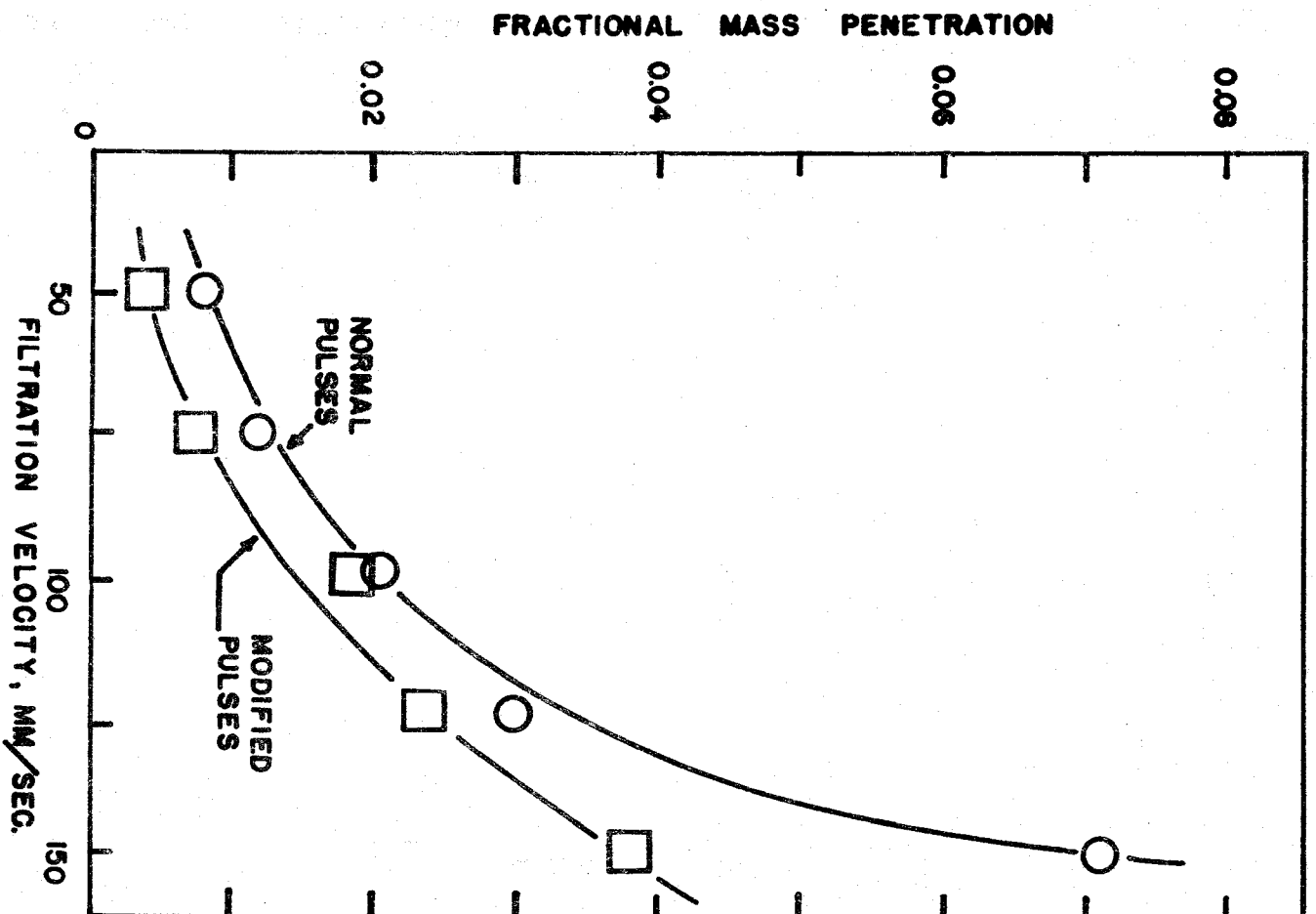


FIGURE 7. Penetration vs. filtration velocity, pulse type as parameter.

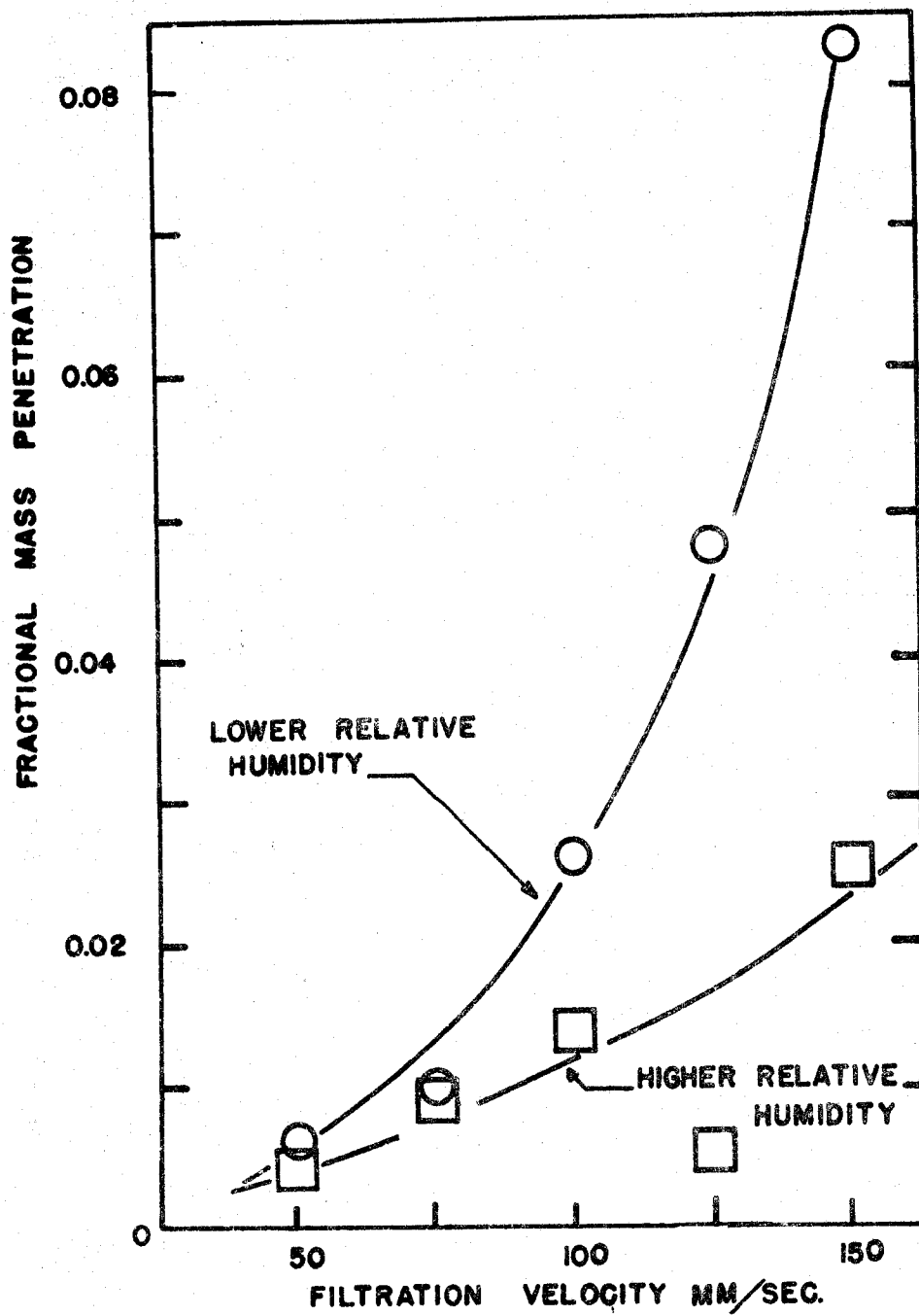


FIGURE 8. Penetration vs. filtration velocity, relative humidity as parameter.



is significantly more rapid at low relative humidity.

As expected, pressure drop increased rapidly with filtration velocity as is shown in Figure 9. An analysis of variance performed on the logarithms of the pressure drop data showed that this increase was significant. There was not a significant pressure drop difference between normal and modified cleaning pulses, or between normal and twice normal pulse volumes.

Relative humidity is the parameter against which pressure drop and filtration velocity are plotted in Figure 9. For both relative humidity conditions, pressure drop increased with velocity. However, contrary to observations for collection of fly ash on woven bags cleaned by shaking,<sup>11</sup> pressure drop in the pulse-jet filter was significantly higher at higher relative humidity.

### Discussion

Pulse form modification is an effective way to reduce dust seepage through a pulse-jet filter, especially at higher filtration velocities. At the highest filtration velocity tested, 150 mm/s, pulse modification lowered fractional penetration by 46%.

Pulse cleaning effectiveness is associated with fabric deceleration as the bag snaps fully open, and with pulse duration sufficient to assure that loosened dust is flushed from the fabric into the filter housing. Because the initial part of a modified and a conventional pulse are the same, they should inflate and flush bags equally well. Modified pulses backflush

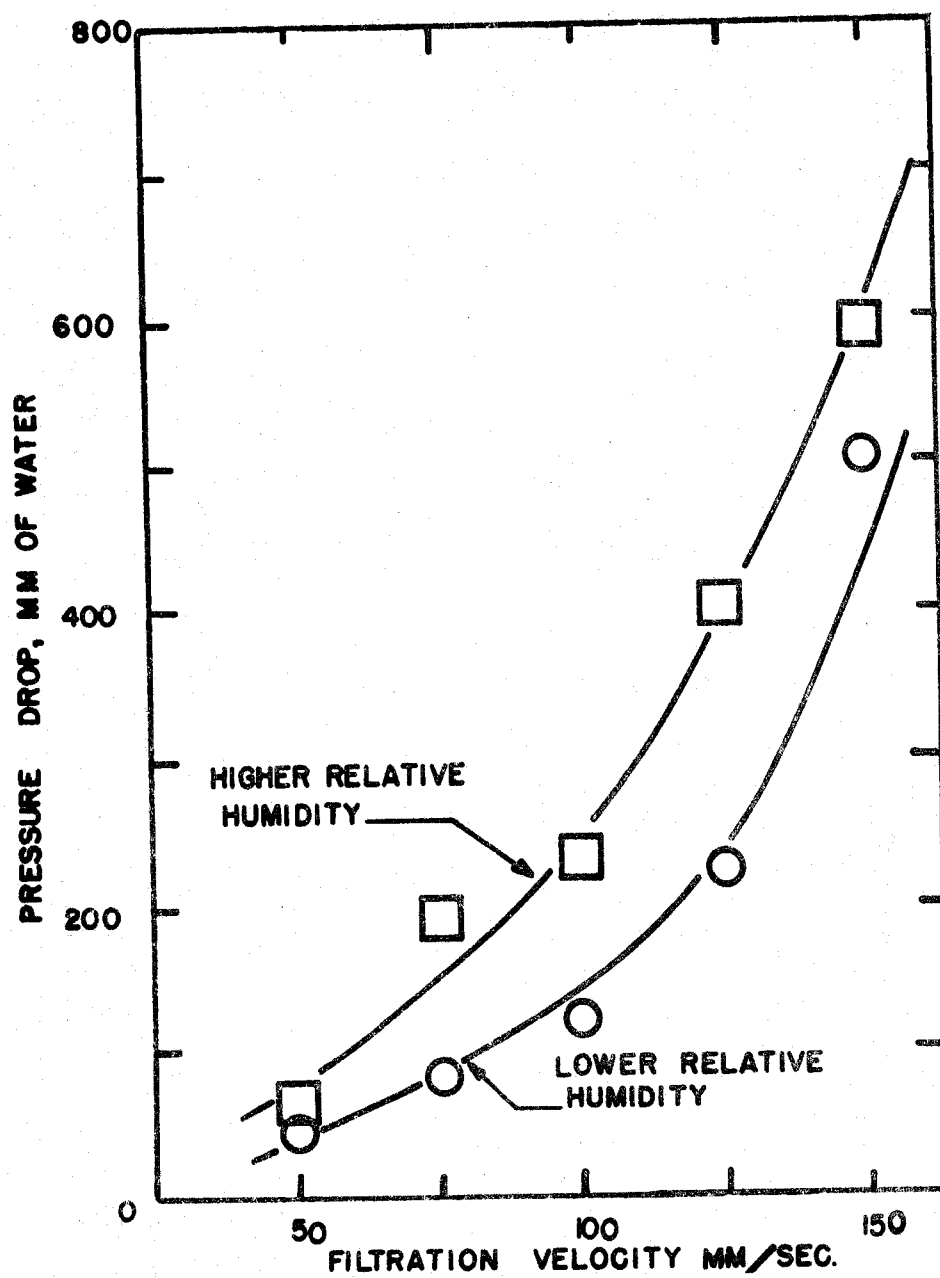


FIGURE 9. Pressure drop vs. filtration velocity, relative humidity as parameter.

bags longer than normal pulses because additional backflow occurs while pulse pressure falls during the final stage of the modified pulse. However, if enough backflow occurs to move loosened dust away from the fabric, additional pulse air brings diminished returns as has been shown by Dennis and Wilder.<sup>10</sup> For these reasons, pressure drops across bags cleaned by conventional and modified pulses were about the same.

There was no difference in penetration between bags cleaned by modified pulses from the 1.6 L pulse chamber and modified pulses from the 3.2 L chamber. This implies that chamber size might be decreased further to save on compressed air, while retaining the form and effect of modified pulses.

For a dust particle or agglomerate to be separated from the fabric, interparticle adhesive forces must be overcome by the deceleration force acting on dust as the bag snaps open at the beginning of a cleaning pulse, or snaps back onto its cage at the end of the pulse. In the former case, the dust flies into the housing from which it can fall to the hopper; in the latter case, the dust separated from the fabric penetrates the filter by seepage. It has been demonstrated that increased relative humidity leads to stronger particle-to-particle and particle-to-fiber bonds,<sup>12,13</sup> which should make separation of the dust deposit from the fabric more difficult. Fly ash may have adsorbed sulfuric acid, which absorbs water at high relative humidities, there strengthening interparticle bonds.

Because the dust deposit is more firmly anchored to the

fabric at higher relative humidity, seepage penetration should decrease. The data confirm this trend. At the same time, stronger interparticle bonds caused by increased relative humidity should make the dust deposit more difficult to clean from the fabric. A dust deposit with higher areal density would account for the higher pressure drops at high relative humidity found in these experiments.

Data for woven fabrics cleaned by shaking<sup>11</sup> and for bench scale new felts<sup>12</sup> show that pressure drop decreases with increasing relative humidity, opposite to the trend found here. Higher interparticle forces could cause a more porous dust deposit structure,<sup>12</sup> one more resistant to compaction with continuous dust addition. Theory<sup>15</sup> confirms that for the same amount of deposited dust, a thicker, more porous structure should have less pressure drop than a thinner, more dense one. However, in the pulse-jet filter cleaning is not wholly effective at removing deposited dust. The effect of increasing the amount of dust retained on the bag at high humidity may be more important than the effect of the more porous structure which that dust forms.

### Summary

Pulse-jet filter show higher seepage penetration at higher filtration velocities. This seepage occurs when the bags return to and strike their rigid support cages at the end of a cleaning pulse, as loosened dust is driven from the bags into the cleaned gas stream. Seepage can be reduced by cleaning the bags with pulses which are identical with conventional pulses at the be-

ginning, but which gradually decrease in pressure at the pulse end, allowing the bags to return gently to their cages. Modified pulses are increasingly effective at reducing dust penetration as filtration velocity increases. At the highest velocity tested, 150 mm/s, modified pulses reduced penetration by 46% but had no effect on pressure drop.

Increased relative humidity caused significantly lower penetration but increased pressure drop. Because increased humidity causes an increase in interparticle bond strength, dust collected at high humidity may be bound more tightly in place and be less likely to seep through the fabric, causing reduced penetration. However, when dust is tightly bound it becomes more difficult to separate from the fabric. At high humidities, an equilibrium dust deposit with higher areal density may build up on the bags causing higher pressure drop.

#### Acknowledgement

This work was supported by EPA Grant R 804700-01, Dr. James H. Turner, Project Officer.

#### References

1. Leith, D. and M. W. First, "Pressure Drop in a Pulse-Jet Fabric Filter", *Filtration and Separation*, 14(5):473 (1977).
2. Leith, D., S. N. Rudnick and M. W. First, High Velocity, High Efficiency Aerosol Filtration, EPA Report EPA 600/2-76-020, Office of Research and Development, Washington, D.C., 1976.
3. Leith, D. and M. W. First, "Performance of a Pulse-Jet Filter at High Filtration Velocity, III. Penetration by Fault Processes", *J. Air Poll. Control Assoc.*, 27(8):754 (1977).
4. Spaite, P. W. and G. Walsh, "Effect of Fabric Structure on Filter Performance", *Am. Ind. Hyg. Assoc. J.*, 24:357 (1963).

5. Ensor, D. S., R. G. Hooper and R. W. Scheck, Determination of the Fractional Efficiency, Opacity Characteristics Engineering and Economic Aspects of a Fabric Filter Operating on a Utility Boiler. EPRI Report FP-297, Palo Alto, CA, 1976.
6. McKenna, J. D., J. C. Mycock and W. O. Lipscomb, "Performance and Cost Comparisons Between Fabric Filters and Alternate Control Techniques", J. Air Poll. Control Assoc., 24:1144 (1974).
7. Turner, J. H., "Extending Fabric Filter Capabilities", J. Air Poll. Control Assoc., 24:1132 (1974).
8. Hobson, M. J., "Review of Baghouse Systems for Boiler Plants", in Proceedings, the User and Fabric Filtration Equipment II, Air Pollution Control Association, 4400 Fifth Ave., Pittsburgh, PA (1975).
9. Leith, D. and M. W. First, "Performance of a Pulse-Jet Filter at High Filtration Velocity, II. Filter Cake Redeposition", J. Air Poll. Control Assoc., 27(7):636 (1977).
10. Dennis, R. and J. Wilder, Fabric Filter Cleaning Studies, EPA Report EPA-650/2-75-009, Office of Research and Development, Environmental Protection Agency, Washington, D.C. (1975).
11. Durham J. F. and R. E. Harrington, "Influence of Relative Humidity on Filtration Resistance and Efficiency", Paper 4e presented at 63rd Annual Meeting of American Institute of Chemical Engineers, Chicago, IL, 1970.
12. Ariman, T. and D. J. Helfritch, "How Relative Humidity Cuts Pressure Drop in Fabric Filters", Filtration and Separation, 14:127 (1977).
13. Corn, M. and F. Stein, "Re-entrainment of Particles from a Plane Surface", Am. Ind. Hyg. Assoc. J., 26:325 (1965).
14. Löffler, F., "Investigating Adhesive Forces Between Solid Particles and Fiber Surfaces", Staub (English Translation), 26:19 (1966).
15. Stephan, D. G., G. W. Walsh and R. A. Herrick, "Concepts in Fabric Air Filtration", Am. Ind. Hyg. Assoc. J., 21:1 (1960).



## CURRENT AND FUTURE EPA FILTRATION RESEARCH

James H. Turner  
Environmental Protection Agency  
Industrial Environmental Research Laboratory  
Research Triangle Park, N. C. 27711

3rd EPA Fabric Filter Symposium  
Tucson, Arizona  
December 5-6, 1977



## CURRENT AND FUTURE EPA FILTRATION RESEARCH

### Introduction

The Third EPA Fabric Filter Symposium is itself largely a review of current and future EPA filtration research:

Kenneth Ladd and Jack Smith: reasons for using a baghouse on a large utility boiler burning low sulfur western coal.

Richard Dennis: formulation of a mathematical model of fabric filtration for combustion sources using glass bags. This model is based on extensive field and laboratory testing.

John Mycock: performance of a pilot baghouse on a trash-to-energy incinerator.

Dale Harmon: use of a mobile pilot baghouse to perform field tests and relate field and laboratory results.

John McKenna: demonstration of a high velocity fabric filter system on two industrial boilers.

Robert Bradway: performance of a fabric filter system on a small electric arc furnace.

Melvin First, David Leith and Steven Rudnick: high velocity filtration in a pulse-jet baghouse and fundamentals of fabric filtration and cake formation.

George Lamb: effects of fiber properties (rather than fabric properties) on filtration performance.

Robert Donovan: electrostatic effects in a pulse-jet baghouse.

Dennis Drehmel and Mike Shackleton: filtration under conditions of high temperature and high pressure.

## Purpose

These various programs all fall into just a few categories:

- Assessment of full scale projects.
- Field and laboratory testing and measurements.
- Fundamental studies.

Most of the work is done in external programs; i.e., contracts, grants or interagency agreements. The purpose of EPA's fabric filtration research is to aid in the improvement of particulate control technology by supporting appropriate projects. These projects may originate either within or outside EPA.

## Other Projects

In addition to the projects identified above, two others are being supported by IERL-RTP. These are fabric comparisons and math modeling being done in Poland, and work on electrostatic effects being done at Carnegie-Mellon University.

The Polish work is being performed at the Institute of Cement Building Materials (IPWMB) in Opole, Poland, and the Principal Investigator is Jan Koscianowski. At the laboratory and pilot level he is directing an effort to compare the performance of both U. S. and Polish fabrics in Polish equipment. There are several differences between U. S. and Polish practice: the Poles use fabrics with plied yarns and high counts; they clean (at least in this case) with a short stroke, vertical shake. There is also some work with reverse air cleaning. Comparisons are being made with cotton, polyester, glass and Nomex fabrics. As well as comparing fabrics, the Poles are endeavoring to describe the filtration process mathematically. The final reports for the work should be available by mid- to late 1978.

Probably the most challenging work being done, other than convincing the new purchaser that baghouses are the perfect answer, is in the area of trying to understand the role and importance of electrostatics in fabric filtration. Gaylord Penney and Edward Frederick (Carnegie-Mellon) have been jointly exploring this area: one from the viewpoint of determining basic electrical effects, and the other of empirically classifying various dust/fabric systems according to electrostatic properties and applying these observations to select the optimum fabric to collect a specific dust. As with the earlier Frederick paper (1), the final report from Carnegie-Mellon (due about April) is bound to be read and re-read.

### Future Work

The work at Southwestern Public Service will continue for at least the next 2 years, and there are options for extended testing and for a slaved pilot baghouse to test various operating modes or fabrics.

The Dennis model for fabric filtration will be tested against a variety of operating conditions and also will be put in simplified form for use by a greater number of people. Computer tapes of the model will be available through the National Technical Information Service.

The mobile baghouse will be used next to compare the filterability of eastern and western low sulfur coal flyashes from pulverized coal boilers. A report, based on tests at Southwestern Public Service Company's Harrington Station and at Michigan State University's boiler house will be prepared during the summer of 1978.

The high velocity Enviro-Systems baghouse at Kerr Industries will be operated for a second year, and other fabrics (besides the current Teflon and GoreTex) will be tested. There is also an option for  $SO_x$  removal using an injected sorbent ahead of the baghouse.

Fundamental work on high velocity filtration, mechanisms and fiber property influence will continue under the grants held by Harvard and

the Textile Research Institute. The in-house work at EPA will continue on electrostatic effects, new fabric evaluation, and investigation of fine particle penetration. Additional work will be done in the area of high-temperature filtration and high- temperature/high- pressure filtration both in-house and under contract.

One new contract that is expected will be for pilot scale assessment of dry sorbent collection of  $SO_x$  in a baghouse. This work will be a three party endeavor involving the City of Colorado Springs, Buell/Envirotech and EPA. Given the water problems, high resistivity coal and close source of a good sorbent (nahcolite) in the west and southwest, the dry sorbent/baghouse approach should be attractive. The pilot assessment will consider disposal methods for spent sorbent/flyash as well as the process techniques and economics. The contract for this work should be signed in mid-1978.

### Summary

EPA's programs in fabric filtration are meant to encourage development and dissemination of technology primarily in areas mandated by the Clean Air Act and its amendments. With a few exceptions, the individual projects are described in detail in other papers presented at the Third EPA Fabric Filter Symposium. Emphasis has been on control of combustion sources.

Now that baghouses are beginning to be used on utility and industrial boilers, perhaps the greatest need, and one voiced by many people at the Symposium, is for reliable field measurements to be taken and distributed to designers and potential users.

### References

1. Frederick, E. R., "How Dust Filter Selection Depends on Electrostatics," Chemical Engineering, pp. 107-114, June 26, 1961.



CONTRIBUTING ROLE OF SINGLE FIBER PROPERTIES TO  
NONWOVEN FABRIC PERFORMANCE

---

G. E. R. Lamb, P. A. Costanza, and D. O'Meara

Textile Research Institute  
Princeton, New Jersey

An early study [1] established that geometric properties of the constituent fibers in a nonwoven fabric could affect its filtration performance. Table I shows results of a  $2^4$  factorial experiment which examined the effect of cross-sectional shape, surface roughness, crimp, and fiber diameter. A second phase [2] of this work therefore examined these effects over a wider range of variables. Figure 1 shows that the effects of surface roughness and of cross-sectional shape on capture efficiency are evident in the capture of particles smaller than  $1\text{ }\mu\text{m}$ . Figure 2 shows that in comparison with a filter made of round fibers, one made of bilobal fibers is less efficient but one made of tri or pentalobal fibers is more efficient. The poor performance of bilobal fibers appears to be due to the strong dependence of single fiber efficiency on fiber orientation. Figure 3 and Table II show that, while the presence of crimp gives an advantage over a filter made of uncrimped fibers, the crimp frequency does not affect performance.

Figures 4 and 5 show the effect on penetration and on specific cake resistance of varying the fiber diameter for two weights of polyester fabric, at constant fabric density. Measurements with fibers having a range of surface roughness were not made because such fibers are not available.

A one-bag baghouse was made and two bags were tested, one made of round, the other of trilobal polyester fibers. Figures 6 and 7 show that the trilobal bag gave lower pressure drop and higher efficiency, the penetration for the trilobal bag being approximately one half that for the round bag. This is the only baghouse-scale confirmation of an effect of fiber geometry. It indicates that this approach can be expected to give better performance in commercial application. The cost of the modification would be almost zero.

Current efforts are aimed at finding explanations for the effects described above. To date, only the effects of cross-sectional shape have been studied in greater detail. The efficiency  $E$  of a filter is given by  $\ln(1-E) = -2\alpha\chi/(1-\alpha)\pi R$  where  $\alpha$ =packing density,  $\chi$  = filter thickness, and  $R$  = fiber radius. Figure 7 shows that the ratio of penetration (round to trilobal) between two 15-oz. fabrics is about 2. This would be consistent with a difference in single fiber efficiency of about 20%, which is roughly the increase in effective diameter due to the change in shape. However, measurements on layered filters indicate that the different performance is only associated with the presence of dust deposits. Figure 8 shows calculated single fiber efficiencies for the various layers in a 4-layer filter, and the trilobal efficiency is higher for the trilobal only in the upstream layer, where the dust cake is located. An interesting consequence of this finding is shown in Table III, which compares performance

of layered fabrics in which the upstream layer was different from the rest of the filter. The table shows that the performance of the filters is dominated by the thin upstream layer. These facts prompted a study of dust cake structure, aimed at the determination of any features of the structure built on different substrates that would explain the lower pressure drop given in some cases by trilobal fabrics as well as the higher efficiencies and the patterns described above. Microscopical examination has so far proved unsuccessful in describing any such features.

In a separate approach, single fiber efficiencies have been calculated for capture in the presence of an electric field. Figure 9 shows collection efficiency for fibers having different numbers of lobes, and shows that it increases both with increasing number of lobes and with increasing lobe height. It is possible that the effects we have seen may originate from interactions of charged particles with electric fields due to previous deposition of charged particles. Experimental verification of this hypothesis is the object of future work.



#### REFERENCES

1. B. Miller, G. E. R. Lamb, and P. Costanza, "Influence of Fiber Characteristics on Particulate Filtration," EPA-650/2-72- January 1975.
2. B. Miller, G. Lamb, P. Costanza, and J. Craig, "Nonwoven Fabric Filters for Particulate Removal in the Respirable Dust Range," EPA-600/7-77-115, October 1977.

## FIGURE CAPTIONS

Fig. 1 Capture efficiencies of three nonwoven PET fabrics made of various fibers, as shown, when filtering a flyash aerosol.

Fig. 2 Ratios of outlet concentrations for filters made of fibers with 2, 3 and 5 lobes to outlet concentrations for round fiber filter.

Fig. 3 Capture efficiencies for nonwoven rayon filters made of fibers with various levels of crimp as shown, when filtering a flyash aerosol.

Fig. 4 Penetration (equal to 1-efficiency) for PET and polypropylene filters of constant weight and density but made of fibers of different diameters.

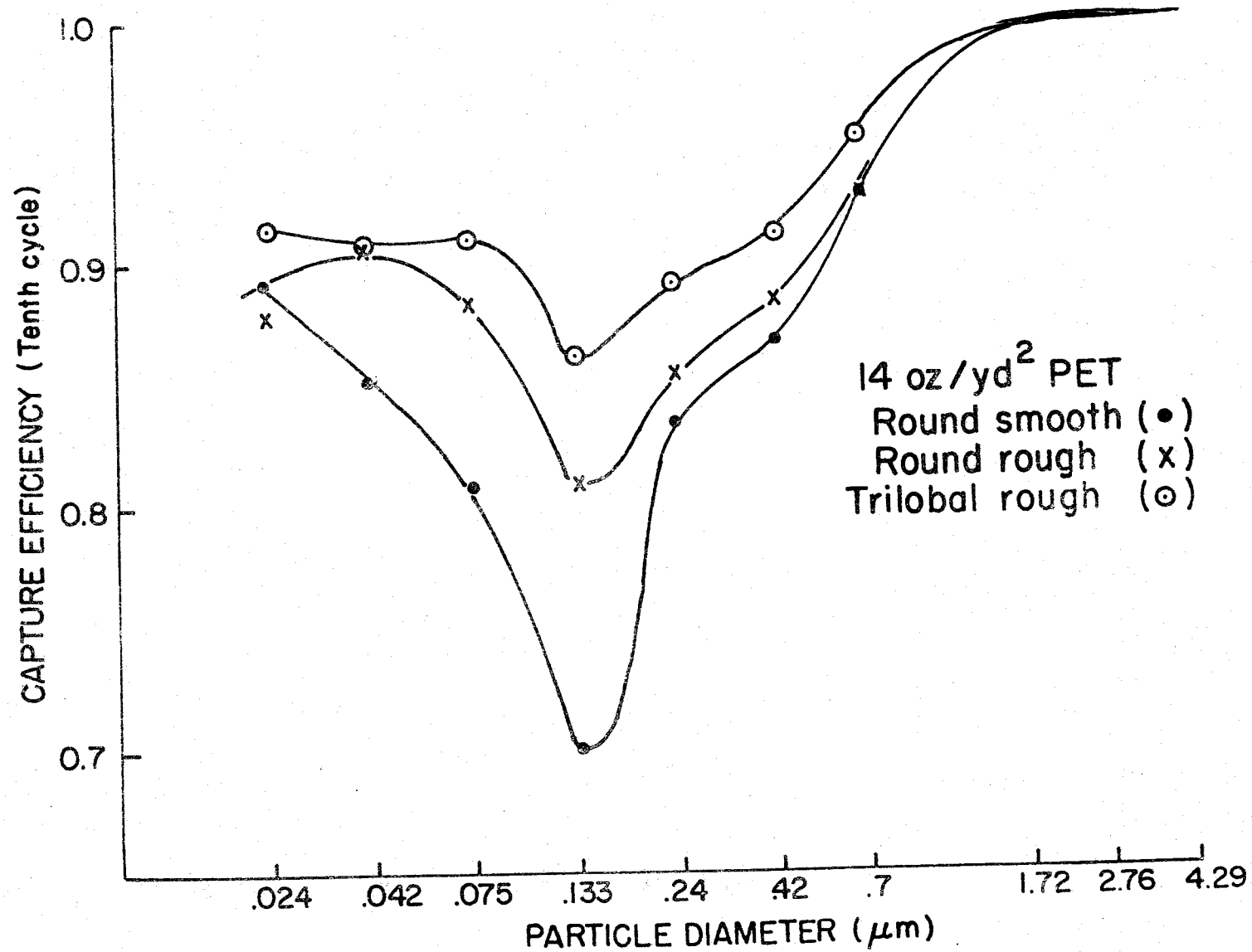
Fig. 5 Specific cake resistance for the filters in Figure 4.

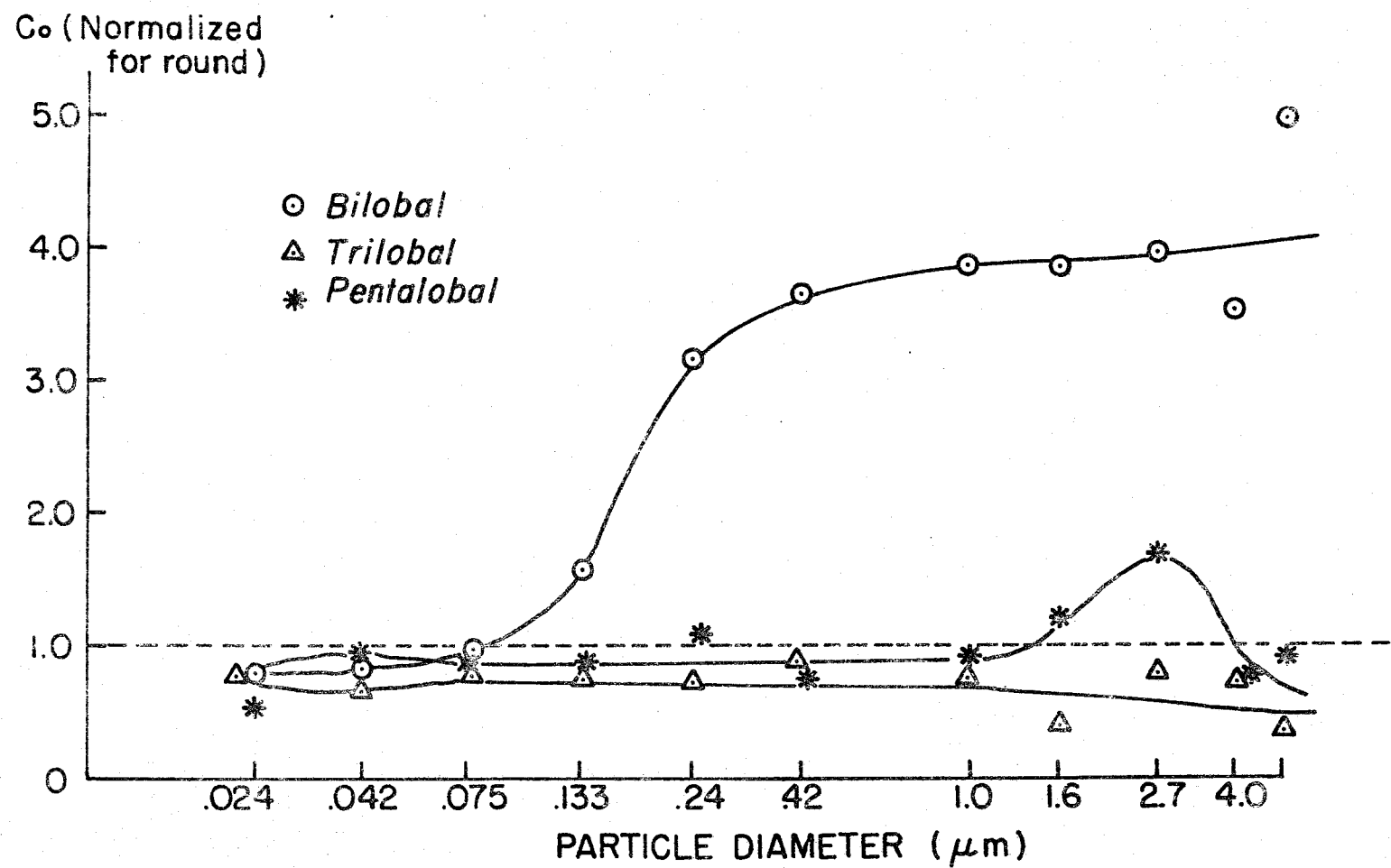
Fig. 6 Pressure drops at beginning and end of filter cycle ( $\Delta P_i$  and  $\Delta P_f$ ) for conditioned bags made of round and trilobal PET fibers.

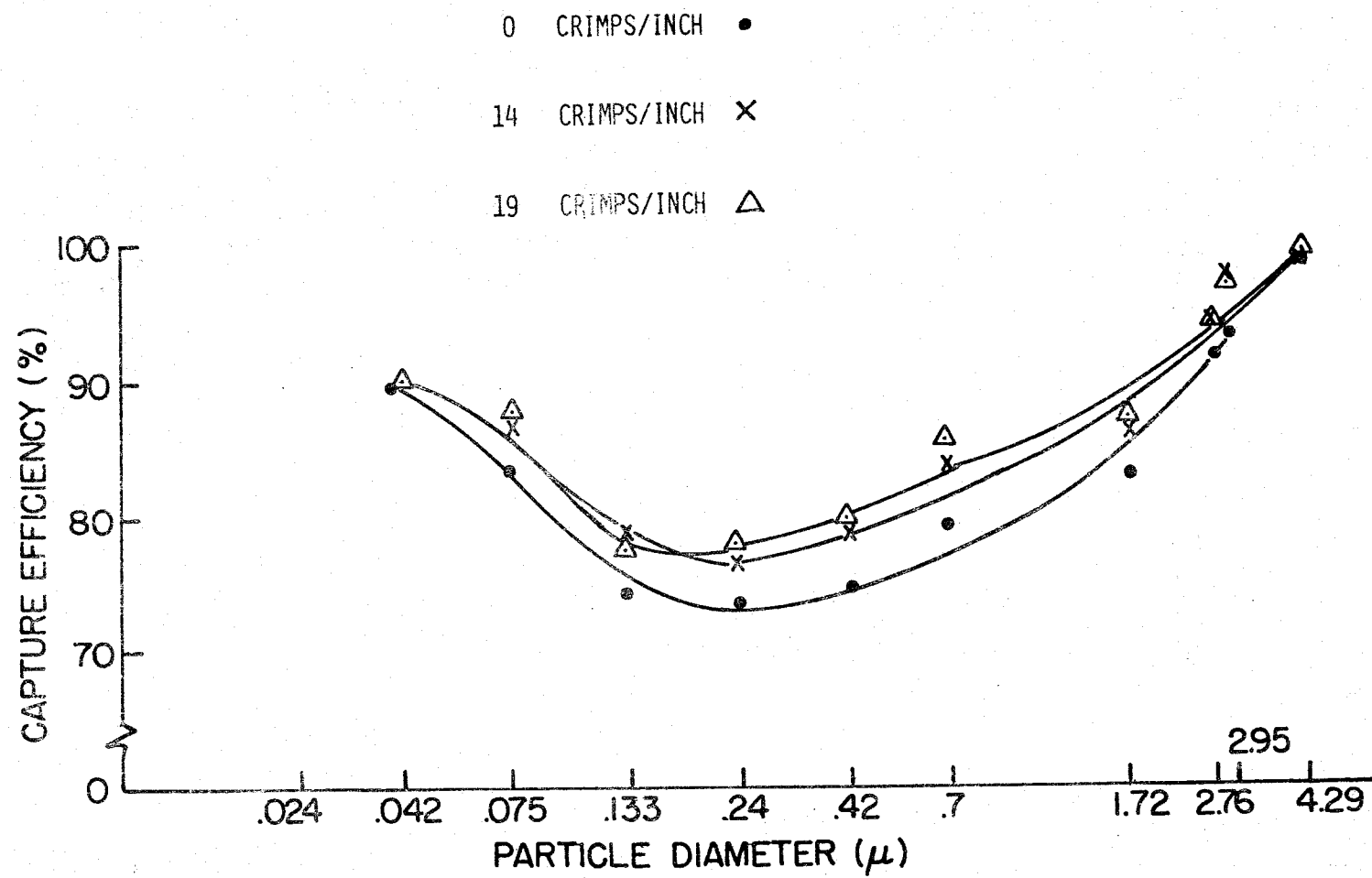
Fig. 7 Outlet concentration ratios for bags in Figure 6.

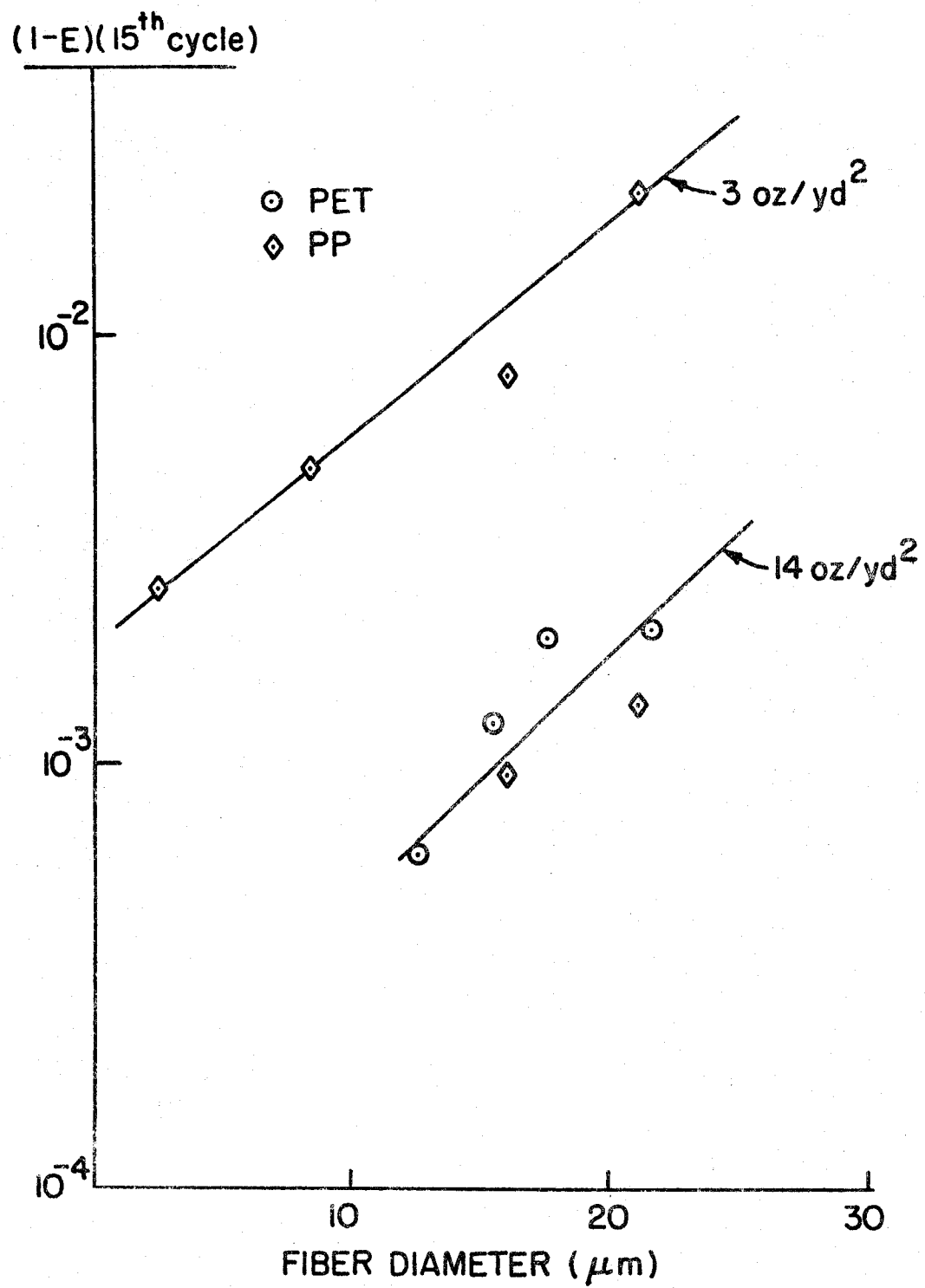
Fig. 8 Single fiber efficiencies for each layer in layered filters made of round and trilobal fibers.

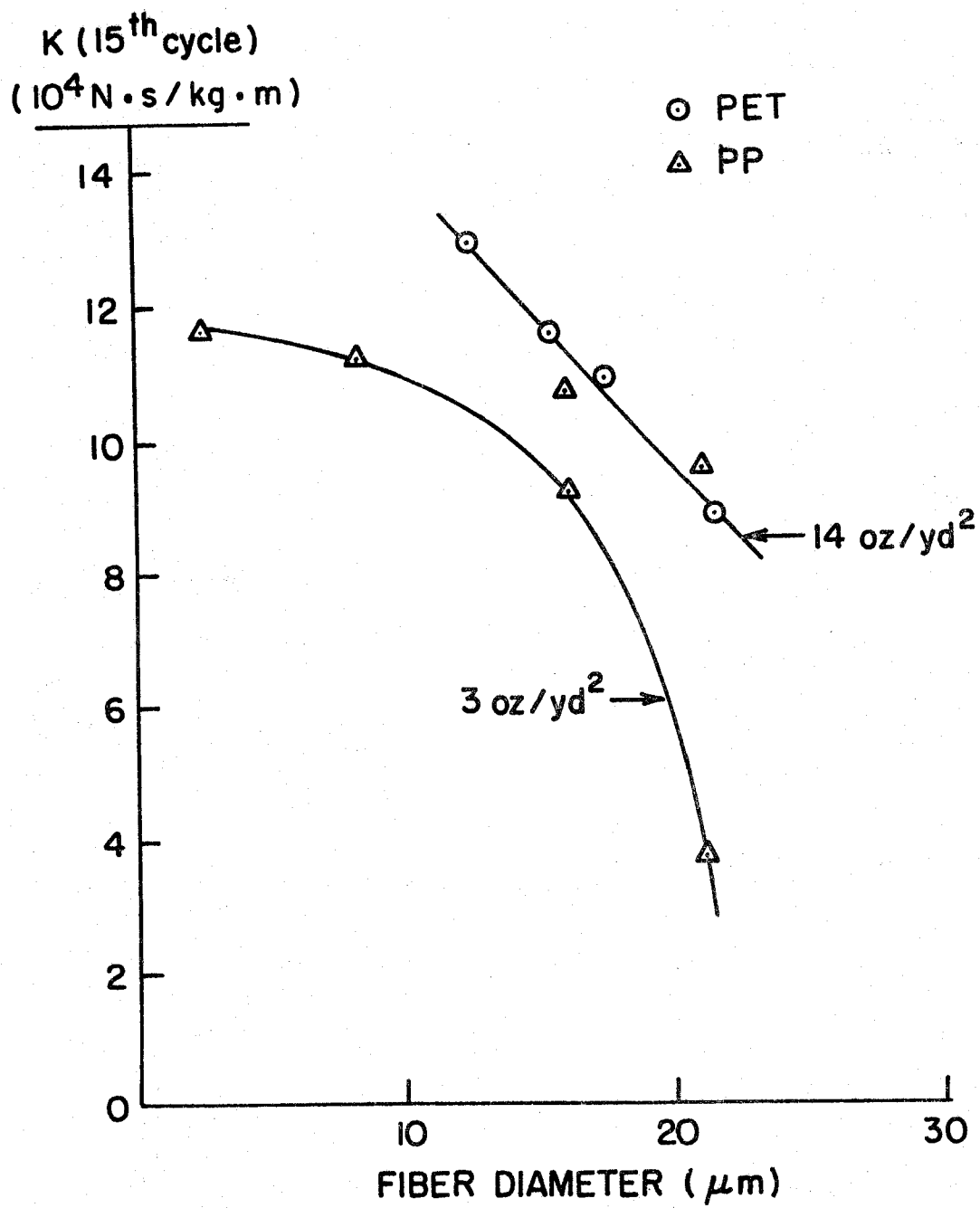
Fig. 9 Calculated single fiber efficiencies for fibers with cross sections  $\rho = 1 + \varepsilon \cos m(\phi+c)$  where  $m$  = number of lobes and  $\varepsilon$  indicates the lobe depth.



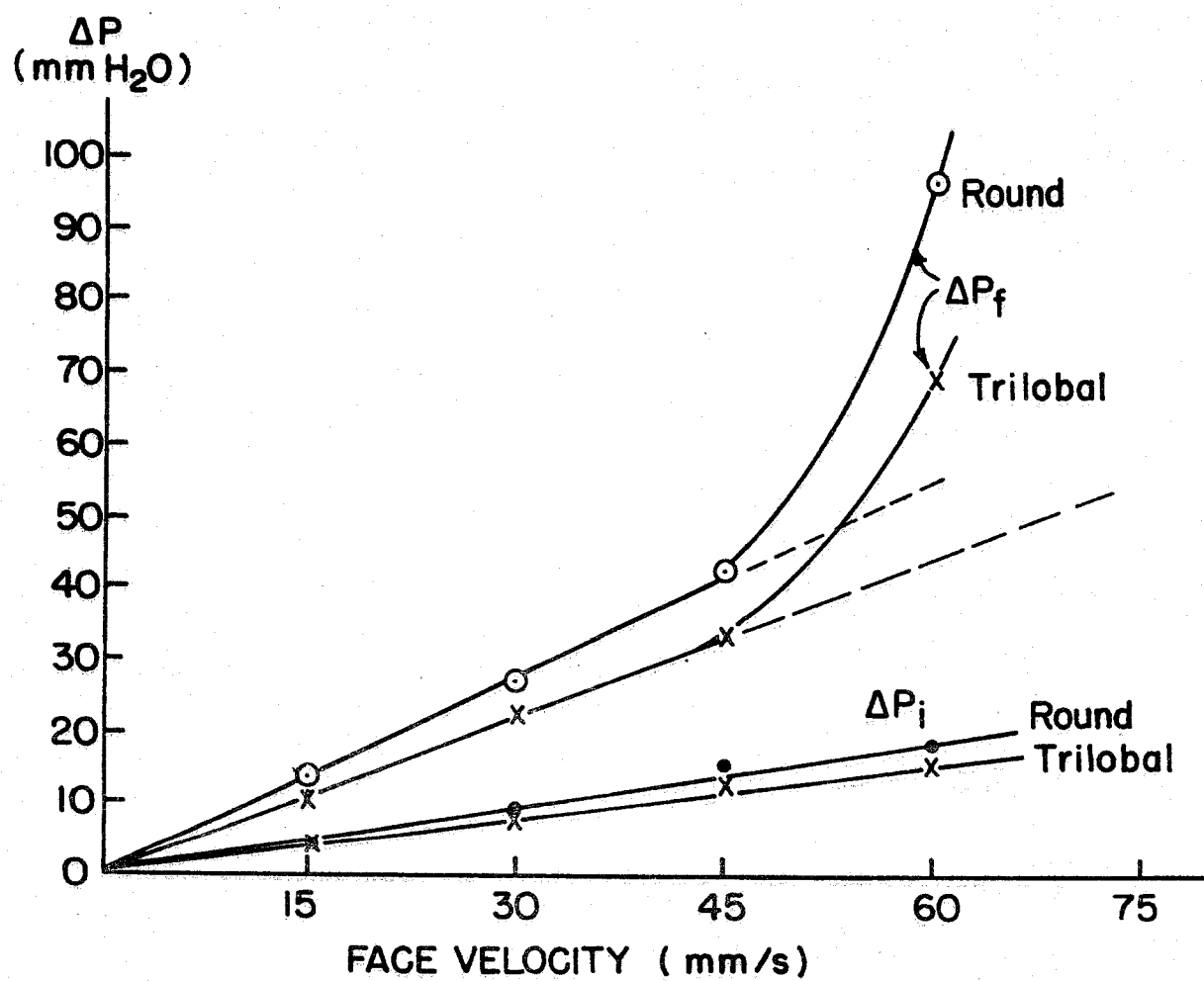


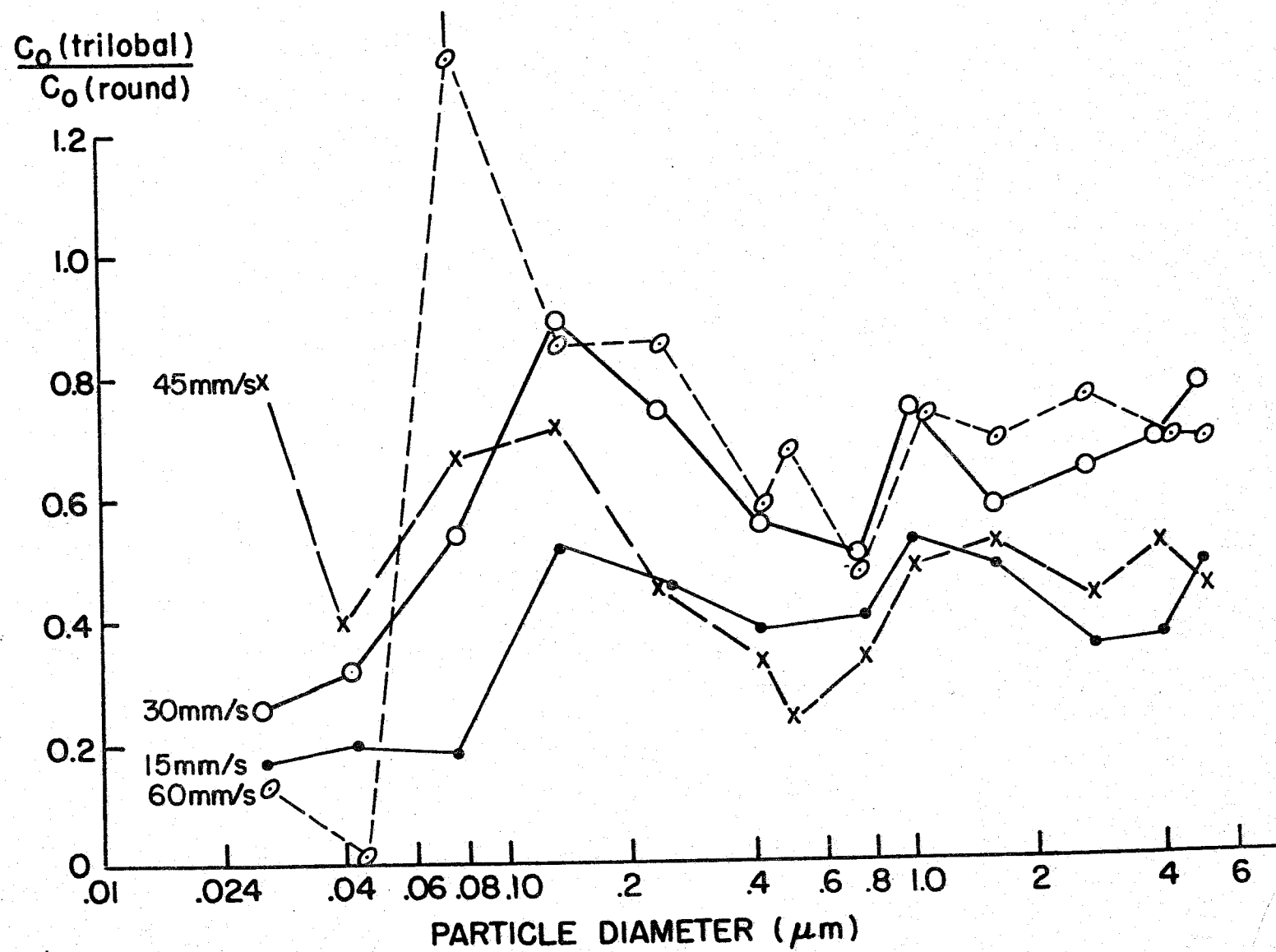


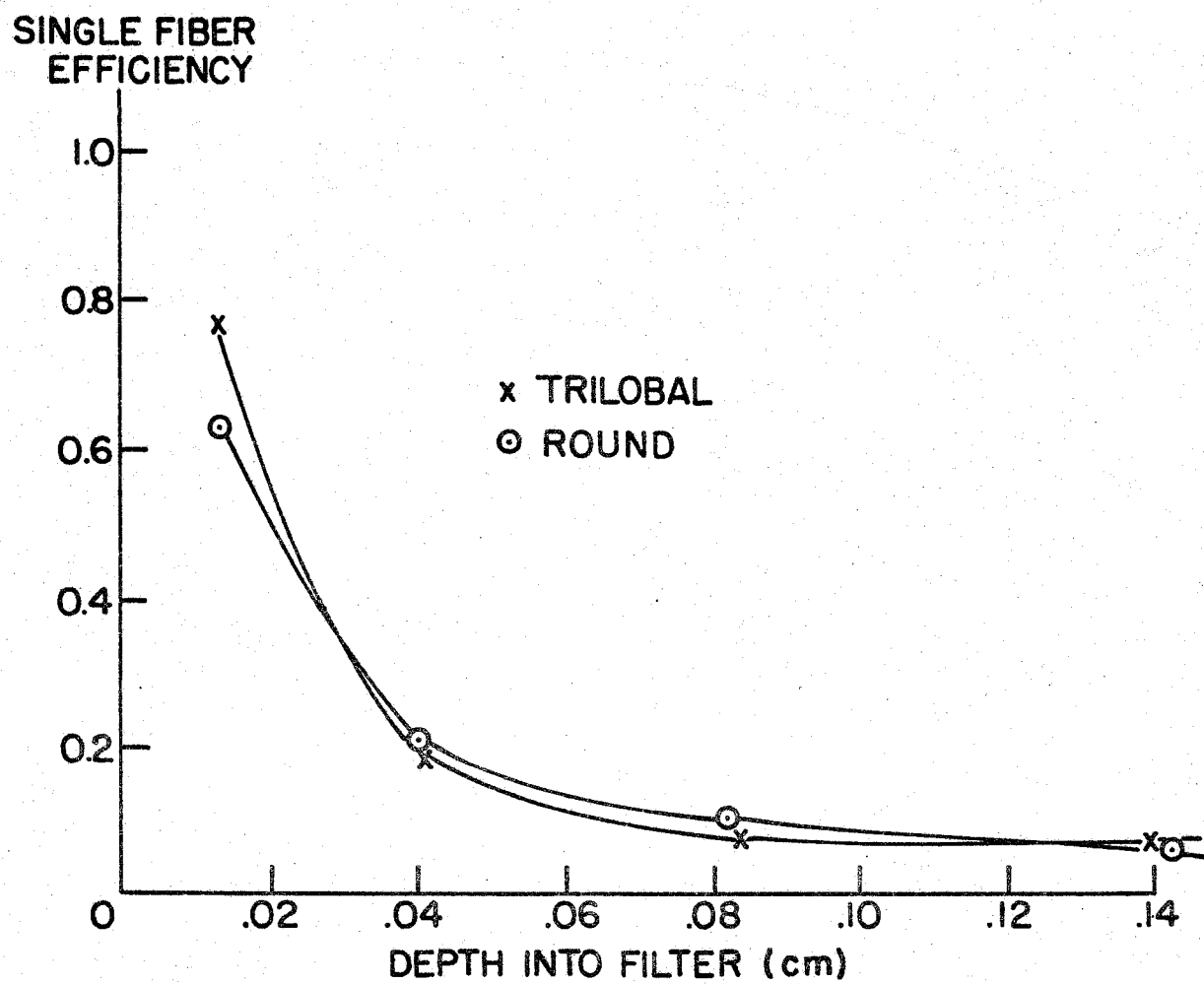


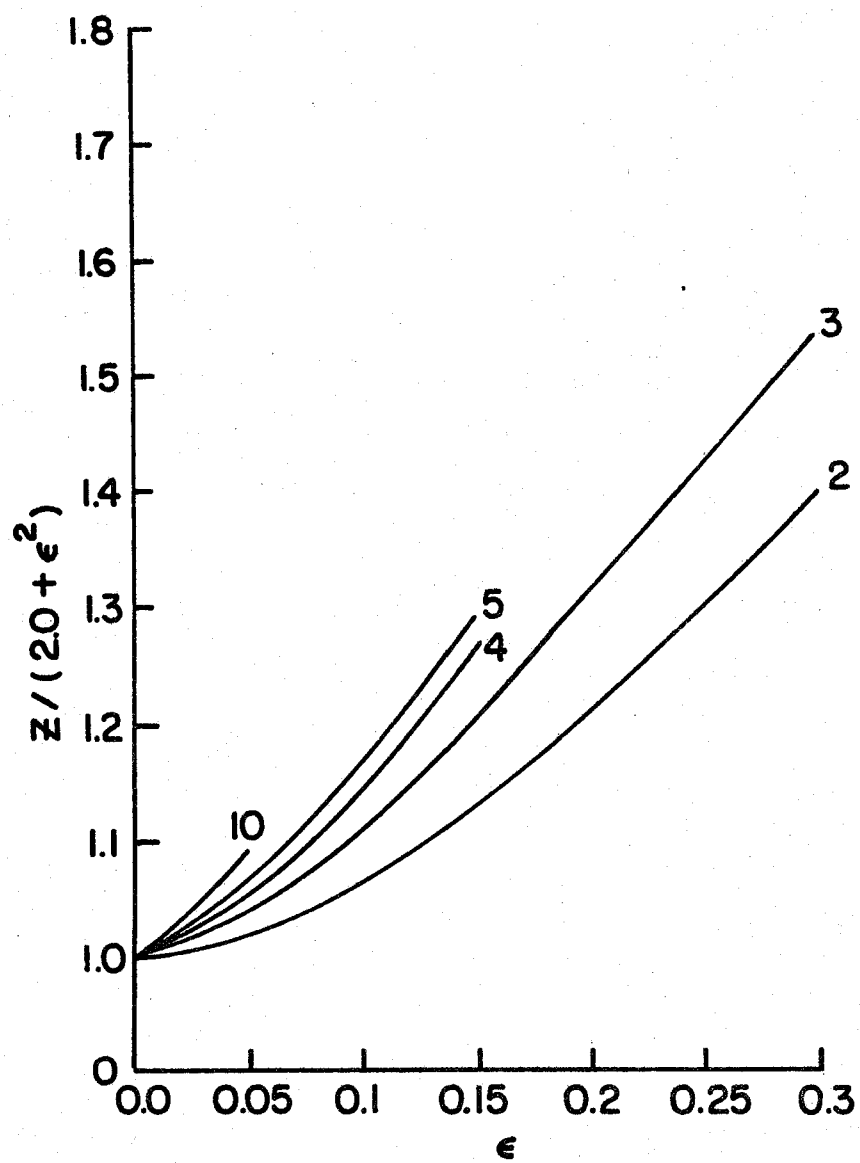














Specific Resistance ( $K_2$ ) of Filter Dust Cakes:  
Comparison of Theory and Experiments

by

Stephen N. Rudnick\* and Melvin W. First

Harvard University  
School of Public Health  
Department of Environmental Health Sciences  
665 Huntington Avenue  
Boston, Massachusetts 02115

Abstract

The specific resistance ( $K_2$ ) of filter cakes formed from elutriated AC-Fine test dust was measured at air to cloth ratios between 7.1 and 56 mm/s (1.4 and 11 fpm) in an apparatus in which other operating conditions including aerosol size distribution remained invariant. Cake porosity and particle size distribution, shape, and density, which affect the specific resistance of dust cakes, were also measured. It was found that the Kozeny-Carman equation, which treats a dust cake as a collection of capillaries, seriously underestimated specific resistance. It is believed that this discrepancy occurs because the high porosity of air-deposited filter cakes makes them more closely resemble an assembly of individual particles than a collection of capillary passages. A simple model based on Stokes' law indicates that the Kozeny-Carman equation predicts  $K_2$  values for air-deposited filter cakes which are less than the minimum theoretical specific resistance. Predictions of  $K_2$  made from the Happel "free surface" model, which treats the dust cake as an assemblage of particles rather than capillaries, compared favorably with experimental values after accounting for nonuniform particle size, nonspherical shape, and gas slip. No empirically fitted constants derived from the measured values of  $K_2$  were required.

\*To whom inquiries should be addressed

## Nomenclature

### Roman

- a cloth area with dust deposit,  $m^2$
- A constant which characterizes interaction between gas and solid surface, dimensionless
- B permeability coefficient in Darcy's equation,  $m^3 \cdot s/kg$
- $C_s$  slip correction factor, dimensionless
- D particle diameter,  $\mu m$
- $D_e$  diameter of sphere with same volume as particle,  $\mu m$
- $D_p$  projected area diameter,  $\mu m$
- $D_s$  sedimentation diameter,  $\mu m$
- $\bar{D}_{vl}$  volume-length mean (sedimentation) diameter in Equation (15),  $\mu m$
- $\bar{D}_{vs}$  volume-surface mean diameter in Equation (10),  $\mu m$
- k Kozeny constant, dimensionless
- $K_2$  specific resistance of dust cake,  $sec^{-1}$
- Kn modified Knudsen number, dimensionless
- L dust cake thickness, m
- m mass of dust cake, kg
- n number fraction, dimensionless
- N number of particles in dust cake
- R resistance factor, dimensionless
- S specific surface area of particles,  $m^{-1}$
- V superficial velocity, m/s
- w weight fraction, dimensionless
- W areal density,  $kg/m^2$

#### Greek

- $\alpha$      solidity, dimensionless
- $\Delta P$     pressure drop, Pa
- $\epsilon$      porosity, dimensionless
- $\lambda$      mean free path of gas, m
- $\mu$      viscosity, Pa·s
- $\rho_p$     particle density, kg/m<sup>3</sup>
- $\tau$      particle relaxation time, s
- $\tau_{vl}$     particle relaxation time based on  $\bar{D}_{vl}$ , s
- $\phi_{vl}$     shape factor relating  $D_p$  to  $D_s$  in Equation (19), dimensionless
- $\phi_{vs}$     shape factor relating  $D_p$  to  $\bar{D}_{vs}$  in Equation (11), dimensionless
- $\chi$      dynamic shape factor, dimensionless

#### Subscript

- $i$      particle size category



## Introduction

Determination of the permeability of porous media to fluids has produced a voluminous literature<sup>1,2</sup> concerned to a large extent with the prediction of permeability from the properties of the porous structure and gaseous medium and confirmation of these relationships by experiment. Various theories and empirical formulations have been proposed, but the general consensus, until recently, has been that the Kozeny-Carman equation<sup>3</sup> is the most reliable, and considerable experimental data have been published to support this contention.

The Kozeny-Carman equation was first applied to the filtration of dusts on fabrics by Williams, Hatch, and Greenburg<sup>4</sup> and, despite a lack of experimental verification, has found wide acceptance<sup>5,6,7</sup>. Generally, only the permeability of the dust cake has been measured as it is considerably more difficult to determine the parameters required for insertion in the Kozeny-Carman equation. In particular, measurement of filter cake porosity is especially difficult because the dust cake is normally a very thin, fragile structure supported on a fabric which is not flat and whose fibers mingle to varying degrees with the particles in the cake. For these reasons, the porosities of dust deposits on operating fabric filters have not previously been measured experimentally<sup>8</sup>.

## Darcy's Law

The fundamental relationship governing noncompressible, creeping flow through porous media, Darcy's law, states that the

rate of flow is directly proportional to the pressure gradient causing the flow<sup>1</sup>, i.e.:

$$V = B \frac{\Delta P}{L} \quad (1)$$

where  $V$  is superficial velocity,  $B$  is Darcy's permeability coefficient,  $\Delta P$  is pressure drop, and  $L$  is thickness of the porous medium. Because the thickness of a dust cake is difficult to measure, Williams, Hatch, and Greenburg<sup>4</sup> substituted the areal density,  $W$ , (i.e., weight of dust on the filter per unit of cloth area) from the following expression:

$$L = \frac{W}{\rho_p(1-\epsilon)} \quad (2)$$

where  $\rho_p$  is the density of the particles in the dust cake and  $\epsilon$  is the dust cake porosity (void fraction). After substituting Equation (2) into (1), Darcy's law becomes:

$$K_2 = \frac{\Delta P}{VW} \quad (3)$$

where  $K_2 = [B\rho_p(1-\epsilon)]^{-1}$ . The quantity " $K_2$ ", the specific resistance of the dust cake, has been employed extensively in fabric filtration studies<sup>4,5,7</sup>. It was first called " $K_2$ " by Billings and Wilder<sup>9</sup> and this designation has become synonymous with specific resistance. The reciprocal of  $K_2$ , the permeability of the dust cake, has also been used for characterizing dust cakes<sup>6</sup>. Equation (3) is a definition of specific resistance and Darcy's law simply states that it is constant for a given porous and

flow medium.

#### Stokes' Law

Because a dust cake is composed of small particles, Stokes' law can be used as a model to predict specific resistance if it is assumed that there is no hydrodynamic interaction between particles. For spheres of uniform size, the sum of the drag forces on each particle in a unit mass of dust cake is equal to pressure drop per unit of areal density, or:

$$\frac{\Delta P}{W} = \frac{\sum \text{Drag Force}}{\sum \text{Mass}} = \frac{(3\pi\mu VD/C_s)N}{(\frac{\pi}{6}D^3\rho_p)N} \quad (4)$$

where N is number of particles in the dust cake,  $\mu$  is gas viscosity, D is particle diameter, and  $C_s$  is slip correction factor. Combining Equation (4) with the definition of  $K_2$  (Equation 3) yields:

$$(K_2)_{\text{minimum}} = \frac{18\mu}{\rho_p D^2 C_s} = \frac{1}{\tau C_s} \quad (5)$$

where  $\tau = \rho_p D^2 / 18\mu$ . Inasmuch as the velocity on the surfaces of the particles is zero (ignoring slip), as the particles get closer together the absolute value of the velocity gradient between particles increases resulting in larger shear stress in the fluid and greater drag on the particles<sup>10</sup>. Therefore, Equation (5) is an expression for the minimum specific resistance because the particles are assumed to be far apart (i.e.,  $\epsilon \rightarrow 1$ ). It is also important to note that the minimum specific resistance is equal to the reciprocal of the slip-corrected particle relaxation time,  $\tau$ ,

which plays a prominent role in the mechanics of aerosols. Although  $K_2$  depends on the density of the particles, as does the terminal settling velocity of a particle, pressure drop is independent of density. For a dust cake composed of unit specific gravity spheres, the minimum specific resistance for ambient air flow based on Equation (5) is shown in Table I.

It may be deduced from Equation (5) that smaller values of the minimum specific resistance will be obtained whenever small particles accumulate in clusters which mimic larger particles. As observed by Carman and Malherbe<sup>11</sup>, this situation can exist with uncompacted fine powders because of the presence of a relatively large surface force compared to the gravitational force on the particles. A different situation exists in a dust cake because the flow, itself, creates the porous medium. Therefore, when flow resistance in one portion of the dust cake is less than in another, the flow rate is greater in that portion with lower resistance, and hence a larger number of particles will deposit in this region causing an increase in flow resistance. Consequently, the distribution of particles in the dust cake tends toward uniformity. An exception to this tendency occurs when the aerosol being filtered is composed predominantly of complex aggregates because particle deposition in the internal recesses of an aggregate may not be possible.

Inasmuch as Stokes' law places a minimum constraint on any model proposed for predicting pressure drop across a dust cake,

TABLE I. Minimum Specific Resistance

<u>Particle Diameter, <math>\mu\text{m}</math></u>	<u>Specific Resistance</u>	
	<u><math>(\text{ms})^{-1}</math></u>	<u><math>\text{in. water}/(\text{fpm}\cdot\text{lb}/\text{ft}^2)</math></u>
50	0.13	0.013
10	3.2	0.32
5	13	1.3
1	280	28
0.5	980	98

a new quantity, the resistance factor,  $R$ , may be defined by the following equation:

$$K_2 = \frac{R}{\tau C_s} \quad (6)$$

$R$  is a number greater than one which, when multiplied by the minimum specific resistance, defined in Equation (5), gives the specific resistance of the dust cake (for  $C_s$  equal to unity).  $R$  generally is only a function of dust cake porosity, although the porosity is influenced by the conditions prevailing when the dust cake is formed (e.g., velocity, humidity) and the properties of the dust. The value of  $\tau$  is affected solely by the properties of the dust. The slip correction factor,  $C_s$ , is a function of both particle size distribution and porosity and will be discussed in detail later.

#### Kozeny-Carman Equation

The Kozeny-Carman equation<sup>3</sup> is a semi-empirical relationship which assumes that a dust cake can be represented by a collection of parallel capillaries whose total surface area is equal to the surface area of the particles and whose total volume is equal to the void volume of the dust cake. It can be written as follows:

$$R = \frac{2k(1-\epsilon)}{\epsilon^3} \quad (7)$$

where  $k$  is the Kozeny constant which Carman<sup>3</sup> determined to be equal to 4.8 for spheres and 5.0 for various irregularly shaped particles over a wide range of experimental conditions. Substituting the former value into Equation (7), it is found that the-

oretically the Kozeny-Carman equation is invalid at porosities greater than 0.92 because higher porosities would correspond to a value of  $R$  less than unity.

The porosity above which the Kozeny-Carman equation is no longer useful is somewhat nebulous. Billings and Wilder<sup>12</sup> stated that the Kozeny-Carman equation does not apply to high porosity dust cakes because the theory is based on discrete passageways. Specifically, they suggest caution for porosities in excess of 0.7. Carman<sup>13</sup> contended that his theory does not break down until porosity exceeds 0.8.

Although in situ porosities of dust cakes on cloth filters have never been reported in the literature, there are some clues to the range of porosities which can be expected. Billings and Wilder<sup>14</sup> indicated that the porosities of granular powders vary from about 0.40 to 0.99. Orr<sup>15</sup> listed porosities from 0.51 to 0.94 for dust filter cakes composed of particles with diameters from 0.24 to 33  $\mu\text{m}$ . Although these dusts were collected on fabrics, the porosities were apparently those that resulted when the same dusts were placed in glass containers and tapped<sup>16</sup>. Kimura and Iinoya<sup>17,18</sup> used the Kozeny-Carman equation to back-calculate the porosities of dust cakes from experimentally determined values of specific resistance. Their calculated porosities ranged from 0.55 to 0.99. Because a porosity greater than 0.92 calculated from the Kozeny-Carman equation is theoretically impossible, their data is suspect.

In conclusion, it is evident that the Kozeny-Carman equa-

tion is probably of limited utility for the prediction of dust cake specific resistance. In particular, at high porosities, which are not uncommon for dust filter cakes, the Kozeny-Carman equation will seriously underestimate pressure drop.

#### "Free Surface" Model

An alternate approach to a capillary model is to recognize that a dust cake consists of an assemblage of individual particles subjected to aerodynamic drag which can be represented by a collection of uniformly distributed cells, each composed of a spherical particle and a concentric, fluid-filled envelope of such proportion that the porosity of the cell and of the entire granular medium is identical. If appropriate boundary conditions are formulated, the Navier-Stokes equation (neglecting inertial effects) can be solved rigorously.

Happel<sup>19</sup> postulated a "free surface" cell model in which the salient boundary condition is the disappearance of tangential stress on the surface of the spherical envelope. If the size of the spherical envelope is infinite, the result becomes identical with Stokes' law. For prediction of pressure drop through a dust cake, the "free surface" model of Happel can be written in terms of the resistance factor as follows:

$$R = \frac{3 + 2(1-\epsilon)^{5/3}}{3 - 4.5(1-\epsilon)^{1/3} + 4.5(1-\epsilon)^{5/3} - 3(1-\epsilon)^2} \quad (8)$$

Theoretically, this relationship should be valid for all values of porosity and it yields the proper limits, i.e., for  $\epsilon = 0$ ,  $R$  is infinite and for  $\epsilon = 1$ ,  $R = 1$ . It shows good agreement



with published experimental data for hindered settling in the high porosity range (0.95 to 1.0)<sup>19</sup>; and, for packed beds in the low porosity range (0.30 to 0.60), it gives results essentially identical to those derived from the Kozeny-Carman equation, as shown in Table II. The close agreement between the semi-empirical Kozeny-Carman equation and the theoretical relationship of Happel in the low porosity range ( $<0.60$ ) is striking considering that the "free surface" model contains no empirical constants. In the intermediate porosity range (0.60 to 0.95), the experimental results are contradictory, indicating that porosity does not uniquely characterize permeability. Inasmuch as most of the data in this porosity range come from fluidized and sedimenting particle systems, circulation and agglomeration effects would be expected to play an important role and result in increased permeability. This would explain qualitatively discrepancies between the "free surface" model and experimental results. The "free surface" model, however, is in satisfactory agreement with the rather limited experimental data in which circulation and agglomeration effects were eliminated or minimized<sup>19,20</sup>. It seems likely that there are no agglomeration effects present when a dust cake is formed primarily from a nonaggregated aerosol. As discussed previously, a dust cake forms dynamically and it is reasonable to assume that particle deposition tends toward uniformity.

Inasmuch as the "free surface" model is theoretically valid at all porosities, it is tempting to adopt it for dust filter

TABLE II. Comparison of Resistance Factors Predicted by Kozeny-Carman Equation and "Free Surface" Model

Porosity	Resistance Factor (R)		
	Kozeny-Carman Equation (Eq. 7, $k = 4.8$ )	Happel Model (Eq. 8)	Ratio Happel/Kozeny-Carman
.30	250	230	0.92
.40	90	85	0.94
.50	38	38	1.0
.60	18	19	1.1
.70	8.4	10	1.2
.80	3.7	5.6	1.5
.90	1.3	3.1	2.4
1.00	0.0	1.0	$\infty$

cakes but certain important considerations remain unresolved. In particular, the "free surface" model assumes uniform spheres, and does not indicate how nonuniform particle sizes and nonspherical shapes should be handled. In addition, the "free surface" model assumes that particles are sufficiently large that the fluid can be considered as a continuum. This may not be correct for a dust cake composed of very small particles.

#### Effect of Particle Size Distribution and Particle Shape

When the Kozeny-Carman equation is employed, the correct mean particle diameter as given by the hydraulic radius theory is a function of the specific surface area of the granules,  $S$ , (i.e., the surface area exposed to the fluid per unit volume of solid material), or

$$\bar{D}_{vs} = 6/S \quad (9)$$

where  $\bar{D}_{vs}$  is the mean diameter to be used in the Kozeny-Carman equation<sup>21</sup>. This approach automatically corrects for particle shape. For spherical particles,

$$\bar{D}_{vs} = \frac{\sum n_i D_i^3}{\sum n_i D_i^2} = (\sum w_i / D_i)^{-1} \quad (10)$$

where  $n_i$  is the number fraction and  $w_i$  the weight fraction of particles with diameter  $D_i$ .  $\bar{D}_{vs}$  is often referred to as volume-surface mean diameter or the Sauter mean diameter. For irregularly shaped particles

$$\bar{D}_{vs} = \phi_{vs} \frac{\sum n_i (D_p^3)_i}{\sum n_i (D_p^2)_i} \quad (11)$$

where  $\phi_{vs}$  is a shape factor which is assumed here to be independent of particle size and  $D_p$  is the projected area diameter obtained from microscopy.

Some experimental studies using mixtures of various particle sizes have shown agreement with the Kozeny-Carman equation when using  $\bar{D}_{vs}$  as the mean diameter<sup>22</sup>. Carman<sup>3</sup> also showed that the use of  $\bar{D}_{vs}$  gave good results for mixtures of spheres in which the diameter ratio was 2:1 whereas when the diameter ratio was 5:1, the calculated value for  $\bar{D}_{vs}$  was not able to compensate entirely for changes in permeability. Krumbein and Monk<sup>23</sup> used sands having equal mass median diameters but different size distributions and obtained a significant effect of particle size dispersity on specific resistance. Correcting their data to a constant volume-surface mean diameter does not substantially change their results. Carman<sup>24</sup> stated that whereas the permeability method for measurement of particle size does not require particles of uniform size, an excessively wide distribution of sizes should be avoided, and this warning is frequently echoed in texts<sup>25</sup>.

In his original "free surface" model derivation, Happel<sup>19</sup> did not treat nonuniformity in size or nonsphericity, but later<sup>26</sup>, he supported the use of a volume-surface mean diameter. Rather than follow this empirical approach, it can be shown that a mean diameter follows logically from either the Stokes' law or Happel model. For illustrative purposes, if Equation (4), based on Stokes' law is rewritten to apply to a distribution of irregu-

larly shaped particles of various sizes, and if slip is neglected, Equation (4) assumes the following form:

$$\frac{\Delta P}{W} = \frac{\sum \text{Drag Force}}{\sum \text{Mass}} = \frac{3\pi\mu V \sum \chi_i n_i (D_e)_i}{\frac{\pi}{6} \rho_p \sum n_i (D_s^3)_i} \quad (12)$$

where  $\chi$  is a dynamic shape factor defined by Fuchs<sup>27</sup> as the ratio of the resistance of a given particle to that of a spherical particle having the same volume, and  $D_e$  is the diameter of a sphere having the same volume as the particle. From the definition of the sedimentation (Stokes) diameter,  $D_s$ , it can be shown<sup>27</sup> that:

$$\chi = \frac{D_e^2}{D_s^2} \quad (13)$$

Hence, if it is assumed that  $\chi$  is independent of particle size, substituting Equation (13) into Equation (12) yields:

$$(K_2)_{\text{minimum}} = \frac{\Delta P}{WV} = \frac{18\mu}{\rho_p} \frac{\sum n_i (D_s)_i}{\sum n_i (D_s^3)_i} \quad (14)$$

Comparing Equations (14) and (5), it will be seen that the required mean diameter is the volume-length mean diameter based on the distribution of sedimentation diameters:

$$\bar{D}_{v1} = \left[ \frac{\sum n_i (D_s^3)_i}{\sum n_i (D_s)_i} \right]^{1/2} = \left[ \frac{\sum w_i}{\sum (D_s^2)_i} \right]^{-1/2} \quad (15)$$

Alternatively,  $\rho_p$ , can be set equal to unit specific gravity in Equation (14) and an aerodynamic diameter substituted for the sedimentation diameter in Equation (15). The same result is obtained for the "free surface" model with slip included provided the dynamic shape factor is not influenced by porosity. Equation (6) can then be rewritten as follows:

$$K_2 = \frac{R}{\tau_{vl} C_s} \quad (16)$$

where

$$\tau_{vl} = \frac{\rho_p \bar{D}_{vl}^2}{18\mu} \quad (17)$$

When  $\bar{D}_{vl}$  is to be determined by microscopic methods,

$$\bar{D}_{vl} = \phi_{vl} \left[ \frac{\sum n_i (D_p^3)_i}{\sum n_i (D_p)_i} \right]^{1/2} \quad (18)$$

where  $\phi_{vl}$  is a shape factor which is assumed to be independent of particle size and porosity and which relates the sedimentation diameter to the projected area diameter, i.e.,

$$\phi_{vl} = \frac{D_s}{D_p} \quad (19)$$

Although the volume-length mean diameter,  $\bar{D}_{vl}$ , given by Equation (15) differs from the volume-surface mean diameter,  $\bar{D}_{vs}$ , given by Equation (10), the difference is small for spherical particles unless the particle size distribution is fairly broad. For example, if the particle sizes are log normally distributed, these two diameters can be related using the Hatch-Choate equation<sup>28</sup> as shown in Table III. For most of the studies done on granular media, usage of  $\bar{D}_{vs}$  or  $\bar{D}_{vl}$  would give nearly the same results, but for most industrial dust cakes, the difference can be expected to be large because industrial dusts tend to have a geometric standard deviation greater than 2.5.

#### Slip Flow

When particle diameters in a dust cake become small, the gas

TABLE III. Comparison of  $\bar{D}_{vs}$  and  $\bar{D}_{vl}$

<u>Geometric Standard Deviation</u>	<u><math>\bar{D}_{vs}/\bar{D}_{vl}</math></u>
1.0	1.0
1.5	1.09
2.0	1.27
2.5	1.52
3.0	1.83

can no longer be regarded as a continuum and the specific resistance will be less than predicted by theory because the gas velocity will not be zero at the particle surface. Inasmuch as the derivation given by Happel<sup>19</sup> does not account for this slip, the "free surface" model was rederived using the classical slip flow procedure<sup>29</sup> in which the Navier-Stokes equation is solved using boundary conditions which account for noncontinuum effects. This method is valid only for small (<0.25) Knudsen numbers (gas mean free path/particle radius). The result of this derivation is given below in terms of the slip correction factor for use in Equation (16):

$$C_s = \frac{(\sum n_i D_i) \cdot \left( \frac{3+2\alpha^{5/3}}{2-3\alpha^{1/3}+3\alpha^{5/3}-2\alpha^2} \right)}{\sum \left[ n_i D_i \frac{3 + 2\alpha^{5/3} + 6Kn_i(1-\alpha^{5/3})}{2 - 3\alpha^{5/3} + 3\alpha^{5/3} - 2\alpha^2 + 6Kn_i(1-\alpha^{1/3}-\alpha^{5/3}+\alpha^2)} \right]} \quad (20)$$

where  $\alpha$  is dust cake solidity ( $1-\epsilon$ ) and  $Kn_i$  is a modified Knudsen number for a particle of size  $D_i$ , i.e.,  $Kn_i = \frac{2A\lambda}{D_i}$ , where  $A$  is a number close to unity which characterizes the interaction of the gas molecules with the particle surface and  $\lambda$  is the mean free path of the gas.

From Equation (20), when the Knudsen number approaches zero (i.e., no slip), the slip correction factor approaches unity. When porosity is equal to unity and the particles are single-sized:

$$C_s = \frac{1+3Kn}{1+2Kn} \quad (21)$$



Equation (21) is identical to the result given by Fuchs<sup>30</sup> for the slip correction factor for a single particle in an infinite medium, which is valid only for small Knudsen numbers and is approximately equal to the Cunningham slip correction factor.

From theory, Equation (20) should be valid at all porosities (for Knudsen numbers  $< 0.25$ ). It gives excellent agreement with published experimental results for compacted fine powders having porosities from 0.4 to 0.6\* and, as stated above, is in fair agreement with the Cunningham slip correction factor for porosities approaching unity. If a slip correction factor = 1.1 is ignored, a 10% error in the specific resistance will be obtained. From Equation (20), this error corresponds to the particle sizes and porosities shown in Table IV. When either porosity or particle diameter becomes smaller than the value shown in Table IV, neglect of the slip correction factor will yield a value for specific resistance from Equation (16) that will exceed the correct value by more than 10%.

#### Experimental Apparatus

Experimental apparatus was designed to fulfill two key objectives: (1) determination of filter cake specific resistance, and (2) preparation of filter cakes for porosity measurement. Figure 1 shows the bench scale equipment in which dust cakes were formed on various cloth and paper supports at a constant air-to-cloth ratio over a wide range of air-to-cloth ratios such that other parameters (e.g., aerosol particle size distribution and relative humidity) could be held essentially constant during a

\*Confirmation of this statement can be found in Harvard School of Public Health doctoral dissertation by S. Rudnick currently in progress.

TABLE IV. Porosities and Particle Diameters for which  $C_s = 1.1$

<u>Porosity</u>	<u>Particle Diameter, <math>\mu\text{m}</math></u>
0.3	32
0.4	22
0.5	16
0.6	11
0.7	8.2
0.8	5.7
0.9	3.6
1.0	1.1

a run and from run-to-run.

As shown in Figure 1, filtered compressed air was fed to a Wright<sup>31</sup> dust feeder which dispersed the test dust. The resultant aerosol passed through an elutriator in which all particles with an aerodynamic diameter greater than 8.4  $\mu\text{m}$  were removed before reaching the experimental filter. Aerosol in excess of the amount needed for filtration was vented at the inlet to the elutriator. To avoid flow disturbances, a circular frustum with a 7° half angle was used upstream of the filter. The filter holder was composed of two cylindrical pieces with large flanges between which a supporting substrate such as cloth could be clamped with the cloth acting as its own leak tight gasket. Flow measuring and controlling devices, located downstream from the filter, included a manually adjusted control valve to give constant flow over the duration of a run plus a sensitive and accurate pressure gauge placed upstream of a calibrated critical orifice to make it possible to measure mass flow rate. The critical orifice also served to isolate the system from downstream disturbances caused by the vacuum pump. The control valve acted as a high flow resistance in series with the filter so that changes in pressure drop across the filter cake had little effect on mass flow rate. At face velocities below 50 mm/s (10 fpm) flow rate remained constant throughout a run without need to readjust the control valve. Pressure drop across the filter was recorded continuously on a chart recorder. Filter approach velocity was adjusted by varying filter area, i.e., changing the diameter of

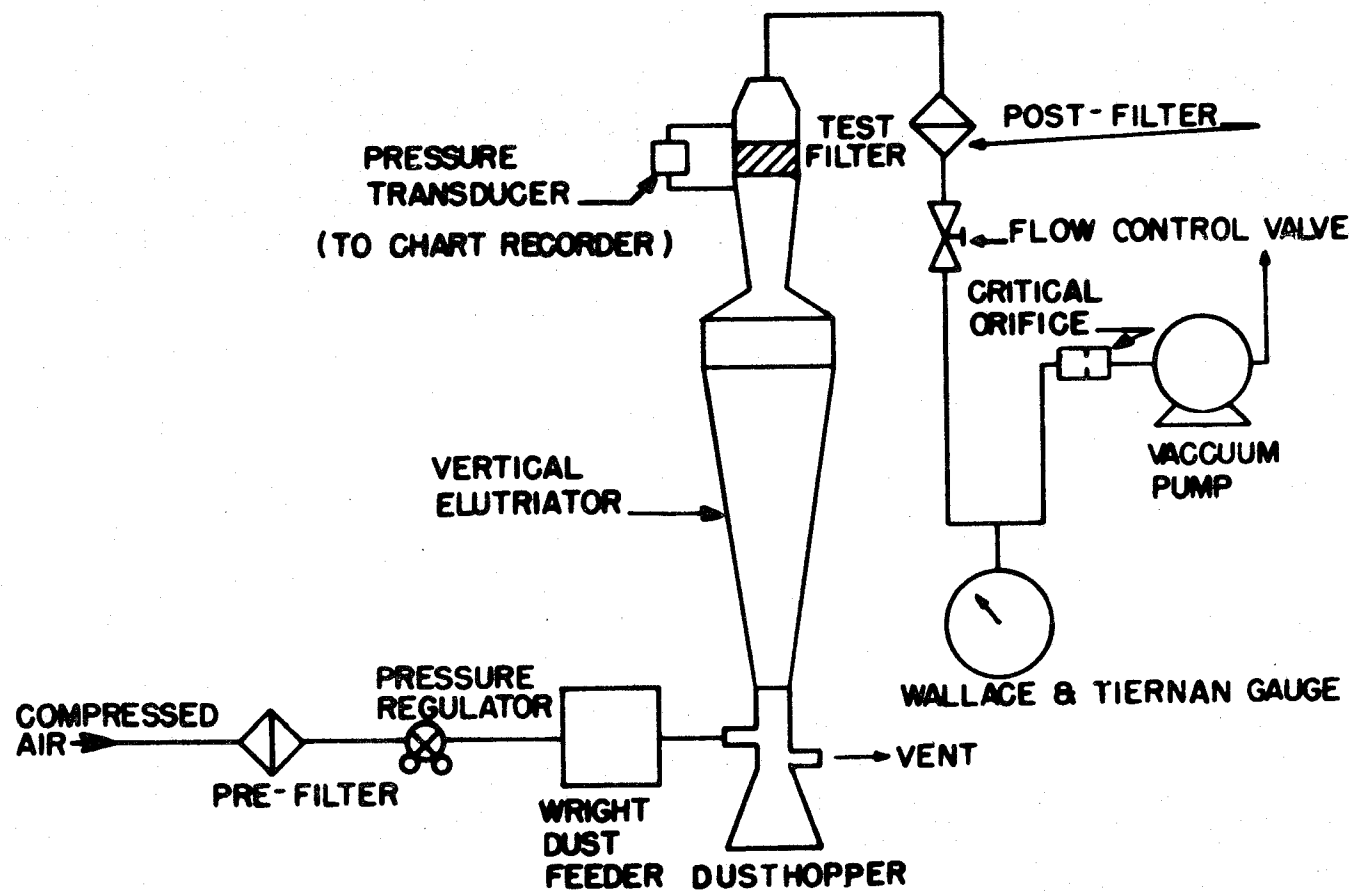


FIGURE 1. Experimental Apparatus

filter holder and connecting pieces. Inasmuch as the filter area was always less than the elutriator cross sectional area, the aerosol size distribution was not affected by changes in filter face velocity.

#### Porosity Determinations

The porosity ( $\epsilon$ ) of dynamically formed dust cakes was calculated from the following working relationship in terms of the measurable parameters:

$$\epsilon = 1 - \frac{m}{a\rho_p L} \quad (22)$$

where  $\rho_p$  is the density of individual particles,  $m$  is the mass of filter cake exclusive of dust retained in the interstices of the fabric,  $a$  is area of the dust deposit, and  $L$  is average thickness of the dust cake. Density of particles removed from filter cakes was evaluated by pycnometry using a nonadsorbing gas, filter cake mass was determined by weighing to the nearest tenth of a milligram, area of the dust deposit was equal to the open area of the filter holder, and cake thickness was measured by the following procedure: A fracture could be induced in most dust cakes by bending the cloth and then the cake could be removed cleanly from one side of the fracture by tapping. This would expose a cross section of the cake such as that shown in Figure 2 on which thickness measurements could be made. During the cleaning cycle of a bag filter, a similar process of fabric bending and cake separation takes place<sup>23</sup>. Alterations of the portion of the dust cake remaining on the fabric that might be caused by the bending

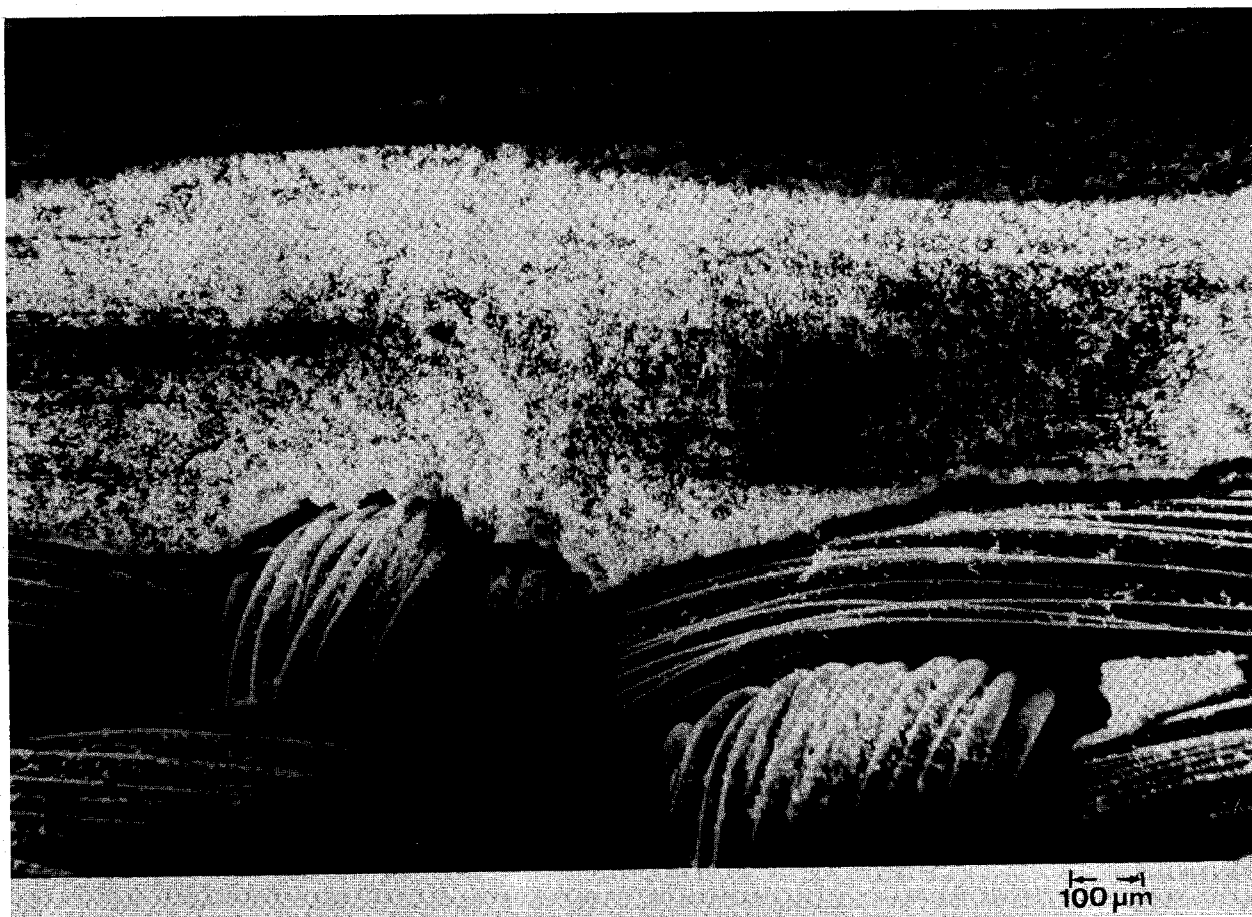


Figure 2. Cross Section of Dust Cake on Woven Fabric

procedure could be detected easily with a stereoscopic microscope. Dust cake thickness was measured by three techniques:

A. Measuring cake thickness with a calibrated graticule in an 84x stereoscopic microscope. The circular dust cake was always flat in the vicinity of its center but it tended to decrease in thickness near the edge. Therefore, dust cake thickness was measured as a function of diameter and converted to a single value of average cake thickness by graphical integration. As this is a lengthy procedure, it was done once at each filter velocity and, thereafter, an experimentally determined correction factor, calculated for each filter velocity, was applied to convert from thickness at the cake center to average dust cake thickness.

B. Measuring the shadow formed in a scanning electron microscope using backscatter electrons. Because the edge of the shadow is cast on a cleaned portion of fabric, this method automatically compensates for the unevenness of the fabric. This procedure is not applicable to the light microscope because of insufficient depth of field. A micrograph of a shadow cast on a woven fabric is shown in Figure 3.

C. Measuring the amount of rotation of a calibrated fine focusing adjustment of a light microscope with a 22x objective by focusing first on the cake surface and then on the fabric surface.

All of these methods worked reasonably well for flat cake supports (paper) but for fabrics, method C gave very inconsistent

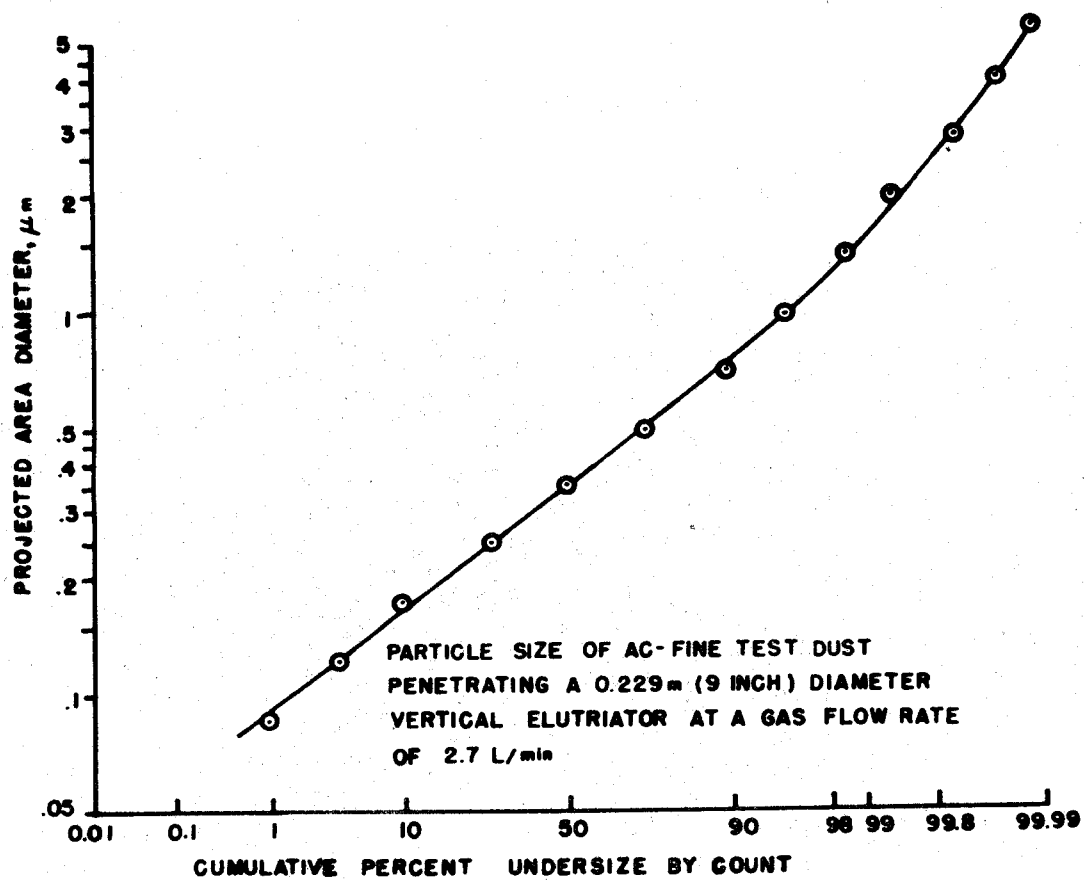


FIGURE 4. Particle Size Distribution



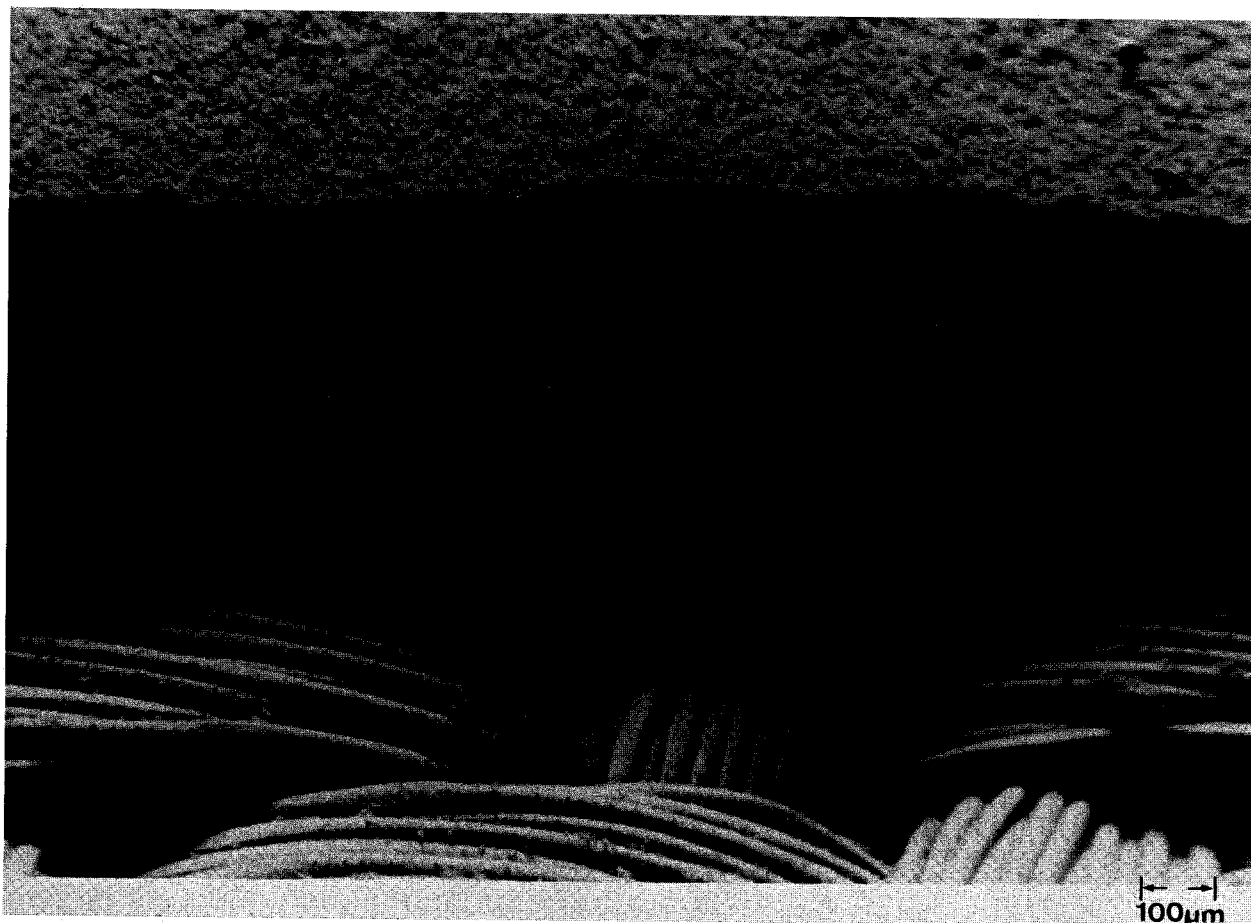


Figure 3. Dust Cake Shadow Cast on Woven Fabric

results. Methods A and B gave reasonably good agreement. Method A is the most accurate and most time consuming.

#### Characterization of the Aerosol

Employing the apparatus shown in Figure 1, representative samples of the aerosol generated from AC-fine test dust (GM Phoenix Laboratory, Flint, Michigan), were collected on two 0.2  $\mu\text{m}$  diameter Nuclepore filters in series separated by an open fibrous mat (Nuclepore D247 POR). All parameters remained the same as during dust cake formation except that the concentration of the aerosol was reduced to produce a deposit suitable for sizing. The filter samples were photographed in a scanning electron microscope at magnifications appropriate for stratified counting. Particles were sorted into geometrically spaced size categories with a transparent overlay patterned after the May-Porton graticule<sup>33</sup>. It was intended that the second Nuclepore filter would be used to measure the fractional efficiency of these filters, but no particles were detected on the second filter.

The projected area diameter distribution of the aerosol used in this study is shown on log probability paper in Figure 4. The volume-length shape factor,  $\phi_{vl}$  (Equation 18), used to convert projected area diameter to sedimentation diameter, was estimated based on (1) the projected area diameter of the largest particles passing through the elutriator determined for photomicrographs, and (2) the sedimentation diameter of the largest spherical particle capable of penetrating the elutriator based on the elutria-

tor center-line velocity assuming Poiseuille flow. This approach is likely to give somewhat large values of  $\phi_{vl}$  because the biggest particles penetrating the elutriator may go undetected by microscopy due to their scarcity. The volume-surface shape factor,  $\phi_{vs}$  (Equation 11), used to convert projected area diameter to volume-surface mean diameter, was determined from (1) projected area diameter distribution, and (2) specific surface area measurements on polished cross sections of particles embedded in plastic resin employing the methods of Chalkley, Cornfield, and Park<sup>34</sup>. It was found for the aerosol used in this study that  $\phi_{vl} = 0.66$  and  $\phi_{vs} = 0.62$ . Both are within the range of values cited in the literature for similarly shaped particles<sup>35,36</sup>.

### Results

Elutriated AC-Fine test dust was collected at various face velocities from 7.1 mm/s (1.4 fpm) to 56 mm/s (11 fpm) on paper and woven fabric supports that included Teflon, polypropylene, Dacron (all 3x1 twill, monofilament yarns), cotton sateen, Whatman 41, and 8.0  $\mu$ m Millipore filter. Specific resistance,  $K_2$ , was determined from the following equation:

$$K_2 = \frac{1}{V} \frac{(\Delta P)_2 - (\Delta P)_1}{W_2 - W_1} \quad (23)$$

where subscript "1" refers to the point at which  $\Delta P$  became essentially linear with areal density and subscript "2" refers to dust flow termination.

Measured values of solidity ( $1-\epsilon$ ) have been plotted against experimentally derived values of the specific resistance,  $K_2$ ,

in Figure 5. Also included in Figure 5 is a curve showing the functional relationship between specific resistance and solidity that we recommend based on Equations (8), (15), (16), (17) and (20) or their composite given as follows:

$$K_2 = \frac{18\mu \left[ \frac{n_1(D_s)_1 \{3 + 2\alpha^{5/3} + 6Kn_1(1-\alpha^{5/3})\}}{3 - 4.5\alpha^{1/3} + 4.5\alpha^{5/3} - 3\alpha^2 + 9Kn_1(1-\alpha^{1/3}-\alpha^{5/3}+\alpha^2)} \right]}{\rho_p \Sigma[n_1(D_s^3)_1]} \quad (24)$$

The experimental results are in considerably better agreement with Equation (24) than with the Kozeny-Carman equation also shown in Figure 5 which greatly underestimated the specific resistance of the experimentally filtered dust cakes. This was expected because the porosity of these dust cakes lies outside the range of validity for the Kozeny-Carman equation. A large portion of the Kozeny-Carman curve lies below the minimum possible specific resistance predicted from the Stokes' law model shown as a single point in Figure 5.

### Discussion

A filter dust cake can be modeled as a collection of capillaries or as an assemblage of particles. Although the latter is clearly a more realistic representation, the Kozeny-Carman equation utilizes the former, and consequently suffers certain limitations. In particular, as the porosity of a dust cake approaches unity, the Kozeny-Carman equation predicts that the specific resistance ( $K_2$ ) will approach zero, whereas in this case, the cumulative frictional and form drag of the isolated particles will define the value of  $K_2$ . As a limiting case,

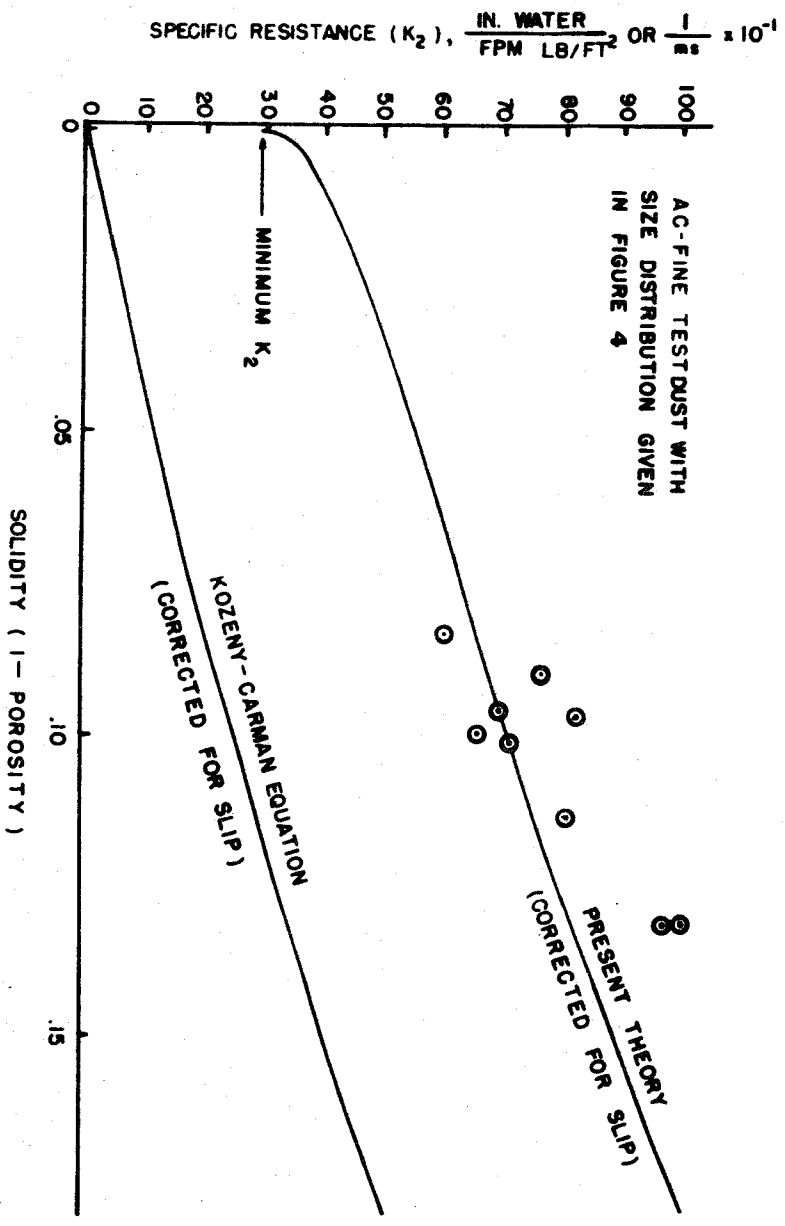


FIGURE 5. Specific Resistance vs. Solidity

applying Stokes' law to flow through a dust cake, leads to Equation (5) which, solely from hydrodynamic considerations, gives the minimum value of  $K_2$  for a given dust. It is clear from Table I that the minimum specific resistance for small particles will be large. For example, a 0.5  $\mu\text{m}$  particle diameter yields a minimum  $K_2$  equal to 980/ms (98 in. water/fpm $\cdot\text{lb}/\text{ft}^2$ ). This example incorporates an important concept: the specific resistance for small particles will always be large, regardless of the magnitude of porosity. A common misunderstanding of fabric filter vendors and users is that fine fumes produce nonporous filter cakes with high flow resistance. Although fine fumes do cause high flow resistance, the dust cakes are, nonetheless, likely to exhibit high porosity. The high flow resistance is due primarily to the small particle size.

An understanding of minimum specific resistance can be helpful in determining whether or not data from lab or field studies are of the correct order of magnitude. When  $K_2$  values less than the calculated minimum specific resistance are obtained, the data must be suspect.

Although the Kozeny-Carman equation (with a suitable correction for slip flow) is presumably valid for dust cakes with porosities less than 0.65, the "free surface" model, modified to treat nonuniform particle sizes, nonspherical shapes, and slip flow, is preferable because it gives good agreement with experimental measurements for the entire range of dust cake porosities. Either model yields essentially the same specific resistance for

porosities less than 0.65. This is fortunate in light of the extensive experimental support of the Kozeny-Carman equation at these porosities. But at porosities above 0.65, which are common in fabric filter dust cakes, the Kozeny-Carman equation underestimates specific resistance whereas the modified "free surface" model gives adequate agreement with experimental results. This is shown in Figure 5.

Both the Stokes' law model and the "free surface" model consider a dust cake to be an assemblage of particles but the "free surface" model differs because the drag force on a particle given by Stokes' law is multiplied by a factor that is greater than unity and increases as dust cake porosity decreases. When porosity approaches one, the two models become identical. The mean diameter appropriate for these models is given by Equation (15) and is calculated directly from the sedimentation diameter distribution or aerodynamic diameter distribution when particle specific gravity is taken in unity in Equation (17). The diameter distribution may be expressed on a number or weight basis, and can often be measured with the aid of an inertial sampling device such as an impactor provided particle size is not too small. In addition to correcting for particle shape based on the aerodynamic properties of particles, this measurement method may also compensate for particle orientation inasmuch as a particle is likely to remain in an aerodynamically stable position after incorporation into the dust cake.

Inasmuch as the "free surface" model also predicts the flow field surrounding a particle in a dust cake, it may be possible to predict SO<sub>2</sub> collection efficiency in fabric filters which remove SO<sub>2</sub> in a reacting chemical precoat or upstream injection. Pfeffer<sup>37</sup> derived a solution for heat and mass transfer in particulate systems based on the "free surface" model which is valid for high Peclet number. Although SO<sub>2</sub> removal in a fabric filter dust cake usually occurs at low Peclet number, development of an approach similar to Pfeffer's which can be applied to SO<sub>2</sub> removal in a fabric filter, may be possible. This type of modeling capability may become very useful if all new coal-fired utility plants are required to use scrubbers or fabric filters with nahcolite injection, as appears likely<sup>38</sup>.

#### Acknowledgement

This work was supported in part by Stone & Webster Engineering Corporation, Boston, Mass. It was performed in partial fulfillment of the requirements for the Sc.D. degree at the Harvard School of Public Health.

#### References

1. Carman, P. C., "Flow of Gases Through Porous Media", Academic Press, New York, NY, 1956.
2. Scheidegger, A. E., "The Physics of Flow Through Porous Media", University of Toronto Press, Toronto, Canada, 1974.
3. Carman, P. C., "Fluid Flow Through Granular Beds", Transactions - Institution of Chemical Engineers, 15:150-166, 1937.
4. Williams, C. E., Hatch, T. and Greenburg, L., "Determination of Cloth Area for Industrial Air Filters", Heating, Piping and Air Conditioning, 12:259-263, 1940.



5. Silverman, L., "Filtration Through Porous Media", American Industrial Hygiene Association Quarterly, 11:11-20, 1950.
6. Stephan, D. G., Walsh, G. W. and Herrick, R. A., "Concepts in Fabric Air Filtration", American Industrial Hygiene Association Journal, 21:1-14, 1960.
7. Billings, C. E. and Wilder, J., "Handbook of Fabric Filter Technology, Vol. I, Fabric Filter Systems Study", National Technical Information Service, PB-200 648, Springfield, VA, 1970.
8. Ibid., p. 2-131.
9. Ibid., p. 2-160.
10. Fuchs, N. A., "The Mechanics of Aerosols", Pergamon Press, Oxford, England, 1964, p. 49.
11. Carman, P. C. and Malherbe P. le R., "Routine Measurement of Surface of Paint Pigments and Other Fine Powders", Journal of the Society of Chemical Industries, London (Transactions), England, 69:134-143, 1950.
12. Billings, C. E. and Wilder, J., Op. Cit., p. 2-117.
13. Carman, P. C., 1956, Op. Cit., p. 15.
14. Billings, C. E. and Wilder, J., Op. Cit., p. 2-134.
15. Orr, C., Jr., "Particulate Technology", MacMillan, New York, NY, 1966, p. 291.
16. Iinoya, K. and Yamamura, M., "Fundamental Experiments With Dust-Collectors", Kagaku Kōgaku, Japan, 20:163-171, 1956, (in Japanese).
17. Kimura, N. and Iinoya, K., "Pressure Drop Characteristics of Filter Cloth for Dust Collection", Kagaku Kōgaku, Japan, 29:166-174, 1965, (in Japanese).
18. Kimura, N. and Iinoya, K., "Pressure Drop Characteristics of Filter Cloth for Dust Collection", Kagaku Kōgaku, Japan, 3:193-196, 1965, (abridged edition in English).
19. Happel, J., "Viscous Flow in Multiparticle Systems: Slow Motion of Fluids Relative to Beds of Spherical Particles", A.I.Ch.E. Journal, 4:197-201, 1958.
20. Happel, J., "Fluid Flow in Multiparticle Systems", Transactions of the New York Academy of Sciences, 20:404-410, 1958.

21. Carman, P. C., 1956, Op. Cit., p. 11.
22. Ibid, p. 18.
23. Krumbein, W. C. and Monk, G. D., "Permeability as a Function of the Size Parameters of Unconsolidated Sand", Transactions of the American Institute of Mechanical Engineers, 151:153-163, 1943.
24. Carman, P. C., 1956, Op. Cit., p. 83.
25. Allen, T., "Particle Size Measurement", Chapman and Hall, London, England, 1968.
26. Happel, J. and Brenner, H., "Low Reynolds Number Hydrodynamics With Special Applications to Particulate Media", 2nd Ed., Noordhoff International Publishing, Leyden, Netherlands, 1973, pp. 395, 418.
27. Fuchs, N. A., Op. Cit., pp. 39-40.
28. Silverman, L., Billings, C. E. and First, M. W., "Particle Size Analysis in Industrial Hygiene", Academic Press, New York, NY, 1971, p. 242.
29. Hidy, G. M. and Brock, J. R., "The Dynamics of Aerocolloidal Systems", Pergamon Press, Oxford, England, 1970, p. 147.
30. Fuchs, N. A., Op. Cit., p. 25.
31. Wright, B. M., "A New Dust-Feed Mechanism", Journal of Scientific Instruments, 27:12-15, 1950.
32. Dennis, R., Cass, R. W. and Hall, R. R., "Observed Dust Dislodgement from Woven Fabrics and Its Measured and Predicted Effect on Filter Performance", Presented at the 70th Annual Meeting of the Air Pollution Control Association, Toronto, Canada, June 20-24, 1977.
33. May, K. R., "A New Graticule for Particle Counting and Sizing", Journal of Scientific Instruments, 42:500-501 1965.
34. Chalkley, H. W., Cornfield, J. and Park, H., "A Method for Estimating Volume-Surface Ratios", Science, 110:295-297, 1949.
35. Mercer, T. T., "Aerosol Technology in Hazard Evaluation", Academic Press, New York, NY, 1973, p. 83.
36. Herdan, G., "Small Particle Statistics", Academic Press, New York, NY, 1960, p. 175.

37. Pfeffer, R., "Heat and Mass Transport in Multiparticle Systems", Industrial and Engineering Chemistry Fundamentals, 3:380-383, 1964.
38. McIlvaine, R. W., ed., "Fabric Filter Newsletter", No. 23, McIlvaine Company, Northbrook, IL, September 10, 1977, p. 8.

THE INFLUENCE OF ELECTROSTATICALLY-INDUCED CAGE VOLTAGE  
UPON BAG COLLECTION EFFICIENCY DURING THE PULSE-JET  
FABRIC FILTRATION OF ROOM TEMPERATURE FLYASH

R. P. Donovan\*  
R. L. Ogan+  
J. H. Turner+

\*Research Triangle Institute  
Process Engineering Department  
P. O. Box 12194  
Research Triangle Park, N. C. 27709

+Environmental Protection Agency  
Industrial Environmental Research Laboratory  
Research Triangle Park, N. C. 27711

## Abstract

In a previous paper an experimental arrangement was described for measuring the effect of electrostatic charge buildup on fabric filters during the room temperature, pulse-jet filtration of re-dispersed flyash--flyash which was originally collected by an electrostatic precipitator scrubbing the effluent of a pulverized coal boiler. A prime justification and advantage of that experimental arrangement was that it required only the attachment of one electrical lead to the cage supporting the bag filter. This simple modification was assumed not to change or influence the dust/fabric interaction being studied in any way.

From the qualitative concepts previously presented, a simple analog equivalent circuit is proposed for relating the charge buildup on or in the fabric to the cage voltage detected by the measuring technique. Since the simple equivalent circuit to be presented explains at least some of the cage voltage features observed so far, it is concluded to be a useful starting point for modeling the interaction.

A second general goal of the experimental program is to relate the electrostatic properties of a given dust/fabric system to its performance as a fabric filter. The initial observation of this portion of the program concludes the paper.

## HISTORICAL BACKGROUND

At least as long ago as 1913 [Reference 1] experiments were being performed which showed that raising clouds of dust produced large amounts of electricity, that the sign of the resultant charge depended on the dust composition and that particle size affected charge quantity. The work included passing particles through metal mesh and light cotton fabrics, and measuring voltages and signs of charge at the mesh or fabric surface and beyond. Passing dust through long tubes (20 feet)\* also generated strong charges.

By 1926 Deodhar [Reference 2] (and Shaw [Reference 2] in discussion following Deodhar's paper) showed that temperature and humidity also affected charge. The beginnings of a triboelectric series for dusts were discussed. In 1950, Kunkel [Reference 3] refined previous work and presented quantitative information about dust clouds. With highly reproducible measurements, he concluded that (1) the particles in a dust cloud are charged, probably as a result of particle to particle separation after contact, (2) the clouds have about equal numbers of positively and negatively charged particles and are therefore neutral (unless a significant portion of the particles strike a dissimilar material), (3) the effect holds for at least over the size range from 0.5 to 30  $\mu\text{m}$ , (4) for the case of metals and insulators being the dissimilar materials,

---

\*Use of metric units exclusively would seriously inconvenience the majority of the intended reading audience. For those readers more familiar with the metric system a conversion table for changing the British units used in the report to their metric equivalent appears in the appendix.

the insulator will invariably have a predominantly negative charge, and (5) because, at least for the quartz powder studies, a one or two molecule thick layer of water remained on the particles even to several hundred degrees centigrade (water vapor moisture plays only a minor role in the electrification process).

About this time interest was generated in the deposition of particles on fibers (and other surfaces) and the effects of electrostatic phenomena on the process. Kraemer and Johnstone [Reference 4] presented equations of motion for a particle influenced by an electrostatic force in a resisting fluid, and equations for the electrostatic force on a particle approaching a collector at constant voltage and for a collector at constant charge. Experimentally they studied charged collector with corona-charged DOP, charged collector with only naturally charged aerosol, and grounded collector with corona-charged aerosol. Their results agreed reasonably well with the various collection parameters they had presented, and led to the suggestion of an electrified mat filter assumed to yield several orders of magnitude increase in collection efficiency over its non-electrified analog. No mention was made, however, of collection by cake established on a fiber or fabric support.

Rossano and Silverman [Reference 5] did experimental work with charged aerosols and/or charged fiber filters (not fabric). They used low concentrations of methylene blue particles ( $0.1$  to  $1.7 \text{ mg/m}^3$ ,  $2 \text{ }\mu\text{m}$  mass median diameter [MMD]) and Saran fiber beds  $1 \text{ in.}$  thick ( $35$  to  $70 \text{ }\mu\text{m}$  curled fibers packed to  $2.6 \text{ lb/ft}^3$ ). Filtration velocity was  $33$  to  $66 \text{ fpm}$ . Their

conclusions were that filtration efficiency increased with increasing fiber charge and decreasing fiber diameter for a negatively charged filter and relatively uncharged aerosol. In the range studied, velocity was not a significant variable (contrary to Kraemer and Johnstone's prediction). For a negatively charged bed and positively charged particles, collection efficiency increased with increasing charge and increasing filter packing density. It should be pointed out that the fiber beds were charged by hand carding just prior to each experiment. An experimental loss in collection efficiency of the bed over a 3 day period (to 45% from 75%) was presumed to be caused by electrical discharge of the bed. Further experimentation of particular (and disturbing) interest to the present work showed that passage of dust through an uncharged bed produced no measurable charge on the bed. Methylene blue at  $1.0 \text{ mg/m}^3$  at velocities of 33 and 70 fpm, and atmospheric dust at 33 to 364 fpm were used.

Although of closer interest to the present work and to baghouse users than much of the preceding work, the Rossano and Silverman experiments still have important differences when compared to fabric filtration. They used thick, open fiber beds which were not cleaned and had no appreciable cake. The fibers were relatively large in diameter and the aerosol loading was low. Velocity was an order of magnitude higher than those used with fabric filters and efficiency much lower (which may be an unfair criticism in view of the low inlet loading).



Rao et al. [Reference 6], in a paper with "Fabric Filtration" in the title, develop a strictly theoretical description and equations for a particle being collected by an array of three parallel cylinders. There may be some confusion in the minds of the authors between fiber and fabric filters. Cleaning and existence of a cake are not mentioned.

Makino et al. [Reference 7], with a reverse twist, studied removal of dust from a filter paper backed up by electrodes. They filtered dusts (Lycopodium, ABS and sinter dust) through the filter with no current through the electrodes, then stopped the dust (but not air) flow, and turned on the electrodes in order to remove dust from the filter (presumably the filter surface was vertical). They used alternating current in three different electrode/filter configurations and concluded that removal efficiency was a function of electrode distance from the filter, electrode diameter, and distance between electrode wires. They also found that removal efficiency increased as the initial electric charge of the dust increased and that filtering velocity was not significant even up to about 50 cm/sec. Optimum removal depended on frequency, with lower frequency being better. Finally, the authors found that continuously moving the filter in relation to the electrodes improved cleaning efficiency (presumably the motion wasn't vigorous enough to approximate shake cleaning).

Numerous authors have studied particle deposition on fibers with the influence of charges or electric fields. When fabrics or filter mats were used the conclusion reached is invariably that charging aids filtration

The experimental method includes measurement of efficiency for clean fabric without, and then with, charging. The efficiency usually goes from some low value to something in the 90's. What is not brought out is the difference between non-cleaned fresh fabrics or mats which filter without significant cake formation, and cleanable fabric filters which depend on the dust itself for very high collection efficiency.

One refreshing change has been the work done by Frederick [Reference 8], and Penney and Frederick [Reference 9] in exploring the role of fabric electrical properties and dust electrical properties in the fabric filtration process.

The present work is predicated on trying to gain still further understanding of electrical effects in an operating fabric filter by taking measurements in a commercial pulse-jet baghouse operated in a laboratory atmosphere.

## REVIEW OF EPA ELECTROSTATIC EXPERIMENT

The experimental apparatus used throughout this work consists of a commercially available, nine-bag MikroPul pulse-jet baghouse. This unit is one of the smallest commercially available baghouses. As such it retains all the features of fuller sized units and lends itself well to laboratory simulation of field experience.

For the electrostatic measurements to be reported here (and as reported previously [Reference 10]), the bag mounting technique was altered from the conventional mounting as shown in Figure 1. The attachment of a banana jack to the cage is the only change from the standard bag mounting procedures. The purpose of this banana jack is to allow monitoring of the electrostatic properties of the dust/fabric system by using the cage as an electrode or electrical contact to the system. As evident in Figure 1, the cage is electrically isolated from the baghouse housing by a single thickness of fabric. Since most of the synthetic fabrics investigated here have high electrical resistivity, the electrical isolation of the cage is generally high. By connecting a high impedance electrometer to the cage, the cage voltage can be monitored without disturbing or altering the filtration conditions.

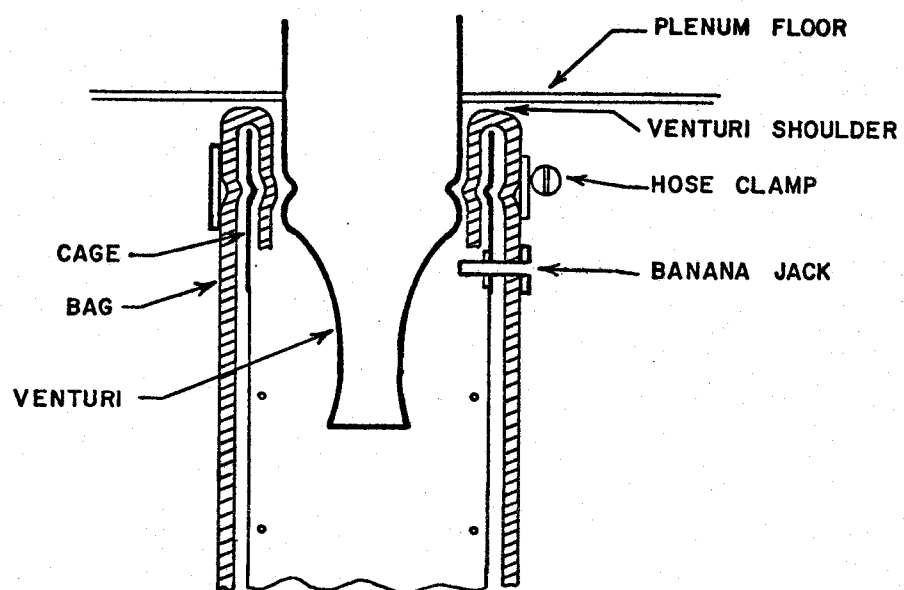


FIGURE 1. CAGE CONTACT

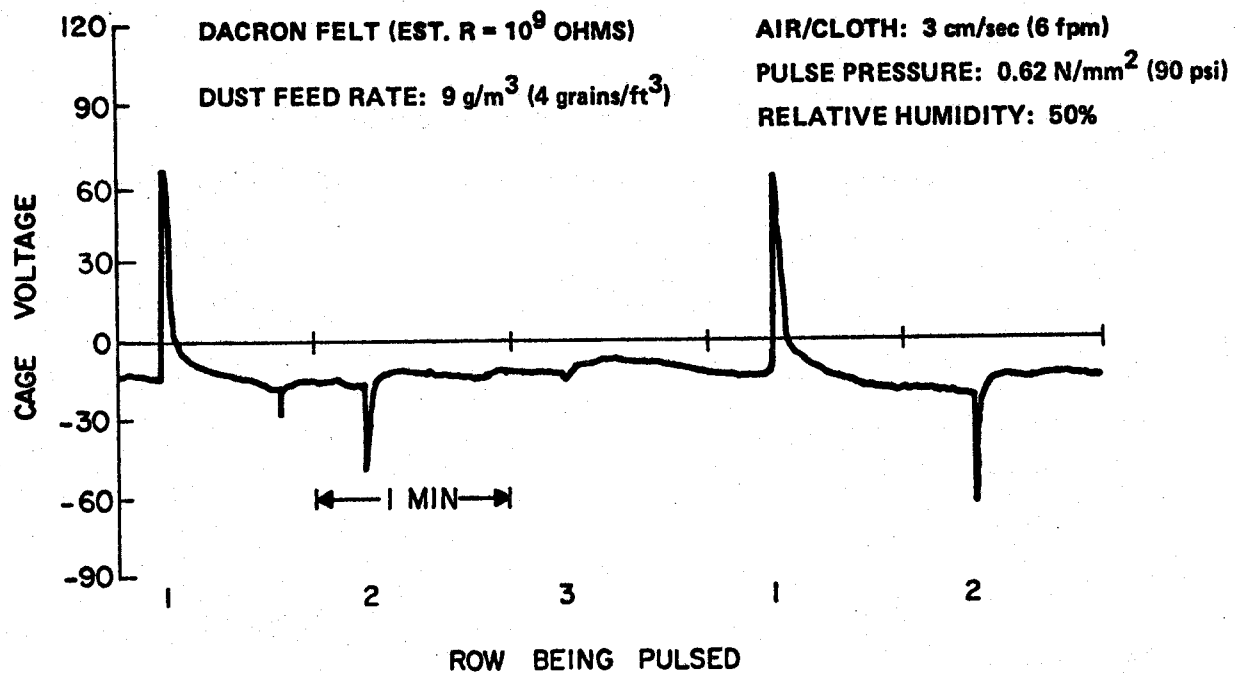
The primary experimental measurement made in this work has been the monitoring of cage voltage as a function of various independent parameters of filtration. As previously described [Reference 10], the voltage on the cage typically displays behavior similar to that illustrated in Figures 2a and 2b. Figure 2a, showing the cage voltage of a polyester felt bag (Dacron\*) filtering flyash, typifies the characteristic of a low resistivity fabric. Figure 2b, showing the cage voltage of a heat treated experimental Nomex\* felt bag, presents the characteristics of a higher resistivity fabric. In both voltage traces, the pulse-jet cleaning of the bags produces a sharp voltage spike, especially when the row of bags pulsed is that to which the electrometer is attached (Row 1, Figure 2a). When neighboring rows are pulse-cleaned, the voltage spike is of opposite polarity and reduced magnitude. The time constants associated with cage voltage recovery depend strongly on fabric resistivity, as is evident in the plots of Figure 2.

Among the conclusions drawn in Reference 1 were the following:

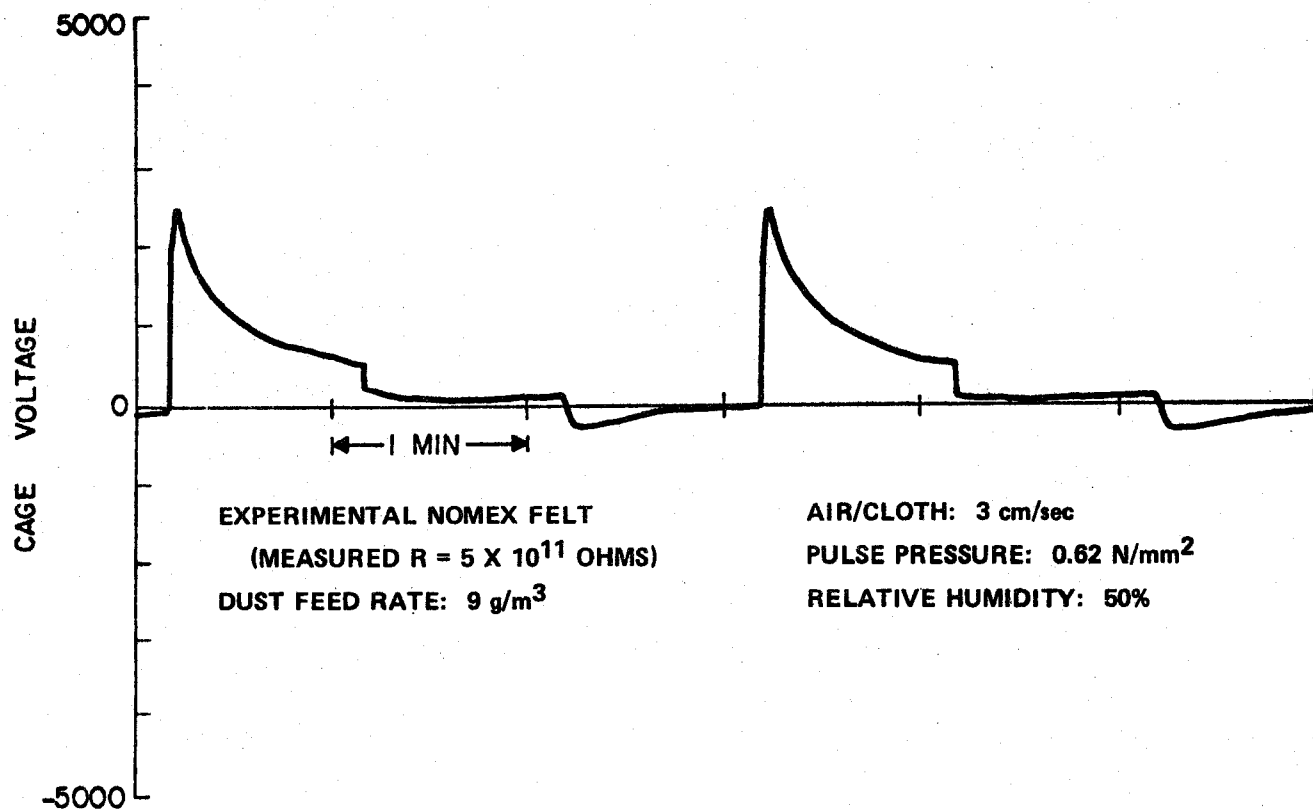
1. The electrostatic charge originates primarily because of triboelectric interactions between the fabric and the dust. Charges on the dust alone do not dominate the observed cage voltage, as is made evident by the

---

\*Tradename of E. I. duPont de Nemours and Company.



a) BAG OF LOW ELECTRICAL RESISTANCE (POLYESTER FELT)



b) BAG OF HIGH ELECTRICAL RESISTANCE (EXPERIMENTAL NOMEK FELT)

FIGURE 2. CAGE VOLTAGE FORMS

dependence of cage voltage upon fabric type. Switching fabrics, while maintaining comparable electrical isolation and filtration conditions, causes significant differences in the observed cage voltage.

2. The pulse-cleaning action creates a voltage spike of sign and magnitude dependent on the bag charge. In this sense the pulse-jet cleaning enhances the signal-to-noise ratio for the detection of electrostatic effects.
3. Pulse-jet cleaning removes charge as well as dust from the bags during cleaning. When a neighboring row of bags is pulse-cleaned, the shift in bag charge is opposite to what it is when the monitored bag's row itself is pulse-cleaned.
4. Air flow alone produces only small cage voltages. With the addition of flyash to the air flow (4 grains/acfm), the cage voltage increases significantly in magnitude and changes sign.

Further exploration of the relationship between electrostatic charge buildup and the resultant cage voltage is one of the two major purposes of this paper and is discussed next. Following that, the final section of the paper relates these cage voltages to fabric filtration performance, the second major purpose of the paper.

## ELECTRICAL EQUIVALENT CIRCUIT

The measurement of static charges on insulators is most often performed by an inductive technique such as the Faraday "pail" method [Reference 11]. In such methods the insulator charges are not required to move but merely to terminate their lines of force on charges induced in an adjacent conducting surface. Since that surface is a conductor, these induced charges can be measured by direct coupling to a conventional electrometer and a measure of the insulator charge is obtained even though no direct contact to it is established.

In the baghouse apparatus employed here, the electrically conductive cage serves as the "adjacent surface" used to detect the charges on or in the fabric. The cage, however, is more than adjacent; it actually makes direct contact with the fabric as well so that the possibility also exists for direct charge flow from the fabric to the cage.

A similar relationship couples the cage charge to the baghouse housing which is electrically grounded. Consequently, at a minimum, the electrical equivalent circuit should consist of two capacitors and resistors in series as sketched in Figure 3.



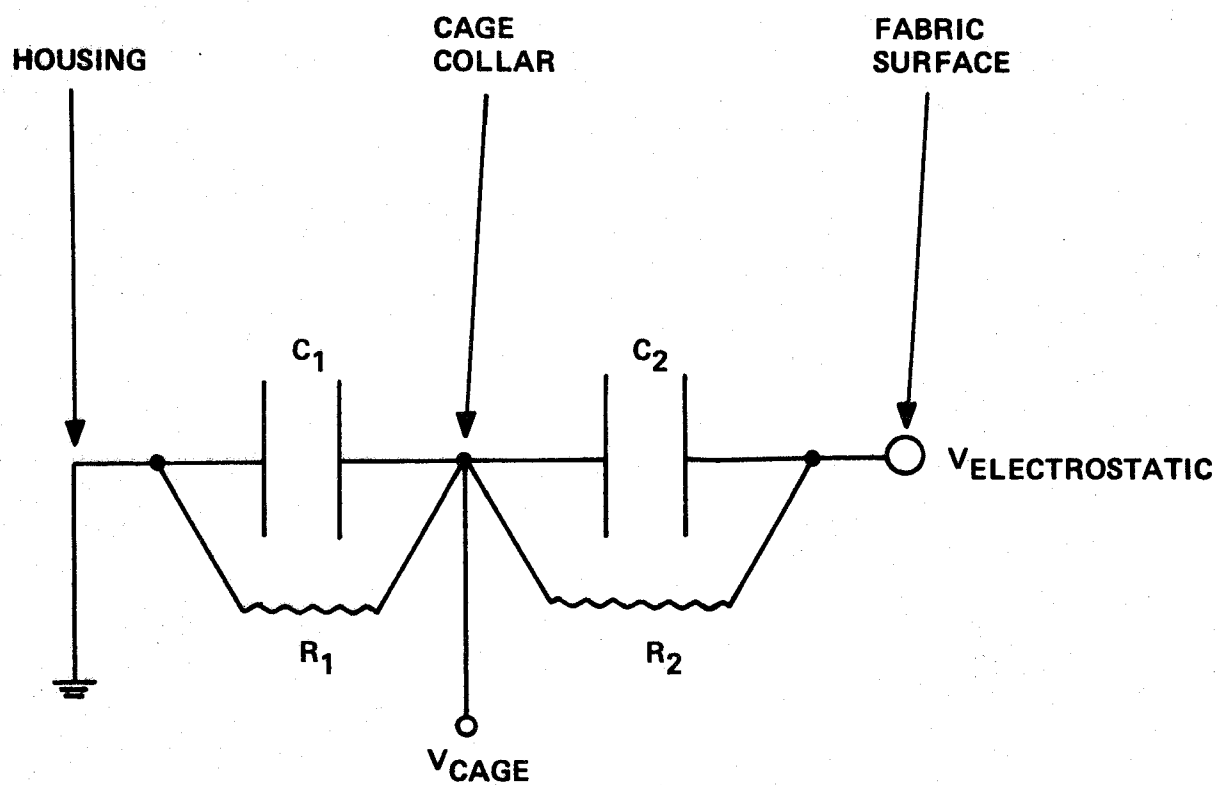


FIGURE 3. BASIC ELECTRICAL EQUIVALENT CIRCUIT

The forcing function,  $V_{\text{Electrostatic}}$ , represents the voltage created by two separate actions:

1. the electrostatic charge generated on the fabric by the dust flow, and
2. the fabric motion during the pulse-cleaning of each row of bags.

If electrostatic charge generation is proportional to gas flow through the bag, this contribution to the forcing function could take on a form such as illustrated in Figure 4. This plot, reproduced from Reference 12, is the calculated gas flow through one bag of a specific pulse-jet baghouse. This calculation is for a 4 x 4 matrix of bags but shows the variation of gas flow to be expected in a pulse-jet baghouse in general. The rapid rise in flow coinciding with the cleaning pulse comes about because of the low flow resistance of a freshly cleaned bag--a bag with little or no filter cake in place. As the cake rebuilds on the cleaned bag, the air flow through it decreases rapidly until the adjacent row is cleaned. The rapid increase in gas flow through this neighboring bag causes a corresponding rapid decrease in flow through the monitored bag which subsequently recovers as the flow through the just cleaned row decreases. And so on for the remaining rows in the baghouse until the monitored bag is pulse-cleaned again.

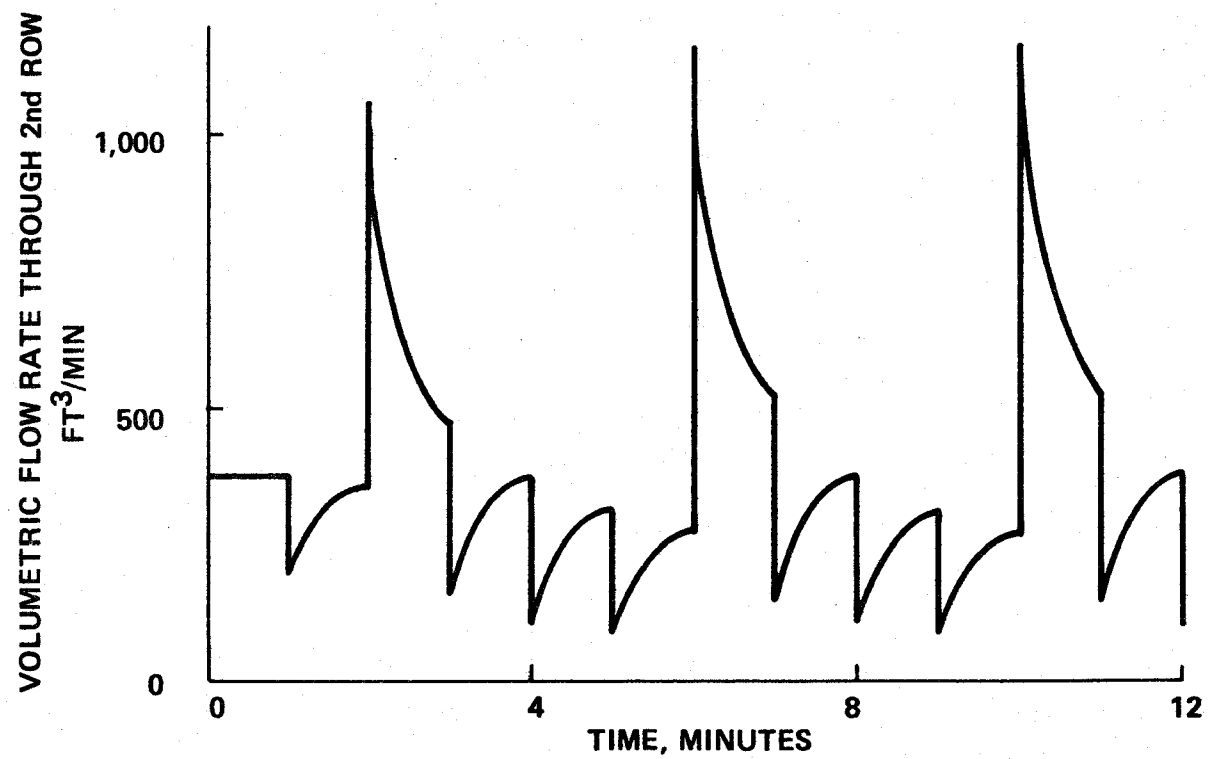


FIGURE 4. GAS FLOW RATE THROUGH ONE BAG OF A FOUR-ROW PULSE-JET ARRAY (REF. 12)

Even without a charge generation function of the form illustrated in Figure 4, the pulse-cleaning action should induce a voltage spike on the cage--simply because of the bag motion during the cleaning. Charge in or on the fabric undergoes a change in position and hence in capacitive coupling to the cage when the bag is pulse-cleaned. This action alone causes a cage voltage spike. In addition the cleaning action can cause a change in the bag charge; the net bag charge may be changed because of the dust removed by the cleaning action.

The cage voltage, therefore, depends upon a number of variables which are not well defined or easy to measure. While the initial simulation of the cage voltage is being carried out with the simple circuit of Figure 3, additional elements, as illustrated by the distributed resistances and capacitances sketched in Figure 5, seem more realistic and will be added as necessary.

Once having settled upon an adequate equivalent circuit, the problem becomes one of accurately describing the forcing function. Many variables could influence the form of the forcing function so that selecting a realistic representation may be neither trivial nor obvious. Further experimentation will be carried out in order to further define its dependencies.

Various combinations of equivalent circuits and forcing functions are now being studied on an Electronics Associates 380 analog computer as preliminary work in the development of a quantitative model.

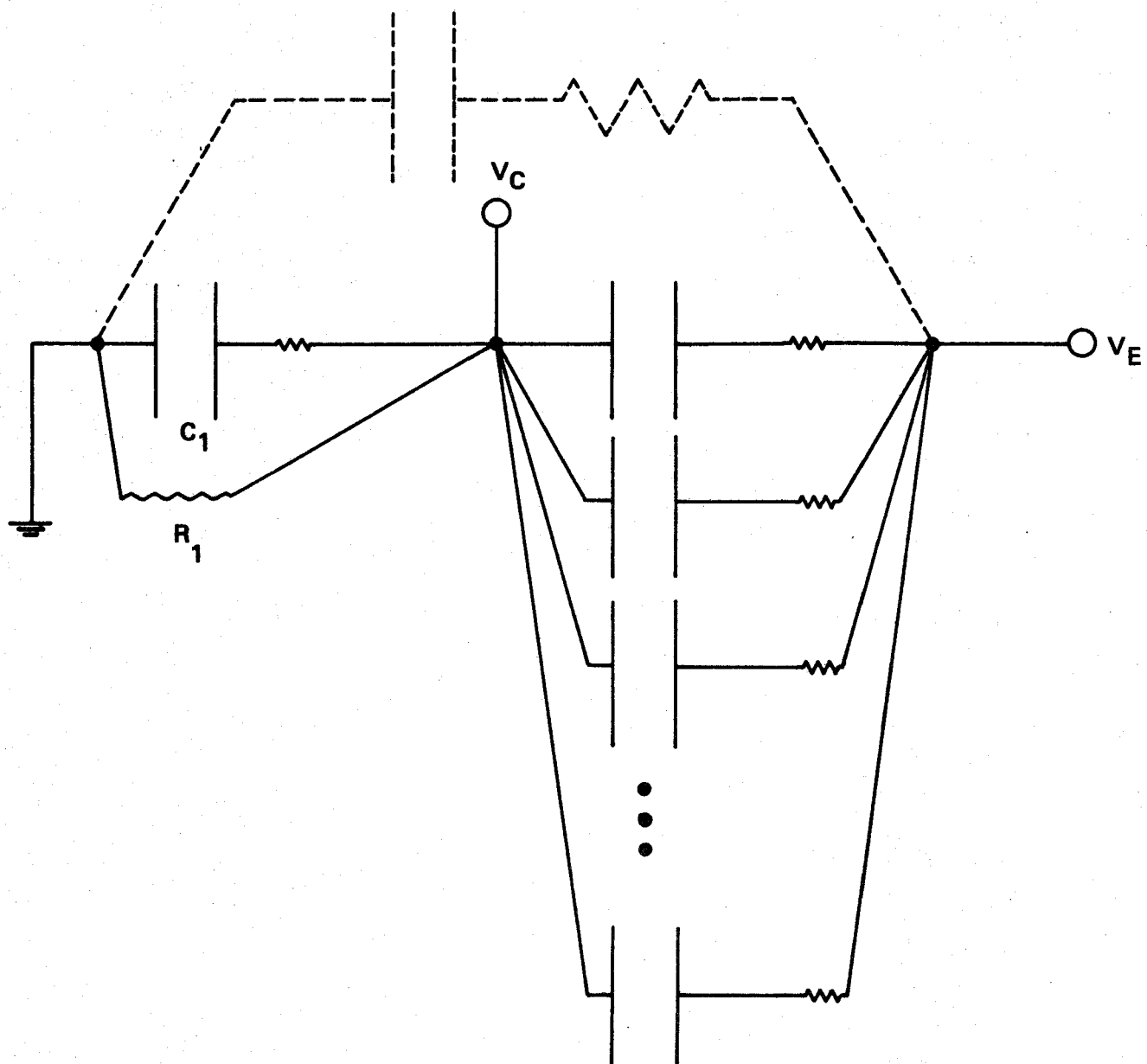


FIGURE 5. MODIFIED EQUIVALENT CIRCUIT CONTAINING DISTRIBUTED COMPONENTS

## RELATIONSHIP BETWEEN FABRIC ELECTROSTATIC PROPERTIES AND COLLECTION EFFICIENCY

Ultimately, interest in the electrostatic properties of a dust/fabric system depends upon the relationship between these electrostatic properties and the performance of the fabric as a filter for the dust. If electrostatics exert little or no influence upon filtration performance, interest in the electrostatic properties of fabric filters will diminish rapidly and rightly so. If, however, electrostatics are important or are important under certain conditions, this information should be better known and increased study of the interaction is warranted.

Evidence is slowly accumulating to suggest that electrostatic interactions can be important second or even first order effects in fabric filtration performance [Reference 9]. Some additional data to further support the significance of electrostatic properties are presented in this section. Both the data reported here as well as those in Reference 9 are based on fabric filtration systems in which the major filtration action comes from conventional, high performance fabric filters--those which conventionally filter with collection efficiencies on the order of 99+%. Variation in the electrostatic properties of the dust/fabric system has

been shown in Reference 9 to alter the operating costs of filtration (by varying the time required between fabric cleaning cycles; i.e., by influencing the drags and specific cake resistance during filtration). In this work we show what we interpret to be an electrostatic influence upon dust cake formation with its attendant effect upon dust collection efficiency.

#### Collection Efficiency Experiment

The relationship between electrostatic properties and collection efficiency suggested itself from independent routine laboratory evaluation of various fabric filters [Reference 13]. In comparing the collection efficiency of an experimental Nomex felt with that of a standard Nomex fabric not having gone through the special heat treatment associated with the preparation of the experimental Nomex, a correlation between the observed electrostatic properties and the collection efficiency was noted. The experimental Nomex bags exhibited very high cage voltages during filtration--the highest values seen in our measurements.

At the same time, they filtered redispersed flyash with uncharacteristically low collection efficiency (~97%). Conventional Nomex felt bags routinely filter this dust source with efficiencies in excess of 99%. The fabric manufacturer (DuPont) expressed surprise at this result and cited his own measurements of collection efficiency in which similarly prepared experimental Nomex bags and comparable-weight standard Nomex bags performed similarly when filtering cement dust. Both filtered cement dust with collection efficiency in excess of 99%.

The thought occurred to us then that the significantly different cage voltage noted on the experimental Nomex was perhaps related to the fabric performance as a filter. The reason for the high cage voltage was hypothesized to be the result of the heat treatment associated with the preparation of these experimental fabrics.\* During the preparation of these fabrics, the fibers are exposed briefly (2-3 min) to a temperature of about 315°C (600°F). This heat treatment probably volatilizes the anti-static coatings normally found on Nomex, rendering the fabric electrical resistance much higher than before the treatment. As can be seen from the equivalent circuits proposed in the previous sections, increasing the resistance between the cage and ground ( $R_1$  in Figure 3) increases the magnitude of  $V_{\text{Cage}}$ , assuming all other parameters, including the charge generation function,  $V_E$ , remain constant.

In order to verify the role of the anti-static coating, two new sets of fabric filters were prepared:

1. The first was the control group, prepared as before, including the heat treating step.
2. The second group was identical to the first except that all bags were sprayed with an anti-static coating after the heat treatment.

---

\*This hypothesis was originated by Dr. H. Forsten, E. I. duPont de Nemours and Company, Wilmington, Delaware.



Table 1 lists the manufacturer's description of the two test fabrics. The fabrics are nominally identical except for the anti-static coating of the second fabric.

### Results

Electrostatically the two test fabrics, not surprisingly, are not identical. The control bags exhibited cage voltage spikes in excess of 1000 volts, while the maximum cage voltage of the coated bags was about 50 volts. While not the actual voltage traces recorded on these test bags, the traces contrasted in Figure 2 correspond roughly to those recorded on the test bags, Figure 2a representing the coated bag and Figure 2b, the control.

Table 2 summarizes the measurements of collection efficiency and outlet concentration. The important conclusion from the data of Table 2 is that the addition of the anti-static coating (Run No. 1) improved bag collection efficiency over that of the uncoated control bag (Runs No. 2 and 4). The run numbers correspond to the chronological order in which the measurements were made. When the measurements are made on the same fabric, the run number tells the order in which the run was made. (In Table 2, Run 4 followed Run 3 which followed Run 2--all on the same set of bags.)

Increasing the relative humidity from 50% to 70% improved collection efficiency even more (Run No. 3). At 70%, relative humidity, the cage voltage changes its character significantly from that at 50% relative humidity (Figure 2b). The voltage spikes associated with the cleaning pulse are reduced in magnitude to the order of

**TABLE 1**  
**EXPERIMENTAL NOMEX TEST BAGS\***  
**(SCRIMLESS FELTS)**

	<u>BAG SET 1 (CONTROL)</u>	<u>BAG SET 2 (CONTROL + ANTI-STATIC COATING)**</u>
<b>BASIS WEIGHT</b> (oz./yd. <sup>2</sup> )	17.0	17.4
<b>THICKNESS</b> (mils)	93	89
<b>AIR PERMEABILITY</b> (cfm/ft <sup>2</sup> at 0.5 in. H <sub>2</sub> O)	12	17

\*Courtesy of H. Forsten, E. I. du Pont

\*\*Sprayed with 1% "Avitex" DN

**TABLE 2**  
**BAG PERFORMANCE SERIES**

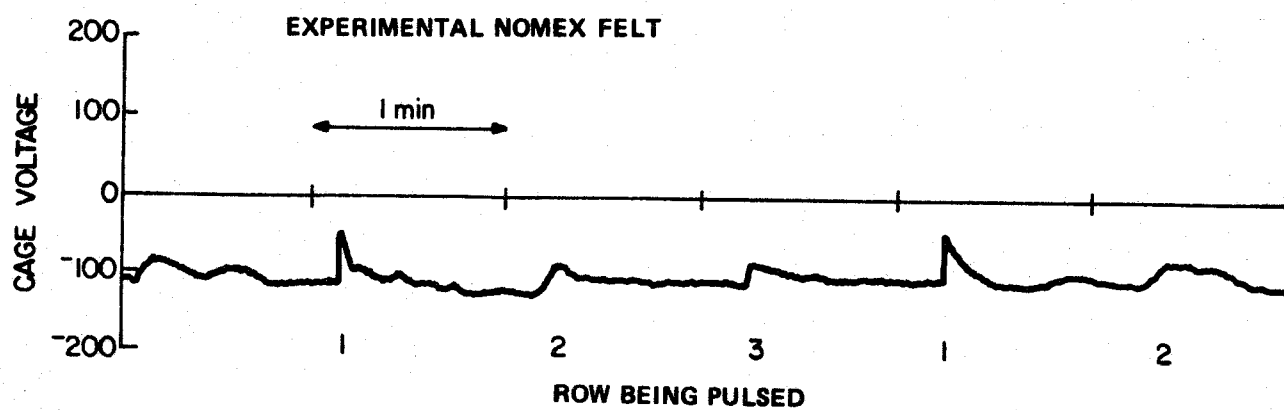
<u>RUN NO</u>	<u>FABRIC</u>	<u>COLLECT. EFF. (%)</u>	<u>OUTLET CONC. (GRAINS/10<sup>3</sup> ft<sup>3</sup>)</u>	<u>BAG PRESSURE CHANGE DURING ONE FILTRATION CYCLE (in. H<sub>2</sub>O) (<math>\Delta P_i - \Delta P_f</math>)</u>
1	CONTROL WITH ANTI-STATIC COATING (50% RELATIVE HUMIDITY)	98.7*	44.6*	0.50 (3.15 - 3.65)
2	CONTROL ALONE (50% RELATIVE HUMIDITY)	97.1	118	0.20 (2.80 - 3.00)
3	CONTROL ALONE (70% RELATIVE HUMIDITY)	99.3	28.2	0.20 (2.80 - 3.00)
4	CONTROL ALONE (50% RELATIVE HUMIDITY)	96.8	128	0.15 (3.55 - 3.70)

\*Average of two runs, 2 days apart

50-70 volts (Figure 6). What also differentiates this cage voltage trace from that of Figure 2a is the relatively high steady state voltage evident in Figure 6. The cage signal in Figure 6 is still better isolated electrically from ground than that in Figure 2a. Whatever else the high relative humidity does, it seems not to degrade  $R_1$  in the elementary equivalent circuit of Figure 3.

These data immediately suggest that a negative cage bias is a desirable operating condition. Such a bias could be externally applied to the cage via the same leads previously used to monitor the cage voltage. The effectiveness of such a bias depends upon the values of  $C_2$  and  $R_2$  (Figure 3) of any given fabric/dust system, since the voltage appearing at the physically poorly-defined  $V_{\text{Electrostatic}}$  terminal of Figure 3 is most likely what the dust being filtered will sense.

Any improved collection efficiency anticipated for operation with a negative bias on the cage did not materialize (Table 3). A bias of -2000 volts applied to all nine cages through a  $10^9$  series resistor produced a cage voltage trace as shown in Figure 7. The Row 3 cleaning pulse appears to be less effective than those of Rows 1 and 2, as indicated by the smaller voltage spike associated with its firing. This condition was also evident in some of the data presented in Reference 10, and was attributed to blow pipe misalignment, pressure leaks, or some other condition not involving electrostatics.



**DUST FEED RATE:  $9 \text{ g/m}^3$  (4 grains/ft<sup>3</sup>)**

**AIR/CLOTH: 3 cm/sec (6 fpm)**

**PULSE PRESSURE:  $0.62 \text{ N/mm}^2$  (90 psi)**

**RELATIVE HUMIDITY: 70%**

**FIGURE 6. CAGE VOLTAGE DURING FLY ASH FILTRATION AT HIGH RELATIVE HUMIDITY**

**TABLE 3**

**CONTROL BAG PERFORMANCE UNDER CAGE ELECTRICAL BIAS  
(ALL RUNS AT 50% RELATIVE HUMIDITY)**

<u>RUN NO.</u>	<u>CAGE BIAS</u>	<u>COLLECTION EFF. (%)</u>	<u>OUTLET CONC. (GRAINS/10<sup>3</sup> ft<sup>3</sup>)</u> <sup>7</sup>	<u>BAG PRESSURE CHANGE (in. H<sub>2</sub>O) (<math>\Delta P_i - \Delta P_f</math>)</u>
315 6	FLOATING	96.6	136	0.28 (4.52 - 4.80)
7	GROUNDING	98.1	75.9	0.18 (4.23 - 4.41)
8	- 2000 VOLTS	97.6	97.0	0.17 (4.14 - 4.31)

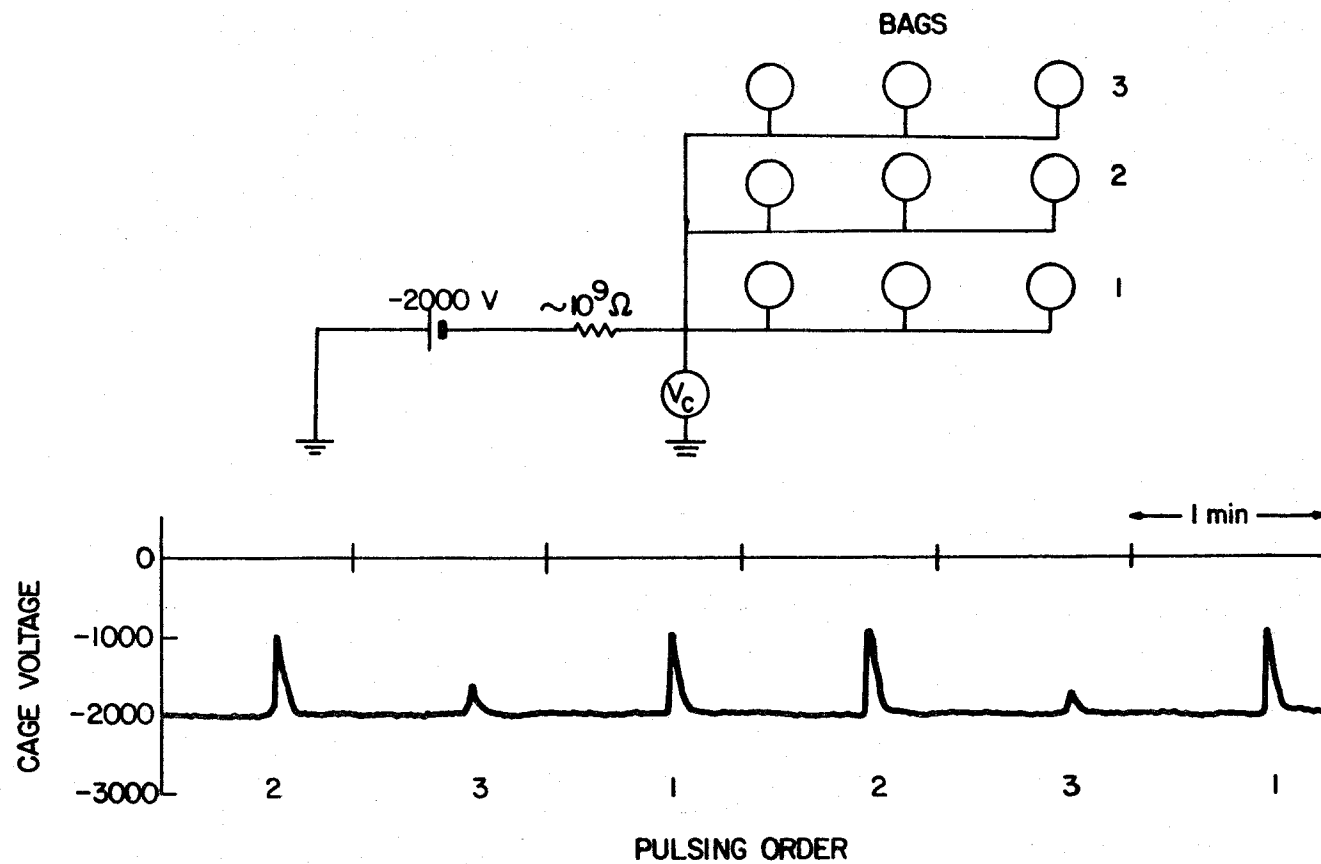


FIGURE 7. CAGE VOLTAGE UNDER AN EXTERNAL BIAS OF -2000 VOLTS

Table 3 shows that the presence of this electrical bias doesn't significantly alter the collection efficiency of the bags--at least not nearly as significantly as the higher humidity operation did (Run 3, Table 2). The opposite polarity (+2000 volts on the cage) also produced no significant change in collection efficiency.

In spite of this low sensitivity to bias levels, cage electrical termination is important as the data of Table 4 show. Low resistance terminations to the cages are superior to the high resistance, floating termination; that is, filtration performance with various cage electrical terminations (Table 4) shows that controlling the electrical termination of the cage does influence filtration performance. These data show that the coupling between the fabric charges (the  $V_E$  terminal, Figures 3 and 5) and the cage is strong enough to allow different cage terminations to influence enough of the active filtering surface as to be detectable by the measurement of collection efficiency. Having the bags tied together electrically (Run 6, Table 4) does not produce a significant change in performance from operation with each bag electrically floating alone (Run 4, Table 4).

The conclusion from the termination and bias data of Tables 3 and 4 is that having a low leakage path for the electrostatically generated cage charges is more important than any arbitrary cage voltage level. Operating with the cage at high electrical isolation from ground degrades collection efficiency. Reducing the cage electrical isolation (whether by humidity, conductive fabrics or



**TABLE 4**  
**CONTROL BAG PERFORMANCE AT VARIOUS CAGE ELECTRICAL TERMINATIONS**  
**(ALL RUNS AT 50% RELATIVE HUMIDITY)**

<u>RUN NO.</u>	<u>CAGE ELECTRICAL TERMINATION</u>	<u>COLLECTION EFF. (%)</u>	<u>OUTLET CONC. (GRAINS/10<sup>3</sup> ft<sup>3</sup>)</u>	<u>BAG PRESSURE CHANGE DURING ONE FILTRATION CYCLE (in. H<sub>2</sub>O) (<math>\Delta P_i - \Delta P_f</math>)</u>
318 4	FLOATING	96.8	128	0.15 (3.55 - 3.70)
5	GROUNDED *	97.9	83.8	0.15 (3.55 - 3.70)
6	FLOATING *	96.6	136	0.28 (4.52 - 4.80)
7	GROUNDED *	98.1	75.9	0.18 (4.23 - 4.41)

\*All nine bags tied together electrically.

direct contact to ground) produces superior performance with respect to dust collection efficiency.

Charge generation is also part of the overall effect and the influence of each of these "corrective" actions upon charge generation is not so clear as their effects upon cage electrical isolation. The total problem, therefore, has only been partially considered; the influence of these variables upon  $V_E$  is yet to be determined.

#### Polyester Felt Experiment

To better establish the tentative relationship illustrated by the measurements made on the experimental Nomex fabrics described in the preceding sections, the experiment was repeated on two sets of felted polyester bags. Both of these sets of needled Dacron felt bags have nominal properties as listed in Table 5.

What has been previously shown is that a bag of high electrical resistance and relatively low collection efficiency can be converted into a bag of lower electrical resistance and higher collection efficiency by spraying the bag with an anti-static coating prior to the filtration tests.

With the two sets of polyester bags (Table 5) the bag electrical properties were changed in the opposite direction to that of the Nomex experiment. Initially both sets of bags have been manufactured with anti-static coatings, the standard procedure. With one set of bags this anti-static coating was removed, at least partially, by repeated soaking (no agitation) in perchloroethylene. Bag resistance increased as a result of this soaking, presumably because of coating removal.

**TABLE 5**  
**PROPERTIES OF NEEDLED POLYESTER FELT FABRIC\***

<b>WEIGHT (oz/yd<sup>2</sup>)</b>	<b>16.0</b>
<b>THICKNESS (mils)</b>	<b>58.0</b>
<b>AIR PERMEABILITY (cfm/ft<sup>2</sup> at 0.5 in. H<sub>2</sub>O)</b>	<b>25.9</b>

**\*Measurements by FRL, an Albany International Co., Dedham, MA**

Table 6 shows that the bags from which the anti-static coating has been removed filter less efficiently than those standard bags on which it remains.

This result corroborates the results of the experimental Nomex bag, linking the bag electrical resistance to its filtration performance. The cage voltage of the soaked polyester felt bags was, perhaps, an order of magnitude greater than what has been seen on standard polyester felt bags (Figure 2a). The lone voltage trace made with the soaked polyester bags was noisier than typical but the magnitude of the primary voltage spikes was about 500 volts, as compared with 50-70 volts usually seen on the standard polyester felt bag.

TABLE 6

## FILTRATION PERFORMANCE OF THE TEST POLYESTER FELTS

<u>FABRIC TESTED</u>	<u>ELECTRICAL RESISTANCE OF MOUNTED BAGS (ohms)</u>	<u>COLLECT. EFF. (%)</u>	<u>OUTLET CONC. (GRAINS/10<sup>3</sup> ft<sup>3</sup>)</u>	<u>BAG PRESSURE CHANGE DURING ONE FILTRATION CYCLE (in. H<sub>2</sub>O) (<math>\Delta P_i - \Delta P_f</math>)</u>
STANDARD POLYESTER FELT	10 <sup>8</sup> - 10 <sup>9</sup>	99.8	6.9	0.10 (1.50 - 1.60)
STANDARD POLYESTER FELT AFTER MULTIPLE SOAKS IN PERCHLOROETHYLENE	$\geq 10^{10}$	97.2	111	0.10 (2.60 - 2.70)

## CONCLUSIONS

1. Bag collection efficiency is highest when:
  - a) Relative humidity is high (70% is better than 50%).
  - b) Fabric resistance is low ( $10^8$  ohms is better than  $10^{10}$  or  $10^{11}$  ohms).
  - c) The cage is electrically grounded (grounded cage is better than floating).
2. These conclusions are valid only for the redispersed flyash used in these experiments and over the specified range of the variables considered, but they show that electrostatic properties can be important in fabric filtration.

## ACKNOWLEDGMENT

Dr. Herman H. Forsten, Textile Research Laboratory, E. I. duPont de Nemours and Company, Wilmington, Delaware, provided advice and assistance in our attempts to relate the cage voltage measurements to the collection efficiency of flyash. He arranged for the fabrication of the Nomex test bags which were donated by DuPont. He also advised us on methods for removing the anti-static coating from the Dacron felts.

## REFERENCES

1. Rudge, W. A. D., "On the Electrification Produced during the Raising of a Cloud of Dust," Proceedings of the Royal Society, Vol. XC-A, pp. 255-272, 1914.
2. Deodhar, G. B., "Electricity of Dust Clouds - Part I," Institute of Physics and the Physical Society. Proceedings of the Physical Society, Vol. 39, pp. 243-249, 1927.
3. Kunkel, W. B., "The Static Electrification of Dust Particles on Dispersion into a Cloud," Journal of Applied Physics, Vol. 21, pp. 820-832, 1950.
4. Kraemer, H. F. and H. F. Johnstone, "Collection of Aerosol Particles in Presence of Electrostatic Fields," Industrial and Engineering Chemistry, Vol. 47, No. 12, pp. 2426-2434, 1955.
5. Rossano, A. T., Jr. and L. Silverman, "Electrostatic Mechanisms in Fiber Filtration of Aerosols," Report No. NYO-1954, Harvard School of Public Health, 1955.
6. Rao, K., S. T. Ariman, K. T. Yang and R. L. Hosbein, "Collection of Dust by Fabric Filtration in an Electrostatic Field," 2nd Annual Environmental Engineering and Science Conference, Louisville, April 1972.
7. Makino, E., K. Iinoya, M. Shibamoto, S. Toyama, and F. Ikazaki, "Experiments on Electrical Dislodging of Dust Layers," Trans. Japan Chemical Engineers Society, Vol 2, No. 1, pp. 31-37, 1976.
8. Frederick, E. R., "How Dust Filter Selection Depends on Electrostatics," Chemical Engineering, pp. 107-114, June 26, 1961.
9. Penney, G. W. and E. R. Frederick, "Electrostatic Effects in Fabric Filtration, final report for EPA Research Grant No. R803020, in preparation.
10. Donovan, R. P., R. L. Ogan, and J. H. Turner, "Electrostatic Effects in Pulse-Jet Fabric Filtration of Room Temperature Flyash," presentation to the Engineering Foundation Conference, "Theory, Practice and Process Principles for Physical Separations," Asilomar Conference Grounds, Pacific Grove, California, October 30 - November 4, 1977.
11. Hersh, S. P., "Resistivity and Static Behavior of Textile Surfaces," Chapter 6 in Surface Characteristics of Fibers and Textiles, Part 1, edited by M. J. Schick, Marcel Dekker, Inc., 270 Madison Avenue, New York, N. Y. 10016 (1975).



#### REFERENCES (Continued)

12. Theodore, L., J. Reynolds, A. Corvini, and A. Buonicore, "Particulate Control by Pulsed-Air Baghouse Filtration: Describing Equations and Solution," pp. 90-103 in The User and Fabric Filtration Equipment II, APCA Specialty Conference Proceedings, Buffalo, New York, October 1975, Air Pollution Control Assn., 4400 Fifth Avenue, Pittsburgh, PA 15213 (1975).
13. Turner, J. H., "EPA Research in Fabric Filtration: Annual Report on IERL-RTP In-house Program," EPA-600/7-77-042 (NTIS No. PB 267441/AS), May 1977.

## APPENDIX

### CONVERSION FACTORS

<u>To Convert From:</u>	<u>To:</u>	<u>Multiply By:</u>
foot <sup>2</sup>	meter <sup>2</sup>	$9.29 \times 10^{-2}$
inch <sup>2</sup>	meter <sup>2</sup>	$6.45 \times 10^{-4}$
yard <sup>2</sup>	meter <sup>2</sup>	$8.36 \times 10^{-1}$
lb (force)	newton	4.45
foot	meter	$3.05 \times 10^{-1}$
inch	meter	$2.54 \times 10^{-2}$
mil	meter	$2.54 \times 10^{-5}$
yard	meter	$9.14 \times 10^{-1}$
grain	kilogram	$6.48 \times 10^{-5}$
lb (mass)	kilogram	$4.54 \times 10^{-1}$
inch of water (60°F)	newton/meter <sup>2</sup>	$2.49 \times 10^{+2}$
lb/inch <sup>2</sup> (psi)	newton/meter <sup>2</sup>	$6.89 \times 10^{+3}$
lb/foot <sup>2</sup>	newton/meter <sup>2</sup>	$4.79 \times 10^{+1}$
foot/min (fpm)	meter/sec	$5.08 \times 10^{-2}$
foot <sup>3</sup>	meter <sup>3</sup>	$2.83 \times 10^{-2}$
inch <sup>3</sup>	meter <sup>3</sup>	$1.64 \times 10^{-5}$
yard <sup>3</sup>	meter <sup>3</sup>	$7.65 \times 10^{-1}$
oz/yd <sup>2</sup>	kg/m <sup>2</sup>	$3.39 \times 10^{-2}$
grains/ft <sup>3</sup>	kg/m <sup>3</sup>	$2.29 \times 10^{-3}$
grains/1000 ft <sup>3</sup>	g/m <sup>3</sup>	$2.29 \times 10^{-3}$
°F	°K	$^{\circ}\text{K} = \frac{5}{9} (^{\circ}\text{F} + 459.67)$



## TEXTILE FILTER MEDIA DURABILITY

Winston F. Budrow

In reviewing the requirements for a textile filter media, three basic primary functions are generated. The first primary function of the filter media is to separate and collect suspended particulate matter from a gaseous stream and allow the cleaned gaseous stream to pass through.

As the filter media collects particulate matter, the fabric achieves a diminishing return in which the filter media will no longer pass air through it at an acceptable level. At this point, it becomes necessary to remove the collected particulate matter and regenerate the filtering qualities of the filter system. For this reason, cleanability becomes a primary function also. The filtering and cleaning qualities are referred to as a cycle. The cycles of filtering and cleaning must be performed in a repetitive fashion, as dictated by economic factors. Therefore, the third primary function is determined, that of durability. These three primary and equally important functions, namely: filterability, cleanability and durability, depict the filter media's ability to perform.

This paper concerns itself with the primary function of durability. Durability can best be defined as the resistance to the chemical and physical breakdown associated with fabric filtration.

The physical breakdown results generally from the filtering and cleaning functions, whereas the chemical breakdown results generally from the chemistry and thermo characteristics of the environment to which the filter media is being exposed.

Chemical breakdown of the filter media is the most common cause of *premature* fabric failure in filtration, primarily due to the fact that it is the least understood. Synthetic organic fibers are generated through chemical reactions to form the polymer phase from the monomer phase. In chemistry, chemical reactions yield the resultant, which indicates the reactions are reversible. There lies the weak link in fabric technology. Any substance or condition which tends to reverse or break down the polymer structure of the fiber will cause premature deterioration of the filter fabric.

In most filtration systems, the one critical ingredient which activates the chemistry of the dust and the gases is moisture. Normally, dust materials, when in a dry phase or void of moisture, are relatively inactive; whereas, in the wet phase or presence of moisture, the dust material or gases are liquified and

become chemically very active and attack the fiber structure, either through a direct reaction or a catalytic reaction. Moisture in itself can cause damage to certain filter media through hydrolysis or oxidation. These reactions can be catalyzed or accelerated due to the presence of an acid condition, alkaline condition and/or temperature elevation.

To combat deterioration situations, a proper fiber selection most resistant to the environmental conditions is the first primary step. Secondly, by understanding the potential chemical activity of the gases and the dust, one can establish the necessary controls and precautions to be taken for prolonging the durability of the filter media.

Physical breakdown of the filter media presents a different type of fiber fatigue or destruction. All fiber filter media will, of course, fail at some point due to use; however, it is the extension of the physical breakdown which is of concern to us.

Normal physical filter media breakdown is the result of work performed. The work performed can be defined as the filtering actions, cleaning actions, and the stress strain associated with those functions.

The filtering phase is probably the most vulnerable to excess physical attack, due to the unpredictable aerodynamics of the air volume. The air volume in combination with the particulate matter enters the cylindrical filter bag at high velocities. If the entry is not perpendicular, dust impingement occurs and gives a sand blasting effect, resulting in premature failure. Even when the dust entry is perpendicular to the bag, however, attack will occur if the bag is not properly installed. An improperly installed bag will result in fabric deformation which allows folds or pleats to be contacted by the high velocity dust, resulting in the same premature failure.

Naturally, many forms of excessive physical attack can occur due to the variety of baghouse designs, filter media types and applications. The important message concerning fabric premature deterioration is to detect the condition and correct the situation.

In summary, durability is a primary function of filter media performance and is the most important subject for proper economical baghouse performance. Filter media life or durability can be substantially extended in most systems by a complete investigation and evaluation of filter media which could yield substantial savings in both the cost of the filter media and the operating costs involved with baghouses.

## HIGH-TEMPERATURE FILTRATION

Dr. Dennis C. Drehmel  
U.S. Environmental Protection Agency  
Research Triangle Park, N.C. 27711

Michael A. Shackleton  
Acurex Corporation  
Mountain View, Calif. 94042

### Abstract

Research on high temperature particle control using ceramic fiber barrier filtration has shown this technique offers promise of successful development. Results of testing of rigid ceramic membrane structures and of ceramic fiber beds including woven, paper and felt ceramic filters are presented.

## HIGH-TEMPERATURE FILTRATION

### Introduction

Removal of particles from high temperature gas streams has been studied for many years. Some of the motivation for this research was the desire to operate coal fired gas turbines.<sup>1</sup> Recently there is renewed interest in the utilization of coal. The processes most actively being studied are pressurized fluid bed combustion (PFBC) and gasification combined cycle (GCC) plants. Both processes are called combined cycle since they generate power by means of gas turbines as well as steam turbines.

In the PFBC, coal is burned in a fluid bed of limestone (which removes the  $\text{SO}_2$ ) and heat is transferred to tubes in the fluid bed. Up to 80% of the recoverable heat value of the coal is removed in the fluid bed, and the gas exits at 1500°F and 10 atm pressure. The gas must now be expanded through a gas turbine to recover the remaining energy. However, previous investigations showed that large particles erode turbine blades and small particles cause deposits that choke the turbine. To protect the turbine, some high-temperature particulate control is required. Moreover, since it would not be economical to duplicate particulate control for environmental regulations at another point of the process, high-temperature control must also meet new source performance environmental standards for coal-fired utilities. Currently, this allows emissions to be no greater than 0.1 #/million Btu.

To meet both the environmental and turbine requirements, a system consisting of two cyclones and a filter is being studied. The two cyclones lower the overall particle concentration but fail to remove small particles. Concentrations leaving the second cyclone can be as high as 1.0 grains/scf and have a mass median diameter of 5.0  $\mu\text{m}$ . The filter can be a ceramic bag filter, a ceramic membrane, or a granular bed.

Research to date has concentrated on the granular bed since it has been considered available technology. However, results of tests at the Exxon PFBC Miniplant have been disappointing.<sup>2</sup> The granular beds tested could barely meet the environmental standard at the beginning of a run and lost efficiency continuously from 95% to as low as 50% within 24 hours. Although granular bed filters may still prove to be a solution to high-temperature particle control, it is now apparent that they will require more developmental work.

Alternative high-temperature filters, using either a ceramic bag or ceramic membrane, are being developed. The remainder of this paper will be devoted to describing ongoing work by the Environmental Protection Agency to assess these high-temperature filters as part of environmental control for the PFBC, although it is expected that results can be extrapolated to the GCC or to high-temperature metallurgical operations.

#### Ceramic Membrane Filters

Several ceramic materials in many configurations were screened as possible high-temperature filters. One of the most promising materials tested was a ceramic cross flow monolith produced by 3M Company under the trade name of Therma-Comb. This material is composed of alternate layers of corrugations separated by thin filtering barriers. This type of configuration affords a large amount of filter surface in a very small volume. Figure 1 shows a piece of this material illustrating the construction.

Bench side experiments were conducted in the high-temperature ceramic test facility at 970°K. Provisions were made to blow back from the clean side and also down the channels on the dirty side so that various cleaning schemes could be investigated. A sequencer was designed to automatically start and operate the cleaning cycle. A 17 cm diameter by 38 cm deep tubular furnace was used to heat the filter. An additional furnace was added to preheat the dust-laden air.



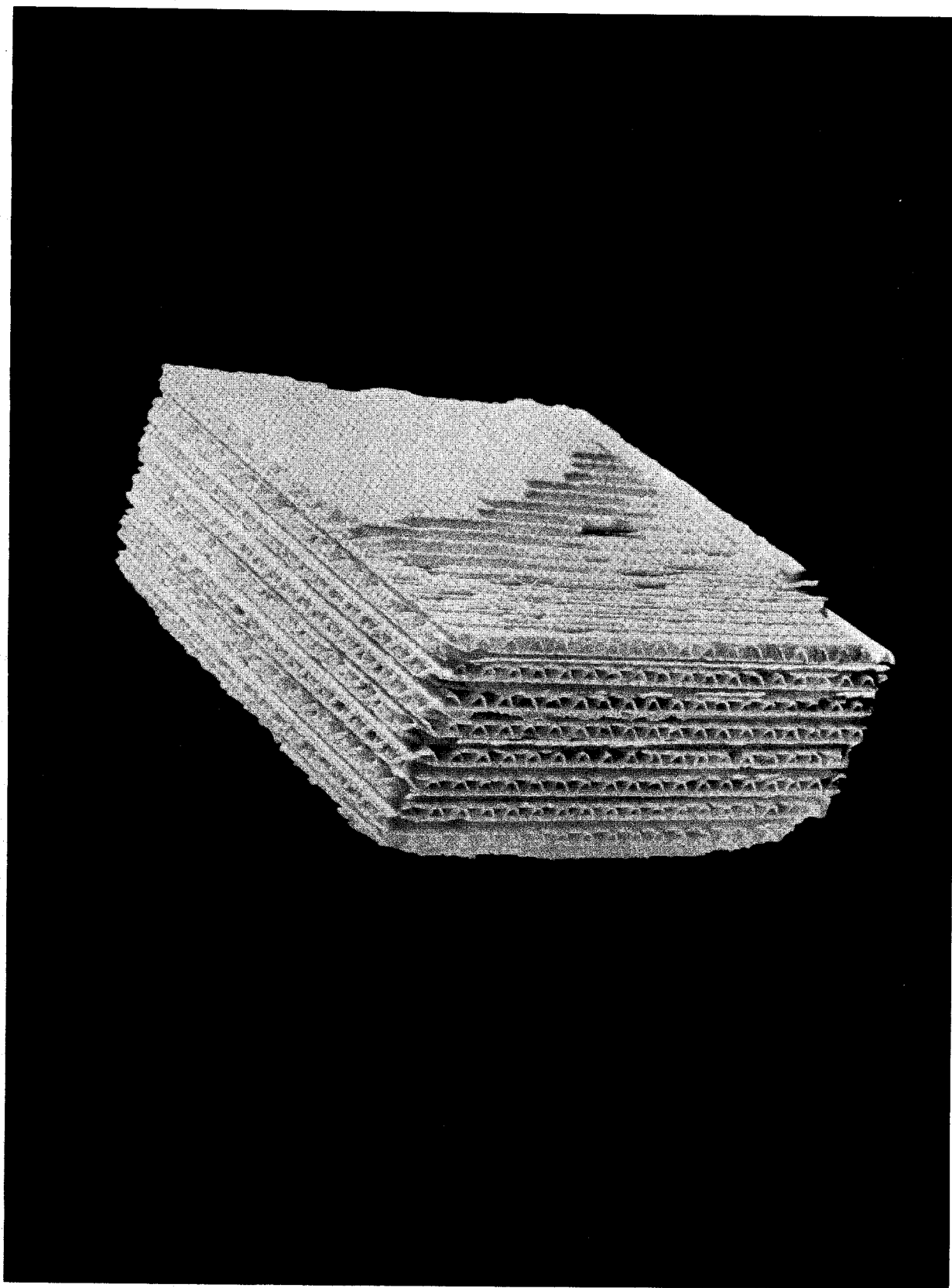


Figure 1. 3-M Company Thermacomb.

Cascade impactors were used to determine the size distribution of the test dust (limestone). The typical mass median diameter was 1.4  $\mu\text{m}$  and the geometric deviation was 3.0  $\mu\text{m}$ . There was some difficulty in maintaining constant feed rate, but dust loadings were maintained at levels from 2  $\text{gm}/\text{m}^3$  to 7  $\text{gm}/\text{m}^3$ .

Typical results for filtering the limestone test dust with the 3M ThermaComb are summarized in Table 1. Table 2 shows the effect of varying the initial pressure of a 0.6-second pulse. Table 2 also shows the result of a similar set of runs except that the pulse time was increased from 0.6 seconds to 5 seconds. These data show that the length of the pulse does not have much effect on the cleaning results. In both runs the collection efficiency was very high (99.6 to 100%) at a linear velocity of 0.41 m/min (1.33 ft/min). Using the 103.4 kPa pressure pulse for cleaning, it was possible to return to a stable pressure drop across the filter in spite of the relatively high dust loadings which in these two runs were 2.6 and 3.75  $\text{gm}/\text{m}^3$ .

Tests using the 3M ThermaComb as a filtering media showed filtering efficiency to be close to 100% even though the test dust had a mass median diameter of 1.4  $\mu\text{m}$  and a significant fraction of sub micron material. Cleanability of the media was verified in experiments evaluating the effect of cleaning pulse intensity and duration. It was determined that the ceramic filter behaved similarly to fabric filters in that the pressure drop could be attributed to a residual pressure drop and that across an incompressible cake.

#### Ceramic Fiber Barrier Filters

Ceramic fibers are produced by several manufacturers. In general, these materials are sold for refractory insulation applications. Many of these ceramic fiber materials are produced in smaller fiber diameters (3  $\mu\text{m}$ ) than are generally

Table 1. Summary of 3M ThermaComb Performance

	<u>Average</u>	<u>Range Tested</u>
Flow rate $\text{m}^3/\text{min}$	0.095	0.04 - 0.16
Filter area $\text{m}^2$	0.0227	-
Inlet/Concentration $\text{gm}/\text{m}^3$	3.6	2.2 - 5.4
Temperature $^{\circ}\text{K}$	990	953 - 1088
Efficiency Percent	96.6	85 - 99.6

Table 2. Effect of Changing Cleaning Conditions

<u>Test Number</u>	<u>Pulse Pressure KPa</u>	<u>Pulse Duration seconds</u>	<u>Cycle Time* minutes</u>	<u>Residual Pressure Drop KPa</u>
1	34.5	0.6	2 - 4	3.5 increasing to limit
1	69.0	0.6	8	3.0 increasing to limit
1	103.4	0.6	12 - 20	2.8
2	103.4	0.6	12	2.8
2	103.4	5	12	2.8

\*as required to lower pressure drop away from the upper limit

available for filtration applications at room temperature ( $20\ \mu\text{m}$ ). This smaller fiber diameter, coupled with high temperature and corrosion resistance characteristics, makes these fibers intriguing candidates for high-temperature filtration applications.

Available ceramic fiber configurations can be classified into the following three groups of materials:

- Woven structures - cloth woven from long-filament yarns of ceramic fibers
- Papers - Ceramic structures produced from short lengths of fibers, generally held together with binders.
- Felts - Structures produced to form mats of relatively long fibers. These materials are known as blankets in the insulation industry. They tend to be less tightly packed than conventional felt materials.

### Theory

Filtration theory supports the contention that ceramic fiber filters should perform adequately at high temperatures and pressures.

There are three particle collection mechanisms generally considered to account for the performance of a bed of fibers in removing particles from gas streams. These mechanisms are: direct interception, diffusion, and inertial impaction. Examining these mechanisms under high temperature and high pressure (800°C and 10 atm) indicates that direct interception and diffusion will be roughly the same as their performance at room temperatures and ambient pressures, while the inertial impaction mechanism will be slightly less effective at high temperatures and pressures. This statement is true when comparing the performance of a clean filter bed (no dust cake) at low temperature/pressure and at high temperature/pressure. This relatively minor performance reduction can be compensated for in the design of the filter media. For example, using smaller diameter fibers in the filter bed can increase collection efficiency far more than the viscosity effect of high temperature reduces it. A fiber bed consisting of 3  $\mu\text{m}$  diameter

fibers, as compared with 20  $\mu\text{m}$  fibers, can be expected to provide equal collection efficiency with a 3  $\mu\text{m}$  fiber bed weighing only one tenth as much on a weight per unit area basis. Figure 2 presents a calculated prediction of collection efficiency for a 3.0  $\mu\text{m}$  fiber bed, consisting of alumina fibers, collecting a 0.5  $\mu\text{m}$  fly ash particle from an air stream at 815°C and 10 atm pressure. The four curves show that for a decrease in solidity\* ( $\alpha$ ) a reduction in efficiency, for a given basis weight, should be expected. Similarly, an increase in airflow velocity causes a small reduction in collection efficiency for a given filter bed (constant basis weight). Note also that by adding fibers (increasing basis weight), all of these effects can be nullified.

The magnitude of predicted efficiency is also interesting. This analysis shows that for a ceramic fiber bed consisting of 3.0  $\mu\text{m}$  alumina fibers a basis weight of 500-600  $\text{g}/\text{m}^2$  should provide 80 to 90 percent collection of a 0.5  $\mu\text{m}$  particle even at the reduced performance levels encountered at high temperatures and pressures.

For comparison, a standard filter media consisting of 20  $\mu\text{m}$  fibers and having a basis weight of 540  $\text{g}/\text{m}^2$  (16  $\text{oz}/\text{yd}^2$ ) can be expected to collect only about 20 percent of 0.5  $\mu\text{m}$  particles at room ambient conditions. Thus, to provide collection efficiency performance equal to a conventional filter requires only about one-tenth the weight of fibers for a 3.0  $\mu\text{m}$  fiber bed. Or, put another way, a ceramic fiber bed of equal media weight to a conventional filter, but made from 3.0  $\mu\text{m}$  fibers, will be much more efficient even at high temperatures and pressures than is normally sufficient in the filtration industry.

---

\*Solidity ( $\alpha$ ) is the fraction of the fiber bed which is solid. A solidity of 0.02 indicates that 2% of the bed is occupied by fibers.

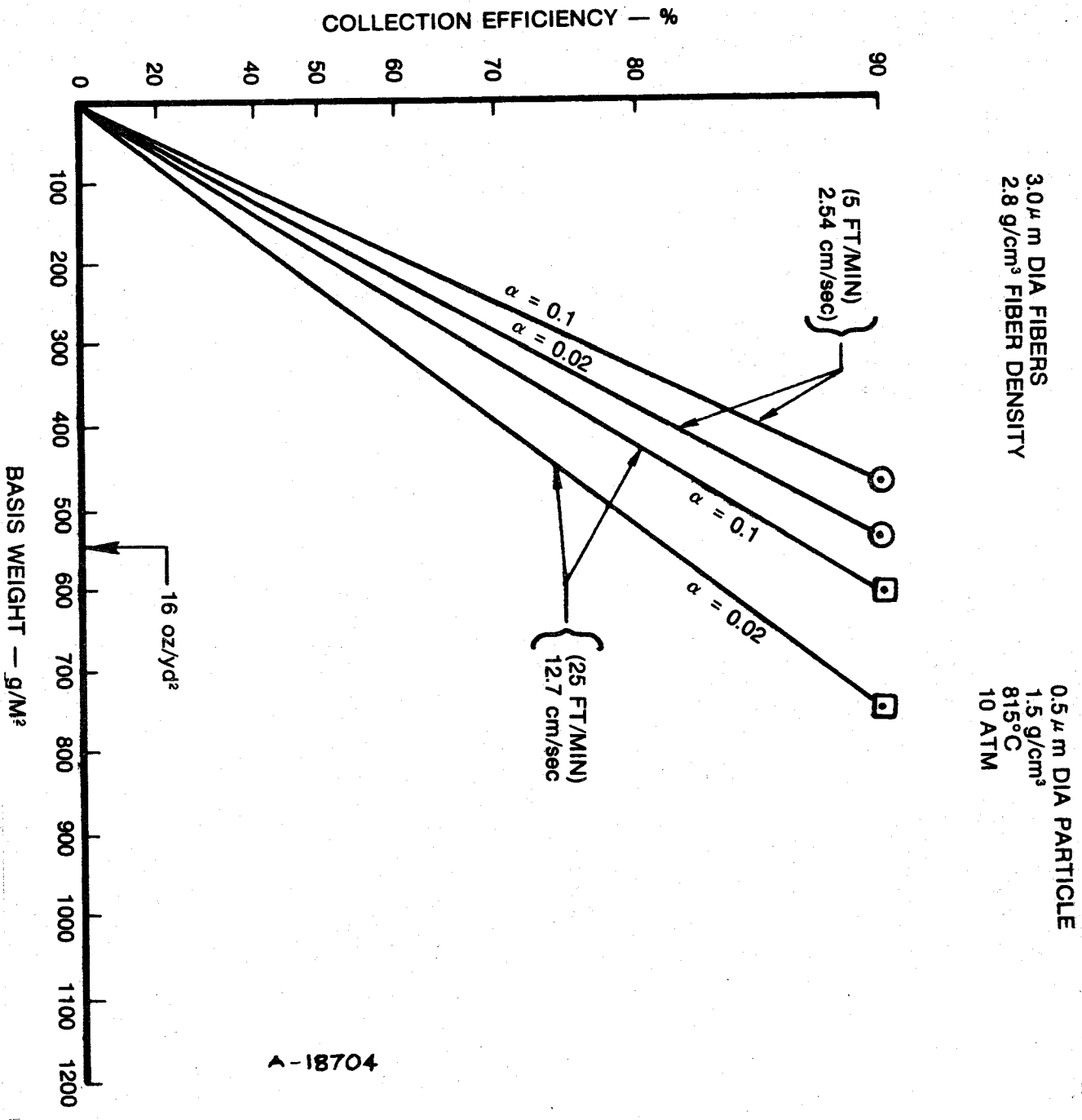


Figure 2. Calculated performance 3.0  $\mu$  m alumina fiber bed.

### Room Ambient Filter Media Tests

A large number of ceramic fiber filter media candidates have been subjected to a series of filtration tests at room ambient conditions. These tests included some examples of conventional filter media for comparison. Included among the tests were:

- Dioctylphthalate smoke (D.O.P) penetration as a function of air flow velocity
- Determination of maximum pore size (in micrometers)
- Measurement of permeability
- Flat-sheet dust loading tests using A.C. Fine test dust. Over-all collection efficiency and dust loading required to develop 3.7 KPa (15 in H<sub>2</sub>O) pressure drop are determined from this test which is operated at 10 cm/sec (20 ft/min) Air-to-cloth ratio.

Data collected from these tests are summarized on Table 3.

Penetration tests using D.O.P. smoke measure the ability of the clean fiber bed to stop fine particles. The D.O.P. smoke generator is adjusted to provide a nominal particle size of 0.3  $\mu$ m diameter which is a "most penetrating" particle size because of the minimal effect of diffusion and inertial impaction at this particle size. The D.O.P. test results should correlate well to the results predicted by analysis since particle collection is provided only by the fibers and not by the dust cake. Figure 3 provides a plot of the DOP efficiency as a function of air flow velocity for all the media tested. Ceramic media data are plotted in solid lines and conventional media in dotted lines. Numbers on the curves refer to those on Table 3. Several interesting observations can be made concerning this data:

- Several of the ceramic materials, especially the ceramic papers and felts, are capable of higher

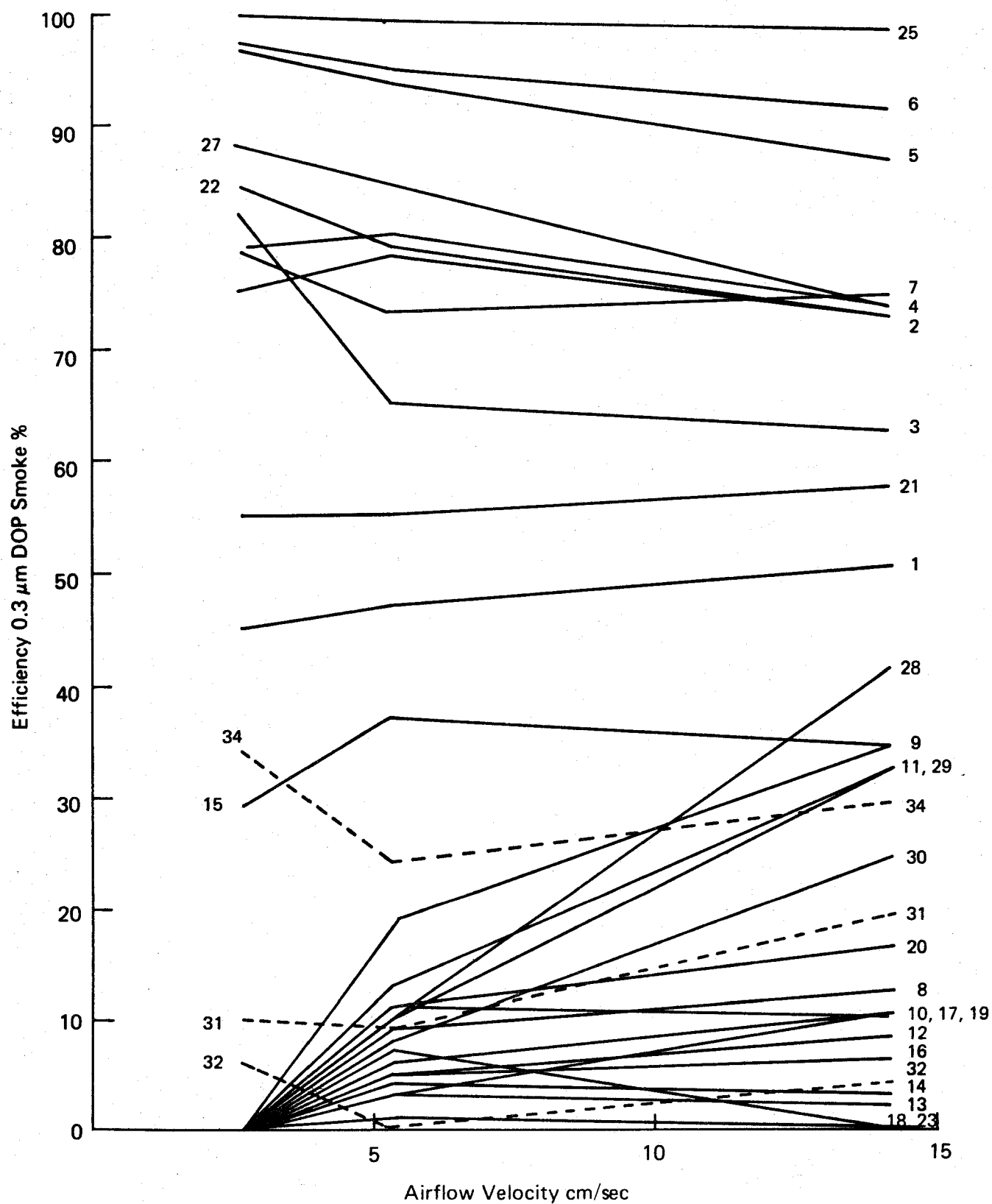


Figure 3. D.O.P. Efficiency fn airflow velocity.



Table 3

## SUMMARY ROOM AMBIENT TEST DATA

(W) Woven (P) Paper (F) Felt	Basis Weight g/m <sup>2</sup>	Percent Efficiency on ACF @ 10 cm/sec (20 ft. min)	Dust Loading g/m <sup>2</sup> to 3.735 KPa (g/ft <sup>2</sup> to 15" H <sub>2</sub> O)	Permeability cm <sup>3</sup> /sec/cm <sup>2</sup> for 0.1245 KPa (ft <sup>3</sup> /min/ft <sup>2</sup> for 0.5" H <sub>2</sub> O ΔP)	Maximum pore size Micrometers	Percent Efficiency on 0.3 μm DOP at cm/sec		
						2.68	5.35	14.22
1. Carborundum Fiberfrax cloth (W) with nichrome wire insert	1366	96.55	239.9 (22.2912)	8.687 (17.1)	248.6	45	47	50
2. Zircar Zirconia felt ZFY-100 (F)	615	95.64	Media Fractured	10.861 (21.38)	59	75	78	72
3. ICI Saffil alumina paper (P) with binder	165	99.805	159.4 (14.81)	9.307 (18.32)	43	82	65	62
4. ICI Saffil mat (F)	355	98.74	Media Fractured	12.395 (24.4)	61.1	79	80	73
5. Babcock & Wilcox Kaowool (F)	746	98.464	118.2 (10.980)	8.067 (15.88)	66.9	96.5	93.5	86
6. Carborundum Fiberfrax (F) durablanket	1363	99.507	146.9 (13.6523)	5.583 (10.99)	68.2	97.1	94.6	90.5
7. John Mansville Fiberchrome (F)	1297	99.654	253.9 (23.59)	11.897 (23.42)	112.3	78	73	74
8. Stevens Astroquartz (W) style 581	283	60.77	Test Stopped - Low Eff.	37.236 (73.3)	248.6	0	9	12
9. Hitco Refrasil C-100-96 (W) heat cleaned	1284	81.97	5.9 (.5482)	1.240 (2.44)	112.3	0	19	34
10. Hitco Refrasil C-100-48 (W) not heat cleaned	667	83.37	11.56 (1.074)	3.099 (6.1)	133.8	0	11	10
11. Stevens Astroquartz cloth (W) style 570	677	56.83	Test Stopped Low Eff.	22.758 (44.8)	267.7	0	13	32
12. 3M AB-312 basket weave (W) cloth	311	51.38	Test Stopped Low Eff.	13.553 (26.68)	870	0	5	8

Table 3 (Continued)

(W) Woven (P) Paper (F) Felt	Basis Weight g/m <sup>2</sup>	Percent Efficiency on ACF @ 10 cm/sec (20 ft. min)	Dust Loading g/m <sup>2</sup> to 3.735 KPa (g/ft <sup>2</sup> to 15" H <sub>2</sub> O)	Permeability cm <sup>3</sup> /sec/cm <sup>2</sup> for 0.1245 KPa (ft <sup>3</sup> /min/ft <sup>2</sup> for 0.5" H <sub>2</sub> O ΔP)	Maximum pore size Micrometers	Percent Efficiency on 0.3 μm DOP at cm/sec		
						2.68	5.35	14.22
13. 3M AB-312 twill weave (W) cloth	231	48.55	Test Stopped Low Eff. (same)	28.448 (56)	435	0	3	2
14. HITCO Refrasil cloth (W) UC-100-48	643	69.26	21.3 (1.98024)	8.687 (17.1)	193.3	0	4	3
15. Zircar Zirconia cloth (W) ZFY-30A	608	99.014	88.1 (8.1853)	5.791 (11.40)	248.6	29	37	34
16. FMI-Stevens Astroquartz (W) cloth crowfoot satin	352	76.19	91.6 (8.5057)	16.556 (32.59)	267.7	0	5	6
17. 3M AB-312 twill weave (W) cloth coated with 3M coating	227	47.64	Test Stopped Low Eff.	65.181 (128.31)	870	0	3	10
18. 3M AB-312 basket weave (W) cloth coated with 3M coating	281	45.65	Test Stopped Low Eff.	47.595 (93.69)	580	0	7	0
19. 3M AB-312 twill weave (W) cloth Menarde coating	254	55.078	Test Stopped Low Eff.	51.211 (100.81)	580	0	6	10
20. HITCO Refrasil cloth (W) UC-100-96 not heat cleaned	1249	68.46	13.68 (1.2708)	3.414 (6.72)	316	0	11	16
21. Carborundum Fiberfrax (W) no insert wire L-126TT	1544	99.21	173.5 (16.1213)	7.447 (14.66)	91.6	55	55	57
22. HITCO Refrasil batt B100-1 (F)	807	99.229	169.1 (15.706)	8.900 (17.52)	64.4	84	79	72
23. HITCO Refrasil standard (W) not heat cleaned very thin UC-100-28	335	84.41	22.88 (2.1257)	11.897 (23.42)	139.2	0	1	0
24. HITCO Irish Refrasil (W) chromized C-1554-48	683	81.476	11.97 (1.1116)	5.121 (10.08)	124.3	2	8	10

Table 3 (Concluded)

	(W) Woven (P) Paper (F) Felt	Basis Weight g/m <sup>2</sup>	Percent Efficiency on ACF @ 10 cm/sec (20 ft. min)	Dust Loading g/m <sup>2</sup> to 3.735 KPa (g/ft <sup>2</sup> to 15" H <sub>2</sub> O)	Permeability cm <sup>3</sup> /sec/cm <sup>2</sup> for 0.1245 KPa (ft <sup>3</sup> /min/ft <sup>2</sup> for 0.5" H <sub>2</sub> O ΔP)	Maximum pore size Micrometers	Percent Efficiency on 0.3 μm DOP at cm/sec		
							2.68	5.35	14.22
25. Carborundum Fiberfrax (P) paper (with binder) 970J		604	99.99	73.7 (6.8442)	26.899 (52.95)	47.7	99.5	99.0	97.6
26. ICI Saffil Zirconia paper (P) (with binder)		212	93.20 *Probable hole	82.2 (7.6374)	8.692 (17.11)	37.4	83	78	74
27. Carborundum Fiberfrax (P) paper (no binder) 970-AH		152	99.91	84.4 (7.8369)	12.416 (24.44)	43.5	88	-	73
28. 3M AB-312 double thick (W) plain weave		1035	43.86	Test Stopped Low Eff.	84.836 (167)	too large to measure with our equipment	0	10	41
29. FMI crowfoot satin cloth (W) astroquartz		905	40.08	Test Stopped Low Eff.	62.078 (122.20)	497	0	10	32
30. 3M AB-312 12 harness satin (W) weave		675	53.73	Test Stopped Low Eff.	75.529 (148.68)	696	0	8	24
31. 630 Tuflex fiberglass# (W)		564	93.982	47.6 (4.4187)	16.038 (31.57)	174	10	9	19
32. 15-011-020 woven filament# (W) polyester		175	96.078	28.0 (2.60163)	6.828 (13.44)	74	6	0	4
33. 25-200-070 polyester felt# (F)		524	99.193	135.3 (12.5688)	11.897 (23.42)	128.9	34	24	29
34. HITCO Refrasil cloth (std) (W) not heat cleaned, med. thickness		637	48.40	34.5 (3.2063)	6.934 (13.65)	-	-	-	-

#These materials are conventional (not ceramic) media.

efficiency collection of fine particles than are media normally used successively in commercial filter units.

- Many of the woven ceramic materials had zero D.O.P. efficiency at low velocity and higher D.O.P. efficiency at higher velocity.

This is contrary to what theory suggests and to the behavior normally seen in tests of conventional filter materials. A likely explanation for this performance is that it is caused by the presence of many large pores in the media. Examination of the pore size data in Table 3 shows that the woven ceramic materials as a group are characterized by larger pore size than are conventional filter materials. Thus, at low airflow velocity, most of the flow passes through the large pores and little filtration takes place. As velocity is increased, flow through the large pores becomes restricted and some of the flow is caused to pass through smaller pores where more filtration can take place.

- The D.O.P. data also supports the theoretical analysis. Efficiency as a function of basis weight for selected ceramic materials is plotted in Figure 4. The materials selected are ceramic papers and felts. These materials provide a fiber bed similar to that for which the analysis summarized in Figure 2 was based. Figure 4 shows that the nominally 3  $\mu$ m fibers do indeed provide higher collection efficiency on a weight-per-unit area basis than conventional media produced with larger diameter fibers.

Maximum pore size data shows that many of the woven ceramic materials had pores larger than those characteristic

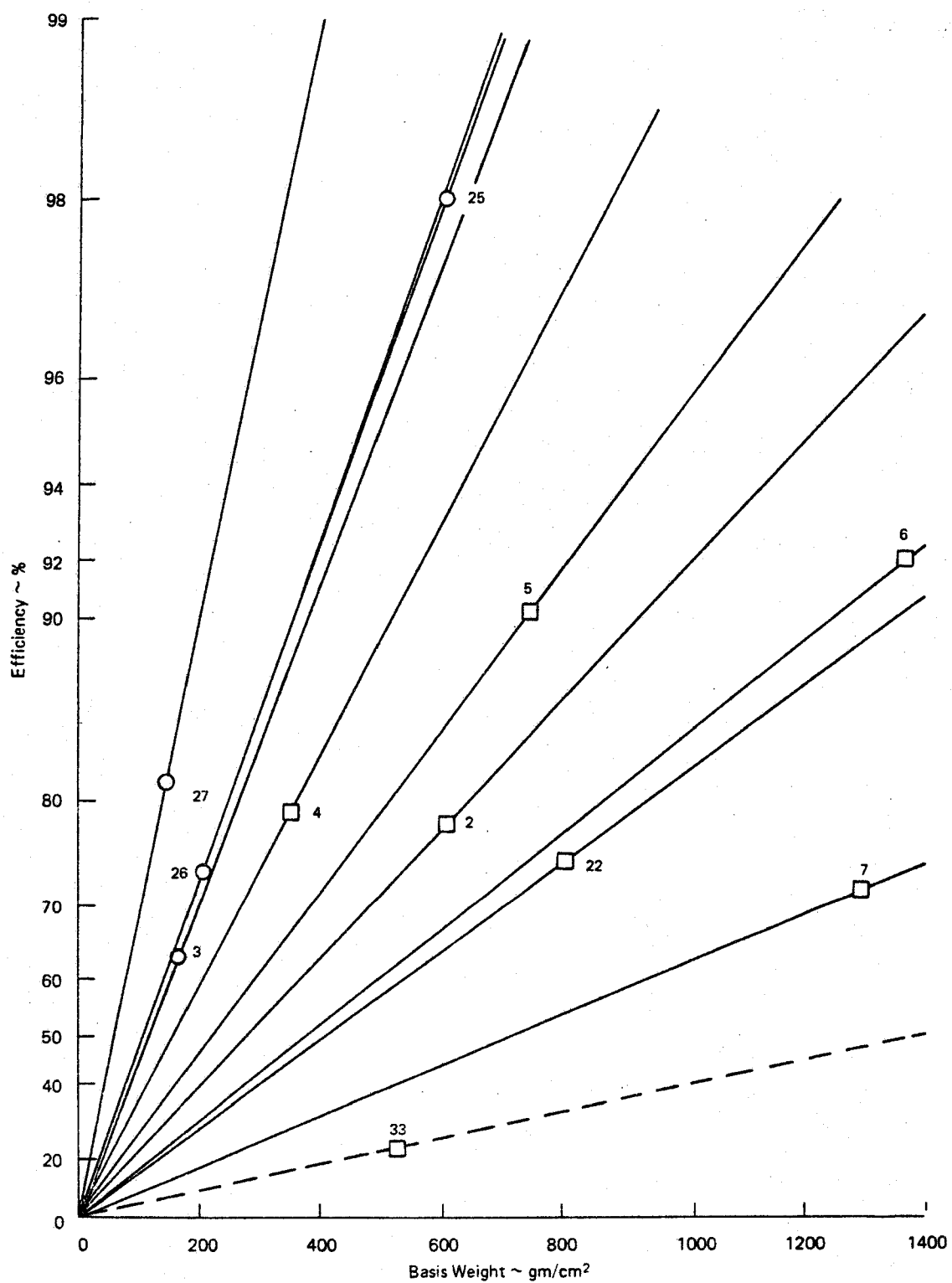


Figure 4. D.O.P. efficiency fn basis weight.

of filter materials. Also, many of the felt and paper materials had pore sizes similar to those of conventional filter materials.

Permeability is measured as the flow per unit area at a constant pressure drop. Thus, a material with low permeability offers a high restriction to gas flow and one with high permeability allows more gas to penetrate for a given pressure drop. Table 3 shows that some ceramic materials are available which have low permeability, while others have high permeability. Some of the woven materials have low permeability and large pore size, while others have high permeability and large pore size. Most of the paper and felt materials have permeability similar to that of commonly used filter materials.

Flat sheet dust loading tests were performed as follows: A 7.62 cm (3 inch) diameter disc of media is suspended across an air stream which is maintained at 10.16 cm/sec (20 ft/min) velocity through the filter media. In this test the media supports itself against the pressure drop (no screen is used). Standard A.C. Fine test dust (0-80  $\mu\text{m}$  silica) was fed to the media at a nominal rate of 0.883 g/m<sup>3</sup> (0.025 g/ft<sup>3</sup>) until a pressure drop of 3.735 KPa (15 in H<sub>2</sub>O) is reached. Pressure drop as a function of time is monitored during the test. This data is presented in Figures 5, 6, and 7 for selected materials. From the data collected, dust loading (g/m<sup>2</sup>) necessary to cause a given pressure drop 3.735 KPa (15 in H<sub>2</sub>O) is determined. Examination of this data in Table 3 shows that some of the woven materials reached high pressure drops while collecting only a small weight per unit area of dust. This is true also of the commercial woven materials (items 31 and 32). Other woven ceramics were penetrated so severely that they would not develop a pressure drop of 3.735 KPa (15 in H<sub>2</sub>O).

Two of the non-woven samples (which were unsupported) fractured as a result of the pressure drop across them. Several of the ceramic paper and felt materials exhibited dust loading, similar to that which is expected from conventional filter papers and felts.

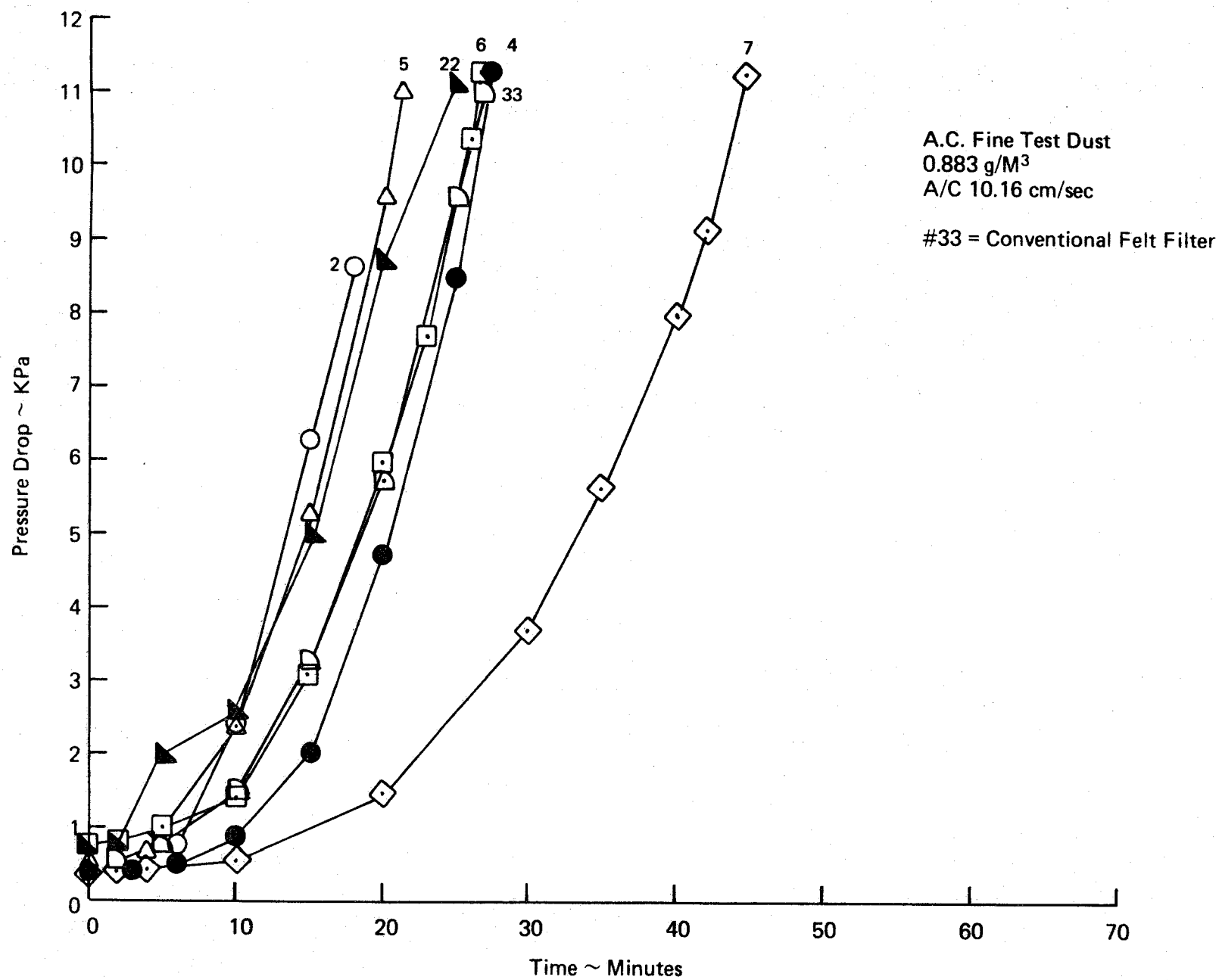


Figure 5. Dust loading of ceramic felts.

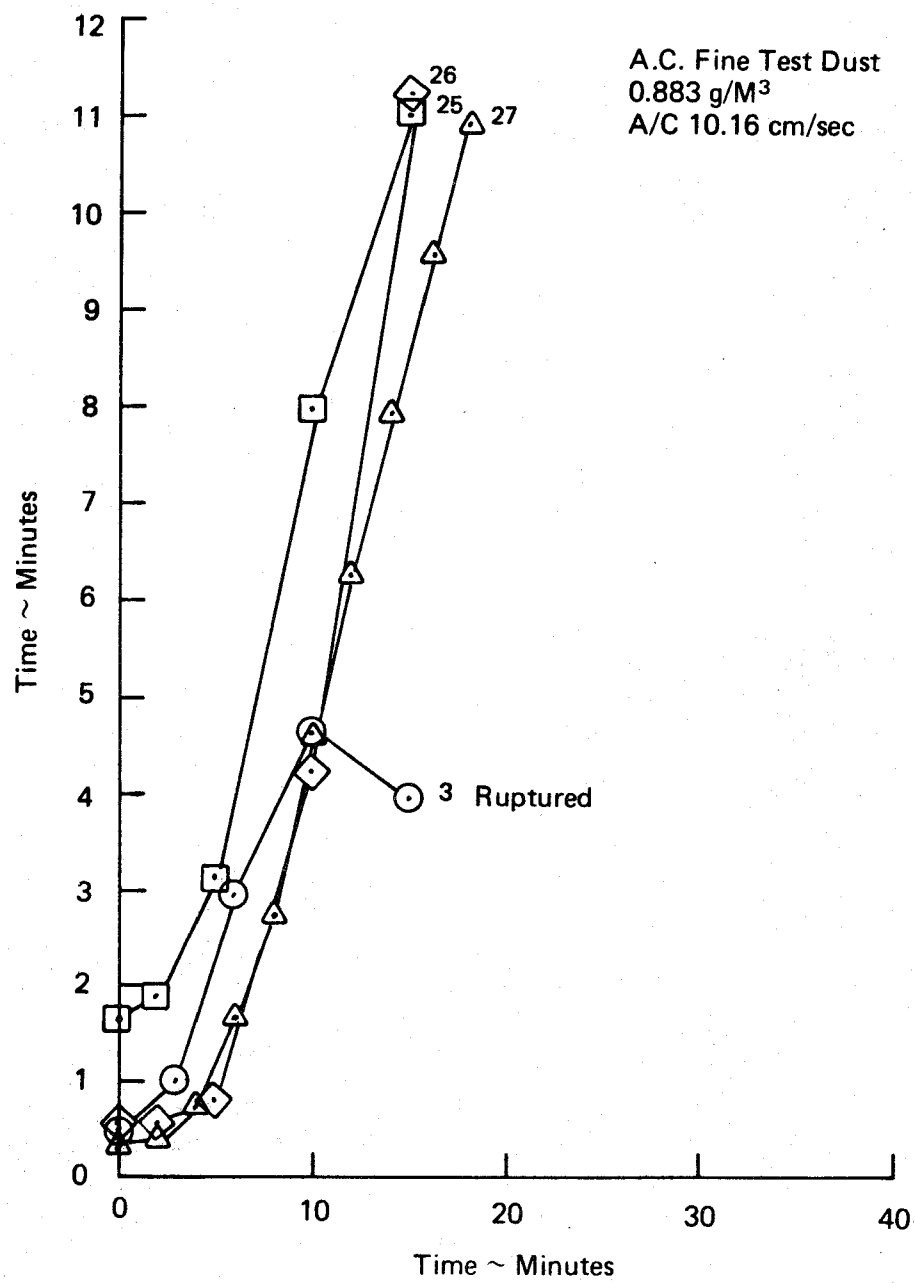


Figure 6. Dust loading of ceramic paper.



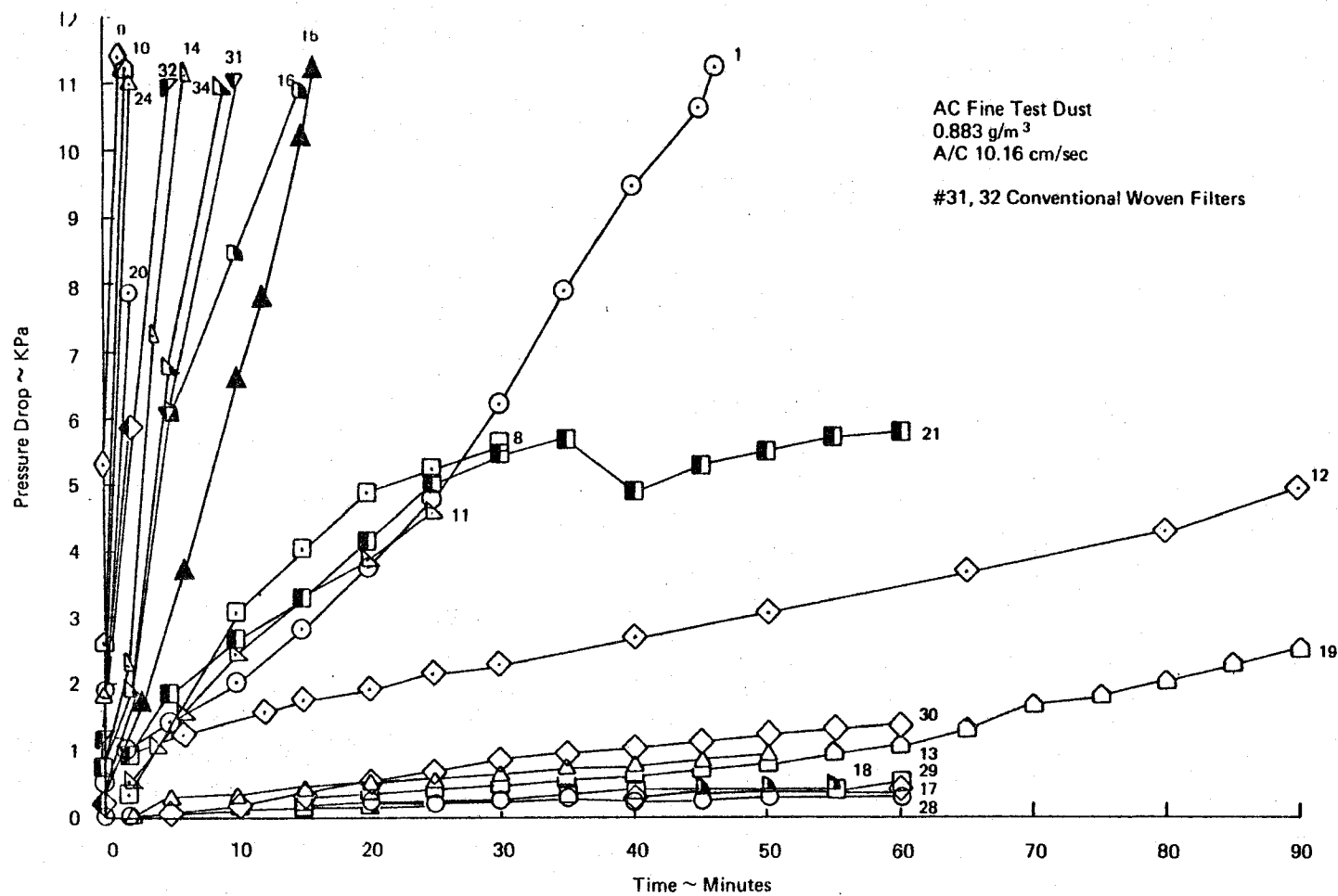


Figure 7. Dust loading of woven ceramic media.

The flat sheet loading tests also provided overall collection efficiency (mass basis) data for the tested materials. Dust penetrating the media was collected in an absolute filter downstream of the test media. Table 3 reveals that most of the woven ceramic materials did not achieve high collection efficiency in this test. On the other hand, woven commercial materials were only moderately efficient. Several of the ceramic paper and felt materials, however, did provide collection efficiency of 99 percent or better. The two materials which fractured would have provided higher efficiency performance had they not fractured. The test was stopped as soon as the fracture was detected.

#### General Conclusions from Room Ambient Tests

- Several of the ceramic paper and felt materials are capable of removing fine particles at high efficiency without excessive filter weights.
- The ceramic paper and felt materials have filtration characteristics and performed similar to paper and felt commercial filter media in a series of filter media tests.
- The ceramic woven materials in general were characterized by large pores and poor collection efficiency in the dust loading tests. The range of parameters exhibited by the various materials, however, indicate that an acceptable woven ceramic filter media can probably be fabricated, but such a filter media would have the same limitations as currently available woven filters. That is, acceptable performance is only probable at low air-to-cloth ratios.

- "Blanket" ceramic fiber materials (felts) consisting of small diameter fibers (3.0  $\mu\text{m}$ ) appear to be the most promising materials for high temperature and pressure tests because of their combination of good filtration performance and relatively high strength.

#### High Temperature/Pressure Tests

Two major questions concerning the suitability of ceramic fibers for filtration need to be answered. These are:

1. How durable are ceramic fiber structures when subjected to environmental conditions associated with filtration applications.
2. How well do ceramic fibers perform as filters in the HTHP environment.

Some preliminary answers are available concerning the first of these questions.

Three ceramic filter media configurations have survived a test during which the filter elements were subjected to 50,000 cleaning pulses. The objective of these tests was to simulate approximately one year of operation of mechanical loads on the media at high temperature and pressure. Test conditions were as follows:

Temperature - 815°C  
 Pressure - 930 KPa  
 Air-to-cloth-ratio - 5 to one (2.54 cm/sec)  
 Cleaning pulse pressure - 1100 KPa  
 Cleaning pulse interval - ~10 seconds  
 Cleaning pulse duration - 100 m second  
 Dust - recirculated fly ash

The three filter media configurations tested were:

- Saffil alumina mat contained between an inside and an outside layer of 304 stainless steel knit wire screen. Figure 8 shows how easily the residual

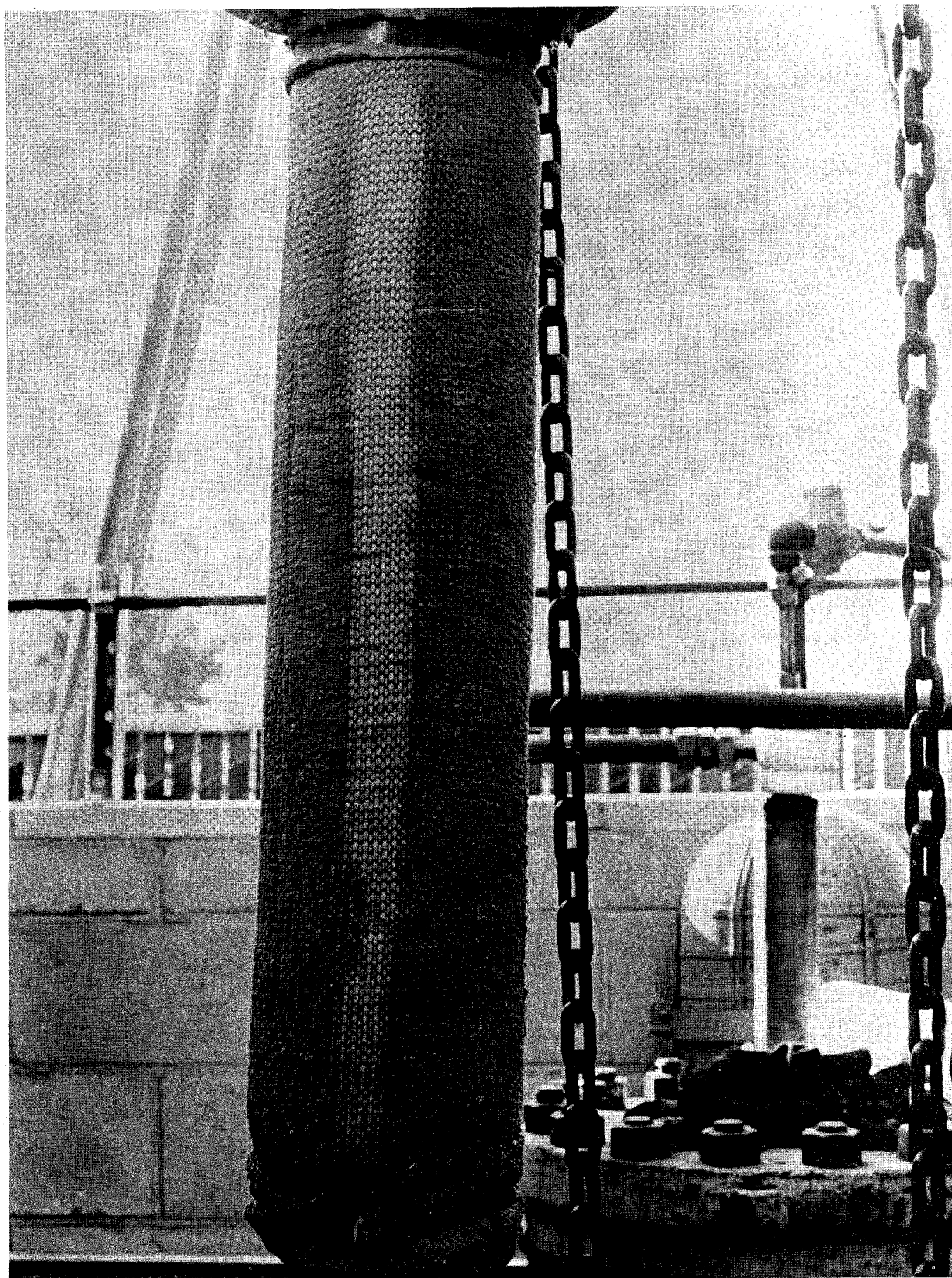


Figure 8. Saffil Alumina—Post Test Dust Cake (Clean strip using Vacuum Cleaner)

dust cake was removed from this media after the test.

- Woven Fiberfrax cloth with nichrome wire scrim insert. Figure 9 shows the dust cake following the 50,000 Pulse test.
- Fiberfrax blanket contained between an inside and an outside cylinder of 304 stainless steel square mesh screen similar to common window screen. The ceramic fiber blanket was held in position between the screens with 302ss wire sewn between the screens. This resulted in about 100 penetrations of the ceramic fiber bed. Figure 10 shows the dust cake following the test.

Pressure drop during the tests was controlled by the rapid cleaning pulses and in general remained less than about 5 KPa (20 in  $H_2O$ ).

Dust penetrating the ceramic test media was collected on a high efficiency filter located downstream (after cooling) of the test chamber. This data is not reported for the Saffil Alumina or for the Woven Fiberfrax Cloth because of a leak discovered in a gasket in the test rig. This problem was corrected before the fiberfrax blanket test was performed. Average outlet loading during this test was  $0.0055 \text{ g/m}^3$  ( $0.0024 \text{ gr/ft}^3$ ). Figure 10 shows that the dust was concentrated near the places where wire penetrated the filter element. This concentration of dust near the wire penetration points could be seen on the inside of the element also. Thus, most of the dust which penetrated apparently did so through the holes made by the wires. It is reasonable to expect that a filter element without holes will experience less penetration. Also a less frequent cleaning pulse interval will reduce penetration. Therefore even better performance than that achieved in this test should result from future tests.

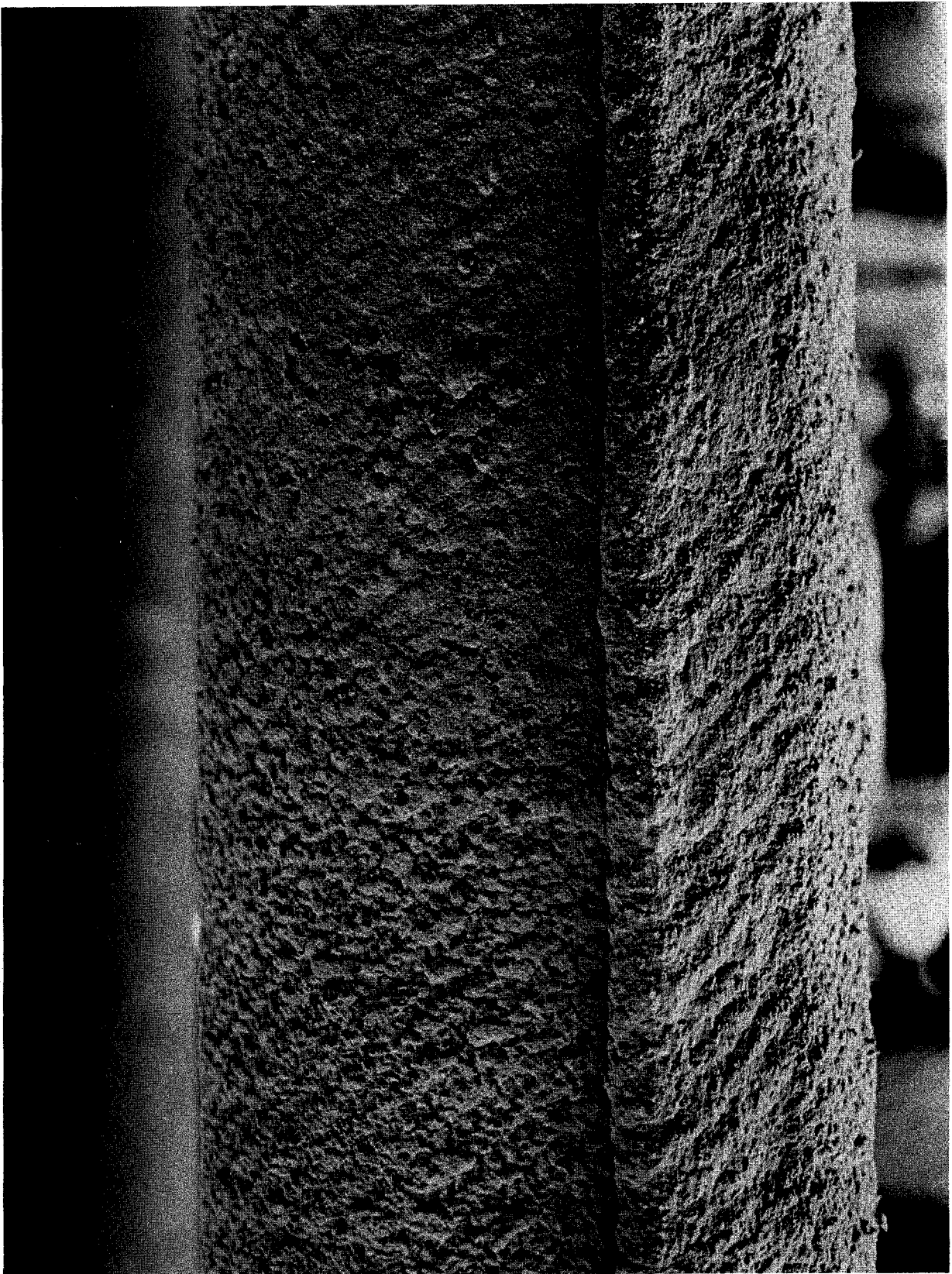


Figure 9. Woven Fiberfrax - Post Test Dust Cake



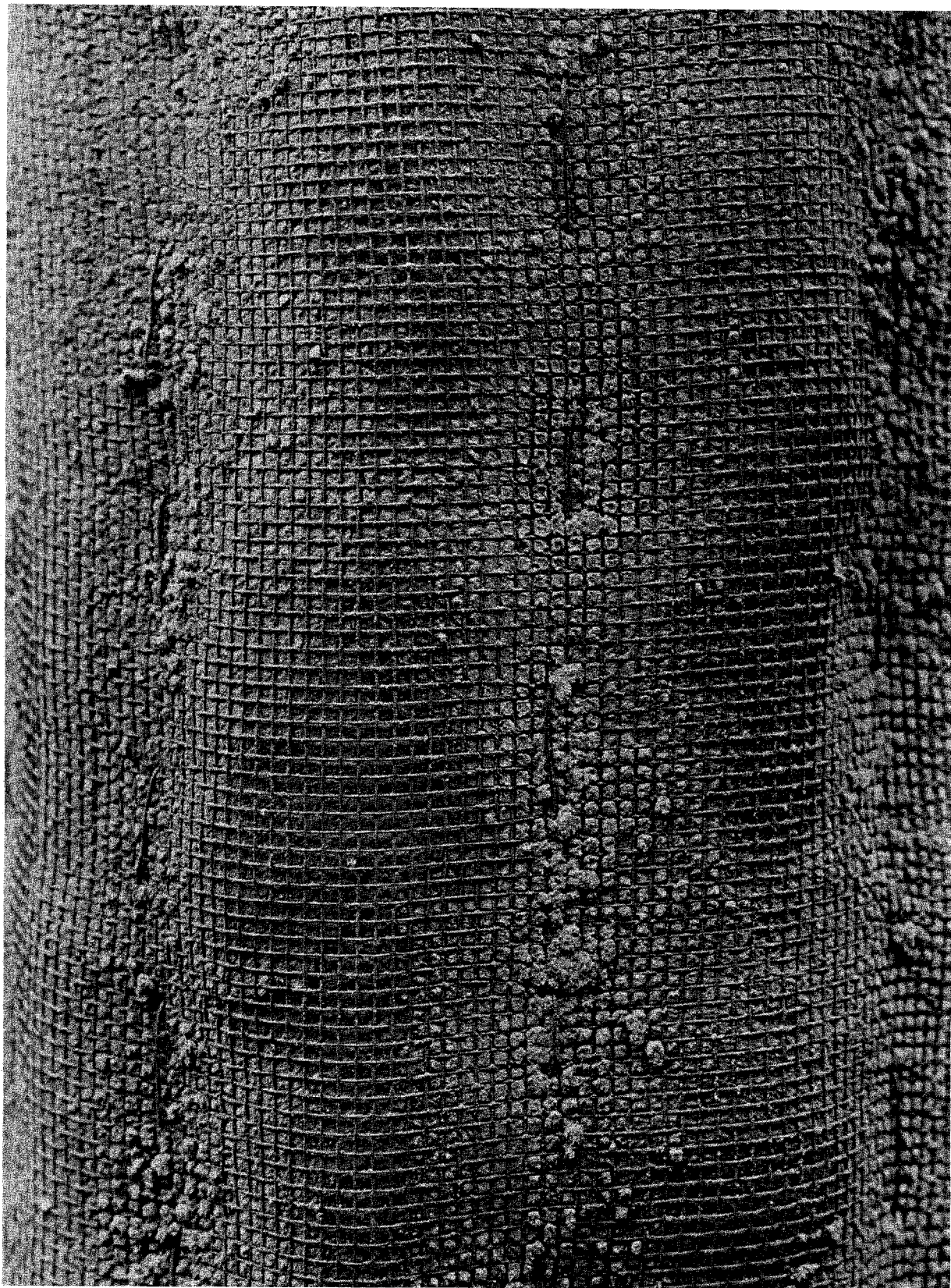


Figure 10. Fiberfrax Blanket - Post Test Dust Cake

## Conclusions

Research on bench scale indicates that fine particle control at high temperature and pressure can be achieved using barrier filtration by ceramic filter beds. Evidence in support of this contention includes the following:

- A theoretical basis exists for it.
- Room temperature tests show that particles including fine particles are collected at high efficiency.
- Tests at high temperatures and pressures show that several ceramic filter structures are capable of surviving in excess of 50,000 cleaning pulses while maintaining pressure drop at acceptable levels and providing efficiency close to the lowest reported turbine requirements.

## REFERENCES

1. Hazard, H. R., "Coal Firing for the Open-Cycle Gas Turbine." Proceedings of the Joint Conference on Combustion, 1955, ATME and IME.
2. Hoke, R., "Ducon Gravel Bed Filter Testing," EPA/ERDA Symposium on High Temperature/Pressure Particle Control, Washington, D.C., Sept. 1977.





## SYMPOSIUM ATTENDEES

K. P. ANANTH  
Midwest Research Institute  
425 Volker Blvd.  
Kansas City, MO 64110

GRANT D. APPLEWHITE  
American Air Filter Co., Inc.  
215 Central Avenue  
Louisville, KY 40277

MARYLIN ARDELL  
McIlvaine Company  
2970 Maria Ave.  
Glenview, IL 60025

B. ARNOLD  
SF Products Canada Ltd.  
4480 Cote de Liesse Road  
Montreal, Quebec  
Canada H4N 2R1

PAUL ATLAS  
J. P. Stevens & Company  
141 Lanza Ave.  
Garfield, NJ 07026

JAMES BALL  
Midland-Ross Corp.  
Capitol Castings Div.  
P.O. 750  
Phoenix, AZ 85001

JOHN BARANSKI  
General Battery Corporation  
Box 1262  
Reading, PA 19603

DUANE BECKNELL  
Lear Siegler, Inc.  
74 Inverness Drive East  
Englewood, CO 80110

WALLACE P. BEHNKE  
E. I. du Pont de Nemours & Co., Inc.  
701 Bldg. Chestnut Run Location  
Wilmington, DE 19898

STEVE BELLMORE  
Fabric Filters  
525 South Hayden Rd.  
Tempe, AZ 85281

LARRY BENNETT  
Fabric Filters  
525 South Hayden Rd.  
Tempe, AZ 85281

ROBERT P. BENNETT  
Apollo Chemical Corp.  
35 South Jefferson Road  
Whippany, NJ 07981

LUTZ BERGMANN  
Milliken & Company  
1304 Washington Street  
LaGrange, GA 30240

CARL H. BILLINGS  
Arizona Bureau of Air Quality Control  
1740 West Adams St.  
Phoenix, AZ 85007

GERRIT W. BLYDORP  
Mobay Chemical Corp.  
Baytex Fibers Div.  
425 Park Avenue  
New York, NY 10022

JOHN BRANCACCIO  
Western Electric Company  
222 Broadway  
New York, NY 10038

ROGER I. BRANDSTETTER  
Industrial Filtration Inc.  
1500 Daisy Ave.  
Long Beach, CA 90813

FREDERICK E. BRANDT  
Johns-Manville Sales Corp.  
Ken-Caryl Ranch  
Denver, CO 80217

WILLIAM J. BRINKMAN  
Magna Copper Co.  
P.O. Box M  
San Manuel, AZ 85631

PETER R. CAMPBELL  
Globe Albany Filtration  
2405 West University  
Tempe, AZ 85281

J. MICHAEL CANTY  
Viking Sales Co.  
Box 50025  
Tucson, AZ 85703

STEPHEN V. CAPONE  
GCA Corporation  
GCA/Technology Division  
Burlington Road  
Bedford, MA 01730

BENGT CARLSSON  
Bahco Systems, Inc.  
3402 Oakcliff Rd., Suite B-1  
(P.O. Box 48116-Atl 30362)  
Atlanta, GA 30340

HUNG BEN CHU  
Los Angeles Department of  
Water & Power  
111 N. Hope St.  
Los Angeles, CA 90051

W. A. CHENEY  
United Air Specialists  
6665 Creek Rd.  
Cincinnati, OH 45242

PETER CHMARA  
Mines Accident Prevention  
Association of Ontario  
290 Second Ave. West  
North Bay, Ontario  
Canada P1B 3K9

JACK CLEMENTS  
Standard Havens, Inc.  
8800 E. 63rd  
Kansas City, MO 64133

JOHN F. COBIANCHI  
J. P. Stevens & Co., Inc.  
1185 Avenue of the Americas  
New York, NY 10036

WILLIAM COLUMBUS  
Arizona State BAQC  
5055 E. Broadway C-209  
Tucson, AZ 85204

ROBERT C. COMER  
W. W. Criswell Co.  
800 Industrial Highway  
Riverton, NJ 08077

EDWARD B. COOPER  
W. L. Gore & Associates, Inc.  
104 Bent Lane,  
Newark, DE 19711

FLOYD B. CORDNER  
State of Utah Department of Health  
150 West North Temple  
P.O. Box 500  
Salt Lake City, UT 84110

RICHARD T. COX  
Huyck Felt-Division of Huyck Corp.  
Washington Street  
Rensselaer, NY 12144

FRED CROWSON  
Naval Surface Weapons Center  
Code CG-31  
Dahlgren, VA 22448

VICTOR M. DAY  
Lear Siegler Inc.  
74 Inverness Dr. E.  
Englewood, CO 80110

EDWARD DE GARBOLEWSKI  
W. L. Gore & Associates, Inc.  
P. O. Box 1220, Rt. 213 North  
Elkton, MD 21921

RONALD L. DEPOE  
J. P. Stevens & Co., Inc.  
1185 Avenue of the Americas  
New York, NY 10036

GORDON A. DICK  
Wheelabrator - Canada  
235 Speers Rd.  
Oakville, Ontario  
Canada L6H-2K9

THOMAS DONNELLY  
Donaldson Company, Inc.  
P.O. Box 1299  
Minneapolis, MO 55440

DAN DOYLE  
Flakt, Inc.  
1500 East Putnam Ave.  
Old Greenwich, CT 06870

DELMAR J. DOYLE  
American Air Filter Co., Inc.  
215 Central Avenue  
Louisville, KY 40277

T. REGINALD DRISCOLL  
Globe Albany - Canada  
Morrow  
Barrie, Ontario  
Canada

STEPHEN B. DUERK  
J. P. Stevens & Co., Inc.  
1185 Avenue of the Americas  
New York, NY 10036

JOHN M. EBREY  
Lodge-Cottrell  
601 Jefferson  
Houston, TX 77005

HEINZ ENGELBRECHT  
Wheelabrator-Frye  
600 Grant St.  
Pittsburgh, PA 15219

DONALD R. ENNS  
Endur Limited  
5379 Fairview St.  
Burlington, Ontario  
Canada L7L 5K4

DAVID S. ENSOR  
Meteorology Research, Inc.  
464 W. Woodbury Rd.  
Altadena, CA 91001

P. S. ESHELMAN  
General Motors Corporation  
Industrial Hygiene Dept.  
GM Technical Center  
Warren, MI 48090

REGINALD G. EVANS  
Canadian Johns-Manville Co.  
P.O. Box 1500  
Asbestos, Quebec  
Canada J1T3N2

J. P. FAGAN  
E. I. du Pont de Nemours  
85 Mill Plain Rd.  
Fairfield, CT 06430

L. W. FERGUSON  
Owens-Corning Fiberglas Corporation  
P. O. Box 415  
Granville, OH 43023

PETER FINNIS  
Wheelabrator - Canada  
235 Speers Rd.  
Oakville, Ontario  
Canada L6H-2K9

E. R. FREDERICK  
Air Pollution Control Association  
P.O. Box 2861  
Pittsburgh, PA 15230

GENE FREDERICK  
Clark-Schweble Fiber Glass Corp.  
14530 South Anson Ave.  
Santa Fe Springs, CA 90670

ROBERT E. FREY  
Torit Div. Donaldson  
P.O. Box 43217  
St. Paul, MN 55164

DALE A. FURLONG  
Buell Division of Envirotech Corporation  
200 N. Seventh Street  
Lebanon, PA 17042

JOHN H. FURSE  
Rexnord APC Div.  
3300 Fern Valley Rd.  
Louisville, KY 40213

R. G. GARCIA  
Duval Sierrita  
Box 125  
Sahuarita, AZ 85629

ROGER L. GIBBS  
Naval Surface Weapons Center  
Code CG-31  
Dahlgren, VA 22448

RONALD GITTELSON  
Southern Silk Mills  
Spring City, TN 37381

HARRY J. GIULIANI  
Wheelabrator-Frye Inc.  
600 Grant Street  
Pittsburgh, PA 15219

A. GOMEZ  
Duval Corp.  
4715 E. Ft. Lowell Rd.  
Tucson, AZ 85712

MANUEL GONZALES  
Los Alamos Scientific Laboratory  
P.O. Box 1663  
Los Alamos, NM 87545

EUGENE E. GRASSEL  
Donaldson Co. Inc.  
P.O. Box 1299  
Minneapolis, MN 55440

PAUL GRIM  
Stearn Rogers  
700 S. Ash St.  
P.O. Box 5888  
Denver, CO 80217

THERON GRUBB  
Burlington Glass Fabrics Co.  
110 Andrew St.  
Greenboro, NC 27406

ARNOLD G. GRUSHKIN  
Research-Cottrell, Inc.  
P.O. Box 750  
Bound Brook, NJ 08805

THOMAS L. HARSELL, JR.  
Harsell Engineering Corp.  
10,000 Santa Monica Blvd., Suite 307  
Los Angeles, CA 90067

BARRY J. HASWELL  
Blast-Tech Ltd.  
1100 Invicta Drive, Unit 12  
Oakville, Ontario  
Canada L6H-2K9

TOM HAYES  
3M Company  
3M Center, Bldg. 230-BE  
St. Paul, MN 55101

J. M. HENRICKS  
Tucson Gas & Electric  
P.O. Box 711  
Tucson, AZ 85702

RICHARD B. HOGUE, JR.  
Viking Sales Co.  
Box 50025  
Tucson, AZ 85703

MARK HOLCOMBE  
Chromalloy, Textile Service Division  
900 N. Alvarado  
Los Angeles, CA 90026

ROBERT P. HOSEMAN  
Pacific Gas & Electric  
77 Beale Street  
San Francisco, CA 94106

RICHARD G. HOSPER  
MRI  
464 W. Woodburg Rd.  
Altadena, CA 91001

CHARLES B. HOTCHKISS  
Menardi-Southern  
1201 Francisco St.  
Torrance, CA 90502

TOM HOYNE  
Buell - Envirotech  
7462 N. Figueroa St.  
Los Angeles, CA 90041

JACK D. JONES  
Southwestern Public Service Company  
Box 1261  
Amarillo, TX 79170

INGEMAR KARVEGARD  
Bahco Systems, Inc.  
3402 Oakcliff Rd., Suite B-1  
(P.O. Box 48116 - Atl. 30362)  
Atlanta, GA 30340

MICHAEL T. KEARNS  
Air Pollution Sysrems Inc.  
1114 Andover Park West  
Tukwilla, WA 98188

THOMAS P. KELLY  
Clark-Schwebel Fiber Glass Corp.  
5 Corporate Park Drive  
White Plains, NY 10604

WILLIAM KELLY  
Environmental Elements  
7249 National Drive  
Hanover, MD 21076

STANLEY K. KEMPNER  
Western Electric  
222 Broadway  
New York, NY 10038

THOMAS J. KILEY  
Griffin Environmental Company, Inc.  
P.O. Box 86  
Baldwinsville, NY 13027

JERRY KRAIM  
Stansteel Corporation  
5001 S. Boyle Avenue  
Los Angeles, CA 90058

PAUL LANGSTON  
DuPont Co.  
114 Mulberry Rd.  
Newark, DE 19711

G. D. LANOIS  
Wheelabrator-Frye Inc.  
600 Grant St.  
Pittsburgh, PA 15219

RICHARD C. LARSON  
Torit Division  
Donaldson Co. Inc.  
1133 Rankin St.  
St. Paul, MN 55165

JOE LEDBETTER  
University of Texas at Austin  
Cockrell Hall  
Austin, TX 78712

WAYNE H. LEIPOLD  
Phelps Dodge  
P. O. Drawer E  
Douglas, AZ 85607

BENJAMIN LINSKY  
West Virginia University  
Fattersall House  
Morgantown, WV 26506

W. O. LIPSCOMB  
Acurex/Aerotherm  
c/o EPA Research Triangle Park  
Durham, NC 27711

JOE LOFLIN  
Texas A & M University  
Zachery Bld. Ind. Eng.  
College Station, TX 77840

ROBERT L. LUCAS  
E. I. DuPont  
Louviers Bldg.  
Newark, DE 19711

CARL E. LUNDBERG  
Contamination Control, Inc.  
1310 Genoa  
So. Houston, TX 88587

TSHIEN MA  
Buell Div. of Envirotech  
200 North Seventh St.  
Lebanon, PA 17042

TERRY MACRAE  
Industrial Clean Air  
2929 Fifth St.  
Berkeley, CA 94710

BRIAN MEAD  
DuPont Company  
PP&R D 13126  
Wilmington, DE 19898

MANAN MEHTA  
Mikropul Corp.  
10 Chatham Rd.  
Summit, NJ 07901

ROBERT C. MEYER  
Envirotech Corporation  
P.O. Box 1211  
Salt Lake City, UT 84117

JAMES A. MITCHELL  
Lodge-Cottrell-Dresser  
601 Jefferson, 27th Floor  
Houston, TX 77005

FRED MORENO  
Acurex Corporation  
485 Clyde Ave.  
Mountain View, CA 94042

ANDY MURPHY  
Acurex Corporation  
3301 Womens Club Drive, Suite 147  
Raleigh, NC 27611

WALLACE G. MURRAY  
Cities Service Co.  
P. O. Drawer 1149  
Franklin, LA 70538

RAYMOND Z. NAAR  
Huyck Research Center  
Washington Street  
Rensselaer, NY 12144

WILLIAM G. NELSON  
U.S. Borax  
Borax Road  
Boron, CA 93516

JOE NOLL  
Flakt, Inc.  
1500 East Putnam Avenue  
Old Greenwich, CT 06870

PETE PETREY  
American Air Filter Co. Inc.  
215 Central Ave.  
Louisville, KY 40277

WALTER PIULLE  
EPRI  
3412 Hillview Avenue  
Palo Alto, CA 94303

CHARLES J. O'BOYLE  
EPA Region VIII  
1860 Lincoln St.  
Denver, CO 80295

PALMER PARSONS  
Filtered Air Corp.  
Perry, OH 44081

MUKESH N. PATEL  
Illinois Institute of Technology  
I. I. T. Centre  
Chicago, IL 60616

MICHAEL A. PETRILLI  
Monsanto Enviro-Chem Systems  
Corporate Square Office Park  
Box 14547  
St. Louis, MO 63178

THOMAS PLUNKETT  
Standard Havens  
8800 E. 63rd  
Kansas City, MO 64133

ED POLLOCK  
SF Products Canada Ltd.  
4480 Cote de Liesse Road  
Montreal, Quebec  
Canada H4N 2R1

W. WALTER RENBERG  
Envirotech Corporation  
Two Airport Office Park  
400 Rouser Rd.  
Pittsburgh, PA 15108

RONALD J. RENKO  
C-E Air Preheater  
P.O. Box 372  
Wellsville, NY 14895

LAMSON RHEINFRANK  
Standard Havens, Inc.  
8800 E. 63rd  
Kansas City, MO 64113

DON RICHMOND  
C-E Air Preheater  
Andover Rd.  
Wellsville, NY 14895

ENRIQUE RODRIGUEZ T.  
Accion Social Regiomontana A.C.  
Box 2034  
Monterrey, N.L.  
Mexico

RICHARD ROLFE  
Joy Manufacturing Co.  
4565 Colorado  
Los Angeles, CA 90039

DONALD H. RULLMAN  
American Air Filter Co., Inc.  
215 Central Ave.  
Louisville, KY 40291

DOUGLAS RYDER  
Globe Albany Corp.  
2405 W. University  
Tempe, AZ 85281

ALBERTO SABADELL  
Mitre Corp.  
McLean, VA 22101

CHARLES A. SALOTTI  
University of Wisconsin - M  
P.O. Box  
Milwaukee, WI 53201

HARRY N. SANDSTEDT  
DuPont  
Centre Rd. Bldg.  
Wilmington, DE 19898

ROBERT W. SCHECK  
Stearns Roger, Inc.  
Box 5888  
Denver, CO 80217

S. P. SCHLIESSER  
Acuretex/Aerotherm  
c/o EPA Research Triangle Park  
Durham, NC 27711

TOM SCHNEIDER  
Bay Area Industrial Filtration  
6355 Coliseum Way  
Oakland, CA 94621

M.P. SCHREYER  
Wheelabrator-Frye Inc.  
14920 So. Main  
Gardena, CA 90248

FREDERICK D. SCHULER  
Donaldson Company  
P.O. Box 1299  
Minneapolis, MN 55440

JOHN H. SCOTT  
Donaldson Company, Inc.  
P.O. Box 1299  
Minneapolis, MN 55440

WILLIAM E. SEBESTA  
300 Florence  
Bay Village, OH 44140

MIKE SHACKLETON  
Acurex Corp. Aerotherm Div.  
485 Clyde Ave.  
Mountain View, CA 94042

JERRY SHANG  
Mitre Corp.  
McLean, VA 22101

J. R. SHEPPARD  
Milliken & Company  
1304 Washington Street  
LaGrange, GA 30240



JOE SIBRAVA  
Flakt, Inc.  
1500 East Putnam Ave.  
Old Greenwich, CT 06870

GLENN A. SMITH, JR.  
BHA Company Div. of Std. Havens  
8800 E. 63rd Street  
Kansas City, MO 64133

GORDON L. SMITH  
American Air Filter  
215 Dentrail  
Louisville, KY 40201

JOHN D. SQUIBBS  
Ford Motor Company  
Michigan Casting Center  
22000 Gibraltar Road  
Flat Rock, MI 48134

J. STEPHENSON  
Ontario Hydro, Central Health  
Physics Services  
757 Mackay Rd.  
Pickering, Ontario  
Canada L1V 2R5

SHARON STORY  
Fabric Filters  
525 South Hayden Rd.  
Tempe, AZ 85281

EMIL STUDINKA  
Texas A & M University  
Zachery Bldg. Ind. Eng.  
College Station, TX 77840

HERB SUERTH  
CEA Carter Day Co.  
500 73rd Avenue, NE  
Minneapolis, MIN 55432

NORM Surprenant  
GCA Corporation  
GCA/Technology Division  
Burlington Rd.  
Bedford, MA 01730

ROBERT D. Sutton  
Public Service Co. of Colorado  
5900 E. 39th Avenue  
Denver, CO 80207

DONALD P. TEIXEIRA  
EPRI  
3412 Hillview Avenue  
Palo Alto, CA 94303

LARRY A. THAXTON  
Buell Emission Control Division  
Envirotech Corporation  
200 N. 7th Street  
Lebanon, PA 17067

FERNANDO ORTIZ THOMAS  
Cristales Mexicanos, S.A.  
Galeana y Ruiz Cortines  
Monterrey, N.L.  
Mexico

TIM THURMAN  
Great Lakes Filter  
18475 Sherwood  
Detroit, MI 48234

ROBERT TISCONE  
Environmental Elements  
7249 National Drive  
Hanover, MD 21076

DAVID W. TOWNSEND  
W. W. Criswell Co.  
3901 W. Beech Ave.  
P.O. Box 130  
McAllen, TX 78501

JOHN W. VAKLYES, JR.  
C-E Air Preheater  
Andover Rd.  
Wellsville, NY 14895

MIGUEL ANGEL VARGAS  
Cristales Mexicanos, S.A.  
Galeana y Ruiz Cortines  
Monterrey, N.L.  
Mexico

THOMAS C. WAGNER  
PPG Industries - Fiber Glass Division  
One Gateway Center  
Pittsburgh, PA 15222

JAMES ZARFOSS  
Environmental Elements  
7249 National Drive  
Hanover, MD 21076

KEN A. WALKER  
Environmental Elements Corp.  
Box 1318  
Baltimore, MD 21203

JOHN ZUTTERMEISTER  
Bechtel Power Corp.  
50 Beale Street  
San Francisco, CA 94598

JACK A. WAUGH  
Kaiser Aluminum & Chemical Corporation  
P. O. Box 98  
Ravenswood, W. VA 26164

FRANK T. WEEMS  
Envirotech Corporation  
3000 Sand Hill Road  
Menlo Park, CA 94025

WAYNE WELLAN  
Combustion Equipment Association  
502 73rd Avenue, NE  
Minneapolis, MN 55432

VINCENT J. WEMLINGER, II  
E. I. DuPont F & F Dept.  
1007 Market St.  
Wilmington, DE 19898

ANDERS WIKTORSSON  
AB Svenska Flaktfabriken  
S-35187  
Växjö, Sweden

CHARLES WRIGHT  
Fabric Filter  
525 Hayden Road  
Tempe, AZ 85281

PAUL YOSICK  
American Air Filter  
215 Central Ave.  
Louisiana, KY 40222

DAVID YOUNG  
Bekaert Steel Wire Corporation  
800 Third Avenue  
New York, NY 10022



<b>TECHNICAL REPORT DATA</b> <i>(Please read Instructions on the reverse before completing)</i>		
1. REPORT NO. <b>EPA-600/7-78-087</b>	2.	3. RECIPIENT'S ACCESSION NO.
4. TITLE AND SUBTITLE <b>Third Symposium on Fabric Filters for Particulate Collection</b>	5. REPORT DATE <b>June 1978</b>	
	6. PERFORMING ORGANIZATION CODE <b>GCA-TR-78-33-G</b>	
7. AUTHOR(S) <b>N. Suprenant, Compiler</b>	8. PERFORMING ORGANIZATION REPORT NO.	
9. PERFORMING ORGANIZATION NAME AND ADDRESS <b>GCA Technology Division Burlington Road Bedford, Massachusetts 01730</b>	10. PROGRAM ELEMENT NO. <b>EHE624</b>	
	11. CONTRACT/GRANT NO. <b>68-02-2177</b>	
12. SPONSORING AGENCY NAME AND ADDRESS <b>EPA, Office of Research and Development Industrial Environmental Research Laboratory Research Triangle Park, NC 27711</b>	13. TYPE OF REPORT AND PERIOD COVERED <b>Proceedings; 6/77-3/78</b>	
	14. SPONSORING AGENCY CODE <b>EPA/600/13</b>	
15. SUPPLEMENTARY NOTES <b>IERL-RTP project officer is Dennis C. Drehmel, Mail Drop 61, 919/541-2925.</b>		
16. ABSTRACT <b>The report presents the 17 technical papers given at an EPA-sponsored symposium, held in December 1977 in Tuscon, Arizona, on fabric filters for particle collection. Emphasis was on current field experience and engineering-oriented research so that potential users could better select and/or design particulate control systems. Technical content focused on fabrics for high temperature filtration, their field behavior with fly ash and other effluents, design criteria and shakedown experience, and new filtration concepts that appear amenable to combustion and other process effluents.</b>		
17. KEY WORDS AND DOCUMENT ANALYSIS		
a. DESCRIPTORS	b. IDENTIFIERS/OPEN ENDED TERMS	c. COSATI Field/Group
<b>Pollution Dust Dust Filters Filtration Fabrics Fly Ash</b>	<b>Pollution Control Stationary Sources Particulate Fabric Filters</b>	<b>13B 11G 13K 07D 11E 21B</b>
18. DISTRIBUTION STATEMENT <b>Unlimited</b>	19. SECURITY CLASS <i>(This Report)</i> <b>Unclassified</b>	21. NO. OF PAGES <b>383</b>
	20. SECURITY CLASS <i>(This page)</i> <b>Unclassified</b>	22. PRICE